Mechanisms for microRNA-mediated silencing in *C. elegans* embryos

Edlyn Wu

Division of Experimental Medicine

McGill University

Montreal, Quebec, Canada

March 2016

A thesis submitted to McGill University in partial fulfillment of the

requirements for the Degree of Doctor of Philosophy

Abstract

MicroRNAs (miRNAs) are small (~22 nts) non-coding RNAs that impinge on post-transcriptional gene silencing to regulate diverse biological processes. miRNAs function as part of the miRNA-induced silencing complex (miRISC) that contains an Argonaute and GW182 proteins at its core. The miRISC typically recognizes and binds partially complementary sequences in the 3' untranslated region (3'UTR) of target messenger RNAs (mRNAs). This interaction initiates a series of gene-silencing mechanisms, which include mRNA translation repression, deadenylation, decapping and decay. The relative contribution of each of these events is still a matter of debate and the series of molecular interactions uniting these events remains to be clarified, and likely depends on cellular context.

To elucidate the mechanism of action by miRNAs, I developed and optimized a cell-free system derived from *C. elegans* embryos that faithfully recapitulates miRNA-mediated translation repression. Using this system, I determined that embryonic miRISC directs the rapid deadenylation of both artificial and natural 3'UTR targets. I also demonstrate a requirement for functional cooperativity between embryonic miRISCs within 3'UTRs in promoting miRNA-mediated deadenylation and silencing. Among the key players in the miRNA pathway, GW182 (AIN-1 and AIN-2 in *C. elegans*) and the multi-subunit CCR4-NOT deadenylase complex effect silencing through their activities and interactions with downstream effector proteins. To resolve the temporal order of events leading up to target silencing, proteomic analyses of AIN-1 and of the scaffolding subunit of the CCR4-NOT complex, NTL-1, were performed. This revealed an extensive interactions network linking the miRNA silencing machinery to P body and germ granule components, including the intrinsically disordered protein MEG-2. Using genetic assays, I identified a role for MEG-1 and MEG-2 for the function of an embryonic miRNA (*lsy-6*).

Using the developed cell-free system, I demonstrate the concerted assemblies of the scanning miRISC to mRNA targets, followed by the CCR4-NOT complex recruitment and nucleation of a microenvironment for consolidating gene silencing. These findings support a continuum of dynamic and specialized miRISC-protein complexes on target mRNAs for gene silencing, and highlight the importance of cellular and developmental contexts.

Collectively, these integrative studies refine our current understanding of the mechanism of gene silencing by miRNAs.

Résumé

Les microARNs (miARNs) sont de courts ARNs non-codants (~22 nts) qui contrôlent l'expression génique au niveau post-transcriptionel dans divers processus biologiques. Ces ARNs régulateurs font partis d'un complexe ribonucléoprotéique de répression induit par les miARNs (miRISCs), qui contiennent en leur centre les protéines Argonautes et GW182. En général, le miRISC cible l'expression des gènes par une hybridation imparfaite avec la région non-codante en 3' (3'UTR) de l'ARN messager (ARNm) ciblé. Cette interaction démarre une série de mécanismes de répression, qui incluent la répression traductionnelle des ARNm, la déadenylation, le décoiffage et la dégradation de l'ARNm ciblé. La contribution de chaque évènement est encore un sujet de débat et la série d'interactions moléculaires qui unit ces évènements demeure incomprise, et dépend possiblement du contexte cellulaire.

Pour élucider le mécanisme d'action des miARNs, j'ai dévelopé et optimisé un système acellulaire à partir d'embryons de *C. elegans* qui récapitule la répression des ARNm par le biais de miARNs. En utilisant ce système, j'ai déterminé que le miRISC embryonique dirige la déadénylation de 3'UTR artificiels et naturels ciblés par les miRNAs. Je démontre aussi qu'une coopérativité fonctionnelle est requise entre les miRISCs embryoniques sur les 3'UTRs pour promouvoir la déadénylation et répression des ARNm. Parmi les joueurs essentiels aux miARNs, GW182 (AIN-1 et AIN-2 chez les *C. elegans*) et le complexe de déadénylase CCR4-NOT effectue la répression à travers leur activités et interactions avec les effecteurs protéiques en aval. Pour résoudre l'ordre des évènements menant à la répression des ARNm cibles, les analyses protéomiques sur AIN-1 et le sous-unité d'échafaudage de la déadenylase NTL-1, sont effectués. Nos résultats révèlent un réseau vaste et qui lie la machinerie des miARNs aux composants de « P bodies » et granules germinaux, incluant la protéine intrinsèquement désordonnée MEG-2.

Par études génétiques, j'ai identifié un rôle pour MEG-1 et MEG-2 dans la fonction de répression d'un miARN embryonique (*lsy-6*). En utilisant le système *in vitro* de *C. elegans*, je démontre l'assemblage d'un miRISC qui balaie l'ARNm, suivi par le recrutement du complexe CCR4-NOT sur l'ARNm ciblé et par la nucléation d'un microenvironnement pour consolider la répression. Ces résultats soutiennent l'existence d'un continuum de complexes dynamiques et spécialisés de miRISC sur les mARNs ciblés pour leur répression.

Collectivement, ces études empiriques par des approches intégratives améliorent notre compréhension actuelle du mode d'action biochimique des miARNs.

Acknowledgments

There are many people whom I must acknowledge for helping me along my PhD journey.

- To my supervisor Dr. Thomas Duchaine, I am sincerely grateful for your mentorship and your encouragement all these years. Thank you for fostering my growth as a scientist, and for the opportunities to be creative and put my artistic skills to work.
- To my thesis committee members: Dr. Maxime Bouchard, Dr. Jean-Claude Labbé, Dr. Christian Rocheleau, and Dr. Monique Zetka, thank you for your support and guidance throughout my doctoral training.
- I thank all the past and present members of the Duchaine lab with whom I have worked with over the years. Caroline Thivierge and Ahilya Sawh, thank you for the fond memories over the years, and sharing the privilege of being the pioneers of the Duchaine lab. To my benchmates Vinay Mayya and ever-so cooperative Mathieu Flamand, thank you for the friendship and support during my highs and lows, the countless scientific discussions, and lightening up life with laughter over entertaining stories, pranks, and even nonsense.
- I am sincerely grateful to Dr. Nahum Sonenberg and current (Clément Chapat) and former members (Géraldine Mathonnet and Marc Fabian) of the Sonenberg lab: thank you for your mentorship, fruitful discussions and collaborations.
- To friends from neighbouring labs, in particular Don Walkinshaw and Soroush Tahmasebi: thank you for making the late nights at the lab during my early grad student life more enjoyable; Richa Sharma, Julianna Blagih, Emma Vincent, Aida Ramdzan, and Simran Kaur – thank you for being wonderful friends.

- To my dear friends outside of the lab, near and far – your friendship and encouragement are invaluable. Thank you for being someone I can count on for a good time, and for understanding when I couldn't make myself available.
- Thesis writing ranks among the most challenging things I have had to do as a grad student. In addition to some of the people I have acknowledged above, another core group of people have rendered the task of thesis writing during my final months of PhD much more bearable. Chers Philippe, Mackie, Alexis, Marc, les deux Charles, Cass, Roxanne, Katheryn, Arianne, Elizabeth, François, Simone et Victor – je tiens à vous remercier pour votre encouragement et accueil chaleureux chaque jour, et de me fournir la meilleure ambiance pour la rédaction de ma thèse.
- I am grateful for the funding I have received from the Canadian Institutes of Health Research, McGill Faculty of Medicine, and the Goodman Cancer Research Centre for supporting my research and trips to conferences. I have had a number of opportunities to travel during my doctoral training and meet other researchers passionate about science. To the wonderful scientists and fellow students I have met abroad, you have made each trip very special and memorable.
- Finally, to my family, especially Mom, Dad, my brother Edwin, and Gramma, for their endless love and support, and for believing me in me every step of the way. I dedicate this thesis to you.

Preface

In compliance with the Guidelines concerning Thesis Preparation of the Faculty of Graduate and Postdoctoral Studies of McGill University, I have chosen to write a manuscript-based thesis composed of two published research articles, and one manuscript in preparation. This thesis is organized into five chapters:

Chapter 1: literature review;

Chapter 2: content was published in

Wu E & Duchaine TF. Cell-free microRNA-mediated translation repression in Caenorhabditis elegans. (**2011**). *Methods in Molecular Biology*. 725: 219-232.

Figure 2-1 (flow chart for the extract preparation) was included in my Master's thesis to present a cell-free extract capable of recapitulating translation. The content presented in this chapter was compiled following the completion of the manuscript included in Chapter 3. Although Chapter 2 was published later, I have chosen to present the *C. elegans* cell-free system earlier, because i) it was my first goal to develop a system that faithfully recapitulates miRNA-mediated silencing and ii) it served as an invaluable tool throughout my thesis work, and from which novel assays were developed. This chapter (and publication) is cited in Chapters 3 and 4 to explain the extract preparation for all the cell-free assays used in each chapter.

Chapter 3: content was published in

Wu E, Thivierge C, Flamand M, Mathonnet G, Vashisht AA, Wohlschlegel J, Fabian MR, Sonenberg N & Duchaine TF (**2010**). *Molecular Cell* 40(4): 558-570.

Two-thirds of the work covered in this chapter was completed during my Master's. A modified version of my Master's thesis was submitted to *Molecular Cell* at the start of my PhD, which contained the following figures:

Figure 3-1, Figure 3-2ABC, Figure 3-3ABD and a less detailed time course for Figure 3-3E, Figure 3-4, Figure 3-5D (except for 2xmiR-35 spaced reporter), Figure A1-3A, and Figure A1-5B (fewer 2'-*O*-Me controls).

To address the requests and comments from reviewers, additional work was carried out during my first year of PhD. This chapter includes the revised manuscript submitted for publication (including the aforementioned figures), and the following figures completed during my first year of PhD:

Figure 3-2DE, Figure 3-3CF and a detailed course for Figure 3-3E, Figure 3-5ABC and Figure 3-5D (2xmiR-35 spaced reporter), all the figures presented in Appendix 1 (except A1-3A and part of A1-5B), additional deadenylation assays were carried out to provide data quantification for the time of half-deadenylation presented in Figures 3-3, 3-5, A1-3, and A1-5;

Chapter 4: manuscript in preparation for *Nucleic Acids Research*.

Wu E, Vashisht AA, Chapat C, Flamand M, Cohen E, Sarov M, Tabach Y, Sonenberg N, Wohlschlegel J & Duchaine TF. A continuum of mRNP complexes in embryonic microRNA-mediated silencing.

The content presented in this chapter represents the bulk of my PhD work;

Chapter 5: General discussion.

Contribution of Authors

Chapter 2: I performed all experiments presented in the manuscript.

Chapter 3: I performed all the experiments presented in the manuscript, except:

Dr. Thomas Duchaine performed the original cap-poly(A) synergy for translation (Figure 3-2A). Caroline Thivierge performed the microRNA expression profiling by northern blots and qRT-PCR (Figure 3-3BCD, A1-1BD, A1-5A, A1-6), the 2'-*O*-Me pulldown experiments (Figure 3-3D, Table 1, Figure A1-2), and assisted with the cloning for the 1x-4xmiR-52 reporters. Mathieu Flamand performed the natural 3'UTR cloning, and the cloning and sequencing of the deadenylated *miR-35* targeted reporters (Figure 3-3D). Former members of Dr. Nahum Sonenberg's laboratory: Dr. Marc R. Fabian conducted the RT-PCR amplification of *miR-35* targeted reporters and Dr. Géraldine Mathonnet trained me on the deadenylation assays. Dr. Ajay Vashisht from Dr. James Wohlschlegel's laboratory carried out the MuDPIT analyses on the 2'-*O*-Me pulldown.

Chapter 4: I performed all the experiments presented in the manuscript, except:

Dr. Ajay Vashisht from Dr. James Wohlschlegel's laboratory carried out the MuDPIT on AIN-1 and NTL-1 IP samples. Dr. Clément Chapat from Dr. Nahum Sonenberg's laboratory suggested and performed the b-isox-mediated precipitation (Figure 4-5 and Figure A3-3). Mathieu Flamand from Dr. Thomas Duchaine's laboratory assisted with the NTL-1 and PAB-1/2 antibody production and with the data analysis from the MNase sensitivity assay (Figure 4-4) using R software. Dr. Emiliano Cohen from Dr. Yuval Tabach's laboratory conducted the computational assessment for siRNA and miRNA pathway proteins (Figure 4-1B and Tables A3-3 and A3-4).

Dr. Mihail Sarov generated the *ain-1::lap* and *ntl-1::lap C. elegans* strains used for immunoprecipitation, DRIP analysis and b-isox-mediated precipitation.

Table of Contents

List of Figures

List of Tables

List of Abbreviations

2'-*O*-Me	2'-*O*-methylated
A-cap	ApppG cap analog
AGO	Argonaute
AIN	ALG-1 interacting protein
ALG	Argonaute-like gene
ARCA	anti-reverse cap analog
ASE	asymmetric expression
ASEL/R	ASE left/right
ATP	adenosine triphosphate
A. thaliana	*Arabidopsis thaliana*
b-isox	biotinylated isoxazole
C	cytosine
CAF1	Ccr4p-associated factor 1
CCF-1	Ccr4-associated factor-1
CCR4	carbon catabolite repressor 4
cDNA	complementary DNA
C. elegans	*Caenorhabditis elegans*
CTP	cytosine triphosphate
DCAP	decapping
DDH	aspartate-aspartate-histidine
D. melanogaster	*Drosophila melanogaster*
DMSO	dimethyl sufoxide
DNA	deoxyribonucleic acid
ds	double-stranded
DTT	dithiothreitol
EDC	enhancer of decapping
EDTA	ethylenediaminetetraacetic acid
EGTA	glycoletherdiaminetetraacetic acid
eIF	eukaryotic initiation factor
FL	firefly luciferase
GFP	green fluorescent protein
GO	Gene Ontology
GTP	guanosine triphosphate
GW	glycine Tryptophan
HEK	human embryonic kidney
HEPES	4-(2-hydroxyethyl)-1-piperazineethanesulfonic acid
Hsa	*homo sapiens*
IP	immunoprecipitation
IPTG	isopropyl β-D-1-thiogalactopyranoside
kb	kilobase
KCl	potassium chloride
kDa	kilodalton
KOAc	potassium acetate
KOH	potassium hydroxide
LAP	localization and affinity purification
lin	lineage
let	lethal
L1-L4	larval stage 1 to 4
LNA	locked nucleic acid
LSM	Sm-like
lsy	laterally symmetric
m^7G	7-methylguanosine triphosphate
mCi	milli Curie
MEG	maternal effect germline
$Mg(OAc)_2$	magnesium acetate
miRISC	miRNA-induced silencing complex
miRNA	microRNA
MNase	micrococcal nuclease
mRNA	messenger RNA
MuDPIT	multi-dimensional protein identification technology
mut	mutant
NaCl	sodium chloride
NGM	nematode growth media
ncRNA	non-coding RNA
ncRNA	non-coding RNA
NOT	negative on TATA
NTL	NOT-like
ORF	open reading frame
p(A)	poly(A)
PABP	poly(A)-binding protein
PAGE	polyacrylamide gel electrophoresis
PAN	poly(A) nuclease
PANL	PAN-like
P body	processing body
P granule	P lineage granule
PCR	polymerase chain reaction
piRNA	PIWI-interacting RNA
PIWI	P element induced wimpi testes
pre-miRNA	precursor miRNA
pri-miRNA	primary miRNA
PTGS	post-transcriptional gene silencing
qRT-PCR	quantitative real-time PCR
RISC	RNA-induced silencing complex
RL	renilla luciferase
RNA	ribonucleic acid
RNAi	RNA interference
RNase	ribonuclease
RNP	ribonucleoprotein
S. cerevisiae	*Saccharomyces cerevisiae*
S. pombe	*Schizosaccharomyces pombe*
SDS	sodium dodecyl sulfate
siRNA	small intering RNA
S2 cells	Schneider 2 cells
SSC	saline sodium citrate
ssRNA	single stranded RNA
T	thymine
$t_{d1/2}$	time of half-deadenylation
TNRC6	trinucleotide repeat containing 6
TRBP	TAR RNA-binding protein64
U	uracil
UTP	uracil triphosphate
UTR	untranslated region
wt	wild-type

Original Contribution to Knowledge

Chapter 2:

Cell-free microRNA-mediated translation repression in *Caenorhabditis elegans*

- Development and optimization of a cell-free system (derived from *C. elegans* embryos) that faithfully recapitulates miRNA-mediated translation repression.
- miRNA-mediated silencing system is based on abundant and phenocritical endogenous miRNAs.

Chapter 3:

Pervasive and Cooperative Deadenylation of 3'UTRs by Embryonic MicroRNA Families

- In *C. elegans* embryos, the abundantly expressed maternal *miR-35-42* and zygotic *miR-51-56* families program a large fraction of the miRISC.
- Cell-free *C. elegans* recapitulation of miRNA-mediated repression on natural 3′UTRs.
- Maternal and zygotic miRISC mediate deadenylation, but not decay of targets *in vitro*.
- miRNA families cooperate to trigger the deadenylation of targets.

Chapter 4:

A continuum of mRNP complexes in embryonic microRNA-mediated silencing

- Establishment of a proteomic network of germ granule and P body components with the miRISC core component AIN-1 and the CCR4-NOT scaffold protein, NTL-1.
- Biochemical isolation of distinct miRISCs: "scanning" vs "effector" miRISC.
- miRISC interaction secludes target mRNAs to nuclease-refractory mRNPs.
- miRISC core components are strongly enriched in selective precipitation of mRNPs.
- The inherently disordered *meg-2* gene is required for embryonic miRNA function.

Chapter 1: Introduction

1. Introduction

The central dogma of molecular biology, established by Francis Crick in 1958, states that the genetic information encoded by DNA is transcribed into messenger RNA (mRNA), which in turn serves as a template for protein synthesis (Crick, 1958). In recent decades, the expansion of non-protein-coding RNAs (ncRNAs) repertoire has unraveled new layers of gene regulation and broadened the roles of RNA from its previously recognized ones. Complete sequencing of the euchromatic region of the human genome by the Encyclopedia of DNA Elements (ENCODE) Project revealed less than 2% of the genome is composed of protein-coding genes, despite the fact that more than 90% of the genome is transcribed, indicating non-coding transcripts make up 98% of the transcriptional output (Amaral et al., 2008; Consortium et al., 2007; Mattick, 2003). These ncRNAs, generally referred to long or short depending on whether they are more or less than 300 nucleotides (nt) in length, have vastly expanded the functions of RNAs. For example, cloverleaf-structured transfer RNAs are fundamental components of the translation machinery that serve as adaptor molecules between mRNAs and amino acids during protein synthesis. In contrast, HOTAIR is a 2.2-kb ncRNA that resides in the *HOXC* locus and has a marked function in epigenetic silencing. It interacts with Polycomb Repressive Complex 2 to modify chromatin (through histone H3 lysine 27 trimethylation) *in trans* of the *HOXD* locus (Rinn et al., 2007). While certain long ncRNAs have specialized roles and others can be assigned to a class with a more global function, RNA research has provided an important new perspective on the role and impact of RNA in controlling gene expression.

Since their discovery in the early 1990s, small RNAs were also found to play an important role in gene regulation. These small RNAs, which include small interfering RNAs (siRNAs), PIWI-interacting RNAs (piRNAs), and microRNAs (miRNAs), associate with members of the Argonaute (AGO) protein family and guide them to their targets to reduce expression of target genes. Yet, these three classes of small RNAs differ in their biogenesis, size, AGO and other protein-interacting partners, mechanism of target regulation, and biological functions. Despite their differences, these three classes function in gene silencing pathways to control target expression and protect the genome from external (eg. viral infection) or internal (eg. transposons) threats (Ghildiyal and Zamore, 2009).

1.1 The origins of miRNAs

In the early 1960s, Sydney Brenner established the nematode, *Caenorhabditis elegans* (*C. elegans*), as a model organism. The ease of maintaining these nematodes and their rapid generation time, coupled to the simplicity of their anatomy and genetics would make *C. elegans* an ideal model to study fundamental mechanisms in embryonic and neuronal development (Brenner, 1974). By the early 1990s, the complete cell lineage of *C. elegans* had already been mapped by tracking the fate of every cell from fertilization through the four larval stages (L1 to L4) and adulthood in living animals (Deppe et al., 1978; Kimble and Hirsh, 1979; Sulston and Horvitz, 1977). Early forward genetic screens were also conducted to identify and characterize genes important for cell lineage (Chalfie et al., 1981; Horvitz and Sulston, 1980; Sulston and Horvitz, 1981). A number of mutants with temporal developmental defects were isolated, more specifically, altered cell lineage patterns and subsequent cell fates, such as skipping or reiteration of stage-specific events (Chalfie et al., 1981; Sulston and Horvitz, 1981). These defects were attributed to mutations in "heterochronic genes" that are important for controlling the proper timing of developmental events (Ambros and Horvitz, 1984; Chalfie et al., 1981). In the early 1990s, while characterizing the heterochronic gene, *lin-4*, the laboratories of Victor Ambros and Gary Ruvkun discovered *lin-4* does not encode a protein, but rather encodes a short 22-nt long RNA that was complementary to seven sites located in the 3'UTR of *lin-14* mRNA (Figure 1-1, Lee et al., 1993; Wightman et al., 1993). Transgenic animals expressing a reporter gene bearing *lin-4* complementary sites exhibited temporal down regulation, indicating a mechanism involving *lin-4* base pairing to *lin-14* 3'UTR (Wightman et al., 1993). Although it is unclear whether *lin-4* occupies all seven sites,

genetic mutants in which all potential *lin-4* miRNA binding sites were deleted result in increased levels of LIN-14 protein, which is abundantly expressed in wild-type late-staged embryos and L1 larvae, and are barely detectable in L2 and later stages (Ruvkun and Giusto, 1989; Wightman et al., 1993). Interestingly, *lin-14* mRNA levels appeared relatively constant throughout development, indicating *lin-14* is negatively regulated at the post-transcriptional level (Wightman et al., 1993). These findings marked the discovery of the first microRNA. In 2000, the Ruvkun laboratory identified another gene that yields a short temporal RNA, *let-7*, which negatively regulates the *lin-41* heterochronic gene by base-pairing to the complementary elements of the *lin-41* 3'UTR (Figure 1-1C, Reinhart et al., 2000). While *lin-4*/*lin-14* regulation is important for transition L1-to-L2 stage, *let-7* is expressed at later stages and controls L4-to-adult transition. In wild-type larvae, epidermal seam cells divide until after the L4 molt, at which point they terminally differentiate and fuse together to form an adult-specific longitudinal structure along the cuticle called the alae (Sulston and Horvitz, 1977). *let-7* mutants fail to execute the L4-to-adult transition and reiterate L4 larval stage. As a result, the alae fail to develop due to ongoing cell division and animals die by bursting through the vulva (Reinhart et al., 2000). This highly penetrant phenotype will later serve as a classical assessment for genes implicated in miRNA function through genetics (Ding et al., 2008; Grosshans et al., 2005; Lin et al., 2003; Parry et al., 2007). The Ruvkun group also showed that *let-7* gene is conserved across a wide range of animal species, including humans, indicating small temporal RNAs are not unique to *C. elegans* (Pasquinelli et al., 2000). Using cloning and bioinformatics techniques, a search for other short 21/22-nt RNAs by the groups of Victor Ambros, David Bartel and Thomas Tuschl revealed many

small RNAs in *C. elegans*, *Drosophila melanogaster* (*D. melanogaster*), and humans, expanding the existence of miRNAs from 2 to 86 (Lagos-Quintana et al., 2001; Lau et al., 2001; Lee and Ambros, 2001). Due to their role in developmental timing in *C. elegans* larvae, the small RNAs encoded by *lin-4* and *let-7* were originally termed as small temporal RNAs. With the discovery of abundant small RNAs in metazoans, this novel class of small RNAs was re-named "microRNAs" (Lagos-Quintana et al., 2001; Lau et al., 2001; Lee and Ambros, 2001). Currently, over 400 miRNAs in *C. elegans* are listed in the miRNA database (www.mirbase.org), whereas 2500 miRNAs are listed for humans.

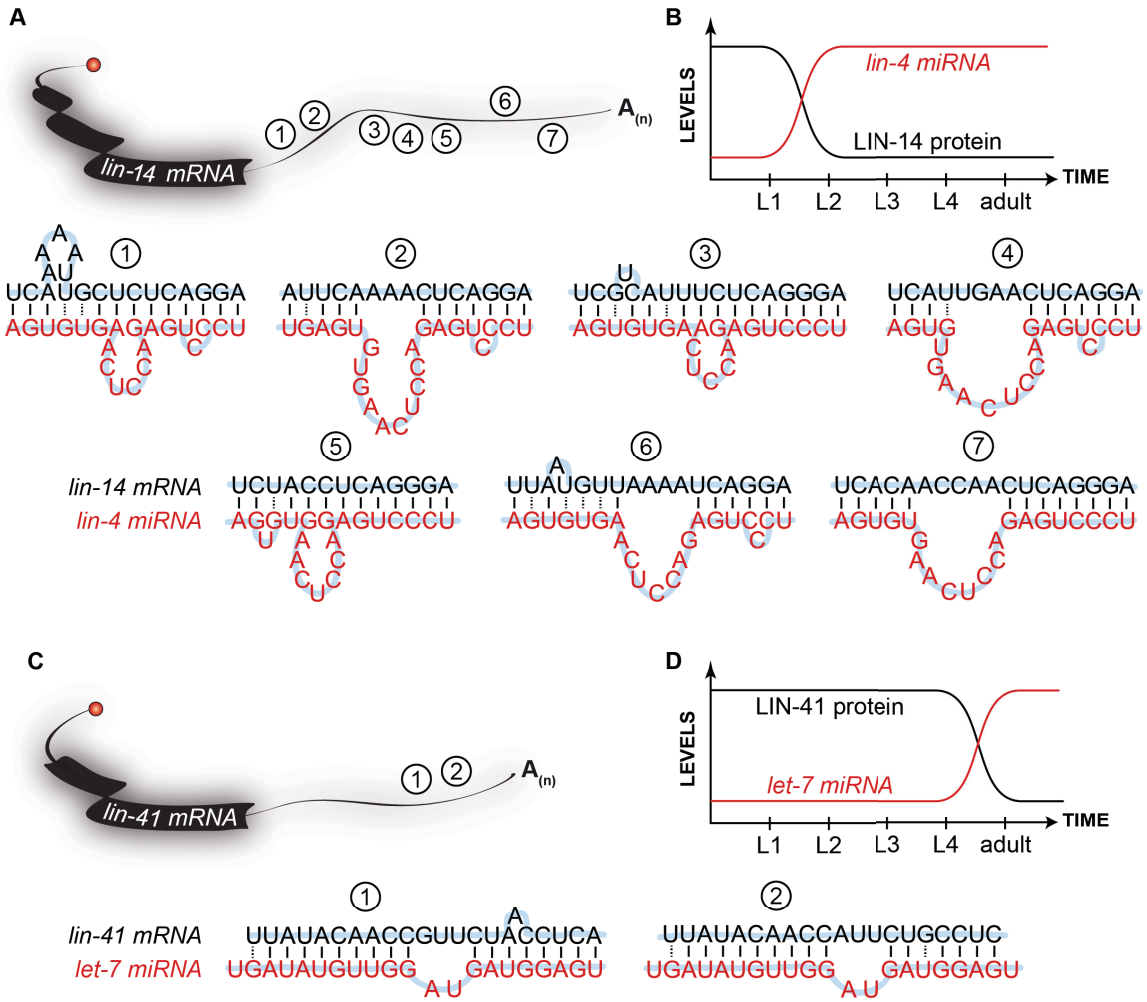

Figure 1-1: *lin-4* and *let-7* mediate developmental regulation via target mRNA binding

The founding members of the miRNA family, *let-7* and *lin-4*, were both discovered in a forward genetic screen for heterochronic mutants (Chalfie et al., 1981; Lee et al., 1993; Reinhart et al., 2000). (A) The 3'UTR of *lin-14* mRNA contains seven sites (numbered 1 to 7) that are complementary to *lin-4* (the predicted *lin-4:lin-14* RNA duplexes are shown as in Wightman et al., 1993). (B) *lin-14* is post-transcriptionally regulated by *lin-4*, and its protein levels are decreased at the end of the first larval stage by the expression of *lin-4*. Similarly, *lin-41* encodes a gene involved in developmental timing. (C) The 3'UTR of *lin-41* mRNA contains two *let-7* sites (predicted *let-7:lin-41* base-pairings are shown as in Reinhart et al., 2000). (D) While *lin-4*-mediated regulation of *lin-14* is essential for L1-to-L2 transition, post-transcriptional regulation of *lin-41* by *let-7* is important for the heterochronic switch from L4-to-adult.

1.2 Biological functions of miRNAs

The identification of hundreds of miRNAs in various organisms brought about questions on their biogenesis, mechanism of gene regulation, and impact on biology. Since their discovery in 1993, miRNAs have been found to play extensive roles beyond regulating developmental timing, including cell differentiation and proliferation, metabolism, pattern formation, and apoptosis (Bartel, 2004). More than 60% of the human genome is predicted to be under the regulation of miRNAs, leading to widespread changes in protein synthesis in response to global miRNA knockdown (Friedman et al., 2009; Selbach et al., 2008). Systematic analysis of miRNA mutants in *C. elegans* and *D. melanogaster* revealed that only specific miRNAs or miRNA families were required for normal development and viability (Alvarez-Saavedra and Horvitz, 2010; Brenner et al., 2010; Leaman et al., 2005; Miska et al., 2007). These studies suggest that while some miRNAs are critical for development or specific biological processes, most may act redundantly with other miRNAs or other gene products, in fine-tuning gene expression. Here, I present a few examples that highlight the diverse roles played by miRNAs.

1.2.1 Neuronal development

While *lin-4* and *let-7* miRNAs are known for their temporal roles in *C. elegans*, *lsy-6* highlights a miRNA involved in spatial patterning during neuronal development. *lsy-6* functions in the specification and differential gene expression of the left/right asymmetric fates of two chemoreceptor neurons that display an asymmetrical expression pattern in the nematode head, ASE left (ASEL) and ASE right (ASER) (Johnston and Hobert, 2003). The *lsy-6* miRNA is specifically expressed in ASEL but not ASER, and downregulates the expression of the transcription factor COG-1, by partially base-pairing to the 3'UTR of *cog-1* mRNA, thereby promoting ASEL fate. In animals lacking *lsy-6* miRNA expression, the ASEL neurons adopt the ASER fate due to failure to repress COG-1 (Johnston and Hobert, 2003). Introduction of a reporter transgene that labels the ASEL fate in a sensitized *lsy-6* mutant background has been extensively used to look at genetic interactions with the miRNA pathway (Hammell et al., 2009; Ren et al., 2016; Vasquez-Rifo et al., 2013; Zhang and Zhang, 2013; Zinovyeva et al., 2014). For instance, the *lsy-6(ot150)* allele harbors a C⟶T point mutation in the *cis*-regulatory element in the *lsy-6* promoter that leads to the reduction of *lsy-6* miRNA, but does not eliminate its function, resulting in a partially penetrant ASEL fate specification phenotype (Sarin et al., 2007). As such, the ASEL-fate defective phenotype can be assessed in progeny arising from genetic crosses between animals carrying a mutation in the gene of interest and the *lsy-6*-sensitized background. An enhancement in ASEL-fate defects is indicative of the requirement for the gene of interest for the function of *lsy-6* miRNA in determining ASEL fate during embryogenesis.

1.2.2 Apoptosis

Proper animal development involves a balance between cell proliferation and cell death. In an effort to study the biological functions of miRNAs during fly development, a collaborative study conducted a systematic analysis of miRNA mutants and examined their loss of function effects upon depleting or inhibiting embryonically expressed miRNAs in *D. melanogaster* early embryos using antisense oligoribonucleotides. More than 50% of these miRNAs gave visible and severe phenotypes when depleted (Leaman et al., 2005). Phenotypes include severe defects in pole cell formation, pattern formation and segmentation, as well as, excessive cell death and lack of cell differentiation, with embryos falling apart on touch at the end of embryogenesis (Leaman et al., 2005). The early onset of apoptosis during embryonic development can be explained in part by the loss of the abundantly expressed miRNA family, *miR-2/6/11/13/308*, that normally suppresses the pro-apoptotic genes *hid*, *grim*, *reaper*, and *sickle* by targeting their 3'UTRs and impinging on translation. These analyses extend on the previous studies that reported the role of other miRNAs, *bantam* and *miR-14*, in regulating cell survival during *D. melanogaster* post-embryonic development (Brennecke et al., 2003; Xu et al., 2003). Thus, miRNAs can target apoptosis with the aim to fine-tune the balance of growing and proliferating cells, and pursue proper animal development.

1.2.3 Maternal-to-zygotic transition (MZT)

While the aforementioned *let-7*, *lin-4*, and *lsy-6* miRNAs are examples of a single miRNA regulating specific mRNA targets, in 2006, Antonio Giraldez and members of the Schier laboratory published a study on the role of a single miRNA, *miR-430*, in early embryonic development of zebrafish (Giraldez et al., 2006). During the maternal-to-zygotic transition, the stage in which developmental control is transferred from maternally provided gene products to the zygotic genome, *miR-430* miRNA directs the destabilization of hundreds of maternal mRNAs containing *miR-430* binding sites in their 3'UTRs through poly(A) tail shortening, or deadenylation (a mechanism described later, section 1.7). Injection of processed *miR-430* rescued developmental defects observed in miRNA processing mutants, including defects in gastrulation, brain morphogenesis, and retinal development (Giraldez et al., 2005). Interestingly, the maternally contributed transcription factors, Nanog, Oct4, and SoxB1 are required to initiate the zygotic developmental program and for the activation *miR-430* expression (Lee et al., 2013).

In *Xenopus laevis (X. laevis)*, a similar phenomenon occurs at the mid-blastula transition (MBT), the stage when zygotic mRNA synthesis begins and cell cycle undergoes remodeling. During MBT, the frog ortholog of *miR-430, miR-427*, triggers the deadenylation of maternal mRNAs, including cyclin A1 and B2 (Lund et al., 2009). Injection of exogenous *miR-427* prior to the expression of endogenous mature *miR-427* triggered deadenylation of both endogenous targets and exogenous reporters, suggesting the timing of the appearance of *miR-427* is essential in activating poly(A) tail removal and subsequent decay of its targets. In flies, the *miR-309* cluster consists of eight miRNAs that are expressed in early zygotes, and function in a manner analogous to *miR-*

430 miRNA by activating the clearance of 138 maternal mRNAs shortly after the appearance of the miRNA cluster (Bushati et al., 2008). Thus, miRNAs play an essential role in remodeling the landscape of gene expression during early animal development in various species.

1.2.4 Cancer

One of the earliest evidence that linked miRNAs to cancer was provided by *let-7* studies. In addition to its discovered function in regulating developmental timing in *C. elegans*, the *let-7* miRNA can also function as a tumor suppressor (Johnson et al., 2005; Mayr et al., 2007; Takamizawa et al., 2004). *Ras* is an oncogene that is activated in many human cancers (Bos, 1989) and its 3'UTR contains multiple sites for *let-7* family members, or other miRNAs sharing the same core motif as *let-7* for targeting (including *miR-84*, features of miRNA:mRNA interactions are described in section 1.4). Both *let-7* and *miR-84* miRNAs negatively regulate *let-60/Ras* gene in hypodermal and vulval precursor cells, respectively (Johnson et al., 2005; Johnston and Hobert, 2003). It was observed that upon overexpression of *miR-84* miRNA, the multi-vulva phenotype was suppressed in activated *let-60/Ras* mutants (Johnson et al., 2005). When extended to mammalian studies, *let-7* directly controlled RAS expression through 3'UTR-mediated repression (Johnson et al., 2005). Closely resembling the suppressive phenotype triggered by over-expression of *let-7* family members in *C. elegans*, over-expression of *let-7* inhibited the growth of cancerous cells by inducing cell cycle arrest and cell death (Esquela-Kerscher et al., 2008; Johnson et al., 2007; Johnson et al., 2005).

To add support to *let-7*'s tumor suppressive properties, in tumor-initiating cells isolated from breast tissues of breast carcinoma patients (BT-IC), which are capable of self-renewal and can differentiate into multiple lineages, levels of *let-7* miRNAs are notably reduced but increased with differentiation (Yu et al., 2007). Upon enforcing *let-7* expression in differentiated BT-IC, or in an immune-deficient mouse injected with tumor cells as an *in vivo* model, proliferation and mammosphere formation were reduced in BT-

IC, and tumor growth was suppressed in mice, indicating loss of self-renewal and tumorigenicity in response to *let-7*. These findings firmly establish *let-7* as a tumor suppressor and point to a promising future for *let-7* and other potential miRNAs in small RNA-based therapeutics (Bussing et al., 2008).

Alterations in miRNA expression can also contribute to diseases. *miR-15* and *miR-16* loci are located at chromosome 13q14, a region frequently deleted in various cancer types, and both genes are deleted or downregulated in 68% of chronic lymphocytic leukemias (CCL) cases (Calin et al., 2002). These findings provided the first link between alterations of miRNA genes and mis-regulation of their expression with human disease. Further mapping of other miRNA genes revealed many of the known miRNA genes are located in chromosomal regions that are frequently altered, either deleted or amplified, in many types of cancers (Calin et al., 2004).

1.3 miRNA biogenesis

miRNAs are derived from the genome and are transcribed mostly by RNA polymerase II, which yields a long primary transcript (pri-miRNA) that is both 7-methylguanosine (m^7G)-capped and polyadenylated, and folds into hairpin structures (Figure 1-2, Lee et al., 2002; Lee et al., 2004). Pri-miRNAs then undergo stepwise processing by two RNase III endonucleases. First, Drosha and its cofactor, DGCR8 (also known as Pasha in *D. melanogaster* and PASH-1 in *C. elegans*), make up the Microprocessor complex, and cleave miRNA-encoding hairpin structures at ~11 bp away from the basal junction and ~23 bp away from the terminal loop, releasing a ~70-nt precursor (pre-miRNA) (Han et al., 2006; Zeng et al., 2005). Exportin 5 then exports the pre-miRNA into the cytoplasm (Gregory et al., 2004; Yi et al., 2003). Once in the cytoplasm, a second RNase III enzyme, Dicer, cleaves the hairpin stem loop of the pre-miRNA to liberate a ~22-nt miRNA:miRNA* duplex (also termed guide and passenger strands, respectively) (Bernstein et al., 2001; Grishok et al., 2001; Hutvagner et al., 2001; Ketting et al., 2001; Knight and Bass, 2001). The duplex possesses a 5' monophosphate end and a 2-nt 3' overhang, a feature of products from RNase III-type endonuclease cleavage reactions (Blaszczyk et al., 2001). One strand is then selected for incorporation into the miRNA-Induced Silencing Complex (miRISC), whose core components are the Argonaute (AGO) proteins and GW182. Once loaded into the RISC, miRNAs bound by AGO proteins are highly stable (Elkayam et al., 2012). The mature miRNA then guides the miRISC effector complex to the 3'UTRs of most targeted mRNAs (see next section for 3'UTR targeting), thereby inhibiting translation and directing deadenylation and/or mRNA destabilization (further discussed in section 1.8.3).

Alternative biogenesis pathways are also used for certain miRNAs, in which specific processing steps are bypassed. For example, *miR-451* is a miRNA conserved in vertebrates and is important for erythrocyte maturation (Pase et al., 2009). The biogenesis of *miR-451* is Dicer-independent, due to structural differences in *pre-miR-451* that renders it incompatible with the recognition and processing by Dicer (Cheloufi et al., 2010; Cifuentes et al., 2010). *Pre-miR-451* is loaded directly into RISC following Drosha cleavage and requires the endonucleolytic cleavage (or "slicing" activity) of Ago2 to further process it into the mature miRNA. Mirtrons are introns that yield pre-miRNA-like hairpins when spliced and debranched, bypassing processing by the Microprocessor. These pre-miRNA-hairpin mimics then enter the canonical miRNA pathway during nuclear export for Dicer processing, followed by incorporation into the RISC (Okamura et al., 2007; Ruby et al., 2007). Clearly, mirtrons are less abundant, and *pre-miR-451* remains the only Dicer-independent miRNA identified to date, but it would not be surprising to discover other anomalous miRNAs recognized and processed in a manner deviating from the canonical pathway. To add another level of complexity, the 5' and 3' ends of miRNAs are sometimes heterogeneous (Azuma-Mukai et al., 2008; Seitz et al., 2008). miRNA processing can also be affected by modifying the 3' ends, either by trimming or non-templated nucleotide(s) addition (Han et al., 2011; Heo et al., 2012; Liu et al., 2011). For example, pre-let-7 is subjected to oligo-uridylation by the terminal nucleotidyl transferase, TUT4/ZCCHC11, in mouse embryonic stem cells (Hagan et al., 2009; Heo et al., 2009). Such modification prevents efficient substrate recognition and processing by Dicer, likely due to masking of the 2-nt 3'overhang on the uridylated pre-let-7. The presence of a U-tail also serves as a decay signal, triggering degradation of

oligo-uridylated pre-let-7 by the exonuclease DIS3L2 (Chang et al., 2013). Mature miRNAs can also be subjected to RNA tailing. Adenylation of maternal miRNAs is conserved in fly, sea urchin, and mouse, and is carried out by the non-canonical poly(A) polymerase, Wispy, in *D. melanogaster* (Lee et al., 2014). In *wispy* mutants, the overall miRNA population are reduced in adenylation, yet upregulated in abundance, suggesting A-tailing by Wispy may contribute to the clearance of maternal miRNAs during early embryonic development (Lee et al., 2014).

Thus, such events could help to offer tighter control in regulating processing and in fine-tuning specific miRNA expression, and in shaping the miRNA and mRNA target landscape during early development.

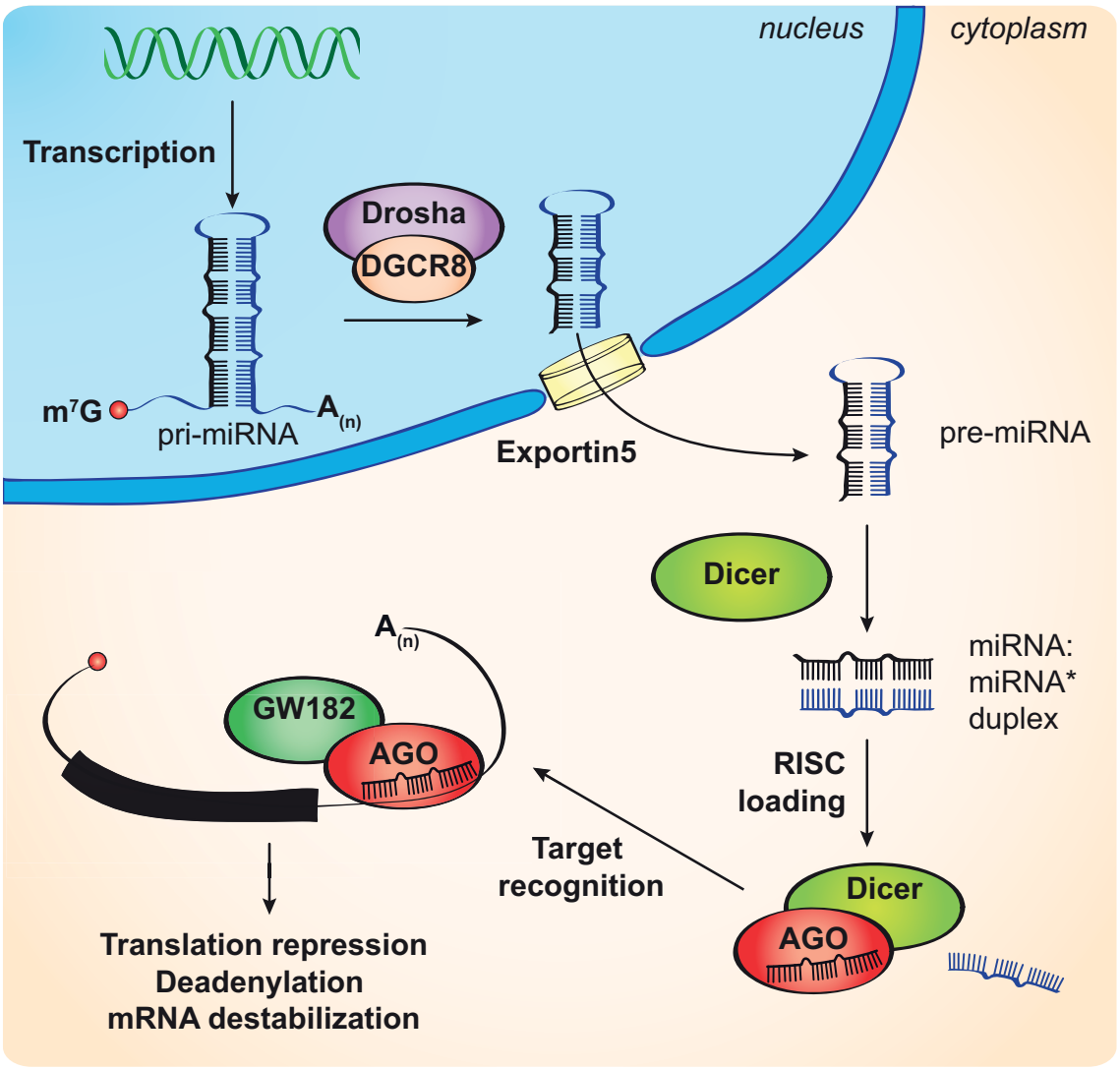

Figure 1-2: miRNA biogenesis and mechanism of action

The majority of miRNAs follows the canonical biogenesis pathway, in which pri-miRNA transcripts undergo step-wise processing by the Microprocessor (Drosha/DGCR8) and Dicer. Alternative pathways have also emerged for the biogenesis of certain miRNAs: *miR-451* (Dicer-independent processing) and mirtrons (bypasses cleavage by Drosha). Only one strand of the miRNA:miRNA* duplex is preferentially loaded into the RNA-induced silencing complex (RISC), which subsequently recognizes target sites and acts on its target by translation repression, deadenylation, and/or mRNA destabilization.

1.4 Principles of target recognition

In plants, miRNAs bind to their target mRNAs with perfect complementarity. This interaction results in mRNA cleavage through the ribonuclease activity of AGOs (Baumberger and Baulcombe, 2005). In metazoans, miRNAs bind only partially to their target mRNAs. Only a small portion of the miRNA, the "seed", binds to its target mRNA with perfect complementarity through Watson-Crick base-pairing (Figure 1-2A). The seed is situated at positions 2-7 from the 5' end of miRNAs and is the main determinant for target recognition (Brennecke et al., 2005; Doench and Sharp, 2004). miRNAs that share identical seeds at positions 2-7 are grouped into "families", and family members can possess widely divergent 3' sequences. For instance, in *C. elegans*, the *miR-35-42* family is comprised of eight miRNA members, of which *miR-35-41* originate from a single polycistronic transcript, while *miR-42* is encoded by another locus (Alvarez-Saavedra and Horvitz, 2010; Lau et al., 2001). In humans, 62 sets of miRNA families have been identified (Lewis et al., 2005).

The thermodynamic stability, or free energy (ΔG), of the seed:mRNA pair is another element that determines the effectiveness of translation repression (Doench and Sharp, 2004). However, as free energy cannot be measured directly in the biological context of miRNA:mRNA interaction, free energy values obtained from algorithms are often used as an overall indicator of miRNA:mRNA pairing stability when predicting miRNA targets (Bartel, 2009).

Using genome-wide computational studies or experimental approaches of artificial reporters in transfection experiments, several groups have investigated the

characteristics of miRNA binding sites and target recognition for efficient silencing. A summary of these findings and target site features is presented in Figure 1-3.

Although the seed is a major determinant in specifying miRNA targeting, a number of features can significantly influence target recognition and silencing (refer to Figure 1-3). Non-canonical seed-target interactions have also been explored, such as those exhibited by *lin-4:lin-14* and *let-7:lin-41* (see Figure 1-1), in which the seed is not fully base-paired to the binding site, yet still maintains extensive complementarity with the target site (Hafner et al., 2010; Loeb et al., 2012; Reinhart et al., 2000; Wightman et al., 1993). Based on transcriptome analyses, non-canonical interactions are associated with less potent effect on mRNA regulation when compared to canonical sites (Hafner et al., 2010; Khorshid et al., 2013; Loeb et al., 2012). Another feature to consider is that multiple sites for the same miRNA or for miRNAs from different families can be present on a single mRNA target. These sites could allow for either a single miRNA to fine-tune the activity of a single gene, or combinatorial regulation by multiple factors simultaneously, adding complexity to gene regulation (Doench and Sharp, 2004).

While miRNAs typically target the 3'UTR, targeting of the 5'UTR and open reading frame (ORF) have also been reported through reporter assays (Kloosterman et al., 2004; Lytle et al., 2007). Genome-wide studies also support these findings, however, 3'UTR targeting by miRNAs is more frequent and efficient (Easow et al., 2007; Grimson et al., 2007; Lim et al., 2005). One explanation for this is that 5'UTRs and ORFs are frequently accessed and occupied by translation factors and ribosomes, making these regions 1) difficult to selectively maintain sequences and motifs for miRNAs and other

RNA-interacting factors, and 2) unfavorable for the miRNA machinery to access (Bartel, 2009).

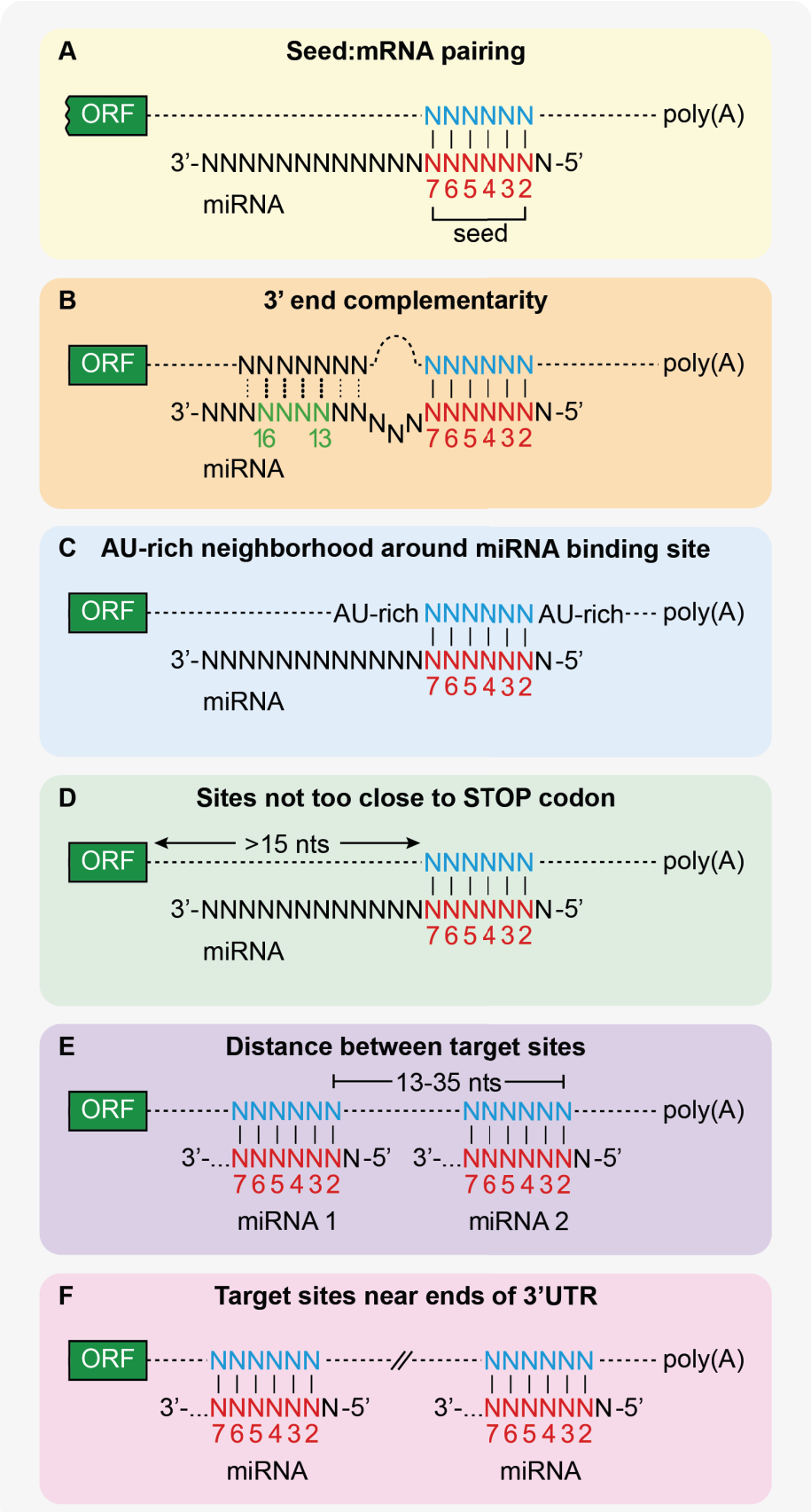
A
Seed:mRNA pairing
ORF
NNNNNN
poly(A)
3'-NNNNNNNNNNNNNNNNNNN-5'
765432
miRNA
seed
B
3' end complementarity
ORF
NNNNNNN
NNNNNN
poly(A)
3'-NNNNNNNNNNNNNNNNNNN-5'
16
13
765432
miRNA
C
AU-rich neighborhood around miRNA binding site
ORF
AU-rich
NNNNNN
AU-rich
poly(A)
3'-NNNNNNNNNNNNNNNNNNN-5'
765432
miRNA
D
Sites not too close to STOP codon
ORF
>15 nts
NNNNNN
poly(A)
3'-NNNNNNNNNNNNNNNNNNN-5'
765432
miRNA
E
Distance between target sites
13-35 nts
ORF
NNNNNN
NNNNNN
poly(A)
3'-...NNNNNNN-5'
765432
miRNA 1
3'-...NNNNNNN-5'
765432
miRNA 2
F
Target sites near ends of 3'UTR
ORF
NNNNNN
NNNNNN
poly(A)
3'-...NNNNNNN-5'
765432
miRNA
3'-...NNNNNNN-5'
765432
miRNA

Figure 1-3: Determinants and features for target recognition and potent silencing

(A) The "seed" (nucleotides 2-7 from the 5' end of the miRNA) is the major determinant for target recognition. This region base pairs perfectly to sites mostly in the 3'UTR of their target mRNAs (denoted in blue). (B) In plants, the miRNA:mRNA interaction is achieved through perfect base-pairing. In metazoans, analysis of miRNA and mRNAs indicate extensive 3' pairing is rarely utilized (Grimson et al., 2007). However, increasing 3' complementarity (especially at position 13-16 of the miRNA, denoted in light green) can help stabilize miRNA:mRNA interaction, particularly when the seed:mRNA base pairing is not perfect (when G:U base pair is tolerated). (C) miRNA binding sites are commonly found in regions enriched in A/U nucleotides. An AU-rich context may render the region more flexible and allow the 3'UTR to be more accessible to the miRNA machinery. (D) Genome-wide analysis also revealed effective miRNA binding sites were preferentially located at least 15 nucleotides from the STOP codon. Providing a minimal distance from the end of the open reading frame may structurally be beneficial, and prevent polysomes from clashing with the miRISC, facilitating miRISC accessibility to the binding site. (E) The distance between target sites can also dictate the efficacy and cooperativity between adjacent miRISC (shown in Chapter 3, Wu et al., 2010). Using artificial reporters bearing two miRNA sites that varied in distance, it was demonstrated that a distance of approximately 13-35 nts between two seeds is needed to achieve optimal translation repression (Saetrom et al., 2007) and deadenylation (shown in Wu et al., 2010). Proximity of miRISCs could allow for greater regulatory effect, as well as, greater sensitivity to small changes in miRNA levels (Grimson et al., 2007). (F) Effective target sites are preferentially located near the ends of the 3'UTR, rather than in the middle. Having the miRNA sites in proximity to the poly(A) tail may facilitate target recognition and allow closer interactions between the miRISC and other downstream effectors, such as the deadenylase machinery. (Figure inspired by the following reviews: Bartel, 2009; Filipowicz et al., 2008).

1.5 The Argonautes

The Argonautes (AGO) are the core components of RNA-mediated gene silencing pathways. The first AGO protein was discovered in *Arabidopsis thaliana* (*A. thaliana*) from a forward genetic screen for genes involved in plant development (Bohmert et al., 1998). Mutants of *ago1* were described as having tubular shaped leaves that resembled the tentacles of an argonaute squid, giving the protein family its name (Bohmert et al., 1998; Mallory and Vaucheret, 2010). Following the initial discovery of AGO1 in plants, related AGO proteins were discovered in various organisms with critical roles in small RNA-guided gene silencing (Catalanotto et al., 2000; Fagard et al., 2000; Tabara et al., 1999). These studies highlighted the conservation of the Argonautes and the significance of RNA silencing by small RNAs in different species.

Based on amino acid sequence similarity, the family of AGO proteins can be classified into two clades: Ago and Piwi (Tolia and Joshua-Tor, 2007). Members of the Ago clades are similar to the *A. thaliana* AGO1, and mainly interact with miRNAs or siRNAs for post-transcriptional gene silencing (Hutvagner and Simard, 2008; Peters and Meister, 2007). Proteins in the Piwi clade resemble the *D. melanogaster* PIWI, the founding member of the clade that is encoded by the *piwi* (*P*-element *i*nduced *wi*mpy testis) gene, which is required for the maintenance and renewal of germline stem cells (Cox et al., 1998; Lin and Spradling, 1997). PIWI proteins are expressed in germ cells, and associate with a distinct class of small RNAs, known as Piwi-interacting RNAs (piRNAs), for the silencing of transposable elements, the development of germ cells, and self-renewal of germline stem cells (Aravin et al., 2001; Cox et al., 1998; Cox et al., 2000).

The family of AGO proteins is highly conserved, yet the number of AGO proteins encoded between species varies enormously. In yeast, *Schizosaccharomyces pombe* (*S. pombe*) expresses a single AGO gene, while *Saccharomyces cerevisiae* (*S. cerevisiae*) lacks any recognizable homologs of Argonautes and other RNAi machinery (Drinnenberg et al., 2009; Verdel et al., 2004). *D. melanogaster* encodes five AGO members: two from the AGO clade and three from the PIWI clade (Williams and Rubin, 2002). In humans and mice, eight AGO protein members have been identified, four in each AGO and PIWI group (Sasaki et al., 2003; Williams and Rubin, 2002). In contrast, *C. elegans* expresses 27 Argonautes: four PIWI and 25 AGO, further expanding the AGO classification to a third clade, known as the WAGO (Worm-specific AGO) clade. WAGO proteins associate with a specific class of 22-nt siRNAs that target germline and somatic-expressed transcripts implicated in promoting proper organization of chromosomes during mitosis (Claycomb et al., 2009; Gu et al., 2009; Yigit et al., 2006). More recently, a subset of the WAGOs was found to be required for silencing of nuclear localized RNAs, or nuclear RNAi (Ashe et al., 2012; Buckley et al., 2012; Guang et al., 2008). These silencing events are necessary for the epigenetic inheritance of RNAi to the progeny and over many generations (Ashe et al., 2012; Buckley et al., 2012; Burkhart et al., 2011; Burton et al., 2011; Gu et al., 2012; Guang et al., 2010; Luteijn et al., 2012; Shirayama et al., 2012).

AGO proteins are composed of three conserved domains: the PAZ, MID, and PIWI. The PAZ (Piwi Argonaute Zwille) domain serves as a docking site for small RNAs, or more specifically, the characteristic 2-nucleotide 3' overhang of small RNAs generated by Dicer (Lingel et al., 2004; Ma et al., 2004). The MID domain serves to anchor the 5' phosphate and terminal nucleotide of the small RNA. The PIWI domain has

a structure similar to RNase H, which cuts the RNA strand of an RNA-DNA hybrid. Some Ago proteins possess a conserved aspartate-aspartate-histidine (DDH) motif in their PIWI domain, a feature also observed in RNase H domains, and which provide the PIWI domain "slicing" activity, or the ability to cleave the target RNA bound to the small RNA (Liu et al., 2004; Rivas et al., 2005). A recent crystal structure of an Argonaute from the yeast *Klyveromyces polysporus* revealed a fourth glutamate residue that constitutes the active site for the catalytic tetrad for slicing Agos (Nakanishi et al., 2012).

As mentioned earlier, *C. elegans* genome encodes 27 AGOs, with several AGOs that evolved with specialized roles in specific RNAi pathways. For instance, the miRNA pathway employs the AGOs, ALG-1 and ALG-2 (Argonaute-Like Gene-1 and -2), for both the maturation of miRNAs and silencing of target mRNAs. In the absence of *alg-1* and *alg-2*, pre-miRNAs accumulate and the population of the corresponding mature 20-25 nt RNAs are reduced, (Grishok et al., 2001; Yigit et al., 2006). Furthermore, *lin-4* and *let-7* miRNAs fail to negatively regulate their targets in *alg-1/2* mutants (Grishok et al., 2001). While the conserved DDH slicing residues are typically found in AGOs implicated in gene silencing pathways mediated by siRNAs, both ALG-1 and ALG-2 also contain the motif. This catalytic triad was reported to coordinate cleavage of a miRNA duplex mimicking Dicer-cleaved pre-miRNA, at least through incubation of the duplex with recombinant ALG-1/2 proteins, and is required for formation of miRISC and, as one would expect, for *C. elegans* viability (Bouasker and Simard, 2012).

Although ALG-1 and ALG-2 share 80% and 88% identity at the amino acid level, respectively, individual knockouts of the two genes differ in their phenotypes. Mutant alleles of *alg-1* are viable, yet display marked developmental abnormalities that render

the animal unhealthy, including bursting vulva (a phenotype due to mis-regulation of *let-7* validated targets, *lin-41* and the *C. elegans* hunchback homolog, *hbl-1*, Grosshans et al., 2005), and temporal mis-specification of seam cell lineages, a phenotype reminiscent of the miRNA loss of function mutants seen in *let-7* and *lin-4* mutants (Grishok et al., 2001; Lee et al., 1993; Reinhart et al., 2000; Tops et al., 2006). However, *alg-2* mutants appear wild type, with subtle defects in fertility and development (Grishok et al., 2001; Tops et al., 2006). In contrast, *alg-1/2* double mutants are lethal, with embryos arresting during the morphogenetic process of elongation (Grishok et al., 2001; Vasquez-Rifo et al., 2012). The observed embryonic lethality phenotype is only observed in double mutants, indicating that the two genes may act in a redundant manner (Grishok et al., 2001; Tops et al., 2006).

While *C. elegans* ALG-1 and ALG-2 evolved to specialize in miRNA-specific activities, *D. melanogaster* produces two AGOs (Ago1 and Ago2) and uses a sorting mechanism, in which the structure of the small RNA duplex dictates which AGO it will be loaded into (Tomari et al., 2007). Ago1 is preferentially loaded with RNA duplexes bearing mismatches or bulges, while duplexes with high degrees of complementarity are sorted into Ago2 (Ghildiyal and Zamore, 2009). Although most miRNAs are loaded into Ago1, a subset of miRNAs are also sorted into Ago2, and both Agos are capable of inducing translation repression, yet only Ago1 can direct mRNA target deadenylation (Iwasaki et al., 2009).

Thus, the Argonaute proteins constitute the fundamental players in various RNA silencing pathways in different organisms. These events require direct binding to small

RNAs, and interaction with other proteins to coordinate the downstream events for gene silencing.

1.6 The GW182 proteins

GW182 is another key component of the miRISC, and bridges AGO proteins to downstream effector complexes, such as the CCR4-NOT deadenylase complex (Jonas and Izaurralde, 2015). GW182 is a protein named after the presence of multiple glycine-tryptophan (GW) repeats and its molecular mass of 182 kDa in human cells. The protein was originally identified using sera from a patient with motor and sensory neuropathy and was found to localize to distinct cytoplasmic foci termed GW bodies (Eystathioy et al., 2002). Subsequent immunostaining studies revealed these GW bodies co-localized with human LSm RNA-binding proteins and Dcp1 decapping proteins, providing the first insights that GW182 may be involved in mRNA metabolism. These GW bodies were thought to be analogous to the processing bodies (P bodies) (Eystathioy et al., 2003).

In mammalians, three paralogs of GW182 have been identified: TNRC6A (trinucleotide repeat containing 6A), TNRC6B, and TNRC6C. In *D. melanogaster*, the ortholog is referred to as Gawky (Schneider et al., 2006), or simply as GW182. The human and fly GW182 members share a similar domain organization. GW182 is composed of two structural domains: an ubiquitin-associated (UBA) domain and an RNA recognition motif (RRM) located in an intrinsically disordered region in the C-terminus, and separated by a glutamine (Q)-rich region (Figure 1-3). It is unclear what the roles of the UBA domain and RRM are, as mutations in these regions do not significantly impact the known functions of GW182. The RRM exhibits no detectable RNA-binding affinity *in vitro* and lacks RNA-binding features (Chekulaeva et al., 2011; Eulalio et al., 2009c; Eulalio et al., 2009d; Lazzaretti et al., 2009; Zipprich et al., 2009). Characterization of the GW182 protein in miRNA-mediated silencing further revealed two functional domains.

The N-terminal Ago-binding domain of GW182, as the name indicates, interacts with mammalian AGO MID/PIWI domain and *D. melanogaster* Ago1, with GW repeats mediating the interactions (Behm-Ansmant et al., 2006; Lian et al., 2009; Takimoto et al., 2009; Till et al., 2007). The silencing domain (SD), which is located near the C-terminus and includes the poly(A)-binding protein (PABP)-interacting motif 2 (PAM2) and C-terminal RNA recognition motif (RRM), is a major effector domain that mediates translation repression and deadenylation of mRNA targets (Eulalio et al., 2009a; Fabian et al., 2009; Huntzinger et al., 2010; Jinek et al., 2010; Kozlov et al., 2010; Lazzaretti et al., 2009; Zekri et al., 2009; Zipprich et al., 2009). Further analysis of the silencing domain revealed distinct sites for GW182 interaction with the CCR4-NOT and PAN2/3 deadenylase complexes. At the extremities of the silencing domain are two CCR4-NOT interacting motifs (CIMs), while PAN2/3 interacts with the PAM2 motif likely through PABP (Braun et al., 2011; Chekulaeva et al., 2011; Fabian et al., 2011).

Two distant homologs of GW182 exist in *C. elegans*, and are referred to as the *A*lg-1 *In*teracting proteins (AIN-1 and AIN-2, or AIN-1/2), namely for their ability to immunoprecipitate with the Argonaute ALG-1 (Ding et al., 2005; Zhang et al., 2007). AIN-1 and AIN-2 share 70% similarity at the amino acid level. The proteins are smaller in size and share little recognizable domain architecture in common with that of mammalian and fly GW182 family members. They lack a defined Q-rich region, UBA domain, RRM, and contain fewer GW repeats (Ding and Han, 2007; Tritschler et al., 2010). Although their structures differ substantially from that of human and fly GW182, at least superficially, they clearly play a critical function in the miRNA pathway (Eulalio et al., 2007a).

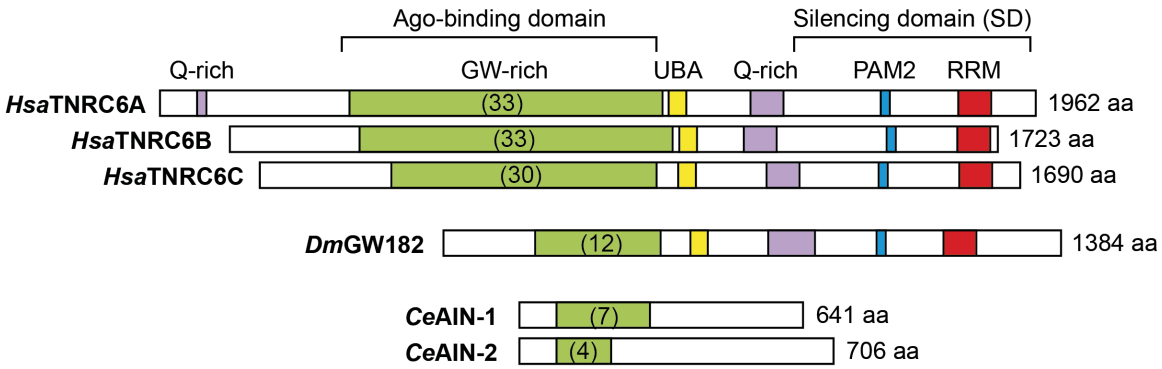

Figure 1-4: Schematic diagram of GW182 family members

Schematic representation of human (*Hsa*), *D. melanogaster* (*Dm*), and *C. elegans* (*Ce*) GW182 proteins. The human and fly GW182 members share a similar domain organization, while *C. elegans* AIN-1 and AIN-2 differ substantially yet function similarly in the miRNA pathway. GW repeats are present throughout the protein, but are enriched in the N-terminal region, which binds Ago proteins (denoted in green, with the number of GW repeats within the Ago-binding region indicated in parentheses). It is important to note that the interaction between *C. elegans* AIN-1/2 with Ago was only studied and demonstrated in *D. melanogaster* S2 cells (Kuzuoglu-Ozturk et al., 2012). GW182 proteins also contain an ubiquitin-associated (UBA) domain (in yellow), a glutamine (Q)-rich region (in purple), and an RNA recognition motif (RRM, in red). The silencing domain includes the RRM and a poly(A)-binding protein (PABP)-interacting motif 2 (PAM2, in blue). (Figure adapted from Tritschler et al., 2010).

Originally, *ain-1* was identified in a genetic screen for mutants that suppress the multi-vulva phenotype caused by the mutations in the *lin-31* gene that encodes for the forkhead transcription factor in the RTK-RAS-MAPK pathway (Ding et al., 2005; Miller et al., 1993). *ain-1* loss of function (lf) mutants do not exhibit drastic defects in vulval or post-embryonic lineages (possibly because of *ain-1/2* functional redundancy), yet the heterochronic pathway was affected, specifically the seam cell differentiation program. In 40% of *ain-1* mutants, significant gaps in the alae were observed and seam cell fusion was retarded. This phenotype was enhanced and observed in a greater population in *ain-1; ain-2* double mutants, suggesting functional redundancy between *ain-1* and *ain-2* (Zhang et al., 2007). These defects in seam cell development are similar to the phenotypes observed in animals with mutations in *lin-4* and *let-7* targets, *lin-14*, *lin-28*, and *hbl-1* (Abrahante et al., 2003; Lin et al., 2003; Moss et al., 1997; Wightman et al., 1993). In addition, *ain-1(lf)* mutants could suppress the precocious alae phenotype in *lin-14(RNAi)* and *hbl-1(RNAi)* animals, indicating *ain-1* regulates developmental timing of seam cell lineages through regulation of the heterochronic genes.

While there appears to be a lack of similarity in domain architecture of AIN-1/2 and its fly and mammalian orthologs (Figure 1-4), both AIN-1 and AIN-2 are also key components of the *C. elegans* miRISC, as revealed by their interactions with ALG-1/2 and the enrichment of associated miRNAs by immunoprecipitation, although AIN-1 and AIN-2 are in distinct complexes (Ding et al., 2005; Zhang et al., 2007). The essential role of GW182 family members in miRNA-mediated silencing is also conserved. In human cultured cells and *D. melanogaster* Schneider 2 (S2) cells, depletion of individual TNRC6 paralogs or *Dm*GW182 abrogates translation repression, deadenylation, and

mRNA decay (Behm-Ansmant et al., 2006; Eulalio et al., 2009a; Eulalio et al., 2008; Jakymiw et al., 2005; Liu et al., 2005a; Meister et al., 2005; Rehwinkel et al., 2005; Zipprich et al., 2009). These results also indicate AGO proteins on their own cannot carry out efficient silencing (Eulalio et al., 2009a; Eulalio et al., 2008). Tethering GW182 proteins to mRNA reporters represses translation and causes mRNA degradation independently of AGO proteins, indicating that AGO proteins recruit GW182 to mRNA targets and GW182 has an essential role in the effector steps of silencing (Behm-Ansmant et al., 2006; Chekulaeva et al., 2011; Eulalio et al., 2009a; Lazzaretti et al., 2009; Zipprich et al., 2009). In mammalian and fly cultured cells, depletion of GW182 abrogates miRNA-mediated silencing (Behm-Ansmant et al., 2006; Eulalio et al., 2008; Liu et al., 2005a; Meister et al., 2005). Similar findings were observed in *C. elegans* (Ding and Grosshans, 2009). Polysome profile analyses and qRT-PCR of several mRNA targets conducted in *ain-1; ain-2* mutants showed translation repression and degradation of target mRNAs were impaired, supporting the notion that these distant homologs of GW182 in *C. elegans* are essential for miRNA-mediated repression (Ding and Grosshans, 2009). Similar to its counterparts in humans and flies, AIN-1 was also shown to co-localize with the P body component DCAP-2, the *C. elegans* ortholog of Dcp2 decapping protein, suggesting *C. elegans* GW182 members are likely to function with miRISC by localizing to P bodies to facilitate target translation repression and degradation of mRNA targets (Ding et al., 2005) (further discussed in section 1.9).

Although GW182 plays an undisputed role in miRNA-mediated silencing, alternative Ago-mediated silencing mechanisms that act independently of GW182 have been described in *D. melanogaster* S2 cells (Fukaya et al., 2014; Fukaya and Tomari,

2012; Wu et al., 2013). In one study, altering the physiological conditions for cell growth revealed the induction of two new forms of miRISC devoid of GW182 (Wu et al., 2013). One complex was found to associate with polysomes and is thought to regulate translation at the elongation step, while the other form appeared to be a miRISC intermediate undergoing recycling (Wu et al., 2013). In another study, GW182 was required for the deadenylation step, yet translation repression was observed in the presence of an Ago1-RISC with or without GW182 (Fukaya and Tomari, 2012). The authors concluded that the silencing pathway employed by different Ago1-RISC could depend on context, such as cell type and cell conditions, RNA target, or availability of GW182 proteins (Fukaya et al., 2014; Fukaya and Tomari, 2012).

While GW182 plays a central role in gene silencing by miRNAs, it is unclear whether GW182 has a role outside the miRNA pathway. One study showed that disrupting GW182 foci by knocking down GW182 interfered with the silencing capabilities of an siRNA specific to another target, lamin-A/C (Jakymiw et al., 2005). This finding suggests a role for GW182 bodies in siRNA-mediated pathways, and it would be interesting to see if GW182 can effect silencing of targets independently of small RNAs.

1.7 The Deadenylases

In eukaryotes, poly(A) tails are added co-transcriptionally to the 3' end of transcripts and are required for mRNA export and stabilization. The poly(A) tail is coated with the poly(A)-binding protein (PABP), which promotes translational efficiency by forming a "closed loop" conformation with the m^7G cap at the 5' end of mRNAs (Gallie, 1991; Jacobson and Favreau, 1983; Palatnik et al., 1984). These two structures are bridged by the eukaryotic initiation factor 4G (eIF4G) and are key determinants in enhancing translation initiation and protecting transcripts from exonucleases (Gorgoni and Gray, 2004). As such, modulating the poly(A) tail length is a tightly regulated process important for the control of gene expression. Deadenylases catalyze the shortening of poly(A) tails and are key players in mRNA turnover and gene expression. An overview of the deadenylases and deadenylation-coupled decay is provided in this section, while the implications of deadenylation in miRNA-mediated silencing is discussed in the following section (section 1.8.4).

1.7.1 Diversity of deadenylases

In metazoans, deadenylases are diverse and can be classified into two groups, based on their nuclease domains (Table 1-1). The DEDD nucleases are named after the four invariant aspartic acid (D) and glutamic acid (E) residues dispersed between three exonuclease motifs that are necessary for catalytic activity (Goldstrohm and Wickens, 2008; Zuo and Deutscher, 2001). DEDD-type nucleases include the Ccr4-associated factor 1 (CAF1), the poly(A) ribonuclease (PARN), and the poly(A) nuclease 2 (PAN2). The exonuclease-endonuclease-phosphatase (EEP) superfamily, which includes CCR4 and Nocturnin, is characterized by conserved glutamic acid (E) and histidine (H) residues

in their nuclease domains (Goldstrohm and Wickens, 2008). Orthologous family members and their impact on the biology of the animal are presented in Table 1-1.

Loss or disruption of specific deadenylases can result in extreme phenotypes that vary between organisms: in yeast, none of the deadenylases are essential for viability, while loss of *C. elegans ccf-1* or *Drosophila* Pop2 result in embryonic lethality, and sterility is observed in *ccr-4* mutants in both organisms (Molin and Puisieux, 2005; Morris et al., 2005; Nousch et al., 2013; Temme et al., 2010; Tucker et al., 2001). Mutation or depletion of other deadenylases, such as Pan2 or PARN, results in reduced fertility only at elevated temperature in *C. elegans*, and a weak effect on poly(A) tail removal (Lee et al., 2012; Nousch et al., 2013). These observations indicate that while certain deadenylases may play a predominant role in specific biological processes, other deadenylases could function redundantly with paralogs or be compensated by other decay pathways (Goldstrohm and Wickens, 2008). Such diversity could also allow for spatial and temporal regulation that depend on cellular context, target mRNAs location, or expression pattern of the deadenylases (Garneau et al., 2007).

Sc	*Ce*	*Dm*	*Hsa, Mm*	Description	Function	Mutation or depletion effects
DEDD-type nucleases						
Pop2	CCF-1	POP2	CAF1/ CNOT7	*Ccr4-associated factor 1*; CCR4-NOT complex component	Deadenylation; translation repression; transcription regulation	Sterility, embryonic and larval lethality (*Ce*); sterility in *Cnot7* knockout mice (*Mm*)
(Berthet et al., 2004; Goldstrohm and Wickens, 2008; Molin and Puisieux, 2005; Nakamura et al., 2004)						
Pan2	PANL-2	PAN2	PAN2	*Poly(A) nuclease* (PAN) complex	Initial phase of poly(A) tail shortening	Reduced fertility at elevated temperatures (*Ce*); weak reduction in rate of mRNA deadenylation (*Sc*)
(Boeck et al., 1996; Goldstrohm and Wickens, 2008; Nousch et al., 2013; Uchida et al., 2004)						
	PARN-1		PARN	*Poly(A)-specific ribonuclease*; Adenosine-specific 3'→5' exonuclease	Deadenylation; active in nonsense-mediated mRNA decay	Stabilization of subsets of transcripts containing premature nonsense codon or involved in specific cellular activities (*Hsa*, *Mm*); reduced fertility (*Ce*)
(Godwin et al., 2013; Lee et al., 2012; Lejeune et al., 2003; Nousch et al., 2013)						
EEP-type nucleases						
Ccr4	CCR-4	CNOT6	CNOT6/ CCR4a	*Carbon catabolite repression 4*; CCR4-NOT complex component	Deadenylation; translation repression; transcription regulation	Cell cycle defects (*Dm*, *Sc*); smaller brood size (*Ce*)
			CNOT6L /CCR4b		Deadenylation	Reduced cell proliferation and cell survival (*Hsa*)
(Denis and Chen, 2003; Mittal et al., 2011; Morris et al., 2005; Nousch et al., 2013)						
		NOC	NOC/ CCR4l	*Nocturnin*; CCR4 family member; circadian deadenylase	Deadenylation of metabolic genes under circadian control	Metabolic phenotypes in *Noc* knockout mice fed with a high-fat diet (*Mm*)
(Douris et al., 2011; Green and Besharse, 1996)						
Ngl1	ANGL-1	ANGEL1	ANGEL1 /CCR4e	*Angel*; CCR4 family member	Angel proteins are thought to function as deadenylases based on sequence similarity to CCR4 family members, however deadenylase activity has not been detected	
Ngl3						
Ngl2		ANGEL2	ANGEL2 /CCR4d		Inhibits cell proliferation and cell cycle arrest in G1 phase	Promotes cell growth and cell cycle progression (*Hsa*)
(Godwin et al., 2013; Goldstrohm and Wickens, 2008; Temme et al., 2010; Yi et al., 2012)						

Table 1-1: Table of eukaryotic deadenylases

Sc, *Saccharomyces cerevisiae*; *Ce*, *Caenorhabditis elegans*; *Dm*, *Drosophila melanogaster*; *Hsa*, *Homo sapiens*; *Mm*, *Mus musculus*. (Table adapted from Goldstrohm and Wickens, 2008).

The CCR4-NOT and PAN2/3 complexes are the most characterized deadenylases, due to their prominent roles in mRNA regulation. PAN2/3 is a heterodimeric complex comprised of PAN2 and its cofactor, PAN3. PAN2/3 is recruited to the poly(A) tail by PABP, which also stimulates its deadenylase activity (Boeck et al., 1996; Brown et al., 1996; Uchida et al., 2004). Genetic studies in yeast and nematodes reveal that loss of PAN2 and PAN3 has no obvious or only a mild effect on the biology of the organism (Boeck et al., 1996; Nousch et al., 2013). *panl-2* and *panl-3* mutants display reduced fertility at elevated temperatures, suggesting the PANL-2/3 complex is important for germline function under stress conditions (Nousch et al., 2013). mRNAs isolated from *panl-2* or *panl-3* mutants revealed only mild changes in the poly(A) tail length, whereas mRNAs isolated from *ccf-1*, *ccr-4*, and *ntl-1* mutants displayed long poly(A) tails, suggesting that the CCR4-NOT complex constitute the main deadenylase activity in mRNA regulation (Bonisch et al., 2007; Nousch et al., 2013; Tucker et al., 2001). In mammals, PAN2/3 is thought to carry out the initial shortening of the poly(A) tail by trimming typical 200 nt-long tails to a length of approximately 80 nts (Yamashita et al., 2005). Subsequently, a second deadenylase complex, the CCR4-NOT complex, trims the remainder of the poly(A) tail (Yamashita et al., 2005).

The CCR4-NOT complex was first discovered in *S. cerevisiae* where, curiously, many of its subunits were involved in the negative regulation of RNA polymerase II-directed transcription and linked to non-fermentative processes and cell-cycle regulation and progression (Collart and Struhl, 1993, 1994). These genes lacked a canonical TATA box in their promoters, resulting in the inheritance of the "NOT (Negative On TATA-less)" gene nomenclature (Liu et al., 1998). The yeast Ccr4 and Caf1/Pop2 subunits

provide the catalytic deadenylase activity for the complex (Daugeron et al., 2001; Denis, 1984; Denis and Malvar, 1990; Tucker et al., 2001). In yeast, the complex exists in two forms of 1.2 and 2 MDa that is built around a core of 7 subunits: the two deadenylases, Ccr4 and Caf1p/Pop2, and the NOT subunits (NOT1-5) (Chen et al., 2001; Liu et al., 1998). NOT1 makes up the bulk of the deadenylase complex, with a molecular mass of approximately 250 kDa, and serves as the central scaffold to which other subunits are associated to directly or indirectly. The overall architecture of the complex and the core subunits are evolutionarily conserved (Liu et al., 1998; Nousch et al., 2013; Temme et al., 2010).

1.7.2 Deadenylation and mRNA turnover

In eukaryotes, modulation of the poly(A) tail length is a tightly regulated process and extensive deadenylation can trigger mRNA degradation (Garneau et al., 2007). Decay is believed to occur through two major pathways that are conserved in eukaryotes. Both decay pathways use exonucleases to remove the body of the transcript and decapping enzymes to metabolize the cap structure. However, the two processes employ distinct sets of enzymes and accessory proteins, and differ in their sequence of events (Figure 1-5).

In the 5'→3' decay pathway, deadenylation of transcripts is followed by the removal of the m^7G cap structure on mRNAs, an irreversible decapping step that involves hydrolysis of the cap by the Dcp1/2 complex, releasing m^7GDP and a mono-phosphorylated mRNA (Lykke-Andersen, 2002; van Dijk et al., 2002; Wang et al., 2002). It is suggested that the interaction between Dcp1 and Dcp2 is weak, and requires binding partners, such as the WD40 motif-containing EDC4 scaffold protein, to bridge or

stabilize their interaction (Fenger-Gron et al., 2005; Jonas and Izaurralde, 2013; Yu et al., 2005). A set of accessory proteins is required for efficient decapping, including the heptameric complex of Sm-like (Lsm) proteins, the Enhancer of decapping (Edc) proteins, Pat1, and the DEAD-box RNA helicase, DDX6 (Table 1-2). The decapping step is an irreversible process in that it prevents additional loading of ribosomes and re-synthesis of new polypeptides, thus preventing the reuse of the transcript. Once decapped, the exposed 5' end of the mRNA is then digested by the 5'→3' exonuclease, Xrn1 (Decker and Parker, 1993; Hsu and Stevens, 1993). Although the pathway was first described in *S. cerevisiae*, many of the components are conserved and active in mammalians and nematodes (Cohen et al., 2005; Couttet et al., 1997; Lall et al., 2005; Wang et al., 2002).

Alternatively, the 3'→5' pathway involves degradation of the mRNA body that is carried out by the exosome, a complex composed of 10 to 12 subunits of 3'→5' exoribonucleases with similar homology, and RNA helicases (Anderson and Parker, 1998; Garneau et al., 2007; Mukherjee et al., 2002; Wang and Kiledjian, 2001). The remaining cap structure is turned over by the scavenger decapping enzyme, DcpS (Liu et al., 2002).

Sc	*Ce*	*Dm*	*Hsa*	**Description / Cellular functions**
Decapping factors				
Dcp1p	DCAP-1	DCP1	Dcp1	Partner of Dcp2/DCAP-2
Dcp2p	DCAP-2	DCP2	Dcp2	Decapping enzyme
(Behm-Ansmant et al., 2006; Cougot et al., 2004; Ingelfinger et al., 2002; Lall et al., 2005; Sheth and Parker, 2003; Squirrell et al., 2006; van Dijk et al., 2002)				
DcpS	DCS-1	DcpS	DcpS	Scavenger decapping enzyme
(Lall et al., 2005; Liu et al., 2002; Wang and Kiledjian, 2001)				
Lsm1-7	LSM-1-7	LSM1-7	Lsm1-7	Heptameric complex, decapping activator, Sm domain
(Cougot et al., 2004; Gallo et al., 2008; He and Parker, 2001; Ingelfinger et al., 2002; Tharun et al., 2000; Tharun and Parker, 2001)				
Pat1p	PATR-1	HPat	Patl1	Decapping activator
(Boag et al., 2008; Gallo et al., 2008; Ozgur et al., 2010; Sheth and Parker, 2003)				
Edc3p	EDC-3	EDC3	Edc3	Enhancer of decapping (Edc) proteins;
	EDC-4	EDC4/ Ge-1	Edc4/ Ge-1	WD repeats in Edc4
(Fenger-Gron et al., 2005; Kshirsagar and Parker, 2004; Sheth and Parker, 2003; Yu et al., 2005)				
Dhh1p	CGH-1	Me31B	DDX6/ RCK/p54	DEAD-box RNA helicase Decapping activator
(Boag et al., 2008; Coller et al., 2001; Cougot et al., 2004; Fenger-Gron et al., 2005; Navarro et al., 2001; Sheth and Parker, 2003)				
Decay factor				
Xrn1p	XRN-1	XRN1	Xrn1	5'→3' exonuclease, degrades decapped 5' monophosphate RNA
(Decker and Parker, 1993; Hsu and Stevens, 1993; Ingelfinger et al., 2002; Lall et al., 2005; Sheth and Parker, 2003)				
Exosome complex				Complex of 3'→5' exonucleases
(Gallo et al., 2008; Mitchell et al., 1997; Sheth and Parker, 2003; van Hoof et al., 2000)				
Deadenylases				
Ccr4p	CCR-4	CCR4	CNOT6	CCR4-NOT complex
Pop2p	CCF-1	POP2	CNOT7	
(Andrei et al., 2005; Cougot et al., 2004; Gallo et al., 2008; Sheth and Parker, 2003; Temme et al., 2004)				
Pan2	PANL-2	PAN2	PAN2	PAN2/3 complex
(Boeck et al., 1996; Brown et al., 1996; Zheng et al., 2008)				

Table 1-2: Machinery implicated in mRNA turnover

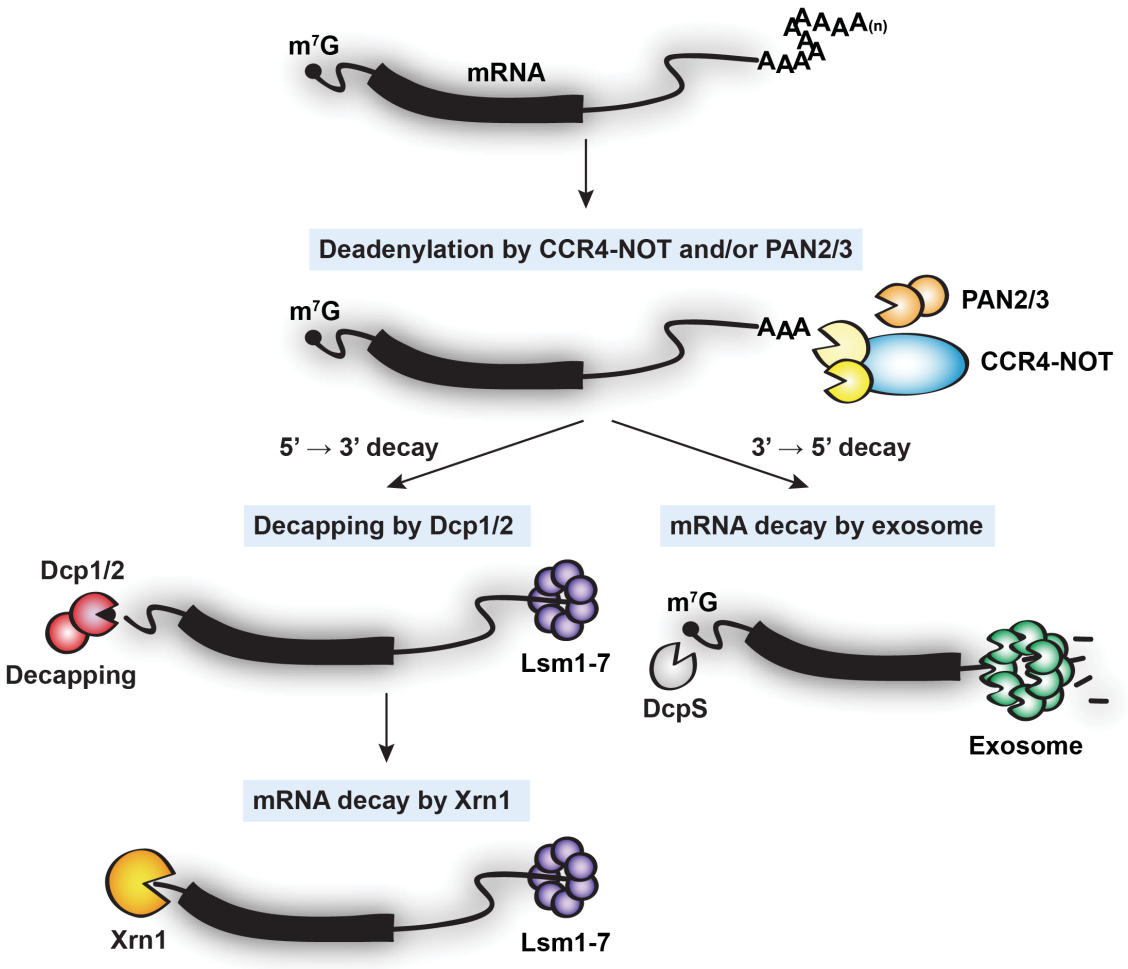

Figure 1-5: mRNA decay pathways

In eukaryotes, the two mRNA decay pathways are initiated by shortening of the poly(A) tail by the CCR4-NOT and/or PAN2/3 deadenylase complexes. Deadenylated mRNAs can be degraded via the 5'→3' decay pathway, or in a 3'→5' manner. The two pathways differ in the order of cap metabolism and mRNA body removal, and the use of distinct sets of enzymes and accessory proteins for mRNA decay.

1.8 The mechanisms of miRNA-mediated silencing

In plants, miRNAs exhibit a high degree of complementarity to their mRNA targets and direct cleavage of the targets within the region of complementarity, in a manner similar to the slicing endonuclease activity by the Argonautes in gene silencing by siRNAs (Llave et al., 2002; Tang et al., 2003). The resulting fragments are then degraded by the 5'→3' exoribonuclease, XRN4, and the exosome (Branscheid et al., 2015; Ibrahim et al., 2006; Shen and Goodman, 2004; Souret et al., 2004). While few miRNAs in animals exhibit extensive complementarity with their targets and direct Argonaute-catalyzed mRNA cleavage, imperfect base pairing is much more common (Davis et al., 2005; Karginov et al., 2010; Yekta et al., 2004).

In the past decade, much progress has been made in elucidating the mechanism for mRNA target regulation by miRNAs. Three distinct models were proposed over the years: repression at the level of translation initiation, repression at the translation elongation step, and target deadenylation and decay (Figure 1-6). A brief overview of the findings and emerging picture for the proposed models are discussed below.

1.8.1 Translation repression at the elongation step

The first insight into how miRNAs mediate silencing was provided by the miRNA pioneers, the groups led by Victor Ambros and Gary Ruvkun, when they noticed that *lin-14* mRNA levels remained constant while the protein levels decreased dramatically when *lin-4* miRNA was expressed (Olsen and Ambros, 1999; Wightman et al., 1993). Both *lin-4* and *lin-14* RNAs were also detected in polysomes, and the polysome profile remained unchanged with accumulation of *lin-4*, suggesting the regulation of *lin-14* does not involve the inaccessibility of the transcript to the translation machinery (Olsen and

Ambros, 1999). Subsequent analyses of *lin-4* regulation on *lin-28* also showed similar results, leading to the conclusion that miRNAs act at the level of translation without triggering decay (Moss et al., 1997; Seggerson et al., 2002).

Further studies using mammalian cells appeared to support this model. Upon treatment with puromycin, an inhibitor that causes premature polypeptide termination and polysome disassembly, a shift in sedimentation was observed for reporter mRNAs, indicating reporter RNAs were actively translated (Maroney et al., 2006; Nottrott et al., 2006). Furthermore, using a translational switch system in which luciferase reporter RNAs bearing iron-response elements that are bound by iron regulatory protein-1 (IRP-1) under conditions of iron deprivation, protein levels were undetectable and the reporter RNAs sedimented with non-translating RNP. Several explanations were proposed for these findings: i) miRNAs cause premature termination and polysome breakdown, causing ribosomes to disassemble into subunits or "drop off" (Maroney et al., 2006; Nottrott et al., 2006; Petersen et al., 2006), and ii) nascent polypeptide chains derived from target mRNAs are degraded co-translationally (Nottrott et al., 2006). While no proteases associated to the miRNA silencing machinery have been identified to date, these findings have been challenged by other studies that have provided more mechanistic insights into miRNAs acting at the translation initiation level, and through mRNA deadenylation and decay.

1.8.2 Translation initiation block

The first evidence that miRNAs inhibit translation initiation came from two studies conducted in HeLa cells (Humphreys et al., 2005; Pillai et al., 2005). A similar methodology was used by both groups, in which reporter RNAs were transcribed *in vitro*

and the translation activity mediated by *let-7* (Pillai et al., 2005) and a synthetic CXCR4 miRNA (Doench et al., 2003; Humphreys et al., 2005) was examined. These studies reported that translation was inhibited only when reporters bear the m^7G cap, while reporters substituted with an ApppG-cap or a viral internal ribosome entry site (IRES) were immune to repression, suggesting miRNAs target the early steps of initiation, likely the cap recognition step. It was also shown that these repressed mRNAs did not localize to polysomes, a finding that differs from the polysome gradient analysis conducted on *lin-4* targets in *C. elegans*, and subsequent mammalian studies. These studies were further supported by the use of cell-free systems derived from rabbit reticulocyte lysates, HEK293F cells overexpressing miRNA pathway components, mouse Krebs2 ascites, and *Drosophila* embryos (Mathonnet et al., 2007; Thermann and Hentze, 2007; Wakiyama et al., 2007; Wang et al., 2006). Each *in vitro* system provided additional mechanistic insights and supportive findings for translation repression at the initiation level. In mouse Krebs2 ascites cell extract, translation was restored upon addition of purified cap-binding complex, eIF4F, but not when other initiation factors were added, suggesting the miRNA machinery targeted the cap recognition step (Mathonnet et al., 2007). Furthermore, subjecting the extract to glycerol gradient centrifugation revealed a reduction in 80S ribosomal complex formation on target mRNAs, indicating miRNAs impinge on ribosomal 80S assembly (Mathonnet et al., 2007). Similarly, when the cell-free system derived from *Drosophila* embryo was analyzed on a sucrose gradient, the assembly of the ribosomal 80S complex was prevented on *miR-2* reporter RNAs, yet these targets sedimented in denser messenger ribonucleoprotein particles (mRNP) (Thermann and Hentze, 2007). Upon blocking *miR-2* with anti-*miR-2* oligonucleotides, these mRNPs

were no longer detectable and the formation of the 80S complex was restored. These data also support a model in which miRISC interferes with the 80S complex assembly, but can additionally induce the formation of non-polysomal mRNPs, or "pseudo-polysomes" (Thermann and Hentze, 2007). Finally, both extracts prepared from HEK293F and rabbit reticulocyte lysates revealed translation of miRNA reporter RNAs relied on both the presence of the 5' m^7G cap and 3' poly(A) tail, supporting the model of miRNA silencing machinery interfering with the synergistic interaction between the m^7G cap and poly(A) tail (Wakiyama et al., 2007; Wang et al., 2006).

Several studies have also proposed alternative mechanisms for repression at the translation initiation step, though these findings are not well supported and have been challenged by others. The translation initiation factor, eIF6, was reported to co-immunoprecipitate with the human Ago2-Dicer-TRBP complex (Chendrimada et al., 2007). Partial depletion of eIF6 impaired *let-7*-mediated regulation in human cells, as well as, *lin-4*-mediated regulation in *C. elegans* on *lin-14* and *lin-28* mRNA levels and the corresponding target proteins (Chendrimada et al., 2007). Subsequent studies conducted in *Drosophila* S2 cells revealed that eIF6 is not required for miRNA-mediated gene silencing, and genetic studies showed the precocious heterochronic phenotypes exhibited by the *C. elegans let-7* hypomorph were suppressed rather than enhanced upon depletion of eIF6 (Ding et al., 2008; Eulalio et al., 2008).

Ago2 was also proposed to be a key component in impinging on the cap recognition step or "closed loop" mRNA conformation. Bioinformatics analysis of the human Ago2 revealed a motif similar to the cap-binding domain of eIF4E. Mutations in the aromatic residues within this motif that are required for the cap binding of eIF4E

impaired the ability of Ago2 to repress translation when tethered to target mRNAs (Kiriakidou et al., 2007). These findings led to the conclusion that Ago2 can compete with eIF4E and directly bind to the m^7G cap of mRNAs, thus preventing eIF4E recruitment and translation initiation of mRNAs. However, one study later reported that the impairment in translation repression of reporters by Ago2 with the same mutations in the aromatic residues was due to its inability to interact with GW182 and miRNAs (Eulalio et al., 2008).

1.8.3 miRNA-mediated deadenylation and decay

In striking contrast to the initial findings in which *lin-14* mRNA levels appeared unaffected by *lin-4* regulation, a subsequent study by Amy Pasquinelli's group revealed that RNA levels of several *lin-4* and *let-7* targets were decreased in response to corresponding miRNA accumulation (Bagga et al., 2005). Along with findings by other groups, these unexpected results were the first to report miRNAs triggering mRNA destabilization in animals without requiring perfect miRNA:mRNA base-pairing (Bagga et al., 2005; Jing et al., 2005; Krutzfeldt et al., 2005; Lim et al., 2005; Wu and Belasco, 2005). Additional studies reported on Ago and GW182 co-localizing with Dcp1/2 decapping factors to P bodies (Behm-Ansmant et al., 2006; Liu et al., 2005b; Pillai et al., 2005; Sen and Blau, 2005). Based on these findings, a new model was proposed for miRNA-mediated silencing, in which miRNA-mediated silencing results in mRNA decapping and degradation, likely through the 5'→3' decay pathway.

Detailed examination of target mRNA integrity over time and of decay intermediates revealed that this miRNA-induced decay also involved changes in the poly(A) tail length (Behm-Ansmant et al., 2006; Giraldez et al., 2006; Wu et al., 2006).

Knockdown of the major deadenylases, CCR4, CAF1, and PAN2 in *Drosophila* cells resulted in stabilized miRNA targets (Behm-Ansmant et al., 2006), thus implicating the deadenylase complexes in miRNA-mediated deadenylation and decay. These findings were further supported by extensive studies that mapped the involved protein-protein interactions. A methodology based on the tethering of proteins of interest fused to a peptide lambda N (λN) or MS2 coat protein with a specific RNA-interacting sequence, boxB (Baron-Benhamou et al., 2004) or MS2 site (Fouts et al., 1997; Valegard et al., 1997), respectively, was also instrumental in deciphering the contributions of the miRISC components and interactors in silencing. These studies revealed that the miRISC and CCR4-NOT deadenylase complex are bridged by GW182/TNRC6 through the silencing domain of GW182/TNRC6 and the C-terminus of CNOT1 (Braun et al., 2011; Chekulaeva et al., 2011; Fabian et al., 2011). The silencing domain of GW182 can also associate with PAN2/3 through a separate motif, yet PAN2/3 appears to be dispensable for miRNA-mediated silencing (Braun et al., 2011; Chekulaeva et al., 2011; Fabian et al., 2011). Other studies have also reported other ways in which GW182 may recruit the deadenylase machinery. TNRC6C was also shown to directly contact the CNOT9 subunit of the CCR4-NOT complex, which itself is associated with CNOT1 (Chen et al., 2014; Mathys et al., 2014). The DEAD box RNA helicase, DDX6, interacts with the decapping stimulating factors, Pat1 and Edc3, and was also recently identified as a partner of the deadenylase complex by interacting with the MIF4G domain of CNOT1 (Chen et al., 2014; Mathys et al., 2014; Rouya et al., 2014).

Another factor implicated in miRISC function is PABP, known for its critical role in translation initiation and mRNA stability. PABP is detected in Ago

immunopurifications (Fabian et al., 2009; Hock et al., 2007; Landthaler et al., 2008). In a PABP-depleted mouse Krebs ascites extract, deadenylation of reporter RNAs was severely impaired, but restored upon addition of recombinant PABP (Fabian et al., 2009). The direct interaction between PABP and miRISC was mapped to the C-terminus of GW182 (Fabian et al., 2009; Huntzinger et al., 2010; Jinek et al., 2010; Zekri et al., 2009). While these findings demonstrate that PABP is required for miRNA-mediated deadenylation, it is not required for the miRISC or deadenylase complex association to targets (Fabian et al., 2009). In contrast, two studies have reported apparently conflicting findings in *Drosophila* cell-free extracts, one from S2 cells (Fukaya and Tomari, 2011) and the other derived from embryos (Moretti et al., 2012). In the former study, PABP was dispensable for both miRNA-mediated translation repression and deadenylation, while in the latter study, PABP was reported to facilitate miRISC association to mRNA targets, but is displaced prior to mRNA deadenylation.

More recently, studies on an eIF4E-binding protein and putative decay factor, 4E-transporter (4E-T), shed light on the mechanism of translation repression and mRNA decapping that could extend to targets under the regulation by miRNAs (Ferraiuolo et al., 2005; Nishimura et al., 2015; Waghray et al., 2015). Affinity purification of 4E-T and associated proteins showed that 4E-T interacts with mRNA decapping and decay factors, suggesting 4E-T is a key player in physically linking the decapping and decay machinery associated to the 3' end of transcripts to the m^7G cap for mRNA turnover via its interaction with eIF4E (Nishimura et al., 2015).

1.8.4 Translation repression versus mRNA deadenylation and decay

Ample evidence now point to two non-mutually exclusive mechanisms for miRNA-mediated silencing: translation repression at the initiation step, and mRNA deadenylation and decay. However, the temporal order of each event, their contributions toward silencing, whether and how they are coupled, and whether translation repression is strictly a consequence of mRNA deadenylation and decay, are questions that are still being tackled by a number of research groups.

In a non-steady state, the Giraldez group monitored the ribosome occupancy and mRNA levels for *miR-430* targets using ribosome profiling and RNAseq during early zebrafish development (Bazzini et al., 2012). Their findings showed an overall decrease in translation of *miR-430* targets without any detectable changes in the mRNA levels when *miR-430* is predominantly expressed at 4 hours post-fertilization (hpf), while mRNA destabilization is prominently observed later by 6 hpf, indicating translation repression occurs before mRNA decay (Bazzini et al., 2012). These findings are indicative of a developmental switch from translation repression to mRNA destabilization mechanisms by a specific miRNA. This report is consistent with a study that used SILAC (stable isotope labeling with amino acids in cell culture) to measure changes in global cellular protein synthesis in response to miRNA induction or knockdown (Selbach et al., 2008). At an early time point after miRNA transfection and early pulse-labeling (8 hours), most targets were only downregulated at the protein level, while at a later time-point (32 hours), the protein and mRNA levels were reduced. Detailed kinetic analysis conducted in HeLa cells and *D. melanogaster* S2 cells reached the same conclusion;

translation repression by miRISC precedes mRNA deadenylation and destabilization (Bethune et al., 2012; Djuranovic et al., 2012).

The findings mentioned above are very different from those reported by an initial ribosome profiling study conducted by the Bartel group. Using cultured mammalian cell lines to assess the effects of ectopic *miR-155* on protein and mRNA levels, they showed significant reduction in mRNA levels that accounted for decreased protein production in >84% of transcripts with *miR-155* sites, while only an estimated ~15% of silencing was attributed to reduced translation efficiency (Eichhorn et al., 2014; Guo et al., 2010). They later modified their approach and used poly(A) tail profiling on RNAs isolated from various species, tissues, and cell lines, which provided better resolution of the tail length of global mRNAs (Subtelny et al., 2014). Their latest findings showed a strong correlation between the poly(A) tail length and translation efficiency, in particular in critical contexts such as early embryo development, as was initially reported by the Giraldez group.

While the reports mentioned above provided a view of the global effects of miRNAs on mRNAs and protein output, studies have also provided mechanistic insights into the requirements for translation repression and deadenylation mechanisms. It was reported that miRNA-mediated deadenylation was not impaired when blocking translation of miRNA reporters using the following approaches: substituting the m^7G cap with A-cap, adding a structured RNA in the 5'UTR to interfere with ribosomal subunits joining, using reporters bearing no open-reading frame but only miRNA target sites, blocking the start codon with an antisense oligonucleotide, or adding cycloheximide (Eulalio et al., 2009b; Fabian et al., 2009; Giraldez et al., 2006; Wakiyama et al., 2007).

Conversely, reporters with an internalized poly(A), or wherein it is replaced with a stable histone-stem loop, were still subjected to translation repression even without any possible mRNA destabilization (Eulalio et al., 2009b; Fukaya and Tomari, 2012; Wu et al., 2006).

The relative contributions of translation repression and deadenylation and decay are still a matter of debate. Taken together, these studies suggest that i) miRNAs act at the translation level and mRNA decay may serve to consolidate silencing following translation repression; ii) mRNA deadenylation and decay may be predominant in the embryo; and iii) how each mechanism contributes and regulates different genes may depend on miRNA:mRNA pair, 3'UTR context, cell type, or biological context.

To add another layer of complexity to miRNA-mediated silencing, one study showed that miRNA-mediated silencing may be reversible under specific conditions. Under stress conditions, such as amino acid deprivation and arsenite treatment, the cationic amino acid transporter 1 (CAT-1) mRNA and reporters bearing its 3'UTR can be relieved from *miR-122* translation repression (Bhattacharyya et al., 2006). Such relief under conditions of stress is accompanied by relocalization of CAT-1 mRNA from P bodies and an increase in polysomal fractions (Bhattacharyya et al., 2006).

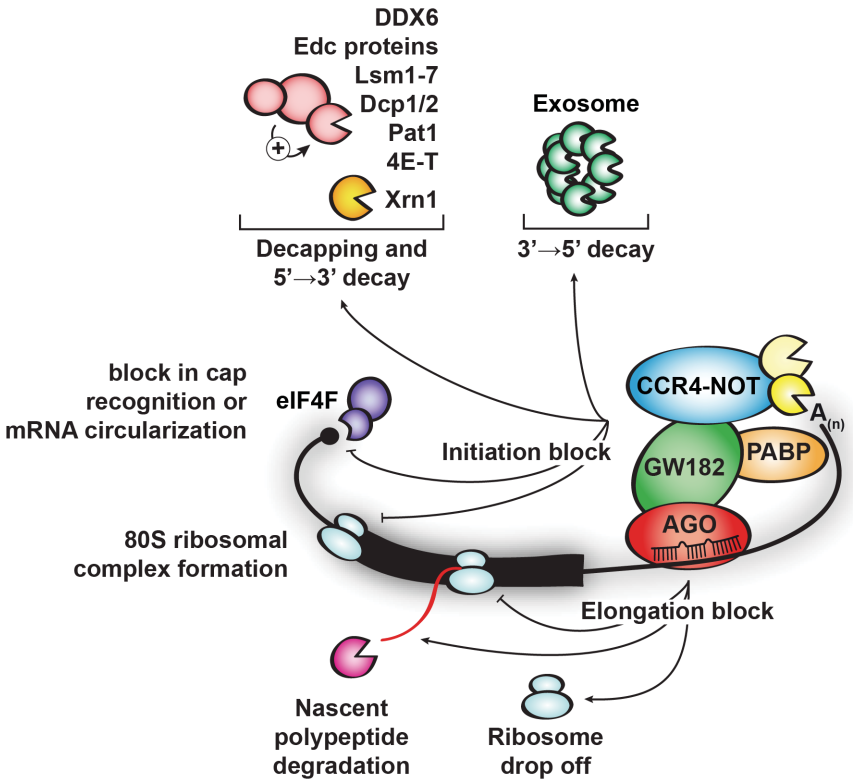

Figure 1-6: Proposed mechanisms for miRNA-mediated silencing

The miRISC can block translation at the elongation step (Moss et al., 1997; Olsen and Ambros, 1999; Seggerson et al., 2002; Wightman et al., 1993), as a result of slowed elongation, ribosome drop off, or degradation of nascent polypeptide chains (Maroney et al., 2006; Nottrott et al., 2006; Petersen et al., 2006). More compelling evidence instead indicates that miRNAs can act at the initiation step, by preventing the assembly of the 80S ribosomal complex (Mathonnet et al., 2007; Thermann and Hentze, 2007) or cap recognition (Doench et al., 2003; Humphreys et al., 2005; Mathonnet et al., 2007; Pillai et al., 2005; Wakiyama et al., 2007; Wang et al., 2006), which in turn can prevent the closed loop conformation of the mRNA for efficient translation. miRISC also interacts with the CCR4-NOT complex and decapping machinery to induce poly(A) tail shortening and mRNA decay (Bagga et al., 2005; Behm-Ansmant et al., 2006; Braun et al., 2011; Chekulaeva et al., 2011; Fabian et al., 2009; Giraldez et al., 2006; Wu et al., 2006). Recent studies indicate DDX6 serving as the link in uniting the two ends of the mRNA through its interaction with CNOT1 and the decapping machinery (Chen et al., 2014; Mathys et al., 2014; Rouya et al., 2014).

1.9 miRNA-mediated silencing and P bodies

As briefly described earlier, P bodies are distinct cytoplasmic foci that contain a conserved set of proteins involved in mRNA processing and decay along with non-translated mRNAs, leading P bodies to be attributed to mRNA degradation (Andrei et al., 2005; Brengues et al., 2005; Ferraiuolo et al., 2005; Teixeira et al., 2005). P bodies belong to a diverse group of membrane-less compartments, referred to as messenger ribonucleoprotein (mRNP) granules, that include germ granules, stress granules, chromatoid bodies in male germ cells, and neuronal granules (Buchan, 2014; Schisa, 2012; Voronina et al., 2011). mRNP granules are classified based on their protein composition, cellular context in which they are formed, and their presumed function attributed to the localized proteins. Stress granules, as indicated by the name, are formed in response to environmental or cellular stress conditions. Similar to P bodies yet functionally distinct due to the presence of translation initiation factors (eIF4E, eIF4G, eIF4A, eIF3 and eIF2) and the 40S ribosomal subunit, the residing non-translated mRNAs are thought to be stalled in translation initiation under conditions of stress (Anderson and Kedersha, 2006; Decker and Parker, 2012), but can exit and return to translation under recovered favorable conditions (Parker and Sheth, 2007). Closely related to P bodies and stress granules are germ granules, which are referred to as P granules in *C. elegans* for their segregation within the P lineage, or germ blastomeres (Strome and Wood, 1982). In flies and nematodes, germ granules are believed to play an important role in the localization and storage of mRNAs for germ cell lineage fates and functions (Ephrussi and Lehmann, 1992; Gruidl et al., 1996; Kawasaki et al., 1998; Knaut et al., 2000; Lehmann and Nusslein-Volhard, 1986).

Due to a significant fraction of AGO and GW182 localizing to P bodies, P bodies were considered likely to be sites for miRNA target decay (Behm-Ansmant et al., 2006; Ding et al., 2005; Jakymiw et al., 2005; Liu et al., 2005b; Meister et al., 2005; Pillai et al., 2005; Sen and Blau, 2005). To further support the role for these bodies in miRNA function, when GW182 or other P body components, including Dcp1/2 and Pat1, were depleted in human or in *D. melanogaster* cells, silencing of reporter mRNAs by miRNAs was impaired (Behm-Ansmant et al., 2006; Chu and Rana, 2006; Eulalio et al., 2007b; Jakymiw et al., 2005; Liu et al., 2005a; Rehwinkel et al., 2005). Intriguingly, depletion of the decapping activators, Lsm1 or Lsm3, results in the dispersion of P bodies yet translation repression was still observed (Eulalio et al., 2007b). These findings led to the conclusion that microscopically visible P bodies may not be required for silencing, but may instead be formed as a consequence of the silencing activity. It does not exclude, however, the possibility of minimal structures on target mRNAs that could still contribute to silencing.

1.10 Rationale and Thesis Objectives

Since the introduction of *C. elegans* as a model organism by Sydney Brenner, *C. elegans* has established itself as an invaluable research tool, with an extensive resume highlighting the diverse genetic approaches that include transgenics, mutagenesis, and RNAi. These powerful genetic tools have established a framework for diverse regulatory pathways that govern animal development. Among the breakthrough genetic studies was the discovery of *lin-4* and *let-7* miRNAs in 1993, followed by the substantial expansion of small RNAs that marked the beginning of the changing landscape of gene regulation in a broad variety of species. Yet, how miRNAs directly impinge on the expression of their mRNA targets in diverse biological processes and in different cellular contexts are not well understood. For a more thorough understanding of the mechanistic aspects underlying miRNA action, one needs to turn to biochemical approaches.

The development of such biochemical tools and assays is a key component of my thesis work. My first objective was to develop a system that faithfully recapitulated miRNA-mediated silencing. In Chapter 2, I detailed the properties of such an extract, derived from *C. elegans* embryo, and its optimization for miRNA-mediated translation repression assays. With such a biochemical tool in hand, in Chapter 3, I sought to use this system in miRNA-directed deadenylation assays and investigated the molecular mechanism of action of abundant miRNA families on their mRNA targets in *C. elegans* embryo. Finally, in Chapter 4, I aimed to resolve and delineate the temporal order of events from target recognition by miRISC, to the recruitment of the effector CCR4-NOT complex assembly on target mRNAs, in nucleating a microenvironment that drive target mRNA silencing. The work presented in this thesis integrates biochemistry, proteomics,

cell-free assays, and genetics to provide a greater understanding of the mechanism of gene silencing by miRNAs.

Chapter 2: Cell-free microRNA-mediated translation repression in *Caenorhabditis elegans*

Wu E and Duchaine TF. Cell-free microRNA-mediated translation repression in Caenorhabditis elegans. (**2011**). *Methods in Molecular Biology*. 725: 219-232.

The numberings for some of the headings and subheadings have been altered to adapt to the format of this thesis.

2.1 Preface

In this chapter, I outline the details for the preparation of the cell-free extract derived from *C. elegans* embryos. This system served as an invaluable tool throughout my thesis work, and from which the following assays were developed to study miRNA-mediated silencing:

- translation repression assays: this chapter and Chapter 3
- deadenylation assays: Chapter 3
- deadenylated RNA-immunoprecipitation: Chapter 4
- micrococcal nuclease sensitivity assay: Chapter 4

Several modifications have been made since the release of this manuscript for publication in 2011. The list of updates can be found in Appendix 1.

2.1 Abstract

In vitro recapitulation has recently led to significant advances in the understanding of the molecular functions of microRNAs. Cell-free systems allow a direct perspective on the different steps involved, and provide the experimenter with the opportunity to directly interfere with, or alter the implicated factors. In this chapter, we describe a cell-free translation system based on *Caenorhabditis elegans* embryo, which faithfully recapitulates miRNA-mediated translation repression. Because of the genetic and transgenic flexibility of this animal model, such a system provides a unique experimental resource to study the mechanism and the functions of miRNAs, the Argonautes, and the RISC.

2.2 Introduction

MicroRNAs (miRNAs), when embedded within the RNA Induced Silencing Complex (RISC), base pair with their messenger RNA (mRNA) targets to subdue gene expression. Ambros and colleagues reported in 1999 that this gene repression occurs at post-transcriptional levels (Olsen and Ambros, 1999). More than a decade has passed since this publication, and the details of the mechanism of action of miRNAs at the molecular level are still not fully understood. Even since the identification of the Argonaute proteins as the core component of the RISC, the molecular basis for miRNA-mediated silencing has proven hard to refine (Filipowicz et al., 2008). This is likely because the mechanism(s) is complex, but possibly also because the predominant mechanism involved may be different in distinct developmental, or cellular contexts where miRNAs were studied.

In the vast majority of mRNA::miRNA targeting events in animals, base pairing is incomplete and does not activate the *Slicer* activity of the Argonautes (Bartel, 2009). What happens then, to the expression of an mRNA target, and to its integrity, once it is targeted by the miRISC? Just like with other fundamental mechanisms of gene expression and regulation, elucidation of the underlying mechanisms only became possible when recapitulation was achieved, in cell culture, and *in vitro*. mRNA reporter systems based on transfection or transgenic expression, for example, provided much insight on the mechanism. This strategy, however, bears some significant limitations stemming from the fact that the reporter activity is examined several hours, if not days after transfection. This severely impinges on the possible insight on the nature, or the order of the very first events following mRNA::miRNA recognition. In addition, with such designs, it is difficult to gain a direct and unambiguous view on the relative contribution of the different steps involved. Thus, on these aspects in particular, *in vitro* reconstitution systems are irreplaceable in providing a *direct* perspective on the complexity of the mechanism of miRNA-mediated silencing. A number of cell-free miRNA-mediated silencing systems have recently emerged, derived from *Drosophila* embryo and cultured cells, rabbit reticulocyte, or mouse, and human cell cultures (for examples see Fabian et al., 2009; Gebauer and Hentze, 2007; Wang et al., 2006). Most recently, we developed an *in vitro* translation system from *C. elegans* embryo, which critically relies on both the 5' cap and 3' poly(A) tail determinants to initiate translation on exogenously-provided transcripts. We further showed that this system faithfully recapitulates a miRNA-mediated silencing response based on endogenous miRNAs, and requires ALG-1 and

ALG-2, the two Argonautes dedicated to miRNA-mediated silencing in *C. elegans* (Chapter 3, Wu et al., 2010).

In this chapter, we provide a detailed method to prepare this translation-competent extract derived from *C. elegans* embryos, and to assay for miRNA-mediated silencing. Specifically, this chapter describes the protocols for the preparation of *C. elegans* embryos, the preparation of the translation extracts, the design and the preparation of the mRNA reporters for miRNAs, and the translation repression assay itself. Finally we describe an alternative method that is based on 2'-*O*-methylated, sequence specific inhibitors.

2.3 Materials

2.3.1 Preparation of *C. elegans* embryo, and extracts

1. Agar/NGM 150 mm plates for *C. elegans* cultures (Hope, 1999).
2. OP50 paste, as a food supply for the large-scale *C. elegans* cultures (Hope, 1999).
3. Bleaching solution: 0.25 M potassium hydroxide (KOH), 0.6% Sodium hypochlorite (Fisher Scientific).
4. 1X M9 saline: 3 g Anhydrous potassium phosphate monobasic (KH_2PO_4), 6 g Sodium phosphate (dibasic) anhydrous (Na_2HPO_4), 5 g Sodium chloride (NaCl), 1 mL 1 M magnesium sulfate ($MgSO_4$), add water to 1 L. Sterilize by autoclaving (Hope, 1999).
5. Sephadex G-25 Superfine beads (Amersham Bioscience): Suspend the contents of the container in 500 mL of nuclease-free water. Sterilize by autoclaving.
6. 10 mL Poly-Prep Chromatography Columns (Bio-Rad).
7. 15 mL Dounce glass homogenizer with pestle 'tight-fitting' (Kontes).
8. 1 M Dithiothreitol (DTT); store at -20°C.
9. Buffer A: 10 mM N-2-hydroxyethylpiperazine-N'-2-ethanesulfonic acid (HEPES)-KOH pH 7.4, 15 mM Potassium chloride (KCl), 1.8 mM Magnesium acetate ($Mg(OAc)_2$), 2 mM DTT. Prepare fresh, and keep on ice.
10. Buffer B: 30 mM HEPES-KOH pH 7.4, 100 mM Potassium acetate (KOAc), 1.8 mM $Mg(OAc)_2$, 2 mM DTT. Prepare fresh and keep on ice.
11. Protein Assay Dye Reagent Concentrate (Bio-Rad).

2.3.2 Preparation of RNA substrate

1. pCI neo plasmid (Promega): To be used as a backbone into which the miRNA-response elements (miR-complementary sites) are cloned.

2. The *Renilla* Luciferase 6x target mRNAs (RL 6xmiR-52 and 6xmiR-52 mut): encode the *Renilla* luciferase coding sequence and six copies of a target site (Note 1).
3. The 6x target was synthesized as a miniGene (IDT) and was purchased as an insert into the pIDT Smart vector in its XbaI and NotI sites: 5'-GCGGCCGCGAATTCATTAACACCCGTACATTTTCCGTGCTATTAACACCCGTACATTTTCCGTGCTCAATTCATTAACACCCGTACATTTTCCGTGCTATTAACACCCGTACATTTTCCGTGCTATTAACACCCGTACATTTTCCGTGCTCAATCACCCGTACATTTTCCGTGCTTCTAGA-3' (RL 6xmiR-52 wild-type) and 5'-GCGGCCGCGAATTCATTAACGTTTGTACATTTTCCGTGCTATTAACGTTTGTACATTTTCCGTGCTCAATTCATTAACGTTTGTACATTTTCCGTGCTATTAACGTTTGTACATTTTCCGTGCTATTAACGTTTGTACATTTTCCGTGCTCAATCGTTTGTACATTTTCCGTGCTTCTAGA-3' (RL 6xmiR-52 mut). The 6x target cassette is digested with XbaI and NotI and subcloned into pCI neo to the RL open reading frame. The poly(A) tail is prepared by annealing oligonucleotides containing a stretch of 90 adenines, and compatible ends for annealing into pCI neo RL using the HpaI and MfeI sites (Note 2).
4. MEGAscript T7 Transcription Kit (Ambion).
5. m^7(3'-*O*-methyl)G(5')ppp(5')G anti-reverse cap analog (ARCA) (Ambion) or ApppG (New England Biolabs).
6. Pre-mixed Phenol:Chloroform:isoamyl alcohol (25:24:1, Bishop).
7. 3 M Sodium acetate.
8. 100% Ethanol.
9. Sephadex RNA mini Quick Spin columns (Roche Applied Science).

10. 4% Polyacrylamide (19:1 acrylamide/bisacrylamide)-8 M urea denaturing gel.
11. Gel loading buffer II (Ambion).
12. RiboRuler High Range RNA Ladder (Fermentas).

2.3.3 Translation conditions

1. 2.5 mM Spermidine (Sigma Aldrich), store at -80°C.
2. Total L-amino acid mix: prepare 1 mM of each amino acid from stock commercial powders (Sigma Aldrich and/or Bioshop). Alternatively, this mixture can be prepared using an amino acid powder kit (Sigma Aldrich). Store 1 mL aliquots at -80°C.
3. 1 M HEPES-KOH pH 7.5.
4. 10 mM $Mg(OAc)_2$, sterilize by filtration.
5. 2 M KOAc, store at -80°C.
6. 5 µg/µL calf-liver tRNA (Novagen, Note 3).
7. RiboLock RNase inhibitor (Fermentas): 40 U/µL.
8. 1 M Creatine phosphate (Roche Applied Science).
9. 3 µg/µL Creatine phosphokinase (from Rabbit skeletal muscle, Calbiochem).
10. 40 mM ATP: Dilute 100 mM ATP stock in sterile water, store at -80°C.
11. 10 mM GTP: Dilute 100 mM ATP stock in RNase free water, store at -80°C.
12. Master mix: 0.1 mM Spermidine, 60 uM amino acids, 24 mM HEPES-KOH (pH 7.5), 1.28 mM $Mg(OAc)_2$, 25 mM KOAc, 0.1 µg/µL Calf-liver tRNA, 0.096 U/µL RiboLock RNase Inhibitor (Fermentas), 16.8 mM Creatine phosphate, 81.6 ng/µL Creatine phosphokinase, 0.8 mM ATP, 0.2 mM GTP (see Table 2-1 and Note 4).
13. Dual-Luciferase Reporter Assay (Promega).
14. GloMax 20/20 Luminometer (Promega, Note 5).

15. The 2'-*O*-methylated oligonucleotides (Dharmacon) were designed as antisense oligonucleotides to the mature miRNAs according to Wormbase registry (www.wormbase.org). Oligonucleotides were resuspended in water to a concentration of 100 ng/uL. In this chapter we used the *miR-52* 2'-*O*-Me (α-miR-52) sequence: 5'-UUAAUAGCACGGAAACAUAUGUACGGGUGUUAAU-3'; *miR-1* 2'-*O*-Me (α-miR-1) sequence: 5'-UCUUCCUCCAUACUUCUUUACAUUCCAACCUU-3'.

A

Reagent	Volume (µL)	Final added conc.
2.5 mM Spermidine	0.5	0.1 mM
1 mM Amino acid mix	0.75	0.06 mM
1 M HEPES-KOH (pH 7.5)	0.3	24 mM
10 mM $Mg(OAc)_2$	1.6	1.28 mM
2 M KOAc	0.156	25 mM
5 µg/µL calf-liver tRNA	0.25	0.1 µg/µL
RNase Inhibitor (40 U/µL)	0.03	0.096 U/µL
1 M Creatine Phosphate	0.21	16.8 mM
3 µg/µL Creatine Phosphokinase	0.34	81.6 ng/µL
40 mM ATP 10 mM GTP mix	0.25	0.8 mM ATP 0.2 mM GTP
Extract	5	n/a
Total master mix volume	9.386	n/a

B

	Reagent	Volume (µL)	Final concentration
no 2'-O-Me	Master mix	9.386	n/a
	mRNA	1	1 nM
	RNase-free water	2.114	n/a
	Total reaction volume	12.5	n/a
with 2'-O-Me	Master mix	9.386	n/a
	mRNA	1	1 nM
	625 nM 2'-O-Me	1	50 nM
	RNase-free water	1.114	n/a
	Total reaction volume	12.5	n/a

Table 2-1: *In vitro* translation mix preparations.

Reaction mixes assembly for a 12.5 µl translation reaction in the absence (A) or presence (B) of 2'-*O*-Me inhibitors.

2.4 Methods

The following method starts with the harvest of large-scale cultures of *C. elegans* gravid adults (animals with rows of embryo in their uteri), and extends until the actual miRNA-mediated translation repression assays. In our lab, we often use variations of this method to take advantage of the genetic flexibility of *C. elegans.* Extracts can be generated from viable mutant strains, or after growing the animals on a bacterial strain (usually HT115) which drives the over-expression of dsRNA to silence target genes (Timmons et al., 2001).

2.4.1 Culture and harvest of *C. elegans* embryos

1. Harvest embryos from large-scale cultures of *C. elegans* on large NGM-Agar plates, and using OP50 as food. For a suitable scale of preparation (a typical batch), harvest embryos from 30x150mm plates each containing approximately 50,000 synchronous animals each (1,500,000 animals total).
2. Harvest gravid adults in 1X M9, and distribute equally in 15 mL Falcon table-top centrifuge tubes. We usually pool the animals from two or three plates per tube for the hypochlorite step.
3. Treat the adults with freshly prepared hypochlorite solution. Animal suspensions are treated for 2 minutes with mild, but constant hand agitation followed by 20 seconds centrifugations in a table-top centrifuge at 680 x g and then remove all the supernatant.
4. Add hypochlorite solution to the animal pellet, and repeat step 3 until the suspension is completely devoid of adult cuticles. Monitor the progress of the treatment under a dissection microscope. Complete dissolution of cuticles typically requires three to

four suspension-centrifugation cycles, and leaves a small, beige embryo pellet of approximately 1/5th to 1/10th the initial animal volume. Following the final centrifugation, carefully remove all of the supernatants.

5. Completely resuspend the pellet of embryo in M9 saline, and centrifuge again in a table-top centrifuge.
6. For the second wash, add 1 mL of 1 M HEPES-KOH pH 7.5, and complete to a final volume of 15 mL with M9 in the Falcon tube.
7. Proceed to 2 additional washes with 15 mL of M9 saline.
8. Finally, wash the embryonic pellet three more times in RNase-free water to completely remove the sodium ions (which are known to inhibit protein synthesis when present at high concentration). We usually pool all the embryo pellets in a single Falcon tube at this step.
9. After the final centrifugation, carefully remove all the residual supernatant. Typically this results in a pellet of 500 µL to 1 mL of stacked embryos.
10. Flash-freeze in a 15-mL Falcon tube by immersion in liquid nitrogen.
    - Following this step, embryos may be stored at -80°C for at least 2 years.

2.4.2 Preparation of *C. elegans* embryonic extract

A broad diversity of methods is available for the preparation of *in vitro* translation systems that are derived from tissues or cell cultures from various species. Most of these methods were not directly adaptable to *C. elegans* extracts. In fact, a large number of parameters had to be tuned before we obtained robust and reproducible translation initiation in *C. elegans* extracts, and often even the slightest deviations greatly affected the recovered activity. For example, in some systems micrococcal nuclease treatment (to

remove the endogenous mRNAs) is required for the translation of exogenous mRNAs (Scott et al., 1979). Such a treatment kills translation initiation in the *C. elegans* embryonic extract. Among the other critical parameters are the monovalent, and divalent ion concentrations, the temperature, and the presence of 5'-cap and 3'-poly(A) tail on the reporter mRNA.

A flow chart illustrating the preparation of the extracts is shown in Figure 2-1. Every step of the extract preparation should be conducted at 4°C, or in a cold room.

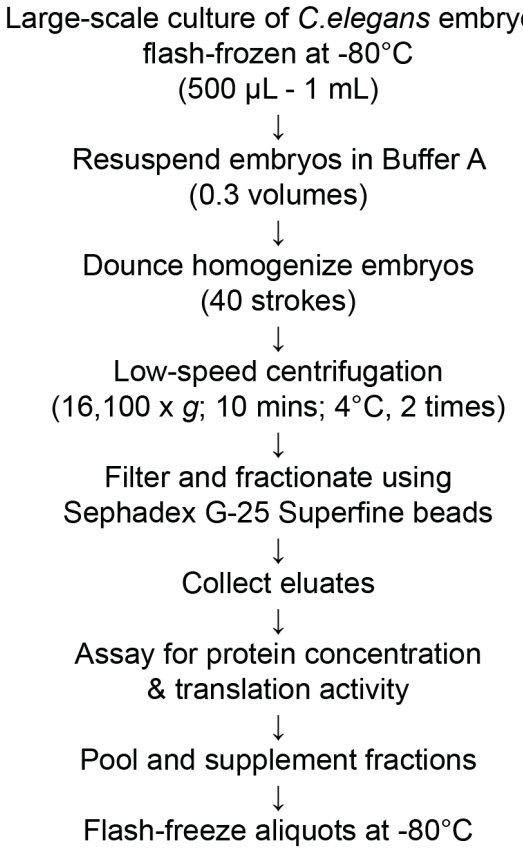

Figure 2-1: Flow chart of the procedure for the preparation of the *C. elegans* embryonic extracts.

1. Rapidly thaw the embryonic pellets in hand and keep it on ice until used.
2. Resuspend the embryonic pellet in 0.3 volumes of Buffer A (Note 6).
3. Transfer the slurry to a clean, pre-chilled Dounce homogenizer. Break the embryos with 40 strokes (total), by series of 10 strokes to allow cooling between the series (Note 7).
4. Confirm the lysis of the embryo by visual inspection of 0.5 µL aliquots on a glass slide using a dissection microscope.
5. Transfer the slurry to an RNase-free microcentrifuge tube. Centrifuge the slurry at 16,100 x g for 10 min at 4°C.
6. Recover the supernatant and centrifuge once more in the same conditions. Retain a 2 µL aliquot of the resulting supernatant to monitor the dilution of the extract during the fractionation step (Note 8).
7. Fractionate the extract by size-exclusion chromatography using Sephadex G-25 Superfine beads (Note 9). For this, wash the beads three times with Buffer B by suspension-centrifugation in a 15-mL Falcon tube and using a table-top centrifuge at 680 x g. Beads should make up approximately four times the volume of the extract supernatant.
8. Settle the beads into a 10-mL Poly-Prep chromatography column, and allow Buffer B to flow through until it reaches the surface of the matrix.
9. Load the supernatant onto the column slowly, and directly onto the matrix (drop-wise). Allow the supernatant to completely enter the matrix by gravity.

10. Load the column with 1 extract volume of Buffer B. Discard the dead volume. Start collecting fractions in a 1.5 ml RNase-free microcentrifuge tubes as soon as tint of yellow is visible in the eluate (Note 10).
11. Once the flow from the first elution volume stops, add 0.3 volumes of Buffer B and collect fractions. Repeat the elution five to six times or until the eluate appears completely clear.
12. Remove 2 µL aliquots from each fraction, and assess their protein concentration by Bradford assay (Note 11).
13. Save a small aliquot (5 µL) of each fraction to test for translation activity using luciferase reporters (see Section 2.4.4) (Note 12).
14. Supplement the fractions that are active for translation by following Table 2-1A. For this, the most active fractions can be pooled (Note 13).
15. Aliquot the supplemented fractions and flash-freeze as aliquots in liquid nitrogen. The extract remains active for at least 2 years when stored at -80ºC.

2.4.3 Preparation of the RNA substrate

1. Transcribe RL 6xmiR-52, and RL 6xmiR-52 mut at 30ºC for 4 hours with the ARCA cap analog using the MEGAscript kit (Note 14).
2. Following transcription, add 1 µl of DNase Turbo I, and digest the template DNA for 15 minutes at 37ºC.
3. Adjust the volume of the reaction to 70 µl with RNase-Free water.
4. Purify the RNA by phenol/chloroform extraction. For this, add 1:1 volume of phenol/chloroform/isoamyl alcohol and vortex for 15 s.
5. Centrifuge for 30 s in a table-top centrifuge at 16,100 x g.

6. To remove any residual, unincorporated nucleotides, transfer the aqueous phase to a Sephadex RNA Mini Quick Spin column, and proceed to filtration according to the supplier's instructions.
7. Quantify the recovered RNA, and monitor the size and quality of the transcript on a 4% polyacrylamide-urea denaturing gel and by Ethidium bromide staining. A single band should be visible. Store the RNA as aliquots at -80ºC.

2.4.4 miRNA-mediated translation repression

To assay for miRNA activity, we use a Luciferase reporter mRNA that is fused to a 3' UTR encoding six copies of a miRNA-binding site (RL 6xmiR-52) (Figure 2-2A). Our data and other published reports indicate that translation repression increases with additional copies of miRNA-complementary sites (Chapter 3, Doench and Sharp, 2004; Wu et al., 2010).

In the first protocol, we determine the repressive effect of a specific miRNA by comparing the translation of RL 6xmiR-52, with a reporter bearing six copies of binding sites bearing a mutation within the seed complementary sequence (positions complementary to nt 2 to 4 of miR-52; RL 6xmiR-52 mut).

Note that for our typical experiments, we use a final concentration of 1 nM of reporter mRNA. This is far less than the miR-52 concentration in the extract, but still allows sufficient sensitivity to detect the translation of the reporter. The investigator is encouraged to determine the precise concentration of their favorite miRNA by qRT-PCR in the embryonic extract, prior to a translation repression assay.

1. Thaw the frozen extract, and assemble the translation reactions in microcentrifuge tubes on ice. For convenience, the master mix content is also outlined in Table 2-2B (no 2'-*O*-Me).
2. For every 1x reaction, add 2.114 µl of water to the master mix.
3. Dispense 11.5 uL of the master mix (completed with water) to 1 µL of mRNA per tube (1 nM final mRNA concentration). We usually work with duplicates of each time-point, and carry parallel reactions for the RL 6xmiR-52 and RL 6xmiR-52 mut mRNAs.
4. Mix each reaction by tapping the tubes gently. Avoid frothing.
5. Incubate the reactions at 17ºC for 0 to 6 hours in a water bath (see Note 15).
6. Once translation reactions are complete (at each time-point), place tubes on ice and withdraw 2 µL from each reaction tube to measure the luciferase activity using the Dual-Luciferase Reporter Assay (see Note 16).

Using this method, translation of RL 6xmiR-52 reaches a plateau and is usually fully repressed between the 1 and the 3-h time-points, while RL 6xmiR-52 mut mRNA remains un-repressed during the entire time-course (Figure 2-2B). Since the translation of RL 6xmiR-52 is arrested, and translation of 6xmiR-52 mut mRNA persists, the extent of the 'repression' detected using this method depends on the time of incubation. Typically for miR-52, a 3-h time-course leads to an approximately threefold difference in overall translation.

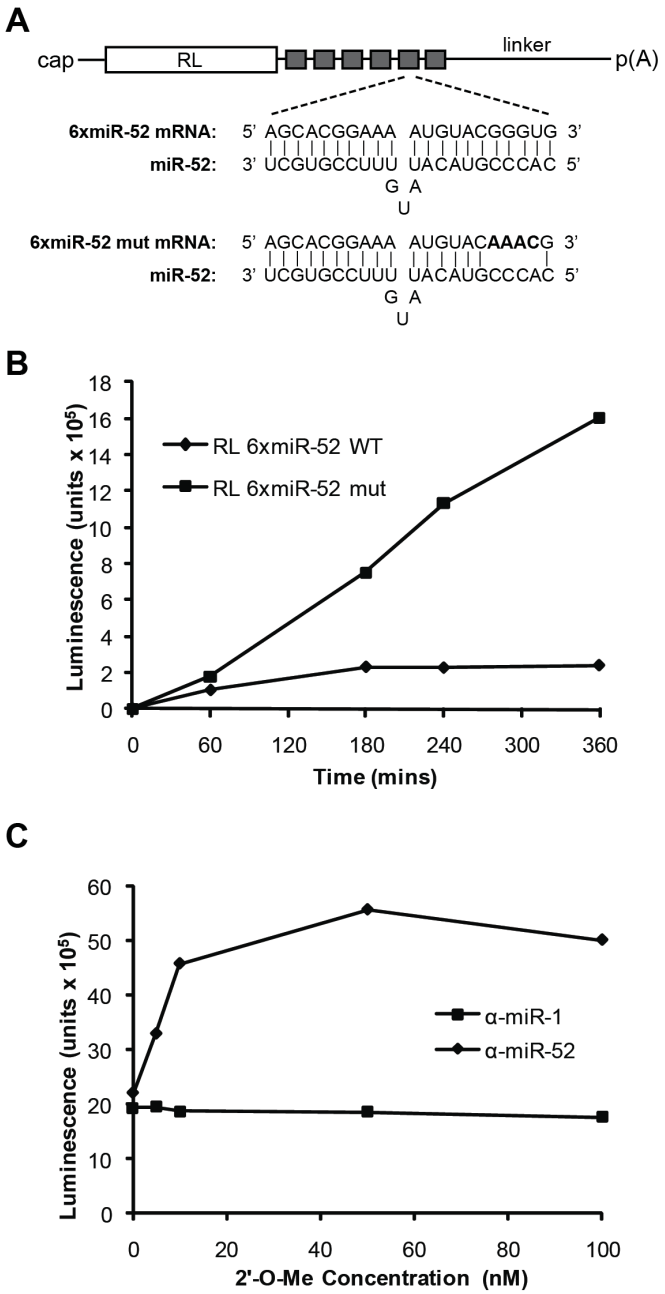

Figure 2-2: Translation repression by miRNAs in *C. elegans* embryonic extracts.

(A) Diagram of the Luciferase miR-52 reporters used to assay for translation repression. (B) Translation repression time-course of RL 6xmiR-52 vs. 6xmiR-52 mut reporter mRNAs. (C) Dose-response translation de-repression using α-miR-52 (specific) and α-miR-1 (negative control) 2'-*O*-Me.

2.4.5 Alternative method: miRNA-mediated translation repression as revealed with 2'-*O*-Me inhibitors

In vitro transcription efficiency and the quality of the resulting mRNA are very sensitive to the quality of the DNA template, its linearization, and concentration. Accordingly, the result of the translation assay will vary with each RNA preparation in a manner that depends on parameters that are not only due to the effect of the miRNA. For this reason, it is crucial to prepare the 6xmiR-52 and the 6xmiR-52 mut in parallel, and using the very same conditions. To circumvent the problem of batch-to-batch variation, we propose an alternative approach that relies on a single mRNA reporter. For this, we use 2'-*O*-methylated oligonucleotides (2'-*O*-Me) as miRNA inhibitors to specifically prevent the repression of the RL 6xmiR-52 reporter. 2'-*O*-Me inhibitors encode a sequence that is complementary to the miRNA of interest. Their inclusion in the reaction results in irreversible hybridization with the miRNA and hence, prevents the repression of the target mRNA. Translation repression is revealed when comparing with a non-related 2'-*O*-Me (here α-miR-1), used at the same concentration. As an alternative to 2'-*O*-Me inhibitors, Locked nucleic acids (LNA) may also be employed (Chan et al., 2005; Orom et al., 2006).

1. Thaw the frozen extract, and assemble the master mix as in Table 2-1B, *with* 2'-*O*-Me.
2. Prior to mRNA addition, the extract is incubated with 1 µL of either α-miR-52 (specific) or α-miR-1 (control) 2'-*O*-Me, which sets a final concentration of 50nM of

2'-*O*-Me (Note 17). Mix by tapping the tubes gently while avoiding frothing. Pre-incubate for 30 minutes at 17°C in a water bath (Note 18).

3. After the 30 minutes of pre-incubation, add 1 μL of the RL 6xmiR-52 mRNA target (1nM final) to each reaction tube, mix with 11.5 μL of the 2'-*O*-Me pre-incubated mastermix and allow the reaction to proceed at 17°C.
4. Incubate the reactions at 17ºC for 3 hours in a water bath (Note 19).
5. Place tubes on ice, and withdraw 2 μL from each reaction tube to measure the luciferase activity using the Dual-Luciferase Reporter Assay.

Including α-miR-52 leads to a 3-fold de-repression when monitored at the 3-h time-point, while the addition of the non-related control α-miR-1 does not significantly affect translation at concentrations up to 100 nM (Fig. 2-2C). Results with this method are usually similar to the 6xmiR-52 mut reporter comparison method, but are less sensitive to mRNA reporter prep-to-prep quality variations.

2.5 Notes

1. The 6x target site is partially complementary to the guide strand of the miRNA, leading to a 'bulge' in the seed-complementary region and hence imperfect base pairing between the miRNA and the mRNA.
2. Note that cloned poly(A) tail-encoding sequences are inherently unstable in bacteria, and should be resequenced every time a preparation is made. Sequencing of *midi* or *maxi* scale preparations is recommended to ensure that batches with predetermined poly(A) tails remain available. Plasmids encoding a poly(A) tail no less than 80 A residues are used.

3. We also successfully used tRNA isolated from cultured cells such as Krebs-2 ascites and *C. elegans* embryos.
4. The optimal concentration for the supplementation with K^+ and Mg^{2+} may vary from batch to batch, especially when the experimenter prepares the extract for the first few times. We have established an optimal range of 1.5–3 mM for Mg^{2+} and 60–75 mM for K^+. Optimally, the salt concentrations should be adjusted for each batch of extract that is prepared. In typical batches, we set the final salt concentrations in translation reactions at 2 mM for $Mg(OAc)_2$ and 65 mM for KOAc.
5. Lumat LB 9507 (Berthold Technologies GmbH & Co. KG) can also be used.
6. Diluting the extract too much can dramatically reduce the translation activity of the embryonic extract.
7. Make sure to keep the pestle in contact or close to the embryo suspension while homogenizing, i.e. no more than 1 cm above the slurry of embryos. Lifting the pestle too high will result in a reduction of yield of the embryonic extract. The slurry is viscous, and will remain on the walls of the homogenizer, making it difficult to recover after homogenization.
8. The protein concentration of the lysates prior to filtration typically ranges from 20 to 60 μg/μl.
9. The step of fractionation on Sephadex™ G-25 Superfine beads *is absolutely required* to obtain translation activity. Centrifugation-based and gravity-based chromatography may both be used, but the gravity-based method yields more consistent results.
10. To follow the activity, we count the elution fractions passed the matrix dead volume. We do this by following the brown-yellowish tint of the extract. Alternatively, you

may wish to simply follow the protein concentration by mixing 1 µl of each fraction with a Bradford assay, as you recover them.

11. Fractions 1–4 (when counting *after* the beads dead volume) typically have highest protein concentration, with fractions 2 and 3 usually being the most concentrated. Concentration within these two fractions is only slightly lower than the concentration prior to filtration. The protein concentrations for fractions 1–4 can range from 5 to 35 µg/µl, with batch-to-batch variations.
12. Fractions 1–4 typically yield the highest translation activity. Like protein concentration, the elution profile for translation activity is also typically bell-curved. We usually combine the fractions yielding similar translation activity to prepare the supplemented extract.
13. Fractions can also be frozen prior to supplementation. However, supplementing on the day of the preparation of the extract leads to a better consistency for subsequent experiments.
14. Our system is highly dependent on the presence of both 5' cap and 3' poly(A) tail. Translation of Luciferase reporters bearing either regular or ARCA-capped analogs yields translation activity, although translation of the ARCA-capped mRNA is most efficient.
15. Translation is active over temperatures ranging from 10 to 25ºC, but the optimal temperature for *in vitro* translation in our *C. elegans* embryonic extract is 17ºC.
16. Ensure that the luciferase reagents (substrates mix) are at room temperature prior to mixing and the measurement of luminescence, as this will greatly affect the read out for luciferase activity.

17. When using a different miRNA, a pilot translation experiment with varying concentrations of 2'-*O*-Me should be performed to select for the optimal concentration at which translation is efficiently de-repressed. This is particularly essential when assaying for miRNAs of unknown concentration in the extract.
18. This pre-incubation, prior to translation, allows for the annealing of the 2'-*O*-Me with the endogenous miRNA (Mathonnet et al., 2007).
19. In the alternative method, we use a single 3-h time-point. A time-course (as in section 2.4.4) may also be conducted. The time-course design is often more suitable, as it is more informative.

2.6 Acknowledgements

We thank Ahilya Sawh and Mathieu Flamand for their comments on the manuscript. This work was supported by Canadian Institute of Health Research (CIHR), the Canada Foundation for Innovation (CFI), and the Fonds de la Rercherche en Santé du Québec (FRSQ) (Chercheur-Boursier Salary Award J.1) to T.F.D.

Chapter 3: Pervasive and Cooperative Deadenylation of 3'UTRs by Embryonic MicroRNA Families

Edlyn Wu, Caroline Thivierge, Mathieu Flamand, Geraldine Mathonnet, Ajay A. Vashisht, James Wohlschlegel, Marc R. Fabian, Nahum Sonenberg & Thomas F. Duchaine (**2010**). *Molecular Cell* (40): 558-570.

3.1 Abstract

To understand how miRNA-mediated silencing impacts on embryonic mRNAs, we conducted a functional survey of abundant maternal and zygotic miRNA families in the *C. elegans* embryo. Here, we show that the *miR-35-42* and the *miR-51-56* miRNA families define maternal and zygotic miRNA-induced silencing complexes (miRISCs), respectively, which share a large number of components. Using a cell-free *C. elegans* embryonic extract, we demonstrate that miRISC directs the rapid deadenylation of reporter mRNAs with natural 3'UTRs. The deadenylated targets are translationally suppressed and remarkably stable. Sampling of the predicted *miR-35-42* targets reveals that roughly half are deadenylated in a miRNA-dependent manner, but with each target displaying a distinct efficiency and pattern of deadenylation. Finally, we demonstrate that functional cooperation between distinct miRISCs within 3'UTRs is required to potentiate deadenylation. With this report, we reveal the extensive and direct impact of miRNA-mediated deadenylation on embryonic mRNAs.

3.2 Introduction

Since their discovery, the small (~18-25 nt) non-coding microRNAs (miRNAs) have reshaped the landscape of genetic networks in a broad variety of species. Accumulating data indicate that miRNAs directly regulate >60% of the human coding genome (Friedman et al., 2009) and leave very few (if any) genetic pathways untouched. Validated miRNA targets are now known to be implicated in a wide range of cellular functions in developmental, steady-state, and disease contexts (Bartel, 2009).

Most miRNAs are generated as primary transcripts that are sequentially matured by two RNaseIII enzymes and their associated proteins. The nuclear Drosha protein cleaves these transcripts into hairpins of ~60 nt in length (pre-miRNA) (Lee et al., 2003). Pre-miRNAs are then exported to the cytoplasm and processed by Dicer (DCR-1 in *C. elegans*) into mature miRNAs (Grishok et al., 2001; Ketting et al., 2001). The processing of miRNAs by DCR-1 is coupled with their assembly into the miRNA-induced silencing complex (miRISC), which is composed at its core of specific members of the Argonaute family of proteins (ALG-1 and -2 in *C. elegans*), and additional proteins such as the GW182 homologs (AIN-1 and -2 in *C. elegans*). Base-pairing interactions between a miRNA and a target mRNA are required for silencing by miRISC. In canonical mRNA-miRNA interactions, the 5' region of the miRNA (nucleotides 2-7), coined the "seed", is an important determinant in the recognition of miRNA target sites, which are typically located within the 3'UTRs of target mRNAs. miRNAs sharing the same seed sequence are said to belong in the same "family" (Ibanez-Ventoso et al., 2008).

The mechanism, or the diversity of mechanisms through which miRNAs mediate gene silencing, is not fully understood. Pioneering work on the mechanism of miRNA-

mediated silencing in *C. elegans* indicated that the *lin-4* miRNA represses *lin-14* mRNA at the level of translation (Olsen and Ambros, 1999). Since then, several models have been proposed to explain the mode of action of miRNAs (see Filipowicz et al., 2008, for a review). Most recently, a growing body of work indicates that miRNA targeting may often result in mRNA degradation, which in at least some cases is preceded by decapping and/or deadenylation (Baek et al., 2008; Bagga et al., 2005; Eulalio et al., 2009b; Fabian et al., 2009; Giraldez et al., 2006; Selbach et al., 2008; Wu et al., 2006). The differences between the prevailing models may stem from differences in experimental designs, but it may also be interpreted as evidence for the existence of multiple mechanisms of miRNA-mediated silencing. Resolution of these matters currently awaits systematic and comparative mechanistic studies. For example, the question of whether two different miRNA families assemble with similar molecular machineries and silence their targets through the same mechanism remains unanswered.

Here we examine the molecular function of abundant maternally and zygotically contributed miRNA families in *C. elegans* embryo. Using a cell-free system, we compared their mechanism of action and surveyed their mRNA targets. We show the broad and direct impact of miRNAs on embryonic mRNA poly(A) tails, and highlight miRISC cooperation as a key feature in target deadenylation.

3.3 Results

3.3.1 Bulk miRISC programming by a few maternal and zygotic miRNA families in *C. elegans* embryos

The *miR-35-42* and *miR-51-56* families are essential for early development (Alvarez-Saavedra and Horvitz, 2010). The *miR-35-42* family is suspected to be mostly maternally

contributed, while the *miR-51-56* as well as the *C. elegans* (Ce)Bantam families (Figure 3-1A) are thought be broadly if not ubiquitously expressed (Ambros et al., 2003; Lau et al., 2001; Stoeckius et al., 2009). We refined the expression domains of these miRNAs using northern blot and qRT-PCR (Figures 3-1B to 1D). Expression of *miR-35* and its precursor is very dynamic. It was strongest in early embryonic preparations (EE) but was rapidly lost at the L1 stage (Figure 3-1B). In contrast, *miR-52* and *miR-58* (Bantam) expression increased as the embryo matured, and was highest during the L1 larval stage preparations, consistent with zygotic transcription accounting for most of their expression (Figures 3-1C and 1D). Similar expression analysis of the other members of these families also indicated zygotic expression (data not shown). *miR-35* is absent in germline-depleted preparations, indicating a germline origin, while *miR-52*, and *miR-58* (bantam) were enriched (Figures 3-1B to 1D, "no germline" lane), indicating somatic expression. Deep sequencing of small RNAs confirmed that *miR-35-42* family members are the most abundantly expressed miRNAs in isolated oocytes (D. Conte, personal communication), hence this family is maternally contributed.

Based on miRNA-specific qRT-PCR, we estimated the concentration of *miR-35* in ME fractions to be approximately 3-8 nM with little batch-to-batch variation, a concentration confirmed using northern blots (see Figure A2-1). To further address the abundance of these miRNAs in embryos, we used biotinylated, nonhydrolyzable 2'-*O*-methylated (2'-*O*-Me) oligonucleotides that mimic miRNA target sites as baits to capture programmed miRISC complexes from embryonic lysates (Figure 3-1E, upper panel) (Hutvagner et al., 2004). The pool of *miR-35-42* miRNAs, even the most divergent family members, was strongly depleted from the lysate using this strategy (Figure A2-2). Pull-

down of *miR-35-42* miRISC in embryonic lysates was effective as indicated by the presence of the Argonautes ALG-1 and ALG-2 (Figure 3-1E, middle panel; note that ALG-1 migrates as multiple species). Quantification indicates that approximately 22% of the entire endogenous embryonic ALG-1/ALG-2 pool is programmed by the *miR-35-42* family alone (Figure 3-1E). In contrast, a *let-7* affinity matrix, which is at most very weakly expressed during embryogenesis, did not pull down significant amounts of miRISC from embryo extracts (Figure 3-1E, middle and lower panels, *let-7* lanes). Using similar capture experiments, we estimate that *miR-51-56* and the *Ce*Bantam families program 13% and 9%, respectively, of the ALG-1/2 pool in ME preparations (Figure 3-1E, lower panel and table). We conclude that a few abundant miRNA families occupy a large fraction of miRISC in *C. elegans* embryos.

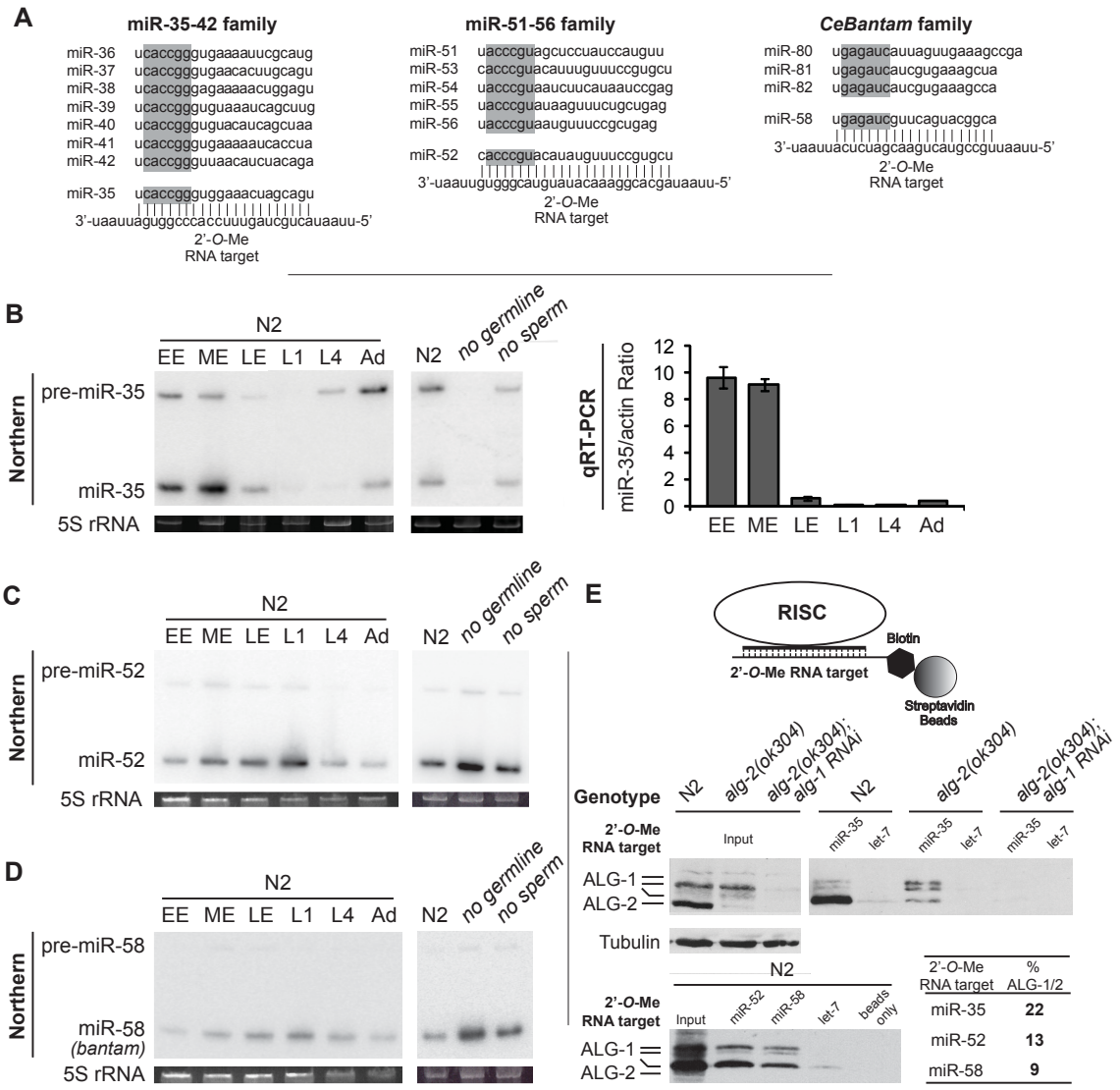
A
miR-35-42 family
miR-36 ucaccgggugaaaauucgcaug
miR-37 ucaccgggugaacacuugcagu
miR-38 ucaccgggagaaaaacuggagu
miR-39 ucaccggguguaaaucagcuug
miR-40 ucaccggguguacaucagcuaa
miR-41 ucaccgggugaaaaaucaccua
miR-42 ucaccggguuaacaucuacaga
miR-35 ucaccggguggaaacuagcagu
3'-uaauuaguggcccaccuuugaucgucauaauu-5'
2'-O-Me
RNA target
miR-51-56 family
miR-51 uacccguagcuccuauccauguu
miR-53 cacccguacauuuguuuccgugcu
miR-54 uacccguaaucuucauaauccgag
miR-55 uacccguauaaguuuucgcugag
miR-56 uacccguaauguuuccgcugag
miR-52 cacccguacauauguuuccgugcu
3'-uaauugugggcauguauacaaaggcacgauaauu-5'
2'-O-Me
RNA target
CeBantam family
miR-80 ugagaucauuaguugaaagccga
miR-81 ugagaucaucgugaaagcua
miR-82 ugagaucaucgugaaagcca
miR-58 ugagaucguucaguacggca
3'-uaauuacucuagcaagucaugccguuaauu-5'
2'-O-Me
RNA target
B
N2
EE ME LE L1 L4 Ad
N2 no germline no sperm
Northern
pre-miR-35
miR-35
5S rRNA
qRT-PCR
miR-35/actin Ratio
12
10
8
6
4
2
0
EE ME LE L1 L4 Ad
C
N2
EE ME LE L1 L4 Ad
N2 no germline no sperm
Northern
pre-miR-52
miR-52
5S rRNA
D
N2
EE ME LE L1 L4 Ad
N2 no germline no sperm
Northern
pre-miR-58
miR-58
(bantam)
5S rRNA
E
RISC
Biotin
2'-O-Me RNA target
Streptavidin
Beads
Genotype
N2
alg-2(ok304)
alg-2(ok304); alg-1 RNAi
N2
alg-2(ok304)
alg-2(ok304); alg-1 RNAi
2'-O-Me RNA target
Input
miR-35
let-7
miR-35
let-7
miR-35
let-7
ALG-1
ALG-2
Tubulin
N2
2'-O-Me RNA target
Input
miR-52
miR-58
let-7
beads only
ALG-1
ALG-2
2'-O-Me RNA target
% ALG-1/2
miR-35 22
miR-52 13
miR-58 9

Figure 3-1: miRISC programming by maternal and zygotic miRNA families in *C. elegans* embryos

(A) Shown are miRNAs and 2'-*O*-Me oligonucleotides used in this study. The seed region for each miRNA is highlighted in gray. (B) Shown is expression profile of *miR-35* by northern and real-time (qRT) PCR analysis. Shown is total RNA from wild-type (N2) early-stage embryos (EE); middle-stage embryos (ME); late-stage embryos (LE); L1-, L4-, and adult-stage animals (Ad); or adult-stage *(glp-4)bn2* (no germline) and *fem-1(hc17)* (no sperm) animals grown at 25°C. 5S ribosomal RNA (rRNA) is indicated as loading control. qRT-PCR results are presented as the mean from triplicate samples and error bars represent standard deviation. (C and D) Shown is northern analysis of *miR-52* and *miR-58* (bantam) expression. (E) (Top) Schematic representation of the miRISC 2'-*O*-Me pull-down strategy. (Middle and bottom) Extracts prepared from wild-type (N2), *alg-2(ok304)*, or *alg-2(ok304); alg-1 RNAi* embryos were incubated with the indicated 2'-*O*-Me matrices. Bound proteins were probed for ALG-1 and ALG-2, and average percentage pulled down of two independent experiments is indicated in bold. See related data in Figure A2-1 of Appendix 2.

3.3.2 Comparative proteomic analysis of embryonic miRISCs

To investigate whether abundant maternal and zygotic miRISC complexes are composed of similar machineries, we used multi-dimensional protein identification technology (MuDPIT) (Wu and MacCoss, 2002) to identify proteins that copurify with *miR-35-42* and *miR-51-56*-miRISC. A set of 15 proteins were identified in at least three independent capture experiments, but were never detected in either mock purifications (beads alone) or using a matrix directed at a nonspecific miRNA (*hsa*miR-16) (Table 3-1). Ten of the interacting proteins were detected in at least one capture experiment for both the *miR-35-42* and *miR-51-56*-miRISC affinity matrices. Known miRISC components (ALG-1, ALG-2, AIN-1, AIN-2) were detected in all affinity purifications for both *miR-35-42*- and *miR-51-56*-directed matrices (five out of five *miR-35* and four out of four *miR-52* captures). Interestingly, DCR-1 was detected in all fractions recovered with both matrices, and its interacting partner RDE-4 (Tabara et al., 2002) was also detected, although less consistently (two out of five *miR-35* and one out of four *miR-52* captures). This observation suggests that, as in mammalians and *Drosophila*, *C. elegans* DCR-1 not only associates with the pre-miRNA maturation machinery but is also a component of the holo-RISC complex (Pham et al., 2004). The capture of these six proteins was further confirmed by western blot (Figure A2-2).

Interestingly, among the detected interactions, TAG-310, SQD-1, and MSI-1 all encode tandem RRM domain proteins and were also previously detected in AIN-1/2 immunoprecipitates (Ding et al., 2005). This raises the possible implication of a new family of proteins in the miRISC. For five of the interacting proteins (Y23H5A.3, MEL-47, SQD-1, MSI-1, and ASD-1), an interaction was only detectable when using the *miR-*

35-42 capture matrix. Although this may reflect differences in the composition of the maternal and zygotic miRISCs, it may also be a consequence of different sensitivities for capture with the two matrices, or a consequence of the less-than-quantitative detection using MuDPIT. Nevertheless, as 10 out of 15 of the consistently detected interactions are common between two capture matrices, our analysis suggests that the maternal and zygotic miRISCs are composed of similar components. This similarity is further supported by the functional analyses provided below.

Gene	Protein Description	% Peptide coverage (# Independent detection)		Western
		α-miR-35	α-miR-52	
C06G1.4	AIN-1 (GW182 homolog)	25.7 (5/5)	14.0 (4/4)	√
B0041.2	AIN-2 (GW182 homolog)	18.5 (5/5)	11.2 (4/4)	√
K12H4.8	DCR-1, Dead box helicase/RNaseIII	16.9 (5/5)	2.0 (4/4)	√
F48F7.1	ALG-1, Piwi/PAZ domain	9.7 (5/5)	5.2 (4/4)	√
T07D3.7	ALG-2, Piwi/PAZ domain	20.1 (5/5)	6.8 (4/4)	√
R10E4.2b	Tag-310, RRM domain	24.7 (3/5)	10.3 (1/4)	
W07B3.2	GEI-4, Coiled-coil domain	11.0 (3/5)	5.4 (1/4)	
T20G5.11	RDE-4, dsRBD	14.0 (2/5)	22.1 (1/4)	√
R09B3.3	Rna15 subunit homolog	32.9 (2/5)	32.9 (1/4)	
F58B3.7	G patch/RRM domain	10.5 (2/5)	7.0 (1/4)	
Y23H5A.3	Novel	7.8 (4/5)	ND	
EEED8.1	MEL-47, RRM domain	8.4 (3/5)	ND	
Y73B6BL.6	SQD-1 (HRP-1 subunit homolog)	19.3 (3/5)	ND	
R10E9.1	MSI-1 (HRP-1 subunit homolog)	12.8 (3/5)	ND	
R74.5a	ASD-1, RRM domain	6.4 (3/5)	ND	

Table 3-1: Comparative proteomic analysis of embryonic miRISCs

MudPIT analysis of proteins interacting with α-miR-35 and α-miR-52 2'-*O*-Me oligonucleotides in wild-type (N2) *C. elegans* embryonic extracts. Identified genes are listed along with their protein description and corresponding peptide coverage (%). The number of times the protein was detected in independent pull-downs is indicated in parentheses. Interactions were confirmed by western blot for those proteins with available antibodies (check marks). ND, not detected. See related data in Figure A2-2.

3.3.3 Cell-free silencing by maternal and zygotic miRNAs

To investigate the mechanism of silencing employed by the *miR-35-42* and *miR-51-56* families, we developed a cell-free translation system from *C. elegans* embryos (see Materials and Methods, Chapter 2, Wu and Duchaine, 2011). Using a *Renilla reniformis* luciferase (RL) reporter mRNA, translation in our system was heavily dependent on 3' poly(A) tail and 5'-m^7GpppG-cap structures (Figure 3-2A). Translation was most efficient for mRNAs bearing both a m^7GpppG-cap and a poly(A) tail and was greater than the additive contributions of either a poly(A) tail or m^7GpppG-cap alone (Figure 3-2A). Hence, this *C. elegans* cell-free translation system recapitulates functional synergy between the 5' m^7GpppG-cap and the 3' poly(A) tail (Gallie, 1991).

To assay for miRNA-mediated silencing activity, we first examined the translation of RL mRNA fused to a synthetic 3'UTR encoding six copies of a *miR-35-42* binding site (Figure 3-2B, 6xmiR-35 mRNA). Reporters were added to the translation system at a concentration of 1nM mRNA, which corresponds to one-third to one-eighth of the measured *miR-35* concentration. Translation of 6xmiR-35 was dramatically impaired in comparison to RL mRNA (compare Figure 3-2A with Figure 3-2C), with activity slowing down and reaching a near-plateau at about 2 hr of incubation (Figure 3-2C). This repression was dependent on *miR-35*, since addition of increasing concentrations of 2'-*O*-Me antisense oligonucleotides to *miR-35* (α-miR-35) released the translation inhibition of 6xmiR-35 (Figures 3-2C and 2D). Derepression reached 3-fold when using 50 nM, for a 3 hr (180 min) translation reaction (Figures 3-2C and 2D). Addition of the same concentrations of a 2'-*O*-Me oligonucleotide complementary to the nonrelated *miR-1* did not affect the translation of 6xmiR-35 (Figures 3-2C and 2D). This

concentration of 2'-*O*-Me oligonucleotide was therefore used for the additional experiments. Similar results were obtained using a *miR-51-56* family reporter and the corresponding 2'-*O*-Me inhibitor (compare Figure 3-2C with 2E). Thus, miRNA-mediated silencing by the *C. elegans miR-35-42* and *miR-51-56* families can be recapitulated *in vitro*.

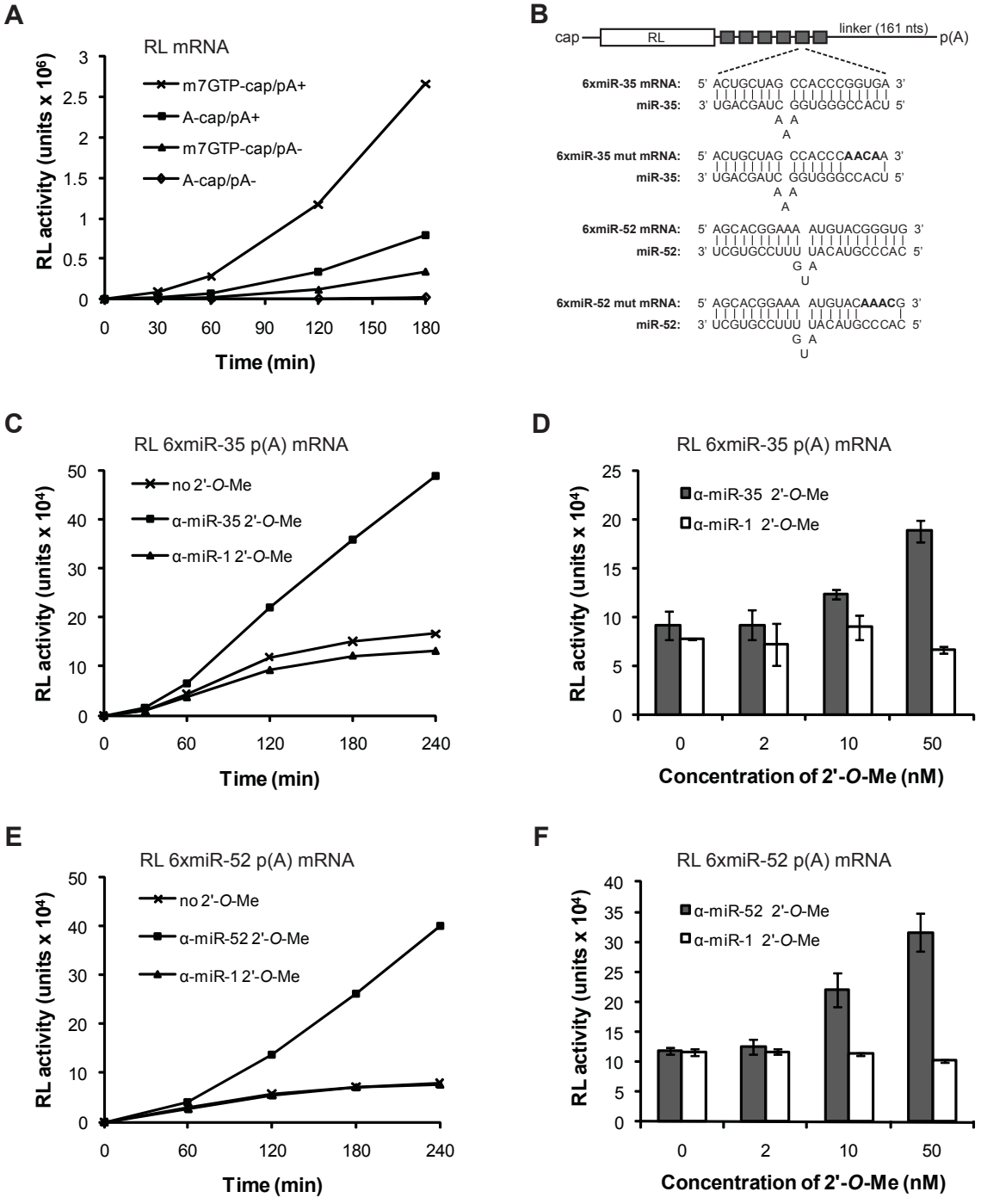
A
RL mRNA
m7GTP-cap/pA+
A-cap/pA+
m7GTP-cap/pA-
A-cap/pA-
RL activity (units x 10⁶)
Time (min)
B
cap
RL
linker (161 nts)
p(A)
6xmiR-35 mRNA: 5' ACUGCUAG CCACCCGGUGA 3'
miR-35: 3' UGACGAUC GGUGGGCCACU 5'
6xmiR-35 mut mRNA: 5' ACUGCUAG CCACCCAACAA 3'
miR-35: 3' UGACGAUC GGUGGGCCACU 5'
6xmiR-52 mRNA: 5' AGCACGGAAA AUGUACGGGUG 3'
miR-52: 3' UCGUGCCUUU UACAUGCCCAC 5'
6xmiR-52 mut mRNA: 5' AGCACGGAAA AUGUACAAACG 3'
miR-52: 3' UCGUGCCUUU UACAUGCCCAC 5'
C
RL 6xmiR-35 p(A) mRNA
no 2'-O-Me
α-miR-35 2'-O-Me
α-miR-1 2'-O-Me
RL activity (units x 10⁴)
Time (min)
D
RL 6xmiR-35 p(A) mRNA
α-miR-35 2'-O-Me
α-miR-1 2'-O-Me
RL activity (units x 10⁴)
Concentration of 2'-O-Me (nM)
E
RL 6xmiR-52 p(A) mRNA
no 2'-O-Me
α-miR-52 2'-O-Me
α-miR-1 2'-O-Me
RL activity (units x 10⁴)
Time (min)
F
RL 6xmiR-52 p(A) mRNA
α-miR-52 2'-O-Me
α-miR-1 2'-O-Me
RL activity (units x 10⁴)
Concentration of 2'-O-Me (nM)

Figure 3-2: Cell-free miRNA-mediated translational repression by maternal and zygotic miRNAs

(A) Cap and poly(A) tail synergy in *C. elegans* embryonic extracts. The translation of 10 nM RL reporters bearing a physiological 5' m^7GpppG-cap, a 5' ApppG-cap, and/or 3' poly(A) tail was monitored over a 3 hr time course. (B) Schematic representation of the RL reporter mRNAs used. Sequences of the miR-35- and miR-52-binding sites (6xmiR-35 and 6xmiR-52) and mutated binding sites (6xmiR-35 mut and 6xmiR-52 mut) are shown. (C and E) Translation time course of RL 6xmiR-35 (C) and 6xmiR-52 mRNAs (E) with or without 50 nM specific (α-miR-35 [C], α-miR-52 [E]) or nonspecific α-miR-1 2'-*O*-Me. (D and F) Dose-response translation derepression by α-miR-35 (D) and α-miR-52 (F) 2'-*O*-Me for a 3 hr reaction. Each bar represents the mean from triplicate independent experiments, and error bars indicate standard deviation.

3.3.4 Zygotic and maternal miRNAs direct deadenylation

To determine the mechanism of miRNA-mediated silencing in our translation system, we examined the integrity of ^{32}P-radiolabeled reporter mRNAs by polyacrylamide gel electrophoresis (Figure 3-3). The RL mRNA reporter was remarkably stable over the 3 hr of incubation (Figure 3-3A, RL panel). In contrast, the RL 6xmiR-35 reporter was completely converted to a second, shorter RNA species within 120 minutes (Figures 3A–3C). Cloning and sequencing revealed that this RNA species corresponds to the deadenylated RL 6xmiR-35 reporter (see below). Quantification of multiple independent experiments, indicates that deadenylation reached half completion ($t_{d1/2}$) within the first 45 min of incubation, with slight variations between the extract preparations (for example, compare Figure 3-3A, $t_{d1/2}$ 30 ± 6 min, and Figure 3-3C, $t_{d1/2}$ 45 ± 2 min).

Three series of control experiments indicate that the deadenylation of RL 6xmiR-35 mRNA is dependent on targeting by miR-35-RISC. First, deadenylation was specifically blocked by the addition of α-miR-35 2'-*O*-Me (Figure 3-3A, + α-miR-35 panel), but was insensitive to the addition of α-miR-1, α-miR-52, or α-let-7 2'-*O*-Me (+ α-miR-1 panel, and data not shown). Second, the deadenylation of RL 6xmiR-35 mRNA was substantially delayed in the *alg-2(ok304); alg-1 RNAi* extract, with less than half of the RL 6xmiR-35 reporter mRNA deadenylated after 4 hr (Figure 3-3B, *alg-2(ok304); alg-1 RNAi*). Third, RL 6xmiR-35 mut reporters, where miR-35 complementary sites have been altered (see Figure 3-2B for mutation design), were not deadenylated in the extract (Figure 3-3C, RL 6xmiR-35 mut panel).

The RL 6xmiR-52 reporter was deadenylated with similar kinetics, and again processing was specifically prevented by a 2'-*O*-Me inhibitor (Figure A2-3, + α-miR-52

panel), or by mutation of the seed-complementary site (Figure A2-3, RL 6xmiR-52 mut panel, see Figure 3-2B for mutation design). We conclude that both *miR-35-42* and *miR-51-56* families direct potent and sequence-specific deadenylation in *C. elegans* embryonic extracts.

To precisely match the timing of translation repression with the fate of the reporter mRNAs, radiolabeled and polyadenylated RL 6xmiR-35 and RL 6xmiR-35 mut reporters were subjected to a time course of miRNA-mediated translation repression, and the same samples were examined for translation and PAGE-autoradiography (Figure 3-3C). Strikingly, the progression of deadenylation paralleled the course of translation repression of the reporters. Considered with the important contribution of the poly(A) tail for translation in our system (see Figure 3-2A), this observation suggests that deadenylation accounts for a major part of the translation repression observed in our system. It does not rule out, however, a minor contribution for additional mechanisms in the early phases of the target recognition by miRISC.

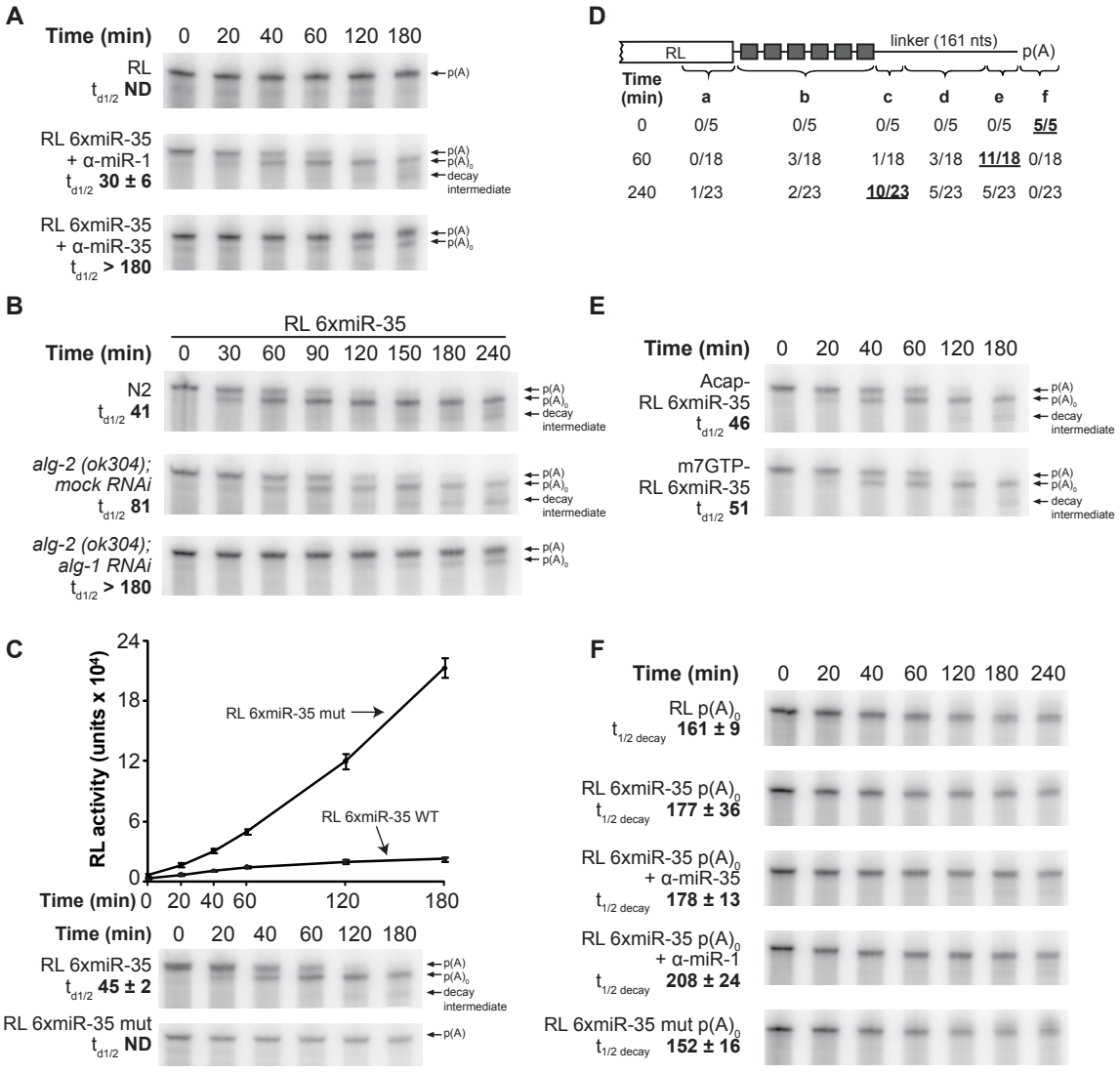
A
Time (min) 0 20 40 60 120 180
RL
$t_{d1/2}$ ND
p(A)
RL 6xmiR-35
+ α-miR-1
$t_{d1/2}$ 30 ± 6
p(A)
p(A)0
decay
intermediate
RL 6xmiR-35
+ α-miR-35
$t_{d1/2}$ > 180
p(A)
p(A)0
B
RL 6xmiR-35
Time (min) 0 30 60 90 120 150 180 240
N2
$t_{d1/2}$ 41
alg-2 (ok304);
mock RNAi
$t_{d1/2}$ 81
alg-2 (ok304);
alg-1 RNAi
$t_{d1/2}$ > 180
C
RL activity (units x 10^4)
24
18
12
6
0
RL 6xmiR-35 mut
RL 6xmiR-35 WT
Time (min) 0 20 40 60 120 180
Time (min) 0 20 40 60 120 180
RL 6xmiR-35
$t_{d1/2}$ 45 ± 2
RL 6xmiR-35 mut
$t_{d1/2}$ ND
D
RL
linker (161 nts)
p(A)
Time (min) a b c d e f
0 0/5 0/5 0/5 0/5 0/5 5/5
60 0/18 3/18 1/18 3/18 11/18 0/18
240 1/23 2/23 10/23 5/23 5/23 0/23
E
Time (min) 0 20 40 60 120 180
Acap-
RL 6xmiR-35
$t_{d1/2}$ 46
m7GTP-
RL 6xmiR-35
$t_{d1/2}$ 51
F
Time (min) 0 20 40 60 120 180 240
RL p(A)0
$t_{1/2\ decay}$ 161 ± 9
RL 6xmiR-35 p(A)0
$t_{1/2\ decay}$ 177 ± 36
RL 6xmiR-35 p(A)0
+ α-miR-35
$t_{1/2\ decay}$ 178 ± 13
RL 6xmiR-35 p(A)0
+ α-miR-1
$t_{1/2\ decay}$ 208 ± 24
RL 6xmiR-35 mut p(A)0
$t_{1/2\ decay}$ 152 ± 16

Figure 3-3: Embryonic miRISCs direct deadenylation but do not promote target decay *in vitro*

(A and B) (A) Deadenylation time course of RL and RL 6xmiR-35 with the indicated 50 nM 2'-*O*-Me, and (B) of RL 6xmiR-35 in wild-type (N2), *alg-2(ok304); mock (gfp) RNAi*, or *alg-2(ok304); alg-1 RNAi* embryonic extracts. (C) Time course of RL 6xmiR-35 WT and mutant translation and deadenylation. The same samples from each time points were examined in translation (upper panel) and PAGE-autoradiography (lower panels). (D) Schematic representation of 3'RACE products from RL 6xmiR-35 at the indicated time points. The indicated number of reads terminated (a) within the RL open reading frame, (b) between the miR-35 binding sites, (c) within the first 40 nt 3' of the miR-35 binding sites, (d) within the middle region of the 3'UTR, (e) within less than 25 nt 5' of the poly(A) tail, and (f) within the poly(A) tail. (E) Deadenylation time course of RL 6xmiR-35 mRNA bearing a m^7GpppG cap or ApppG cap. (F) Decay time course of unadenylated reporters. (B) and (E) are representative of two independent experiments; (A), (C), and (F) are representative of triplicate experiments conducted using the same extract preparation. Half-deadenylation ($t_{d1/2}$) and half-life ($t_{1/2\ decay}$) were quantified using ImageJ. ± indicates standard deviation. See related data in Figure A2-3.

3.3.5 Embryonic miRISC does not mediate target decay *in vitro*

MiRNAs often direct the destabilization of target mRNAs. In our system, miRNA target reporters proved remarkably stable, even after being fully deadenylated (see Figures 3-3A to 3C, $p(A)_0$ labeled band, average $t_{1/2\ decay}$ 183 min). This observation prompted us to ask whether targeting by embryonic miRISC results in target degradation in addition to deadenylation. Upon close examination of *miR-35-42* and *miR-51-56*-deadenylated reporter autoradiograms, we noticed the appearance of shorter RNA species at or around 3 hr of incubation (Figures 3-3A to 3C, and Figure A2-3, see "intermediate" arrows). These intermediates accumulated in a miRNA- and/or deadenylation-dependent manner, as cognate *miR-35-42* and *miR-51-56* 2'-*O*-Me inhibitors, or genetic depletion of *alg-1/2* prevented their accumulation (see "intermediate" arrow in Figures 3-3A to 3C). Sequencing of the recovered reporter mRNA population indicated that while the vast majority of reads terminated at or very near the polyadenylation site at the 60 min time point (region e in Figure 3-3D), reads from clones recovered after 240 min clustered closely in the 3' region bordering the miRNA-binding site repeats (Figure 3-3D, region c). This indicates that the embryonic extract is capable of mRNA decay. The continuous removal of sequences further upstream of the poly(A) tail over time suggests the involvement of a 3'→5' exonuclease activity.

A number of studies have suggested that miRNA-promoted decay involves a decapping step (Bagga et al., 2005; Behm-Ansmant et al., 2006). To address whether de-capping is involved in the slow turnover of the reporters, we examined the fate of ApppG-capped mRNAs that are not recognized by cellular decapping enzymes (Grudzien-Nogalska et al., 2007; Wang et al., 2002). The time-course of deadenylation

and decay for the ApppG-capped transcript closely mirrored the profile of the m^7GpppG-capped reporters (Figure 3-3E), indicating that reporter decay does not require decapping in the extract. It also further supports the notion that mRNA decay occurs via a 3'→5' activity in the embryonic extracts.

The observed decay could be due to a nonspecific 3'→5' activity acting on every reporter in the extract, or it could be the result of the miRISC actively promoting decay of the deadenylated reporters. Hence, we examined the stability of RL reporters lacking a poly(A) tail but bearing functional (6xmiR-35) or non-functional (6xmiR-35 mut) miRISC-binding sites (Figure 3-3F). RL 6xmiR-35 $p(A)_0$ ($t_{1/2\ decay}$ 177 ± 36 min) was at least as stable as RL 6xmiR-35 mut $p(A)_0$ ($t_{1/2\ decay}$ 152 ± 16 min), or RL $p(A)_0$ ($t_{1/2\ decay}$ 161 ± 9 min). Addition of 2'-*O*-Me oligonucleotides slightly increased the stability of RL 6xmiR-35 $p(A)_0$ but not in a sequence-specific manner, presumably due to competition for nonspecific RNases in the extract. Similarly, the RL 6xmiR-52 $p(A)_0$ reporter was at least as stable as the RL 6xmiR-52 mut $p(A)_0$ (Figure A2-3B). Overall, these results indicate that miRISC does not directly mediate the destabilization of the target mRNA but rather directs the generation of a stable deadenylated mRNA in the embryonic extract.

3.3.6 Pervasive deadenylation of embryonic miRNA targets

To obtain a measure of if and how natural 3'UTRs would undergo miRNA-mediated silencing in this cell-free system, we undertook a survey of mRNA deadenylation and decay by sampling the predicted *miR-35-42* 3'UTR targets. 3'UTRs of *miR-35-42* targets (as per TargetScan (Friedman et al., 2009) and mirWIP (Hammell et al., 2008) predictions) were cloned as fusions to a truncated fragment of RL mRNA sequence to improve gel resolution in the deadenylation assay. Transcripts were then incubated in

embryonic extracts, recovered, and resolved by denaturing PAGE, as presented above. A control experiment with the 6xmiR-35 3′UTR, as well as a representative sample of the natural 3′UTRs surveyed, is presented in Figure 3-4A.

Roughly half of the 3'UTRs examined were rapidly deadenylated in the extract, highlighting the prevalence of deadenylation as an embryonic mRNA regulation mechanism (Figure 3-4A, groups 2 and 3). The rate of deadenylation (compare *spn-4* to *r05h11.2* 3'UTR for example) as well as the pattern (compare *spn-4* and *r05h11.2* to *y71f9b.8* 3'UTRs) varied broadly, indicating the 3'UTR-specific properties of the deadenylation process. Deadenylation of a subset of these targets was substantially blocked by incubation with the α-miR-35 2'-*O*-Me inhibitors but not the α-miR-1 2'-*O*-Me inhibitor (group 2), indicating that deadenylation was dependent on *miR-35*. This subset includes the 3'UTR of the proapoptotic BH3-only homolog *egl-1*, and the toll-ish homolog *toh-1* (Figure 3-4A, group 2). Since all of the natural 3'UTRs were also predicted to be targeted by additional embryonic miRNAs (see 3'UTR legend on left, blue crossbars), deadenylated target 3'UTRs were incubated in extracts depleted of ALG-2 or both ALG-1 and -2 (Figure 3-4B for examples, also see Figure A2-4 for a control of the extract translation activity). Strikingly, depletion of both ALG-1 and ALG-2 together prevented deadenylation for all deadenylated targets screened thus far, including group 3 targets that were resistant to α-miR-35. These data indicate the involvement of embryonic miRISCs in the deadenylation of an important variety of natural 3'UTR targets.

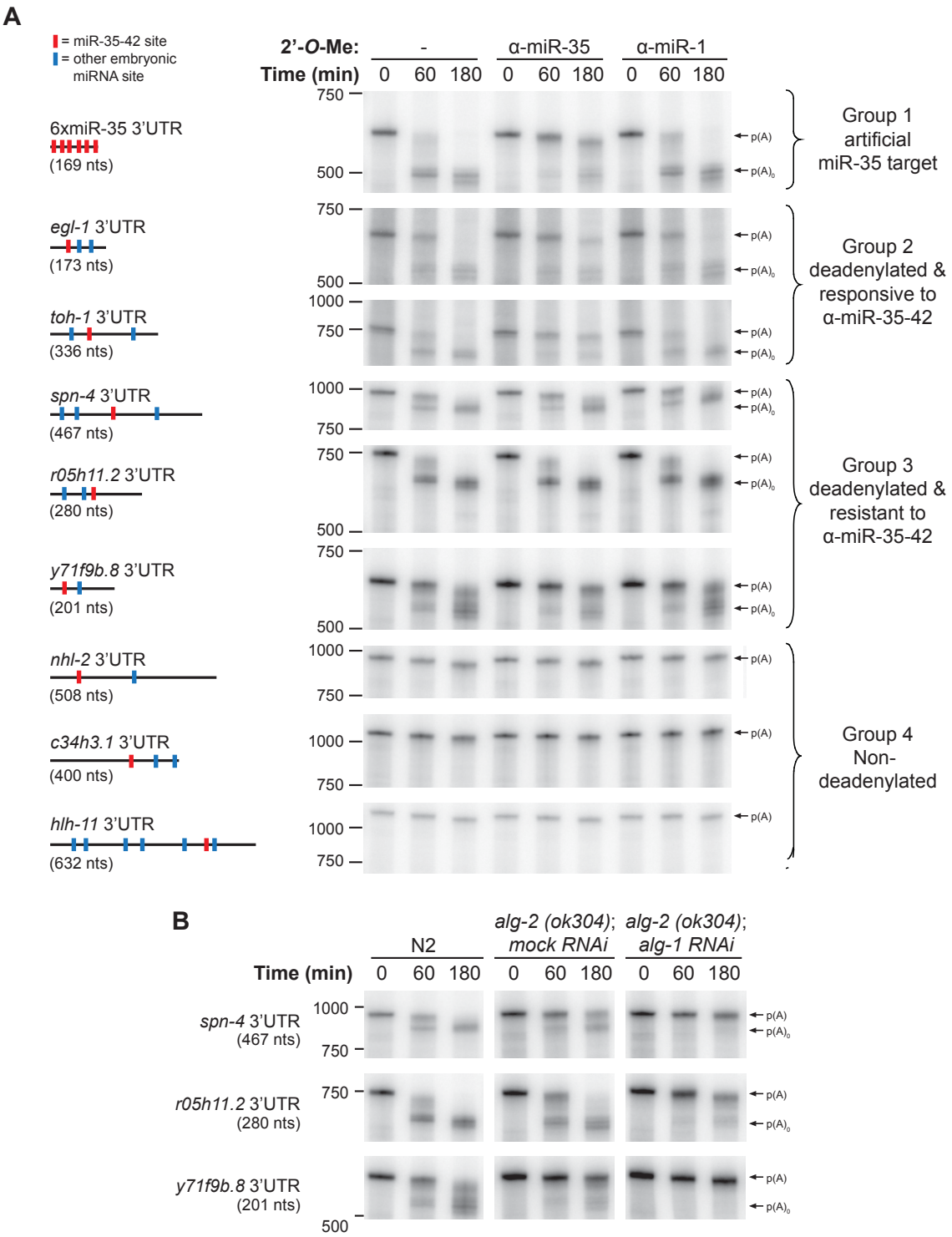
A
= miR-35-42 site
= other embryonic miRNA site
2'-O-Me:
-
α-miR-35
α-miR-1
Time (min)
0 60 180 0 60 180 0 60 180
6xmiR-35 3'UTR
(169 nts)
egl-1 3'UTR
(173 nts)
toh-1 3'UTR
(336 nts)
spn-4 3'UTR
(467 nts)
r05h11.2 3'UTR
(280 nts)
y71f9b.8 3'UTR
(201 nts)
nhl-2 3'UTR
(508 nts)
c34h3.1 3'UTR
(400 nts)
hlh-11 3'UTR
(632 nts)
750
500
1000
p(A)
p(A)0
Group 1
artificial
miR-35 target
Group 2
deadenylated &
responsive to
α-miR-35-42
Group 3
deadenylated &
resistant to
α-miR-35-42
Group 4
Non-
deadenylated
B
N2
alg-2 (ok304); mock RNAi
alg-2 (ok304); alg-1 RNAi
Time (min)
0 60 180 0 60 180 0 60 180
spn-4 3'UTR
(467 nts)
r05h11.2 3'UTR
(280 nts)
y71f9b.8 3'UTR
(201 nts)
1000
750
500
p(A)
p(A)0

Figure 3-4: miRNA-mediated deadenylation is prevalent in embryos

(A) Deadenylation of natural 3'UTR reporters in embryonic extracts. 3'UTRs were fused to a truncated RL fragment (nucleotides 764-936 [172 nt long]), for all UTRs screened except *c34h3.1* where nucleotides 491-936 were included. Reporters also encoded a 161 nt linker and a poly(A) tail of 87 nt. Schematic representation of each 3'UTRs is depicted on the left (size in parentheses). Red bars denote *miR-35-42* sites, blue bars denote sites for miRNA that are known to be expressed in embryos (Stoeckius et al., 2009). Courses were realized with or without 50 nM 2'-*O*-Me (either α-miR-35 or α-miR-1 [C-]). 3'UTRs are divided into four groups: (1) deadenylated artificial miR-35 target (6xmiR-35, control), (2) deadenylated 3'UTR targets that are responsive to α-miR-35, (3) deadenylated 3'UTR targets that are resistant to α-miR-35, and (4) 3'UTRs not subjected to detectable deadenylation. (B) Time course of group 3 in N2, *alg-2(ok304); mock (gfp) RNAi*, and *alg-2(ok304); alg-1 RNAi* embryonic extracts. Experiments were reproduced at least twice in independent extract preparations. See related data in Figure A2-4.

3.3.7 Target deadenylation requires miRISC cooperation

To better understand how *miR-35-42* miRNAs direct deadenylation and repress translation, we further characterized the properties of the *toh-1* and *egl-1* 3'UTRs (Figures 3-5A to 5C). According to the bioinformatic predictions using the TargetScanWorm program (release 5.1), the 3'UTRs of *toh-1* and *egl-1* encode four and five miRNA-binding sites, respectively. Among those, the sites for the *miR-35-42* and *Ce*Bantam families (Figures 3-5A and 5B, colored boxes on UTR legends) match miRNAs that are detectable in the early embryo. The remaining sites (gray boxes) match miRNAs that are undetectable in our system by northern blotting (Figure A2-5A), or that did not have any detectable functional implications when inhibited using 2'-*O*-Me (Figure A2-5B). Strikingly, deadenylation of reporters encoding these 3'UTRs was slowed by negating a single one of these two miRNA families (*miR-35-42* or *Ce*Bantam) using sequence-specific 2'-*O*-Me inhibitors (Figure 3-4, group 2, and Figures A2-5B and 5C), suggesting that both miRNA families are required to initiate efficient deadenylation on these 3'UTRs. To assess the precise contribution of each miRNA-binding site, we mutated the predicted *miR-35-42* and bantam-binding sites within the *toh-1* and *egl-1* 3'UTRs and examined their effects on deadenylation and translation repression assays (Figures 3-5A and 5B). For reporters containing the *toh-1* 3'UTR (RL *toh-1* WT, $t_{d1/2}$ 52 ± 2 min), mutating either the *miR-35-42* or the bantam site alone effectively impaired deadenylation (RL *toh-1* miR-35 mut, $t_{d1/2}$ >>> 180 min; RL *toh-1* bantam mut, $t_{d1/2}$ 152 ± 7 min), whereas no deadenylation could be detected when using the double mutant 3'UTR (RL *toh-1* miR-35 + bantam mut). These reporters were also derepressed to the same extent in translation assays (Figure 3-5A, bottom panel). While these data cannot

rule out a weak and residual activity for the *miR-35-42* site on its own, they indicate that the *miR-35-42* and the *Ce*Bantam miRNA families cooperate synergistically in promoting the deadenylation and silencing on the *toh-1* 3'UTR.

In similar reporter assays, the 3'UTR of the *egl-1* mRNA also mediated a potent translation repression and a rapid deadenylation (Figure 3-5B, RL *egl-1* WT, $t_{d1/2}$ 53 ± 8 min). Mutation of the *miR-35-42* binding site on its own, or in combination with an additional mutation in the predicted bantam site at position 86, completely abrogated reporter deadenylation and translation repression (RL *egl-1* miR-35 mut, and RL *egl-1* miR-35 + bantam mut). Mutation of this bantam target site on its own, however, had only a mild effect on the course of deadenylation and on translation repression (RL *egl-1* bantam mut, $t_{d1/2}$ 79 ± 15 min). This observation first appeared surprising, as bantam-specific 2'-*O*-Me inhibitors efficiently inhibited the deadenylation and derepressed the translation of the RL *egl-1* WT reporter (Figure 3-5C, upper panels, Figures A2-5B and 5C). Further analysis of the *egl-1* 3'UTR using the mirWIP algorithm (Hammell et al., 2008) revealed a second, atypical bantam-binding site in the 5' vicinity of the *miR-35-42* binding site, starting at position 38 (Figure 3-5C, upper panel). This second site (named bantam G:U) base pairs extensively with *miR-58* (ΔG_{hybrid} -17.1 kcal/mol, in comparison to -18.3 kcal/mol for the first bantam site at nt 38) includes four G:U wobble base pairs, two of which are located within the seed sequence region, and also features an extensive base pairing (6 bp) with the 3' sequence of *miR-58*. Interestingly, deadenylation of the RL *egl-1* bantam mut reporter was specifically and potently impaired by the presence of α-miR-58 2'-*O*-Me inhibitor (Figure 3-5C, bottom panel). This suggests that the bantam G:U site accounts for a major part of the impact of bantam miRNAs on the *egl-1* 3'UTR.

These observations also suggest that noncanonical miRNA-binding sites can contribute to the cooperativity between multiple miRNA-binding sites that is required for miRNA-mediated deadenylation.

Thus far, our results indicate that the cooperation between at least two separate miRISC-binding sites in a natural 3'UTR is required to potentiate miRNA-mediated deadenylation. To better define this cooperation, we engineered reporter mRNAs bearing one, two, three, or four *miR-35-42* binding sites, and examined their fate in deadenylation assays (Figure 3-5D). Interestingly, deadenylation was not observed for the artificial reporters bearing one or two *miR-35* target sites. However, increasing the distance between the *miR-35* target sites from 5 to 29 nt in the 2xmiR-35 reporter resulted in a detectable but modest deadenylation (see 2xmiR-35 spaced). Deadenylation was dramatically accelerated by additional *miR-35-42* binding sites, with $t_{d1/2}$ 74 ± 9 min and 46 ± 2 min for 3xmiR-35 and 4xmiR-35, respectively (Figure 3-5D). A similar effect was observed when analogous (1x-4x) *miR-51-56* family reporters were examined (Figure A2-5D). This effect was not the result of varying distances between the sites and the poly(A) tail, as all the reporters encode the same sequence between the last miRNA-binding site and the poly(A) tail, and shortening or doubling the distance to the poly(A) tail had, by comparison, only a minor effect on the course of deadenylation (Figure A2-5E). Altogether, these results demonstrate that miRISC cooperation is required to potentiate miRNA target deadenylation.

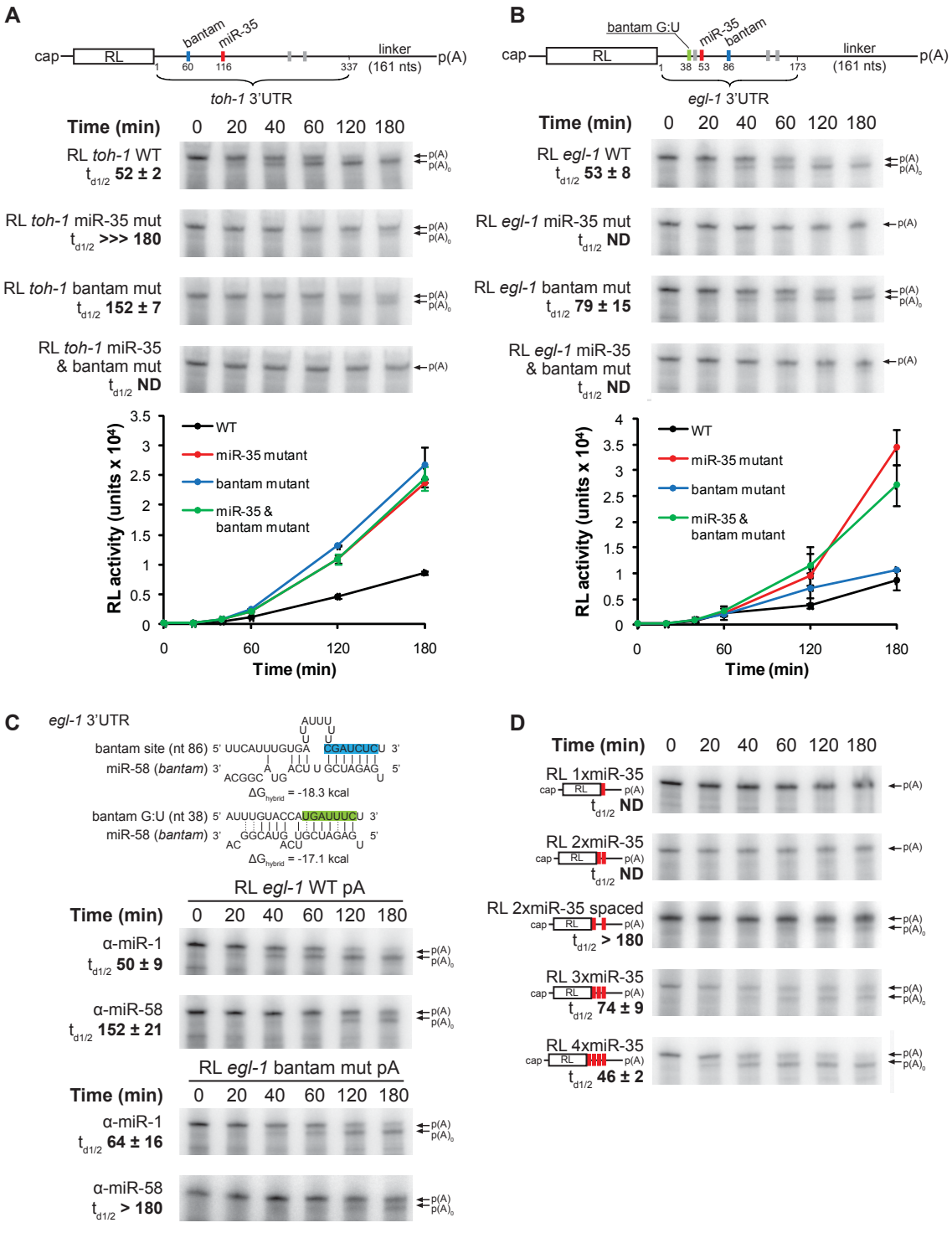
A
cap
RL
bantam
miR-35
linker
(161 nts)
p(A)
1
60
116
337
toh-1 3'UTR
Time (min)
0 20 40 60 120 180
RL toh-1 WT
t d1/2 52 ± 2
RL toh-1 miR-35 mut
t d1/2 >>> 180
RL toh-1 bantam mut
t d1/2 152 ± 7
RL toh-1 miR-35
& bantam mut
t d1/2 ND
p(A)
p(A)0
RL activity (units x 10⁴)
WT
miR-35 mutant
bantam mutant
miR-35 &
bantam mutant
Time (min)
B
bantam G:U
miR-35
bantam
1
38
53
86
173
egl-1 3'UTR
RL egl-1 WT
t d1/2 53 ± 8
RL egl-1 miR-35 mut
t d1/2 ND
RL egl-1 bantam mut
t d1/2 79 ± 15
RL egl-1 miR-35
& bantam mut
t d1/2 ND
C
egl-1 3'UTR
AUUU
bantam site (nt 86) 5' UUCAUUUGUGA CGAUCUCU 3'
miR-58 (bantam) 3' ACGGC UG A ACU U GCUAGAG U 5'
ΔG hybrid = -18.3 kcal
bantam G:U (nt 38) 5' AUUUGUACCA UGAUUUCU 3'
miR-58 (bantam) 3' AC GGCAUG ACU UGCUAGAG U 5'
ΔG hybrid = -17.1 kcal
RL egl-1 WT pA
α-miR-1
t d1/2 50 ± 9
α-miR-58
t d1/2 152 ± 21
RL egl-1 bantam mut pA
α-miR-1
t d1/2 64 ± 16
α-miR-58
t d1/2 > 180
D
RL 1xmiR-35
t d1/2 ND
RL 2xmiR-35
t d1/2 ND
RL 2xmiR-35 spaced
t d1/2 > 180
RL 3xmiR-35
t d1/2 74 ± 9
RL 4xmiR-35
t d1/2 46 ± 2

Figure 3-5: Target deadenylation requires miRISC cooperation

(A and B) Deadenylation and translation time courses of RL *toh-1* WT (A) and RL *egl-1* WT (B) 3'UTR reporters in wild-type (N2) embryo extract. Detailed schematic representation of 3'UTR reporter mRNAs is shown. Red bars indicate *miR-35-42* sites, blue and green bars indicate sites for *Ce*Bantam family members, and gray bars indicate sites for miRNAs that were not detected and/or had no detectable functional implications in our system (see also Figure A2-5). (C) (Top) Pairing of the *egl-1* 3'UTR *miR-58* (bantam) sites; the site with canonical base-pairing is in blue, and the noncanonical site containing G:U wobble base-pairing is in green. (Middle and bottom) Deadenylation time course of the RL *egl-1* WT, and the RL *egl-1* bantam mut mRNA (encodes mutations within the canonical *bantam* site) in the presence of 50 nM α-miR-58, or the negative control α-miR-1. (D) Deadenylation time course of RL reporter mRNAs encoding one to four copies of *miR-35* binding sites. The 2xmiR-35 spaced reporter contains two miR-35 separated by 29 nt. Translation and deadenylation assays were conducted as triplicate of independent experiments. Quantifications of the half-deadenylation ($t_{d1/2}$) were realized using ImageJ. Error bars and ± indicate standard deviation. See related data in Figure A2-5.

3.4 Discussion

3.4.1 Impact of embryonic miRNAs on mRNA polyadenylation and stability

Previous work indicates that miRNA-mediated deadenylation correlates with miRNA-directed destabilization. This has been particularly well supported in zebrafish and *Drosophila* embryos where a few abundant zygotic miRNA families drive deadenylation and rapid turnover of maternal mRNA targets, in a process required for a timely maternal-to-zygotic gene expression transition (MZT) (Giraldez et al., 2006). On this particular aspect, the *in vitro* properties of the *C. elegans* maternal and zygotic embryonic miRISCs appear to contrast. Even though the *miR-35-42*, *miR-51-56*, and *Ce*Bantam miRISCs directed rapid deadenylation of artificial and natural targets, the deadenylated mRNAs remained surprisingly stable. The slow 3'→5' destabilization of mRNA targets in this cell-free embryonic system remained unaffected by alteration of the m^7GpppG-cap structure, and was not directly promoted by miRISC recruitment. Consistent with miRNAs not promoting the destabilization of certain target mRNAs *in vivo*, neither *toh-1* nor *egl-1* mRNA levels were significantly increased in *alg-2(ok304); alg-1 (RNAi)* embryos (Figure A2-6). Transcriptional compensation for rapid miRNA-mediated decay appears unlikely, in particular for maternal miRNA targets, as gene expression in the early embryo is largely governed by maternally provided mRNAs and is under extreme transcriptional restriction (Seydoux and Fire, 1994). We hypothesize, instead, that miRNA-mediated deadenylation in the early *C. elegans* embryo is either completely uncoupled, or only conditionally coupled with target destabilization.

Uncoupling between deadenylation, decapping and decay in the maturing oocyte and in the early embryo may be essential to prevent premature degradation of maternal mRNA targets that are coinherited with highly abundant miRNAs. Such a biochemical condition might be a feature of P bodies (a structure thought to be involved in miRNA-mediated silencing (Ding et al., 2005)) in the germline (Boag et al., 2008) and in the earliest phases of embryonic development (Gallo et al., 2008). A recent study, which revealed that P bodies are inherited with – but are distinct from – germ granules and lack essential decapping activators in the early embryo lends credence to this model. This property may, under certain conditions, allow for the derepression and mRNA expression in a temporal manner via readenylation (see model in Figure 3-6, and figure legends). Interestingly, somatic P bodies "mature" biochemically and later acquire the LSM-1 and LSM-3 decapping activators (Gallo et al., 2008). In time, this maturation, and possibly other means of miRISC regulation could be key events to couple deadenylation with further decay, hence accelerating the degradation of miRNA targets.

3.4.2 3'UTR-specific modulation of miRNA-mediated silencing outcomes

The survey of 3'UTR targets of the *miR-35-42* family unveiled the direct and potentially broad impact of miRNAs on the deadenylation of embryonic mRNAs. The cooperative contribution of neighboring RISC-binding sites on silencing had been noticed through the early studies of artificial reporters in transfection assays, and through genome-wide bioinformatics studies (Grimson et al., 2007; Saetrom et al., 2007). The Grimson study even identified the distance between RISC-binding sites and the poly(A) tail as a significant parameter for the potency of silencing, but how these determinants altered the mechanism of miRNA-mediated silencing was unknown. Our embryonic system allowed

a direct perspective on the mechanistic impact of this cooperation: we show that synergy between distinct miRNA-binding sites can drastically potentiate deadenylation.

Potentiation of deadenylation through miRISC cooperation appears to be a common feature of the two targets studied in details here: the *tollish* family member *toh-1* and the BH3-only protein encoding *egl-1*. In this latter case, the biological implications of the collaborative regulation by multiple miRNA families are potentially immense for embryonic development. A finely tuned level of EGL-1 protein is thought to be the key to trigger apoptosis in a large number of cell lineages in *C. elegans* (Nehme and Conradt, 2008). Our observations also point to a striking evolutionary conservation of the role for miRNA in the regulation of apoptosis: *Ce*Bantam miRNAs, just like the *Drosophila Bantam* miRNA which downregulates *hid* (Brennecke et al., 2003), antagonize apoptosis. Curiously, regulation of *egl-1* homologs by miRNAs also occurs in humans and is often altered in cancer. Mammalian *egl-1* homolog and proapoptotic Bim is a known target of the oncogenic *miR-17-92* polycistron (Inomata et al., 2009; Ventura et al., 2008), and its protein partner BCL-2 is also heavily regulated by miRNAs including *miR-15a*, *miR-16-1* (Calin et al., 2008; Cimmino et al., 2005) and miR-34 (Ji et al., 2009). Hence, coordinated regulation of the *egl-1* transcript by maternal and zygotic miRNAs represents yet another aspect in the tight control of the BH-3 family of proteins in apoptotic cellular decisions.

Some observations in the 3'UTR functional survey may suggest that cooperation between *cis* elements in promoting deadenylation is not restricted to miRISC-binding sites. One example, the *y71f9b.8* 3'UTR, encodes two miRISC-binding sites which match known embryonically expressed miRNAs (i.e., the *miR-35-42* and *miR-72-74*). Yet, this

3’UTR drives efficient deadenylation, even when *miR-35-42* is inhibited, although with a distinct, nonprocessive pattern (Figure 3-4). At this point, we cannot rule out that noncanonical miRISC-binding sites may have been missed in the predictions on *y71f9b.8* 3’UTR sequences. An attractive and alternative possibility, however, is that the miRISC-binding sites may cooperate with additional *cis*-acting sequences within the *y71f9b.8* 3’UTR to promote deadenylation. Such a possibility finds echoes in recent findings by the Ambros group indicating that RNA-binding proteins (Hammell et al., 2009) can be required to potentiate miRISC action on specific targets.

In closing, our survey suggests that an accurate assessment of miRNA-mediated silencing mechanisms requires a careful consideration of context- and 3’UTR-specific outcomes. The modulation of miRNA-mediated silencing mechanisms through miRISC cooperation, or through interactions with additional elements within UTRs, could provide flexibility in adapting the function of miRNAs to different genetic environments such as the transcriptionally silent embryo and fully differentiated somatic cells.

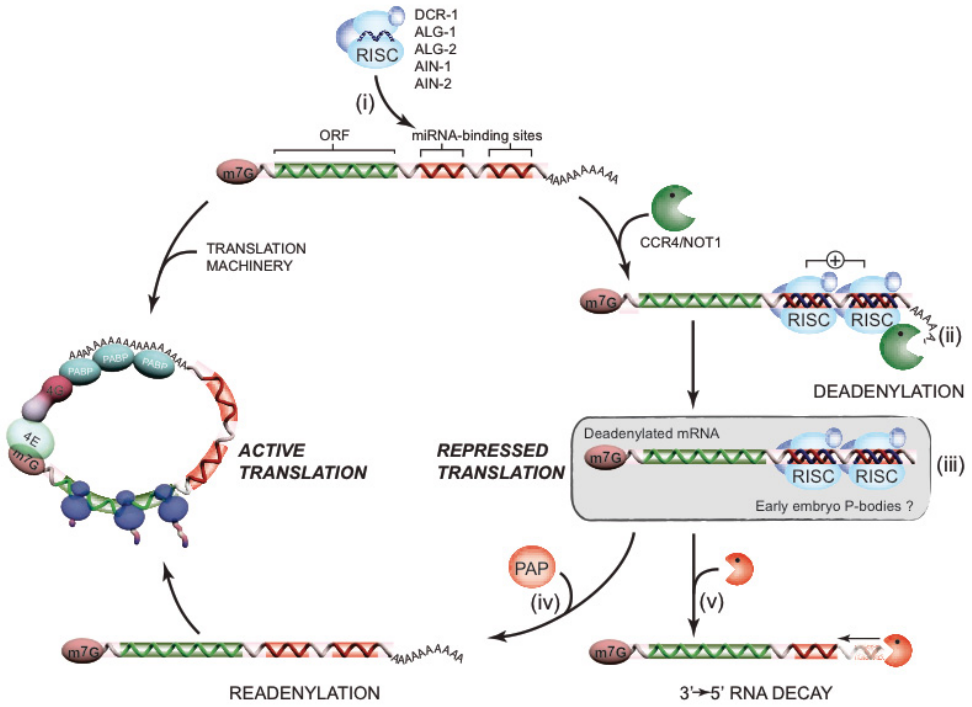
DCR-1
ALG-1
ALG-2
AIN-1
AIN-2
RISC
(i)
ORF
miRNA-binding sites
m7G
AAAAAAAAA
TRANSLATION
MACHINERY
CCR4/NOT1
RISC
RISC
(ii)
DEADENYLATION
PABP
4G
4E
ACTIVE
TRANSLATION
REPRESSED
TRANSLATION
Deadenylated mRNA
(iii)
Early embryo P-bodies ?
PAP
(iv)
(v)
READENYLATION
3'→5' RNA DECAY

Figure 3-6: A model for the deadenylation and decay of early embryo miRNA targets.

The miRISC complex (ALG-1/2, AIN-1/2, DCR-1 and other accessory proteins), programmed by the abundant maternal and zygotic miRNA families, scans and recognizes mRNA targets (i). Through functional cooperation (indicated by a + sign), embryonic miRISCs recruit and/or activate the deadenylase complex (CCR4/NOT was previously identified in a number of studies, including our own) and direct the rapid deadenylation of the target (ii). The stability of deadenylated mRNAs and the association with GW182 proteins AIN-1 and AIN-2 on our target site baits in proteomics suggest that deadenylated targets may be protected and/or stored within the miRISC, or possibly within P body-like structures (iii). One consequence of this stability is the possibility that deadenylation may be reverted or outcompeted by poly(A) polymerase activities (PAP) (iv). Although this last hypothesis remains to be tested, evidence for competing deadenylation and polyadenylation activities exists in paradigms such as the germline and in the early embryo (Goldstrohm and Wickens, 2008). Finally, a fraction of the deadenylated mRNA pool may be decayed through a slow 3'→5' route (v). This destabilization could be accelerated by the recruitment of decapping machinery by the miRISC, for example (see the Discussion).

3.5 Materials and Methods

3.5.1 *C. elegans* strains and RNAi.

N2 was used as the wild-type strain. Alleles used, *glp-4(bn2)*, *fem-1(hc17)*, and *alg-2(ok304)*, were cultured as in Brenner (1974). *alg-2(ok304)* animals were exposed to *alg-1 RNAi* or *gfp RNAi* (mock), starting with L3 larvae. RNAi was carried out as in Fire et al. (1998) and Timmons et al. (2001).

3.5.2 Construction of plasmids.

For the backbone of the reporters, the RL ORF was cloned in NheI-XbaI sites of pCI neo vector (Promega) and a poly(A) tail of 87 nucleotides was cloned into NotI/MfeI. See Appendix 2 for Supplemental Materials and Methods and Table A2-1 for details on the additional reporters.

3.5.3 Northern analysis.

Total RNA from animals taken at different stages was prepared using the TRIZOL (Invitrogen) method. Embryos from adults bearing one to three embryos per animal (EE) were harvested and allowed to further develop for 6 hr at 17°C (ME) and 12 hr (LE) in M9 saline suspensions. Animals were also harvested as synchronous populations of L1, L4, and adult stages. Of total RNA, 10 μg were analyzed by northern as in Duchaine et al. (2006).

3.5.4 Real-Time PCR.

miR-35 real-time PCR analysis throughout *C. elegans* development was performed using methods described in Raymond et al. (2005).

3.5.5 2'-*O*-Methyl pull-down.

2'-*O*-Me pull-down was done as described in Hutvagner et al. (2004). Of the beads, 10 μL were loaded on gel for western blot analysis with a polyclonal antibody against peptides in the C-

terminal region of ALG-1 and ALG-2, rabbit polyclonal antibody against DCR-1, rabbit polyclonal antibody against RDE-4, and GFP as Duchaine et al. (2006).

3.5.6 Multidimensional protein identification

MudPIT was performed as described in Duchaine et al. (2006).

3.5.7 Preparation of embryonic extracts and *in vitro* translation assays

Embryonic extracts and *in vitro* translation assays were performed as described in details in Appendix 2, Supplemental Materials and Methods section.

3.5.8 Deadenylation assays

Deadenylation assays were performed in the same condition as translation (see Appendix 2 Supplemental Materials and Methods section) using 1 ng radiolabeled RNA. Autoradiography was realized as in Fabian et al. (2009).

3.6 Acknowledgments

We thank Darryl Conte Jr., Maxime Bouchard, and Ahilya N. Sawh for their comments on the manuscript. We thank Noriko Uetani for her artistic assistance with the model. We thank Min Han for providing *ain-2::gfp* transgenic animals/worms and rat polyclonal AIN-1 antibody, and Richard E. Davis for providing rat polyclonal DCP-2 antibody. This work was supported by Canadian Institute of Health Research (grants MOP 86577 and 93607), the National Sciences and Engineering Council of Canada (NSERC) (grant RGPIN 86577), the Canada Foundation for Innovation (CFI), and the Fonds de la Rercherche en Santé du Québec (Chercheur-Boursier Salary Award J.1) to T.F.D.

Chapter 4: A continuum of mRNP complexes in embryonic microRNA-mediated silencing

Edlyn Wu, Ajay A. Vashisht, Clément Chapat, Mathieu Flamand, Emiliano Cohen, Mihail Sarov, Yuval Tabach, Nahum Sonenberg, James Wohlschlegel & Thomas F. Duchaine.
Manuscript in preparation

4.1 Abstract

MicroRNAs (miRNAs) impinge on the translation and stability of a wide variety of mRNAs, and play key roles in development, homeostasis and disease. The gene regulation mechanisms they instigate are largely effected through the activities and interactions of the CCR4-NOT deadenylase complex, but the molecular events that occur on target mRNAs and lead to silencing are poorly resolved. Using comparative proteomics, we observed a broad convergence of interactions of germ granule and P body mRNP components on AIN-1/GW182 and NTL-1/CNOT1 in the *C. elegans* embryo. We show that the miRISC progressively matures on the target mRNA from a scanning form into an effector mRNP particle by sequentially recruiting the CCR4-NOT complex, and mRNP components such as the decapping and decay, or germ granule proteins. Finally, we implicate the intrinsically disordered proteins MEG-1 and MEG-2, which scaffold the germ granules, in embryonic miRNA-mediated silencing. Our findings define dynamic steps of effector mRNP assembly in embryonic miRNA-mediated silencing, and identify a functional continuum between germ granules and P bodies in the *C. elegans* embryo.

4.2 Introduction

MicroRNAs (miRNAs) are ~22 nucleotide (nt)-long RNAs that impinge on gene expression to regulate a broad variety of biological processes (Bartel, 2009). miRNAs direct silencing from within the miRNA-induced silencing complex (miRISC), an assembly of an Argonaute (ALG-1 and -2 in *C. elegans*) and GW182 proteins (AIN-1 and -2) (Grishok et al., 2001; Zhang et al., 2007). The miRISC typically recognizes 3' un-translated region (3'UTR) sequences of target messenger RNAs (mRNAs) through imperfect base-pairing with miRNAs (Bartel, 2009). Cognate interactions instigate a series of gene-silencing mechanisms, which include mRNA translation repression, deadenylation, decapping and decay (Bagga et al., 2005; Behm-Ansmant et al., 2006; Eulalio et al., 2007c; Giraldez et al., 2006; Mathonnet et al., 2007; Wu et al., 2006). The relative contribution of each of these events is still a matter of debate, and likely depends on cellular context. The multi-subunit CCR4-NOT deadenylase complex is a key effector in the several mechanistic aspects of miRNA-mediated silencing (Behm-Ansmant et al., 2006; Eulalio et al., 2009b; Fabian et al., 2009). The scaffolding subunit CNOT1 (NOT-like 1, or NTL-1 in *C. elegans*) directly interacts with GW182 *in vitro* (Braun et al., 2011; Chekulaeva et al., 2011; Fabian et al., 2011), and either alone or in combination with other CCR4-NOT subunits (Chen et al., 2014; Mathys et al., 2014), further tethers other effector components such as the RNA helicase DDX6 (Chen et al., 2014; Mathys et al., 2014; Rouya et al., 2014) or the distinct PAN2/3 deadenylase complex (Zheng et al., 2008).

A significant fraction of the Argonaute and GW182 proteins localize to processing bodies (P bodies), which are dynamic assemblies of RNA and proteins observed as distinctively large foci throughout the cell cytoplasm (Behm-Ansmant et al., 2006; Ding et al., 2005; Eystathioy et al., 2002; Jakymiw et al., 2005; Liu et al., 2005b; Meister et al., 2005; Pillai et al., 2005; Sen and

Blau, 2005). Their full composition is unknown, but numerous other factors implicated in mRNA processing, such as decapping enzymes (Dcp1/2) and activators (Pat1 and the Lsm1-7 complex), and the 5'⟶3' exonuclease Xrn1, co-localize in P bodies (Ingelfinger et al., 2002; Lykke-Andersen, 2002; Sheth and Parker, 2003; van Dijk et al., 2002). While they do concentrate several key miRNA co-factors, detectable P bodies as distinct cytoplasmic foci are not required for miRNA-mediated silencing. Genetic depletion of components often results in their reduction in size or abundance without impairing miRNA-mediated silencing (Cougot et al., 2004; Eulalio et al., 2007b; Yu et al., 2005).

P bodies belong to a broad and functionally diverse group of electron-dense and membrane-less cellular foci referred to as messenger ribonucleoprotein (mRNP) granules. mRNPs include stress granules, transport granules, chromatoid bodies in male germ cells, and germ granules in oocytes and embryos (Buchan, 2014; Decker and Parker, 2012; Voronina et al., 2011). mRNP functions have been largely inferred based on co-localization of proteins, enzymatic functions attributed to resident proteins, and interactions *in vitro*. Germ granules are thought to be sites of mRNA storage for germ cell lineage functions (Boag et al., 2008; Gallo et al., 2008; Nguyen Chi et al., 2009; Noble et al., 2008; Soderstrom and Parvinen, 1976), whereas P bodies are instead being primarily associated with mRNA processing and decay (Sheth and Parker, 2003). What determines the structural and functional frontiers or the interactions between the distinct mRNP subtypes is not well defined. High-resolution, live imaging studies in *C. elegans* embryos revealed that germ granules exhibit liquid droplet-like behavior, which allows rapid phase transitions of dissolution and condensation (Brangwynne et al., 2009). Such a behavior is consistent with a dynamic molecular scaffold of multivalent protein-RNA complexes, lending grounds to a model explaining assemblies of large cytoplasmic mRNPs like P bodies and

germ granules (Li et al., 2012). Recent studies uncovered a key contribution for intrinsically disordered regions (IDRs), often encoded in RNA-binding proteins, in mRNP granule architecture and dynamics (Elbaum-Garfinkle et al., 2015; Kato et al., 2012; Lin et al., 2015; Molliex et al., 2015; Nott et al., 2015; Wang et al., 2014). The Maternal-Effect Germline defective (MEG) MEG-1 and MEG-2 are exclusively constituted of IDRs and directly participate in the germ granule assembly in *C. elegans* embryo (Wang et al., 2014).

Through a combination of proteomics, genetics, and novel cell-free assays in *C. elegans,* we delineate the molecular events leading to and occurring during embryonic miRNA-mediated silencing. We identify a striking convergence of interactions between germ granule and P body components with AIN-1 and NTL-1. We further show that scanning miRISC and mRNP components assemble sequentially on mRNA targets. Finally, we reveal the role of intrinsically disordered proteins MEG-1 and -2 in potentiating miRNA-mediated silencing. We thus identify new molecular events underlying embryonic miRNA functions, and a role for mRNP granule components in specializing their silencing mechanism.

4.3 Results

4.3.1 Germ granule and P body proteins are enriched among miRISC interactions

mRNA deadenylation is a prevalent outcome for miRNA targets in diverse systems and this activity has been largely attributed to the CCR4-NOT deadenylase complex (Jonas and Izaurralde, 2015). The molecular interactions of miRISC with mRNA processing machineries in the embryo are still unknown. To capture the physical interactions between miRISC and its effectors in the *C. elegans* embryo, we performed immunoprecipitation (IP)-shotgun proteomics on the miRISC protein AIN-1, a *C. elegans* ortholog to GW182, and on the CCR4-NOT complex scaffold NTL-1, the ortholog of CNOT1. LAP (GFP-3xFLAG)-tagged AIN-1 and NTL-1 proteins were immuno-purified from *C. elegans* transgenic embryos expressing tag fusions at endogenous levels (Figure 4-1A, and see Materials and Methods). Recovered fractions were analyzed using Multi-Dimensional Protein Identification Technology (MuDPIT) (MacCoss et al., 2002; Washburn et al., 2001; Wolters et al., 2001). Six independent biological replicates were analyzed for AIN-1, and three were analyzed for NTL-1. Only candidate interactions detected in at least two independent biological experiments were retained, and proteins also found in negative control samples (non-transgenic strains) were disqualified. A total of 340 proteins were detected in at least two samples for AIN-1 purifications (Table A3-1), while 78 candidate interactions were identified from NTL-1 sample analyses (Table A3-2).

AIN-1 and NTL-1 interaction datasets significantly overlapped with previous phylogenetic profiling (co-evolution), genome-wide RNAi screens, and proteomic analyses that identified genes of the RNAi and miRNA pathways (71/340 for AIN-1, *p*-value: 1.14×10^{-37}; 18/78 for NTL-1, *p*-value: 6.33×10^{-12}; (see Materials and Methods; Tabach et al., 2013) (Figure

4-1B and Tables A3-3 and A3-4). Genes encoding 25 of the 71 proteins shared with AIN-1 proteomics were identified in an RNAi screen for enhancement of the *let-7* phenotypes in a sensitized background (*p*-value: 6.6×10^{-9}) (Parry et al., 2007), and 29/71 displayed the same phenotype in other independent RNAi experiments (*p*-value: 1.7×10^{-12}). Extensive and significant overlap is also observed between AIN-1 datasets and results of a screen for miRNA factors in *Drosophila* (17/71, *p*-value: 3.4×10^{-14}). NTL-1 datasets significantly overlap with *let-7* phenotype screen (6/18; *p*-value: 0.002). Finally, both AIN-1 and NTL-1 interactions further overlap with proteomic and genetic screens for RNAi pathway factors (Figure 4-1B). These results indicate that both AIN-1 and NTL-1 interactions are functionally relevant to the miRNA and RNAi pathways in a diverse variety of cellular and species contexts.

Gene Ontology (GO) classification using the PANTHER system (Mi et al., 2013; Thomas et al., 2003) revealed a strong enrichment for annotations to cytoplasmic RiboNucleoProtein granules (mRNP granules) (Figure 4-1C). Twenty-three out of 329 AIN-1 interactions (*p*-value: 2.1×10^{-20}), among 195/329 proteins with classified terms, and 10 out of 75 NTL-1 interactions (49/75 classified; *p*-value: 4.7×10^{-11}) were annotated as cytoplasmic mRNP granules. More specifically, P body components were enriched among AIN-1 and NTL-1 interactions. P body components were annotated to 9 interactions with AIN-1 (*p*-value: 1.1×10^{-8}), and 6 NTL-1 interactions (*p*-value: 3.7×10^{-8}). Detected P body proteins among the interactions included several of the CCR4-NOT complex subunits, the PAN2/3 deadenylase complex, the decapping enzymes DCAP-1/2 and the decapping activator PATR-1 (Figures 4-1D and 4-1E). Finally NHL-2, a member of the TRIM-NHL family of proteins, and a miRISC cofactor (Hammell et al., 2009) which localizes to P bodies and germ granules based on GO annotations (Hammell et al.,

2009; Hyenne et al., 2008), was among the most consistently detected interactions in both NTL-1 and AIN-1 purifications.

Surprisingly, germ granule (also known as P granules in *C. elegans*) proteins were strongly enriched among AIN-1 interactions (18 interactions, *p*-value: 5.0×10^{-15}), and in NTL-1 interaction datasets (7 interactions, *p*-value: 1.0×10^{-6}) (Figure 4-1D). Interactions detected with AIN-1 include proteins known to play critical roles in germline determination and functions including PGL-1, PGL-3 (Kawasaki et al., 2004; Kawasaki et al., 1998), CCCH Zinc finger proteins PIE-1 (Mello et al., 1996), MEX-5, and MEX-6 (Schubert et al., 2000), the snRNP spliceosome component SNR-7 (Barbee et al., 2002), DEAD-box RNA helicases DRH-3 (Nakamura et al., 2007) and GLH-1 (Gruidl et al., 1996), a close *C. elegans* homolog to Drosophila VASA. eIF4E homolog IFE-1 and 4E transporter and translation regulator IFET-1, both known residents of germ granules in *C. elegans* (Amiri et al., 2001; Sengupta et al., 2013), were detected among interactions with AIN-1.

Whereas some of the detected proteins reside and/or function within germ granules, others are known for their structural function in mRNP assembly itself. This is the case for MEG-2 protein, detected in 3/3 NTL-1 purifications (Figure 4-1D and Table A3-2), and its paralog MEG-1, which was detected with lesser consistency and at lower peptide coverage (not shown). MEG-2 and MEG-1 lack any recognizable domains, are constituted of inherently disordered regions (IDRs) rich in serine, and localize to germ granules (Leacock and Reinke, 2008; Wang et al., 2014). Both proteins act at least in part redundantly in germline development and germ granule assembly and disassembly. Interestingly, MEG-1 was recently shown to be a target of the MBK-2(DYRK) kinase, and of the PPTR-1/2(PP2A) phosphatase, with activities that modulate germ granule assembly (Wang et al., 2014). PPTR-1 is also detected among NTL-

1 interactions, in 2/3 biological replicates (Table A3-2), and MBK-2 was detected with poorer consistency, in 1 out of 3 NTL-1 purification samples (not shown).

Overall, our comparative proteomic analyses reveal the physical linkage of miRISC core component AIN-1 and its effector complex scaffold protein NTL-1 with mRNPs. It further identifies previously unrecognized interactions with key germ granule components.

A

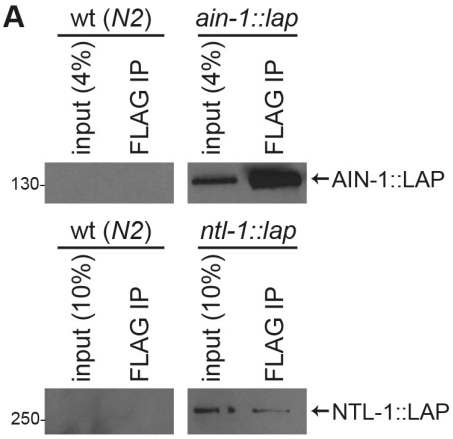

IP: FLAG; WB: α-GFP
(LAP: GFP-3xFLAG)

B

	AIN-1		NTL-1		AIN-1 & NTL-1	
	Overlap	*p*-value	Overlap	*p*-value	Overlap	*p*-value
Genetic screens for miRNA factors						
let-7 phenotype	29	1.7E-12	6	0.0024	4	0.0042
let-7 sensitized	25	6.6E-09	3	0.1805	2	0.1593
Drosophila miRNA	17	3.4E-14	0	1	0	1
Proteomics studies						
DCR-1 Co-IP	11	3.0E-06	5	7.5E-05	1	0.1920
ERI-1 Co-IP	10	1.1E-05	3	0.0080	1	0.1810
AIN-2 Co-IP	6	9.8E-05	0	1	0	1
Genetic screens for RNAi-related pathways						
Suppression of transgene silencing in *eri-1*	61	5.0E-19	11	0.0014	8	0.0004
Drosophila siRNA	21	2.6E-14	2	0.1051	1	0.2362
dsGFP RNAi	13	2.7E-08	2	0.0643	1	0.1828
Germline co-supression defect	10	1.4E-06	4	0.0003	2	0.0110
SynMuv suppression	6	3.0E-05	0	1	0	1
Total number of non-redundant overlapping proteins	71/340	1.14E-37	18/78	6.33E-12	11/38	1.95E-09

C

AIN-1 interacting proteins classified for GO analysis

GO cellular component terms	REFLIST (20490)	AIN-1 IP (329)	*p*-value
ribonucleoprotein complex	295	50	3.1E-32
cytoplasmic ribonucleoprotein granule (mRNP granule)	68	23	2.1E-20
Germ granule (P granule)	58	18	5.0E-15
cytoplasmic mRNA processing body (P body)	18	9	1.1E-08
spindle pole	17	7	7.1E-06
cell cortex	89	11	1.3E-04
CCR4-NOT complex	3	3	7.6E-03
eIF3 complex	14	5	1.6E-03
spliceosomal complex	24	5	2.1E-02

NTL-1 interacting proteins classified for GO analysis

GO cellular component terms	REFLIST (20490)	NTL-1 IP (75)	*p*-value
cytoplasmic ribonucleoprotein granule (mRNP granule)	68	10	4.7E-11
ribonucleoprotein complex	295	14	1.7E-09
cytoplasmic mRNA processing body (P body)	18	6	3.7E-08
Germ granule (P granule)	58	7	1.0E-06
CCR4-NOT complex	3	3	8.9E-05
ESCRT-0 complex	2	2	1.1E-02

D

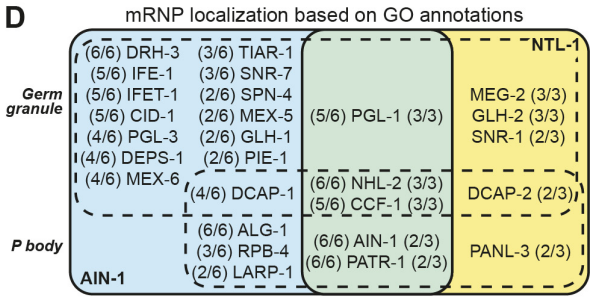

E

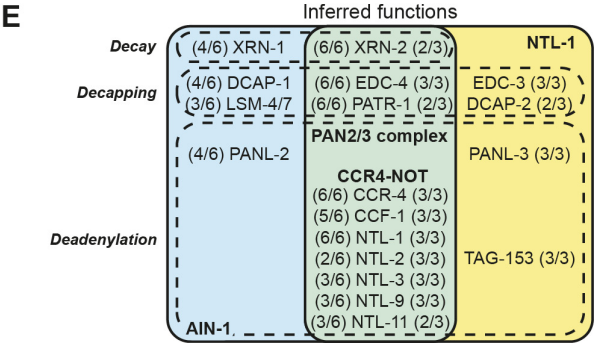

Figure 4-1: Germ granule and P body proteins are enriched among miRISC interactions

(A) Western blots of embryo lysates and FLAG immunoprecipitations (IP) from wild-type non-transgenic (*N2*, left panels) and transgenic animals expressing LAP-tagged AIN-1 (top right panel) or NTL-1 (bottom right panel). (B) The table shows the number of proteins identified in the present Co-IP studies (AIN-1 and NTL-1) that overlap with proteins identified in previous screens and the hyper-geometric *p*-values of the overlap (see Experimental Procedures and Tabach et al., 2013). The studies integrated for the analysis of factors implicated in miRNA and other RNAi-related pathways are as follows: *let-7* phenotype (WormBase (WS220), Tabach et al., 2013), *let-7* sensitized (Parry et al., 2007), *Drosophila* miRNA and siRNA (Zhou et al., 2008), DCR-1 Co-IP (Duchaine et al., 2006), ERI-1 Co-IP (Thivierge et al., 2012), AIN-2 Co-IP (Zhang et al., 2007), suppression of transgene silencing in *eri-1* and dsGFP RNAi (Kim et al., 2005), germline co-suppression defect (Robert et al., 2005), SynMuv suppression (Cui et al., 2006). The right-most columns show the number of proteins identified in both AIN-1 and NTL-1 studies and in previous screens, and the hyper-geometric *p*-value of the three-way overlap. (C) Gene Ontology (GO) analysis of cellular component terms on AIN-1 and NTL-1 proteins detected by MuDPIT. Among the proteins retained from at least 2 biological replicates, only 329/340 AIN-1 interactors and 75/78 NTL-1 interactors were classified for GO analysis. (D) Venn diagram of proteins with GO annotations to cellular component terms related to germ granules and P bodies. (E) Venn diagram of a subset of proteins with inferred functions in deadenylation, decapping, and RNA decay. Fractions in the Venn diagrams indicate the number of times the corresponding protein was detected in each independent IP (out of 6 for AIN-1, and out of 3 for NTL-1). (See also Tables A3-1 to A3-4).

4.3.2 Coupled expression and function of the CCR4-NOT complex subunits in embryonic miRNA-mediated deadenylation

Intersect of the datasets revealed an extensive overlap of the interactions with the CCR4-NOT complex and AIN-1. 48% of the detected NTL-1 interactions were also detected in the AIN-1 IP (Table 4-1), and CCR4-NOT complex components enrichment was un-biasedly highlighted through GO analysis in AIN-1 IP (Figure 4-1C; *p*-value: 7.6×10^{-3}). Among shared interactions, the CCR4-NOT catalytic subunit CCR-4 (CCR-4a/b; orthologous to CNOT6/6L) scored among the very highest in percentage of peptide coverage and in the number of detected peptides, and was detected in all samples analyzed. CCF-1 (CAF1), the other deadenylase catalytic subunit of the complex, was detected in 5/6 AIN-1 samples and in 3/3 NTL-1 samples. Together with CCF-1, CCR-4 and NTL-1, a total of 7 known subunits of the CCR4-NOT complex were common to both AIN-1 and NTL-1 purifications, including NTL-2, NTL-3, NTL-9 and NTL-11 (Figure 4-1E). Decapping co-factors PATR-1 and EDC-4 (named based on homology with human Edc4) and the mRNA decay enzyme 5'→3' exonuclease XRN-2 were also detected in both groups of datasets (Figure 4-1E, Table 4-1). Finally, and in spite of extensive overlap, some of the best detected proteins in NTL-1 purifications were absent from any AIN-1 interaction datasets. In particular, TAG-153 is an un-characterized paralog of NTL-2 (Figure A3-1), a member of the NOT2/3/5 family, and was among the proteins most consistently detected in NTL-1 purifications. While NTL-2 is consistently detected in 3/3 NTL-1 IP, TAG-153 is absent from all six AIN-1 interaction replicates. This may suggest specialization of distinct and functionally non-redundant CCR4-NOT complexes in miRNA-mediated silencing.

These data reveal that embryonic miRISC physically interacts with mRNA deadenylation and decay machineries, and position AIN-1 as a bridge between the miRNA-dedicated ALG-1/2 Argonaute proteins and their gene-silencing effectors.

The CCR4-NOT complex had never been functionally linked to miRNA-mediated silencing mechanisms in *C. elegans* embryo. To formally test the implications of CCF-1 and CCR-4 in embryonic miRNA-mediated deadenylation, we exploited an *in vitro* embryonic extract previously developed in our lab (Wu and Duchaine, 2011; Wu et al., 2010), and proficient for miRNA-mediated silencing and deadenylation. For this, an *in vitro* transcribed, radiolabeled polyadenylated *Renilla reniformis* luciferase (RL) reporter RNA bearing six *miR-35* binding sites (RL 6x pA, Figure 4-2B) was incubated in wild-type (wt) or genetically-depleted extracts over a time-course of three hours. RNA was extracted, and deadenylation was monitored and quantified using denaturing electrophoresis and autoradiography. Because strong genetic depletion of *ccf-1* and *ccr-4* results in pleiotropic defects including sterility and, in the case of *ccf-1* mutants, embryonic and larval lethality (Molin and Puisieux, 2005; Nousch et al., 2013), null alleles or strong RNAi depletions could not be used in extract preparation. Instead, we generated cell-free embryonic extracts wherein *ccf-1* and *ccr-4* expression was mildly reduced by RNAi (Figure 4-2A, see Materials and Methods). In extracts derived from wild-type embryos subjected to mock (*gfp*) RNAi, the RL 6x pA mRNA reached half-deadenylation time ($t_{d1/2}$) at 25 minutes (Figure 4-2B). In contrast, deadenylation of the reporter was significantly delayed under mild *ccf-1 (RNAi)* (74% knockdown, Figure 4-2A), and in *ccr-4 (RNAi)* depletions (54% knockdown, Figure 4-2A), delaying half-deadenylation times to 39 and 41 min, respectively (Figure 4-2B). Interestingly, while examining knockdowns of *ccf-1* and *ccr-4* by western blot, we observed a decrease in CCR-4 protein expression under *ccf-1 (RNAi)* depletion, while *ccr-4*

(RNAi) did not significantly impact CCF-1 protein expression (Figure 4-2A). Furthermore, NTL-1 expression was significantly decreased (47% reduction) even under mild (57%) *ccf-1 (RNAi)* knockdown.

These results are reminiscent of the coupled stability of the CCR4-NOT complex subunits in diverse species (Boland et al., 2013; Nousch et al., 2013; Temme et al., 2010). We note that such results make it difficult to genetically disambiguate the relative or redundant contributions of the catalytic subunits in miRNA-mediated silencing. Nonetheless, these results show that CCR-4 and/or CCF-1 contribute to miRNA-mediated deadenylation in *C. elegans* embryos.

Sequence name	Protein	NTL-1::LAP		AIN-1::LAP		Homology/Domain	Description
		# datasets detected	coverage (peptide counts)	# datasets detected	coverage (peptide counts)		
ZC518.3	CCR-4	3/3	61% (40)	6/6	20% (6)	Ccr4/CNOT6, CNOT6L	CCR4-NOT subunit
F57B9.2	LET-711	3/3	43% (121)	6/6	10% (17)	CNOT1	CCR4-NOT subunit
B0513.1	LIN-66	3/3	10% (4)	6/6	17% (6)	unknown	translational regulation
Y44E3A.6	Y44E3A.6	3/3	12% (7)	6/6	13% (7)	EDC4	decapping activator
C07G1.5	HGRS-1	3/3	6% (3)	6/6	12% (6)	Vps27p,FYVE Zn finger	ESCRT-0 component
F26F4.7	NHL-2	3/3	8% (6)	6/6	10% (6)	TRIM-NHL	miRISC component
F31E3.3	RFC-4	3/3	12% (3)	5/6	13% (3)	RFC4	DNA replication
ZK381.4	PGL-1	3/3	4% (3)	5/6	5% (2)	none detected	RGG box motif, P granules
C18H9.3	C18H9.3	3/3	4% (3)	5/6	4% (2)	GIGYF1/2	GYF domain protein
Y56A3A.20	CCF-1	3/3	39% (19)	5/6	18% (4)	Caf1/CNOT7	CCR4-NOT subunit
T01B7.6	TRCS-2	3/3	4% (3)	5/6	7% (3)	unknown	uncharacterized
H28G03.1	H28G03.1	3/3	13% (3)	4/6	12% (2)	RNA-binding	uncharacterized
Y56A3A.1	NTL-3	3/3	58% (44)	3/6	8% (4)	CNOT3	CCR4-NOT component
F13D12.2	LDH-1	3/3	12% (3)	3/6	15% (4)	LDHB	lactate dehydrogenase
K10B3.8	GPD-2	3/3	14% (3)	3/6	11% (3)	GAPDH	glycolysis
K10B3.7	GPD-3	3/3	14% (3)	3/6	11% (3)	GAPDH	glycolysis
R11A8.7	R11A8.7	3/3	5% (9)	3/6	2% (3)	Q/N-rich domain	uncharacterized
F56A3.4	SPD-5	3/3	4% (3)	3/6	4% (3)	coiled coil domain	cell division
C26E6.3	NTL-9	3/3	45% (27)	3/6	10% (2)	RQCD1	CCR4-NOT component
B0286.4	NTL-2	3/3	42% (14)	2/6	10% (2)	CNOT2	CCR4-NOT component
C06G1.4	AIN-1	2/3	6% (3)	6/6	53% (37)	GW182/TNRC6	miRISC component
F43G6.9	PATR-1	2/3	7% (4)	6/6	10% (5)	PAT1	mRNA decay
Y116A8C.35	UAF-2	2/3	10% (2)	6/6	23% (5)	U2AF35, RRM	splicing
Y48B6A.3	XRN-2	2/3	4% (3)	6/6	13% (7)	XRN2	5'-3' exoribonuclease
F31D4.3	FKB-6	2/3	12% (4)	5/6	8% (2)	TPR repeat	protein folding
C34G6.7	STAM-1	2/3	12% (4)	5/6	16% (4)	Q/N-rich domain, SH3	protein transport
R05D3.7	UNC-116	2/3	11% (7)	5/6	7% (4)	kinesin-1 heavy chain	intracellular transport
T25G12.5	ACDH-7	2/3	7% (2)	5/6	10% (3)	ACADM	acyl-CoA dehydrogenase
Y34D9A.10	VPS-4	2/3	7% (3)	5/6	11% (3)	VPS4B, VPS4A	vacuolar protein sorting
W01B11.3	NOL-5	2/3	6% (3)	5/6	15% (5)	NOP58	nucleolar RNP
Y74C10AR.1	EIF-3.i	2/3	18% (5)	4/6	20% (5)	EIF3I	translation initiation
T12E12.4	DRP-1	2/3	11% (6)	4/6	5% (3)	DRP1	dynamin-related protein
Y73F8A.25	NTL-11	2/3	5% (3)	3/6	8% (3)	CNOT11	CCR4-NOT component
Y54G9A.6	BUB-3	2/3	10% (2)	3/6	12% (3)	BUB3	mitotic checkpoint
F35G12.2	IDHG-1	2/3	8% (2)	3/6	10% (2)	isocitrate dehydrogenase	tricarboxylic acid cycle
Y59A8B.6	PRP-6	2/3	3% (2)	3/6	5% (3)	PRPF6	pre-mRNA processing
T23B5.1	PRMT-3	2/3	3% (2)	3/6	5% (3)	PRMT9	methyltransferase
ZK1053.4	ZK1053.4	2/3	4% (2)	3/6	3% (2)	coiled-coil domain	SEPA-1 family, autophagy

Table 4-1: Comparative proteomics of AIN-1- and NTL-1-interacting proteins

A list of 38 proteins detected in both AIN-1 and NTL-1 immunoprecipitations. Proteins that were detected only once in each immunoprecipitation and found in the negative control (non-transgenic wild-type *N2* background) were excluded. Homology data and description for each protein were obtained from Wormbase WS250 and UniProt database. (See also Tables A3-1 and A3-2).

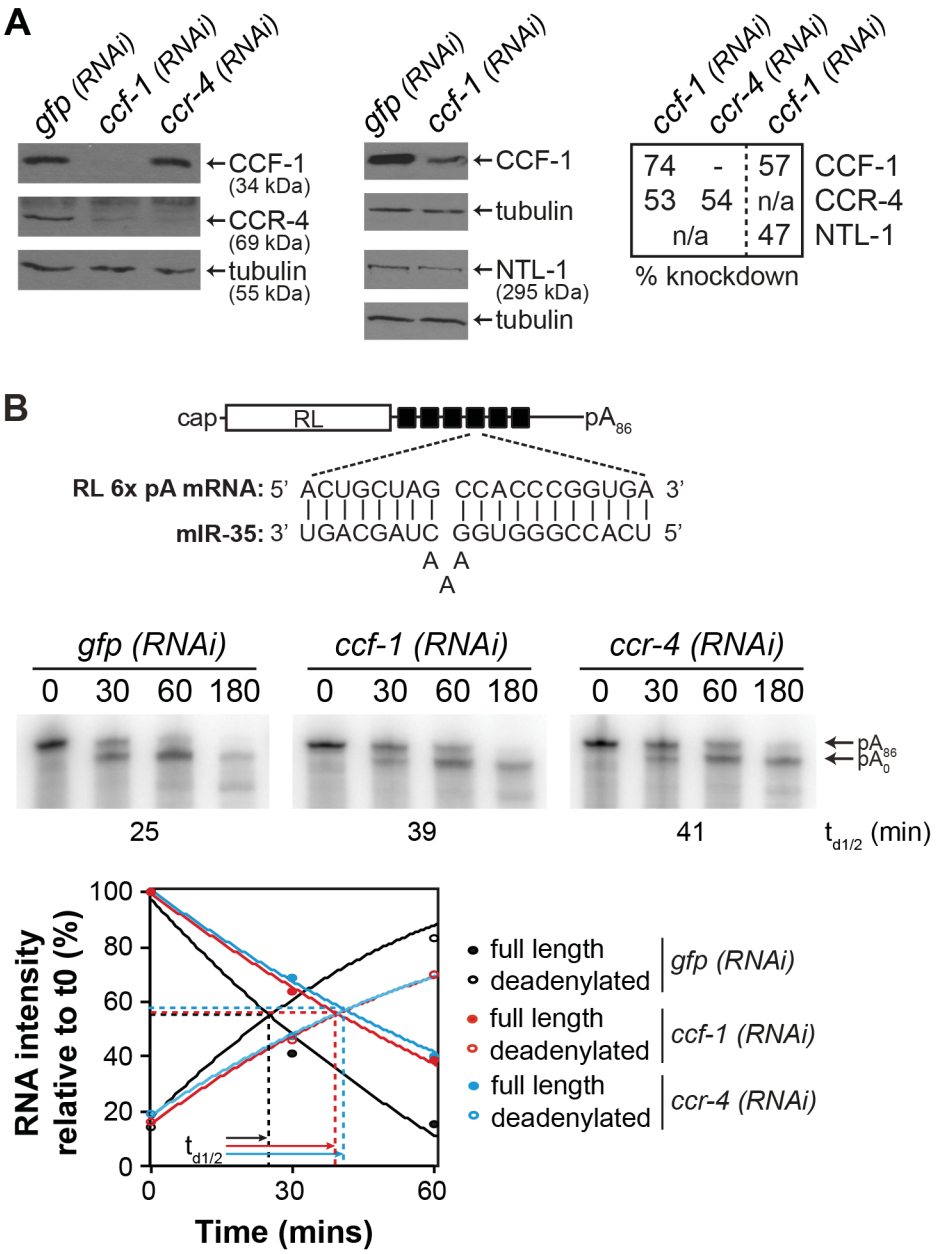
A
gfp (RNAi)
ccf-1 (RNAi)
ccr-4 (RNAi)
←CCF-1
(34 kDa)
←CCR-4
(69 kDa)
←tubulin
(55 kDa)
gfp (RNAi)
ccf-1 (RNAi)
←CCF-1
←tubulin
←NTL-1
(295 kDa)
←tubulin
ccf-1 (RNAi)
ccr-4 (RNAi)
ccf-1 (RNAi)
74 - 57 CCF-1
53 54 n/a CCR-4
n/a 47 NTL-1
% knockdown
B
cap
RL
pA86
RL 6x pA mRNA: 5' ACUGCUAG CCACCCGGUGA 3'
mIR-35: 3' UGACGAUC GGUGGGCCACU 5'
A A
A
gfp (RNAi)
ccf-1 (RNAi)
ccr-4 (RNAi)
0 30 60 180
0 30 60 180
0 30 60 180
←pA86
←pA0
25
39
41
td1/2 (min)
RNA intensity relative to t0 (%)
100
80
60
40
20
0
td1/2
0
30
60
Time (mins)
full length
deadenylated
gfp (RNAi)
full length
deadenylated
ccf-1 (RNAi)
full length
deadenylated
ccr-4 (RNAi)

Figure 4-2: Coupled expression and function of the CCR4-NOT complex subunits in embryonic miRNA-mediated deadenylation

(A) Western blot analyses of embryonic extracts exposed to *mock* (*gfp*) *RNAi*, *ccf-1 (RNAi)*, or *ccr-4 (RNAi)* probed with anti-CCF-1, anti-CCR-4, anti-NTL-1, and anti-tubulin (loading control) antibodies. Percentage of knockdown was quantified using ImageJ on western blots. (B) Deadenylation time course of RL 6x pA in wild-type embryonic extracts exposed to mock (*gfp*) *RNAi, ccf-1 RNAi*, or *ccr-4 RNAi*. The relative intensity of the bands corresponding to full length and deadenylated RNAs was measured using ImageJ. A second-order polynomial regression was used, and the time of half-deadenylation ($t_{d1/2}$, intersection point between the full length and deadenylated RNA) was calculated using the quadratic formula. Schematic representation of the RL 6x reporter RNA used and the sequences of miR-35 and miR-35 binding site are also shown.

4.3.3 Step-wise assembly of miRISC effector complexes on mRNA targets

We had previously performed shotgun proteomic analyses on miRISC captures using miRNA target analogs (2'-*O*-Me modified and biotinylated oligonucleotides) encoding binding sites for the maternal miR-35-42 and the zygotic miR-51-56 embryonic miRNA families (Lau et al., 2001; Stoeckius et al., 2009; Wu et al., 2010). Instead of being based upon relatively stable protein-protein interactions like IP, this strategy of miRISC capture relies solely on its ability to specifically find and bind miRNA target sequences in a single step purification from a complex lysate mixture. When target analog capture and AIN-1 interactions were compared, only 8 proteins were detected in both datasets (Figure 4-3A and Table A3-5), which primarily reflect the known central components of miRISC. AIN-1, AIN-2, ALG-1, ALG-2, and DCR-1 were among the best detected proteins in overlaps between AIN-1 IP, miR-35-42, and miR-51-56 target analog captures. The overlap also revealed factors of unknown or poorly characterized purpose in miRNA functions, which were detected at lower peptide coverage and in fewer replicates (SUP-26, Y23H5A.3, MEL-47). In stark contrast with AIN-1 IP datasets, none of the detected proteins in target analog captures are known components of the CCR4-NOT complex, any of the mRNP granules, or known mRNA decay machineries. Furthermore, while ALG-1 or ALG-2 were the best detected interactions in AIN-1 IP based on coverage percentage or peptide counts (ALG-2: 68% coverage, 72 peptides; ALG-1: 63%, 76 peptides), neither were detected among interactions with NTL-1. Such a discontinuity between miRISC in its target recognition form, as captured using analog pull-down, and the deadenylation and decay machineries interaction with AIN-1, lies at odds with the rapid and processive deadenylation of miRNA targets, which pervades in *C. elegans* embryonic cell-free systems (Wu et al., 2010). We note that since target analog capture identifies endogenous miRISC components on the basis of its

scanning activity, absence of deadenylation and decay machineries cannot be due to protein tagging artifacts.

We reasoned that the interactions detected with AIN-1 and NTL-1 may represent biochemically distinct form(s) of miRISC, involved in the effector step(s) of miRNA-mediated silencing, in contrast to, and perhaps downstream of, target recognition or scanning miRISC. To test this hypothesis, we developed an *in vitro* assay to detect interactions of miRISC components with targeted mRNAs prior to and during the course of deadenylation. The *D*eadenylated *R*NA-*I*mmuno*P*recipitation (DRIP, Figure 4-3B) assay combines the *C. elegans* embryonic cell-free extract capable of miRNA-mediated silencing and deadenylation, with RNA immunoprecipitation using tagged miRISC proteins. Radiolabeled RL 6x pA reporter was incubated in the extract, as above, over a course of three hours. Time points were chosen to reflect the state of the target mRNA prior to (Figure 4-3C, top panel; 0 min), during (30, 60 min), and after deadenylation (120, 180 min). IP was performed at each time point on core miRISC components, the Argonaute ALG-2, the GW182 ortholog AIN-1, and on the scaffolding subunit of the CCR4-NOT deadenylase complex, NTL-1. RNA was then extracted and resolved by urea-polyacrylamide gel electrophoresis and autoradiography. Importantly, the same monoclonal antibody directed against GFP was used for IP, and exhibited minimal background when no fusion was present in the extract (Figure 4-3C, wild-type (wt, *N2*) panel). When GFP-ALG-2 was recovered by IP, both full-length RL 6x pA_{86} and its deadenylated form were detected. Full-length RL 6x pA_{86} was detected at 0, 30, and 60 min, while the deadenylated species was detected at 30 min, and at all later time points of the 3-hr course. A similar profile was observed with AIN-1::LAP IP; AIN-1 associated with both the polyadenylated reporter and the deadenylated RNA species, and remained stably associated post-deadenylation. In contrast, only

the deadenylated species of RL 6x was detected in the NTL-1 IP during the time course (Figure 4-3C, NTL-1 panel). This observation indicates that its association with mRNA targets occurs on the mRNA and later than the initial recognition by scanning miRISC. Furthermore, it is consistent with a highly processive activity of the CCR4-NOT complex. These interactions were maintained in a poly(A) tail-independent manner; ALG-2, AIN-1, and NTL-1 remained stably associated with the target mRNAs long after completion of deadenylation. In line with this conclusion, DRIP profiles of 6x transcripts lacking a poly(A) tail (RL 6x pA_0) closely mirrored the profiles of RL 6x pA_{86} (Figure 4-3D).

Taken together, these results show that the interaction with scanning miRISC precedes the recruitment of CCR4-NOT complex scaffolded by NTL-1 on the target mRNA. It further indicates that their interactions do not depend on the presence of poly(A) tail, and persist long after deadenylation.

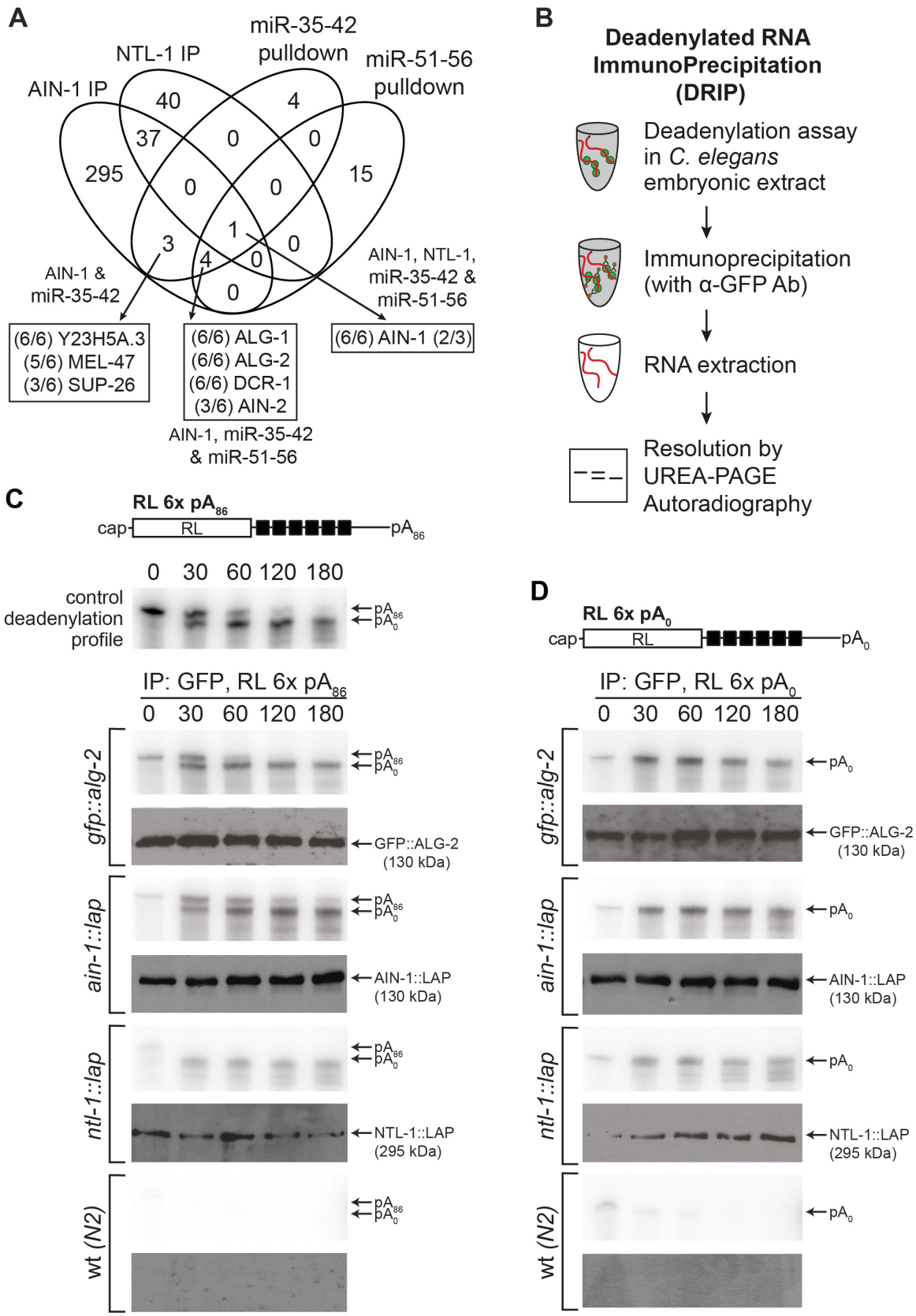
A
AIN-1 IP
NTL-1 IP
miR-35-42 pulldown
miR-51-56 pulldown
40
4
37
0
0
295
0
0
15
1
3
4
0
0
0
AIN-1 & miR-35-42
AIN-1, NTL-1, miR-35-42 & miR-51-56
(6/6) Y23H5A.3
(5/6) MEL-47
(3/6) SUP-26
(6/6) ALG-1
(6/6) ALG-2
(6/6) DCR-1
(3/6) AIN-2
AIN-1, miR-35-42 & miR-51-56
(6/6) AIN-1 (2/3)
B
Deadenylated RNA ImmunoPrecipitation (DRIP)
Deadenylation assay in C. elegans embryonic extract
Immunoprecipitation (with α-GFP Ab)
RNA extraction
Resolution by UREA-PAGE Autoradiography
C
RL 6x pA86
cap
RL
pA86
0 30 60 120 180
control deadenylation profile
pA86
pA0
IP: GFP, RL 6x pA86
0 30 60 120 180
gfp::alg-2
GFP::ALG-2 (130 kDa)
ain-1::lap
AIN-1::LAP (130 kDa)
ntl-1::lap
NTL-1::LAP (295 kDa)
wt (N2)
D
RL 6x pA0
cap
RL
pA0
IP: GFP, RL 6x pA0
0 30 60 120 180
gfp::alg-2
GFP::ALG-2 (130 kDa)
ain-1::lap
AIN-1::LAP (130 kDa)
ntl-1::lap
NTL-1::LAP (295 kDa)
wt (N2)

Figure 4-3: Step-wise assembly of miRISC effector complexes on mRNA targets

(A) Venn diagram of proteins interacting with AIN-1, NTL-1, and 2'-*O*-Me captured miRISC. Fractions indicate the number of times the corresponding protein was detected in each independent IP (out of 6 for AIN-1, and out of 3 for NTL-1). (B) Flow chart of the procedure for Deadenylated RNA ImmunoPrecipitation (DRIP) assay. (C and D) DRIP profiles of RL 6x pA_{86} (C) and RL 6x pA_0 (D) that represent target RNAs associated to immunoprecipitated proteins at each time point, as determined by autoradiography. Top panel in (C) is representative of a deadenylation assay time course carried out in wild-type (wt, *N2*) extract prior to the IP step. Western blots on GFP IPs of embryo-stage transgenic animals carrying GFP::ALG-2, AIN-1::LAP, or NTL-1::LAP using anti-GFP are shown below each autoradiograph. (C) and (D) are representative of at least three independent experiments. (See also Table A3-5).

4.3.4 miRISC interactions seclude target mRNAs in nuclease-refractory mRNPs

Considering the breadth of interactions of miRISC with its effector machinery on target mRNAs, we reasoned that assembly of mRNP granules could sequester mRNA targets. To test this idea *in vitro*, we subjected the assembled complexes to a nuclease-resistance assay (Figure 4-4A). Radiolabeled polyadenylated RL 6x pA was incubated in cell-free extract until its complete deadenylation (180 min), and then challenged with serial dilutions of hindrance-sensitive micrococcal nuclease (MNase) over a 15-minute time-course (Figure 4-4B, Figure A3-2). A mutant reporter encoding unpaired seed-binding sites, which remained polyadenylated (RL 6xmut pA; Wu et al. 2010), was used as control. Both targeted and un-targeted reporters decayed as a result of the MNase treatment, but RL 6x reporters resisted significantly better than the non-targeted RL 6xmut reporter (Figure 4-4B). Full-length RL 6x reporter, and not only the sequence encoding miRNA-binding sites, remained visible at the 6- and 9-min MNase treatment time points, when the RL 6xmut reporter was entirely degraded. Quantitation of independent replicates confirmed that the targeted RL 6x pA reporter was significantly less sensitive to MNase treatment than a non-targeted RL 6xmut pA reporter (Figure 4-4B, graphical panel). When the nuclease assay was conducted on un-adenylated transcripts (RL 6x pA_0 and RL 6xmut pA_0), the same outcome was observed with no significant difference in progression, indicating that mRNP assembly is independent of poly(A) tail presence. Overall, these results imply that miRNP assembly secludes miRNA-targeted mRNA, and raise the possibility that mRNP assembly on target mRNA may contribute to silencing.

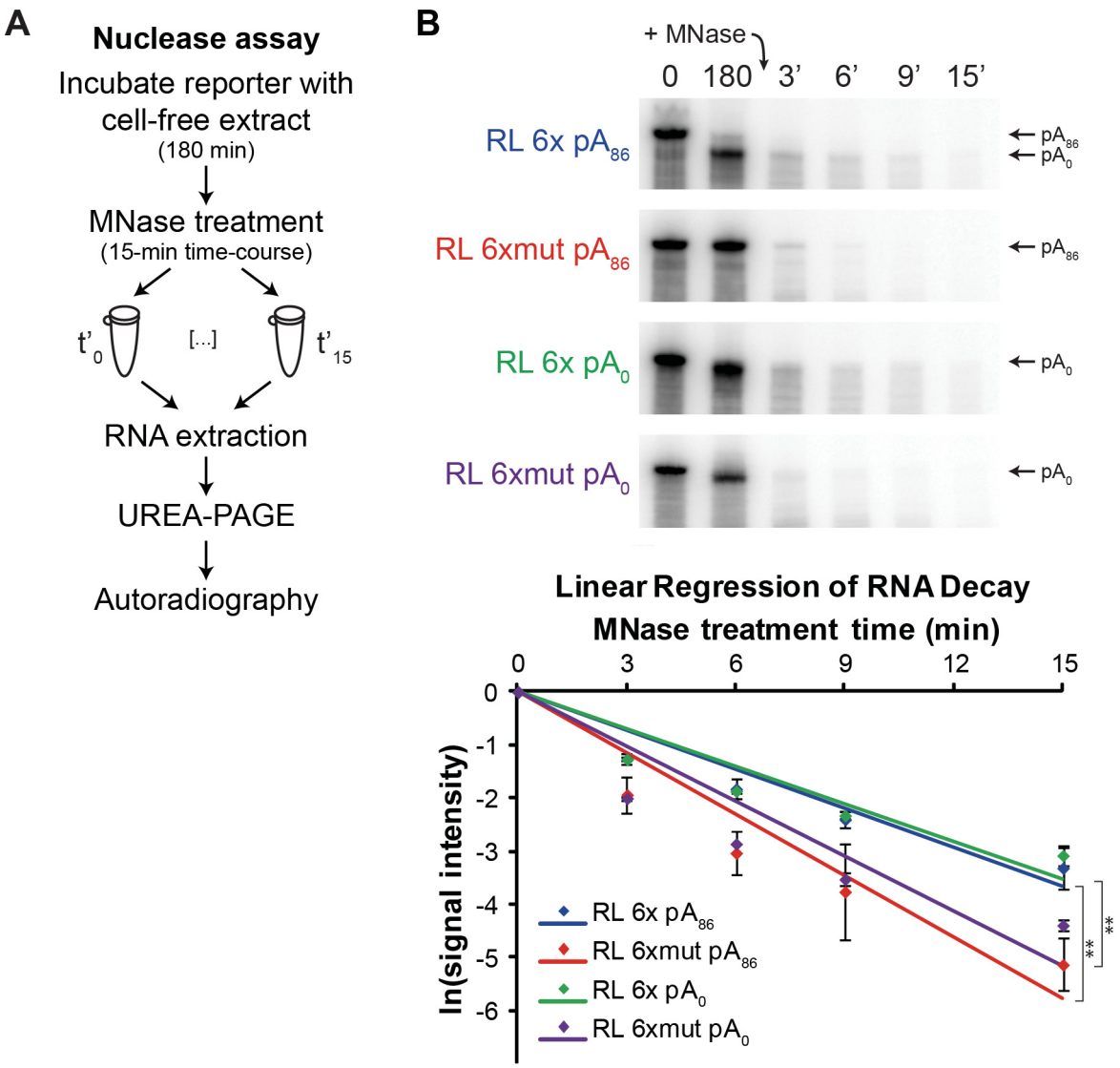
A
Nuclease assay
Incubate reporter with cell-free extract
(180 min)
MNase treatment
(15-min time-course)
t'0
[...]
t'15
RNA extraction
UREA-PAGE
Autoradiography
B
+ MNase
0 180 3' 6' 9' 15'
RL 6x pA86
RL 6xmut pA86
RL 6x pA0
RL 6xmut pA0
pA86
pA0
Linear Regression of RNA Decay
MNase treatment time (min)
ln(signal intensity)
0 3 6 9 12 15
0 -1 -2 -3 -4 -5 -6
RL 6x pA86
RL 6xmut pA86
RL 6x pA0
RL 6xmut pA0
**
**

Figure 4-4: miRISC interactions seclude target mRNAs in nuclease-refractory mRNPs

(A) Schematic diagram of nuclease assay. (B) PAGE-autoradiography of reporter mRNAs (RL 6x and mut, +/- poly(A) tail). RNAs at 0 and 180 min are on the left to show their integrity at the start and end of the 3-hour incubation in the embryonic extract, prior to nuclease treatment. MNase was then added to the reaction after 180 min and RNA integrity was monitored over a 15-min (denoted by t') MNase treatment. The intensity of the RNAs following MNase treatment was quantified using ImageJ from triplicate experiments conducted using the same extract preparation. A logarithmic regression using a linear model was used to analyze the rate of RNA reporter decay. Autoradiograph from one replicate is presented. Experiment was reproduced at least twice in independent extract preparations. Error bars indicate standard deviation. Statistical significance was calculated using one-tailed t-test (**$p<0.01$).

4.3.5 Selective precipitation of miRISC by biotinylated isoxazole

We elected to further characterize the association of miRISC with mRNPs using biotinylated isoxazole (b-isox), a compound causing aggregation of proteins rich in intrinsically disordered regions that are key determinants for mRNP assembly (Decker et al., 2007; Reijns et al., 2008). Precipitation using this reagent selectively enriches constituents of mRNPs, and at least some of their associated proteins (Han et al., 2012; Kato et al., 2012). Selective co-precipitation with b-isox from *C. elegans* embryonic lysates was assessed by western blotting for a panel of proteins related to miRNA function, RNAi, translation, mRNA processing, P bodies and germ granules (Figure 4-5). Strikingly, miRISC components ALG-1/2 and AIN-1 were strongly enriched in the b-isox precipitate. The AIN-1::LAP fusion fractionates in a similar manner (Figure A3-3). NTL-1, the poly(A) binding proteins PAB-1/2, the *C. elegans* DDX6 ortholog CGH-1, and the germ granule constituents (PAN-1, GLH-1, and MEG-1) were all preferentially co-precipitated with b-isox. Curiously, while MEG-1 and MEG-2 paralogs are rich in intrinsically disordered regions, the two FLAG-tagged fusion proteins behave differently with regards to b-isox precipitation. MEG-1 is strongly enriched in the precipitate, while a more limited portion of MEG-2 is selectively precipitated. Interestingly, unlike the CCR4-NOT complex scaffold NTL-1, its catalytic subunits CCR-4 and CCF-1 co-precipitate only in limited amounts. A minor fraction of DCR-1 was also detected in the precipitate fraction. Finally, b-isox precipitation was highly selective; the dsRNA-binding protein RDE-4, the cap-binding proteins IFE-1 and IFE-2, and tubulin were not recovered in the pellet fraction.

With these results and prior work (Han et al., 2012; Kato et al., 2012), the selective precipitation of mRNP proteins with b-isox has now been extensively characterized. However, we still do not rule out that part of the selectivity of b-isox precipitation may be due to its

inherent compatibility or incompatibility with individual proteins. Notwithstanding this reserve, the strong selective enrichment of ALG-1/2, AIN-1, and NTL-1 proteins in b-isox precipitates lends further support to their association with mRNPs. Finally, the distinct behavior of MEG-1 and MEG-2 suggests that they are not constitutively co-assembled.

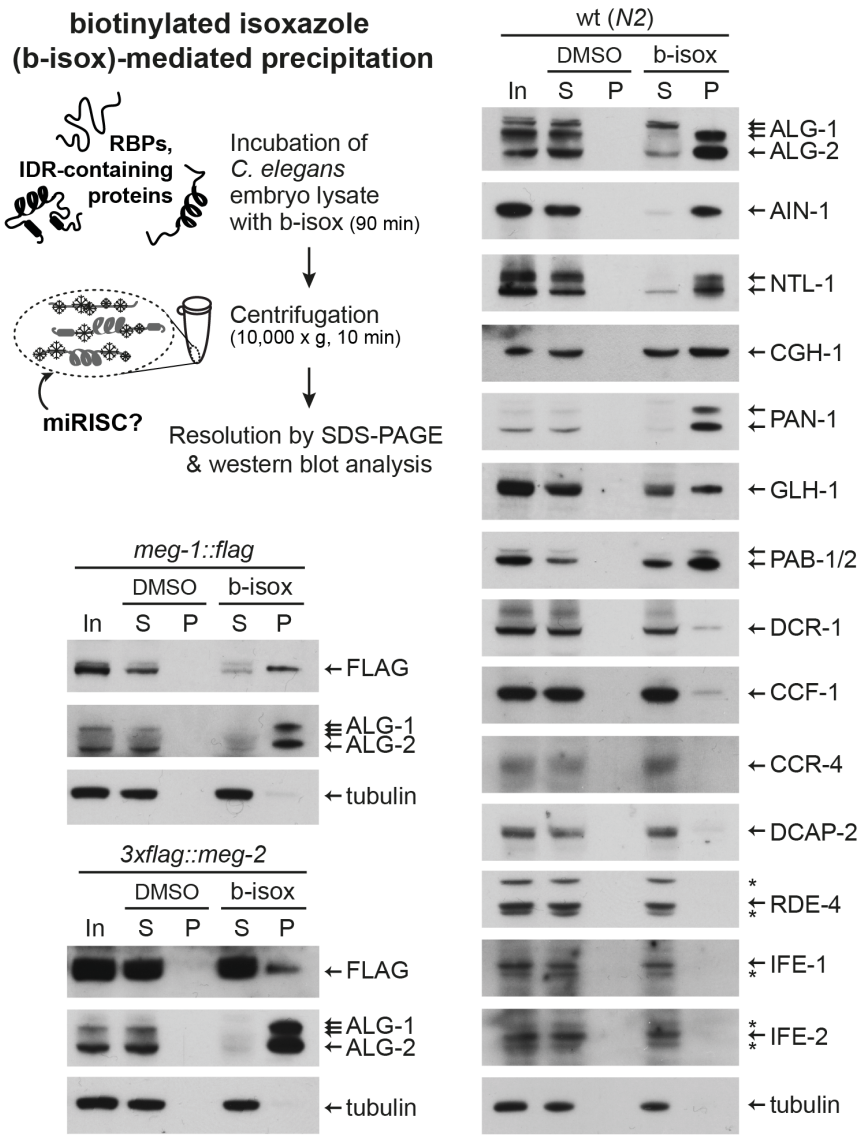

Figure 4-5: Selective precipitation of miRISC by biotinylated isoxazole

Schematic representation of the biotinylated isoxazole (b-isox)-mediated precipitation and western blots on *C. elegans* embryonic lysates (50 µg total protein) following exposure to b-isox (100 µM final). Lysates were derived from wild-type (wt, *N2*), and FLAG-tagged *meg-1* and *meg-2* strains. DMSO, used as the solubilizing agent for b-isox, served as a mock control. In indicates input, S indicates soluble content, and P indicates precipitate. Asterisks (*) indicate non-specific bands. (See also Figure A3-3).

4.3.6 Loss of inherently disordered MEG-1/2 disrupts the regulation of *cog-1* mRNA by *lsy-6* miRNA

The structural role of MEG proteins in germ granule assembly has recently been described (Leacock and Reinke, 2008; Wang et al., 2014). However, the linkage of germ granules in general, and of MEG-1/2 in particular, with miRNA-mediated silencing is unknown. We sought to determine whether intrinsically disordered MEG-1 and MEG-2 are implicated in embryonic miRNA function. For this, we first tested the effects of *meg-2* loss on the activity of the *lsy-6* miRNA (Figure 4-6). *lsy-6* functions during embryogenesis in the developmental specification of two bilaterally asymmetric neurons, ASEL and ASER, by down-regulating its target, *cog-1* (Johnston and Hobert, 2003). Animals lacking *lsy-6* expression fail to down-regulate *cog-1* in the ASEL, resulting in the ASEL neuron adopting the ASER fate. The hypomorphic *lsy-6(ot150)* allele encodes a mutation in the conserved regulatory element in the *lsy-6* promoter that leads to the reduction of *lsy-6*, but does not eliminate its function, resulting in a partially penetrant ASEL fate specification phenotype (Sarin et al., 2007). This sensitized background has been extensively used to look at genetic interactions with the miRNA pathway (Hammell et al., 2009; Ren et al., 2016; Vasquez-Rifo et al., 2013; Zhang and Zhang, 2013; Zinovyeva et al., 2014). ASEL fate was assayed by scoring for the expression of the ASEL-specific *plim-6*::*GFP*, a transcriptional reporter that serves as an indicator for successful *cog-1* silencing by *lsy-6*. Loss of *meg-2* in *lsy-6(ot150)* significantly enhanced the ASEL fate specification phenotype, with the absence of reporter expression in ASEL detected at 21.5%, compared to 8.2% in *lsy-6(ot150)* animals, thus more than doubling the penetrance of the phenotype (Figure 4-6). This effect was modulated by temperature, and the exacerbated *lsy-6* phenotype was more prominent when animals were grown at 16°C than at 19°C (21.5% at 16°C compared to 15.2% at 19°C). In *meg-2* mutants with

wild-type *lsy-6* expression, the reporter was expressed in the ASEL of every animal, indicating that removal of *meg-2* activity on its own did not affect ASEL fate specification. We also tested the loss of *meg-1* on *lsy-6* mutants. While *meg-1* mutants had no effect on *lsy-6* mutants at 16°C, a mild increase in animals displaying defects in ASEL specification was observed when grown at 19°C (from 9.7% to 13.9%).

These results indicate that *meg-2* is required for the full function of *lsy-6* miRNA in silencing *cog-1* expression during embryogenesis, while its paralog *meg-1* may have a partially redundant, or more limited contribution.

T(°C)	Genotype (with *otIs114*)	Animals expressing *plim-6::GFP* (%) ASEL	ASER	ASEL	ASER	n
16	*lsy-6(ot150)*	91.8		8.2		1503
	meg-1(vr10)	100		0		1419
	meg-1(vr10); lsy-6(ot150)	90.3		9.7		1054
	meg-2(ok1937)	100		0		1168
	meg-2(ok1937); lsy-6(ot150)	78.5		21.5		1012
19	*lsy-6(ot150)*	90.6		9.4		1096
	meg-1(vr10)	100		0		1165
	meg-1(vr10); lsy-6(ot150)	86.1		13.9		489
	meg-2(ok1937)	100		0		999
	meg-2(ok1937); lsy-6(ot150)	84.8		15.2		1161

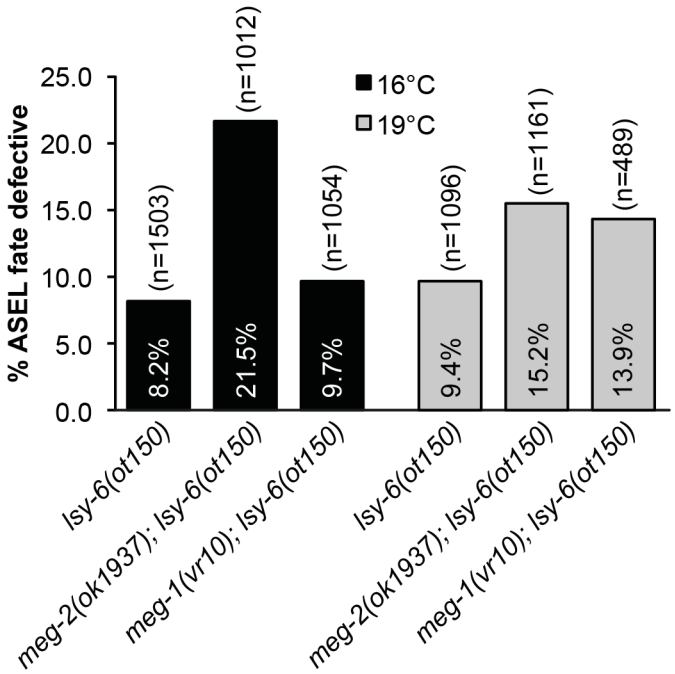

Figure 4-6: Loss of *meg-1* and *meg-2* function disrupts regulation of *cog-1* mRNA by lsy-6 miRNA

The *plim-6*::GFP expression (denoted in black in schematic diagram) indicates ASEL neuronal cell fate. *plim-6::*GFP mis-expression phenotypes were quantified in *lsy-6*, *meg-2*, and *meg-1* single mutants and *lsy-6; meg-2* and *lsy-6; meg-1* compound mutants. n = animals scored for each genotype.

4.4 Discussion

Through concerted proteomics and interaction analyses, cell-free assays and genetics, we resolved temporal events leading to silencing by miRISC, and identified a role for intrinsically disordered proteins recruited by the CCR4-NOT scaffold NTL-1 in the functions of embryonic miRNAs. Our results support a model wherein progressive mRNP assembly on target mRNA is an integral part of the mechanism of miRNA-mediated silencing in the embryo (Figure 4-7). This model improves the previous static view on miRISC interactions, and opens up new possibilities into how developmental contexts modulate silencing mechanisms dictated by miRNAs.

4.4.1 Scanning miRISC and effector miRISC are distinct

We provide three distinct lines of experimental evidence supporting the view that miRISC biochemically matures from a 'free' scanning miRISC, to a mRNA-bound form which tethers effector components of miRNA-mediated silencing. Firstly, interaction datasets generated with AIN-1 IP contrast with miRISC-associated components captured through 2'-*O*-methyl target analog affinity. Whereas in both cases the Argonautes ALG-1 and ALG-2 were the best detected interactions by far, the mRNA deadenylase, the processing machineries, or germ granule components were not detected in target analog captures. Secondly, while NTL-1 could be specifically recruited to miRISC-bound reporters in DRIP assays and AIN-1 was consistently detected among NTL-1 interactions, neither ALG-1 nor ALG-2 Argonautes could be detected in NTL-1 IPs. Thirdly and most decisively, scanning and effector miRISC could be resolved in time; DRIP results indicate that ALG-2 and AIN-1 association on the polyadenylated form of the 6xmiR-35 reporter precedes association with NTL-1, or the consequent mRNA deadenylation.

These findings are in logical line with previous conclusions drawn from *D. melanogaster* and human cells, which biochemically resolved the "miRISC loading complex" or RLC from

mature miRISC. RLC complexes lack GW182, but contain Dicer and exhibit pre-miRNA processing activity, while "mature miRISC" contains GW182 but lacks Dicer and pre-miRNA-processing activity (Fukaya and Tomari, 2012; Miyoshi et al., 2009). Hence, a tentative integrated view on data obtained across species and systems is that Argonaute-containing complexes are progressively remodeled from loading, to scanning, to the several steps of target silencing, to recycling (Gibbings et al., 2009; Lee et al., 2009; Wu et al., 2013).

We note that significant circumstantial evidence supports the possibility that multiple alternative miRISC maturation pathways may co-occur. A previous report examined AIN-2 interactions and mainly revealed interactions with components of the translation initiation machinery, but did not detect deadenylase, decapping, decay or mRNP components (Zhang et al., 2007) that are pre-eminent with AIN-1. The fact that AIN-2 was detected in our AIN-1 proteomic analyses indicates that such pathways may not be mutually exclusive.

4.4.2 CCR4-NOT association nucleates mRNPs on miRNA targets

Our work provides a unique glimpse on the intricate interactions that prevail in embryonic miRISC mRNPs and on their biological significance. The above-described sequential recruitment of the CCR4-NOT scaffold NTL-1 on miRNA targets, the breadth of the interactions of AIN-1 and NTL-1 with P body and germ granule proteins, the refraction of miRNA reporters to MNase challenge, and the selective precipitation of miRISC with biotinylated isoxazole support the assembly of a mRNP microenvironment on miRNA targets. We furthermore note that some of the detected interactions are independently corroborated in a recent protein-protein interaction network involved in embryonic polarity and germ granule assembly (Chen et al., 2016). AIN-1 was detected in PIE-1 and CAR-1 IP proteomics, and NTL-1, CCF-1, CCR-4 and MEG-2 were detected in MBK-2 IPs.

It has long been noticed that a fraction of the miRISC components, such as GW182 homologs, Argonautes, and small RNAs, localize to P body and/or P body like mRNPs (Behm-Ansmant et al., 2006; Ding et al., 2005; Jakymiw et al., 2005; Liu et al., 2005b; Meister et al., 2005; Pillai et al., 2005; Sen and Blau, 2005). A key question is how the mechanisms at work in the assembly of organelle-scale P bodies or germ granules relate to miRISC functions and dynamics. Important insight can be gained by considering a closely related paradigm. The Gavis group used quantitative single-molecule imaging to examine assembly of mRNP into germ granules in the *Drosophila* oocyte (Little et al., 2015). Detailed examination of stoichiometry and mRNP dynamics revealed that localized mRNAs are assembled and transported as single-mRNA RNP complexes into the oocyte, and are later merged as germ granules in the germ plasm. Build-up into germ granules is preferential for mRNPs that contain the same mRNA species, and mimics a positive-feedback dynamic, which could play a role in precipitating high-scale germ granule mRNPs. Altogether, this suggests that the content and assembly processes of single-mRNA and greater-scale mRNPs can be distinctly controlled, and progress along defined spatio-temporal steps (Little et al., 2015). If one projects this concept of mRNP reorganization into a miRNA-mediated silencing analogy, progression from single-mRNA-bound miRISC to greater scaffolds may be a consequence of the recruitment of CCR4-NOT and its associated proteins (Figure 4-7). Specifically, tethering intrinsically disordered proteins such as MEG-1/2 to miRISC through NTL-1 interaction, or their combination with determinants of GW182 homologs (Huang et al., 2013), could trigger phase transition to larger dynamic mRNP granules, and thus provide an enhanced microenvironment for mRNA seclusion, storage, or for decapping and decay.

4.4.3 Context and miRNP function: to decay or not to decay?

De-repression of *lsy-6* reporters *in vivo* under depletion of the MEG-1/2 proteins indicates that miRISC-instigated mRNP assembly contributes to miRNA target silencing in the *C. elegans* embryo. At first glance, this result may stand at odds with experiments in *Drosophila* S2 cells, wherein impairment of P body formation by knock-down of the decapping factors (Lsm1 and Lsm3) did not prevent miRNA reporter silencing (Eulalio et al., 2007b). This observation led to the interpretation that P bodies arise as a consequence of miRNA-mediated silencing rather than being a cause (Eulalio et al., 2007b). Such results, however, could not rule out the possibility that putative P body functions are redundant with other aspects of miRNA-mediated silencing in S2 cells, or that a sufficient function for a lesser-scale miRISC mRNP scaffold on target mRNAs. In addition, substantial evidence supports the idea that developmental context defines the composition and functions of P bodies and mRNPs in general. Work by the Evans group in *C. elegans* has already highlighted the diversity of mRNPs during oocyte maturation and in early embryo. mRNPs that contain components such as CAR-1 and CGH-1 have distinct functions in maternal mRNA translation repression and degradation (Hubstenberger et al., 2015). This work and the results from the Seydoux group further indicate that the composition and function of mRNPs rapidly progress during early development (Gallo et al., 2008; Hubstenberger et al., 2015). This diversity indicates that interactions detected here with NTL-1 and AIN-1 reflect a convolution of functionally distinct germ granule and P body-like particles that occur in the different cell lineages, merged in our embryonic preparations. The interactors PGL-1, GLH-1, and MEG-1 are distinctly detectable in P lineage blastomeres during *C. elegans* embryogenesis, where they are important for germ granule assembly and stability (Gruidl et al., 1996; Kawasaki et al., 2004; Kawasaki et al., 1998; Kuznicki et al., 2000; Leacock and Reinke, 2008; Spike et al.,

2008). MEG-2, while partially functionally redundant with MEG-1 in the germline, is more broadly expressed and extends to somatic blastomeres (Leacock and Reinke, 2008). De-capping factors DCAP-1 and DCAP-2 co-localize with PGL-1 in P1 germline blastomeres in germ granules, but are also closely associated with P bodies throughout *C. elegans* lifespan (Gallo et al., 2008; Lall et al., 2005). The PATR-1 decapping co-factor is also detected both in germline and somatic P bodies, but progressively accumulates in somatic blastomeres (Gallo et al., 2008). The *C. elegans* homolog of the eIF4E-transporter, IFET-1 is partitioned into germ cells after the 4-cell stage, where it functions as a translational repressor of germ granule localized RNAs (Sengupta et al., 2013). Finally, the LSM proteins, thought to couple deadenylation with mRNA decay (Tharun and Parker, 2001), are enriched in somatic P bodies from the 3/4-cell stages, a window that coincides with maternal mRNA decay, and such a localization requires NTL-1 (Gallo et al., 2008; Seydoux and Fire, 1994).

The relative contributions of the translation repression, and deadenylation and decay components of miRNA-mediated silencing is still a matter of debate, and remain under scrutiny in various systems and cell types. Our findings support the possibility that specialization of mRNPs can modulate miRISC output. It is thus reasonable that the extent and nature of functions of mRNPs in miRNA-mediated silencing mechanisms should be systematically considered in specific developmental and cellular contexts.

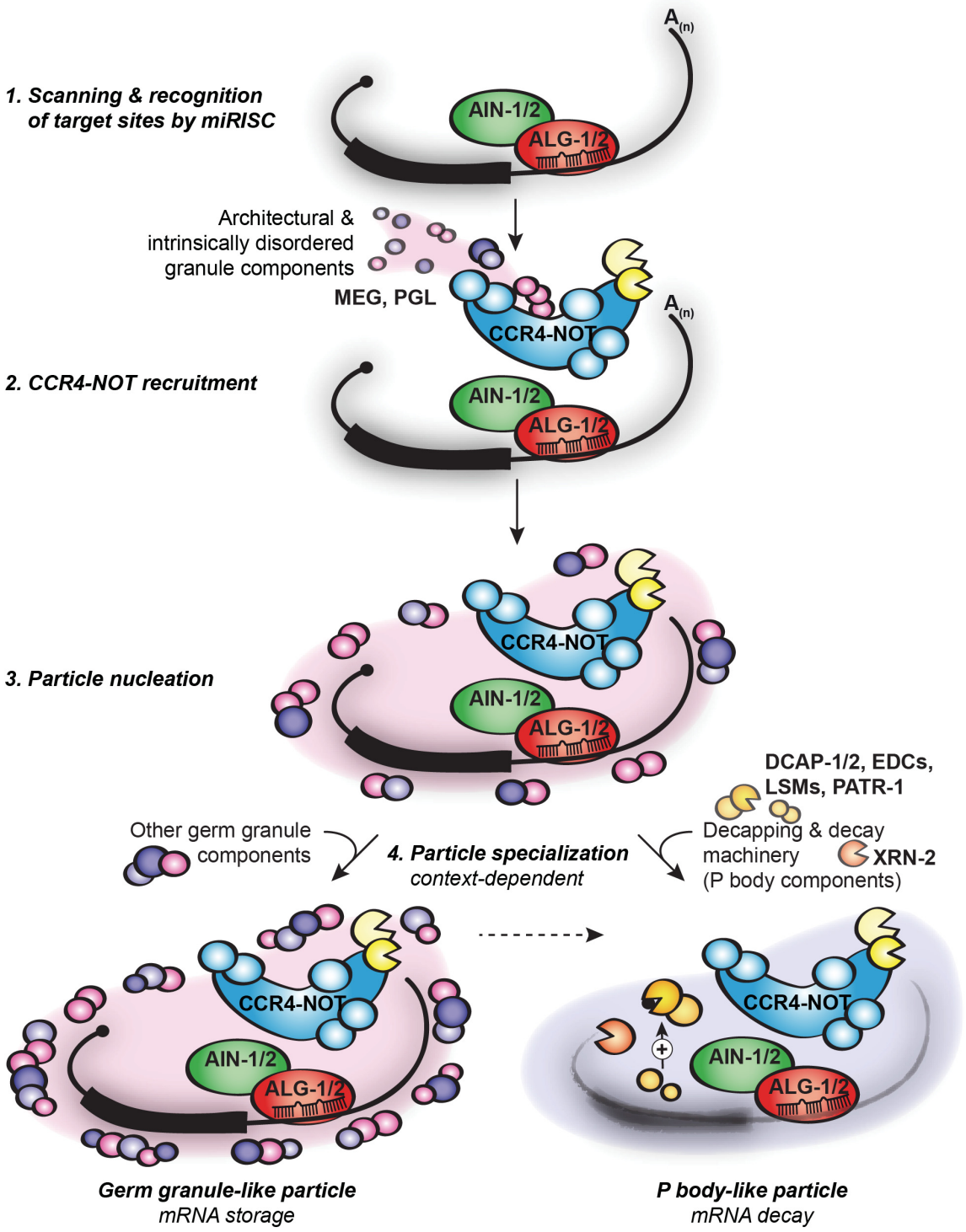
1. Scanning & recognition of target sites by miRISC
A(n)
AIN-1/2
ALG-1/2
Architectural & intrinsically disordered granule components
MEG, PGL
CCR4-NOT
2. CCR4-NOT recruitment
3. Particle nucleation
DCAP-1/2, EDCs, LSMs, PATR-1
Other germ granule components
4. Particle specialization
context-dependent
Decapping & decay machinery (P body components)
XRN-2
Germ granule-like particle
mRNA storage
P body-like particle
mRNA decay

Figure 4-7: Model : mRNP assembly and specialization on target mRNAs in embryonic miRNA-mediated silencing

The miRISC (ALG-1/2 and AIN-1/2, and other accessory proteins) scans and recognizes mRNA targets (1). The CCR4-NOT deadenylase complex, along with tethered architectural and intrinsically disordered granule constituents (MEG-1 and MEG-2, and PGL proteins), is sequentially recruited to target mRNAs (2) and nucleates an mRNP particle (3). Proteomics analyses on AIN-1 and NTL-1 reveal a convolution of germ granule and P body-like mRNP complexes. Such diversity indicates the possibility of particle specialization that depends on cellular and developmental context for modulating the miRISC output on target silencing by storing the mRNA or subjecting it to decay (see Discussion).

4.5 Materials and Methods

4.5.1 *C. elegans* strains and RNAi.

C. elegans were cultured using standard techniques as described (Brenner, 1974). Worm strains used: N2 Bristol (wild-type), MJS26 (ALG-2::GFP, described in Vasquez-Rifo et al., 2012), FD21 (AIN-1::LAP, unc-119(ed3); tagIs1271), EV465 (NTL-1::LAP, described in Nousch et al., 2013), *meg-1(vr10)*, *meg-2(ok1937)*, MH2636 (*otIs114(plim-6::GFP, rol-6, lsy-6(ot150))*), FD14 (*meg-1(vr10); otIs114; lsy-6(ot150), rol-6*), FD15 (*meg-1(vr10); otIs114, rol-6*), FD16 (*meg-2(ok1437); otIs114; lsy-6(ot150), rol-6*), FD17 (*meg-2(ok1437); otIs114, rol-6*), JH3292 (MEG-1::1xFLAG, C-terminal FLAG insertion in the genomic *meg-1* locus and generated using CRISPR/Cas9 system by the laboratory of Geraldine Seydoux), FD22 (3xFLAG::MEG-2, N-terminal 3xFLAG insertion in genomic *meg-2* locus, generated using CRISPR/Cas9 system). All strains were grown at 22°C, except strains used in assessing *meg-1* and *meg-2* genetic interactions with *lsy-6*, which were maintained at 16°C or 19°C, as indicated.

RNAi was performed as in Fire et al. (1998) and Timmons et al. (2001) on L4 animals and progeny (embryos) were harvested. For generating the *ccf-1* RNAi clone, the genomic sequence of *ccf-1* was amplified using forward primer: 5'-TAATACGACTCACTATAGGG AATGGTCAATGACAAAGGAG-3' (Tdo435); and reverse primer: 5'-TAATACGACTCACTATAGGG ATTAGGCCTTGTGGTGTCT-3' (Tdo436). TA cloned into pSC-A-amp/kan and transformed in HT115 bacteria as described in Timmons et al. (2001). The *ccr-4* RNAi feeding vector was obtained from the Ahringer library (Kamath and Ahringer, 2003).

4.5.2 Plasmids.

The RL constructs containing miR-35 wild type or mutated sites have been described in Wu et al. (2010).

4.5.3 Preparation of *C. elegans* embryonic extract for translation assays, deadenylation assays, deadenylated RNA immunoprecipitation (DRIP).

C. elegans embryo extracts were prepared as described in Wu and Duchaine (2011), except that calf-liver tRNA was omitted from the extract.

4.5.4 *In vitro* translation and deadenylation assay.

Assay was setup and performed as described in Wu et al. (2010).

4.5.5 Deadenylated RNA Immunoprecipitation (DRIP).

Deadenylation assay was conducted as described above with the following modification: Prior to deadenylation reaction, *C. elegans* embryonic extract was pre-cleared with pre-equilibrated Dynabeads® Protein G (Life Technologies) for 1 hour at 4°C with rotation in DRIP buffer (24 mM HEPES-KOH pH 7.4, 25 mM KOAc, 1.28 mM $Mg(OAc)_2$, 0.1 U/µl Ribolock RNase inhibitor (Fermentas), 1 mM DTT). 50 µl-deadenylation reaction mixture was setup per time point. Deadenylation assay was then conducted over a three-hour time-course. During incubation, mouse anti-GFP antibody (Roche) was added to Dynabeads® Protein G and incubated for 1 hour at 4°C with rotation. The reaction mixture was then incubated with 50 µl of a 1:1 suspension of anti-GFP-Dynabeads® Protein G for 30 minutes at 4°C with rotation. After the immunoprecipitation step, beads were washed four times with DRIP buffer. Washes were performed at 4°C with rotation. The beads were then transferred into two tubes, one for western blot analysis, and the other for Proteinase K treatment and RNA extraction. Proteinase K

treatment was performed by resuspending the beads in 90 µl Proteinase K buffer (200 mM Tris-HCl pH 8, 25 mM EDTA pH 8, 30 mM NaCl, 2% SDS) and 10 µl Proteinase K (10 µg/µl) for 10 min at room temperature. The eluted RNA was purified using phenol/chloroform and ethanol precipitation, followed by separation on a 4% polyacrylamide/urea gel and autoradiography.

4.5.6 Extract preparation and Multidimensional Protein Identification (MuDPIT).

Embryo pellets were homogenized in lysis buffer (50 mM Tris HCl pH 8, 150 mM NaCl, 1 mM EDTA, 1% Triton X-100 with Complete EDTA-free protease inhibitors (Roche)) and cleared by 16,100 x g centrifugation. FLAG-tagged proteins were purified using ANTI-FLAG M2 Affinity Gel (Sigma-Aldrich A2220) following extract preparation. Prior to adding the matrices, the clarified lysate was quantified and diluted to 5 mg/ml concentration in lysis buffer (50 µl bead slurry was added for 1 ml IP volume). Immunoprecipitations were carried out at 4°C for 2 hours, and beads were then washed four times in the lysis buffer. Bound proteins were eluted using the 3xFLAG peptide (Sigma-Aldrich F4799). A fraction of the eluate (1/10th for AIN-1::LAP and 1/3rd for NTL-1::LAP) was monitored by SDS-PAGE, followed by western blot analysis. Non-transgenic N2 embryos were used as controls for the purifications. MuDPIT was performed as described in Duchaine et al. (2006).

4.5.7 Assessment for siRNA or miRNA pathway proteins.

The studies integrated for the analysis of factors implicated in miRNA and other RNAi-related pathways are as follows: *let-7* phenotype (WormBase (WS220), Tabach et al., 2013), *let-7* sensitized (Parry et al., 2007), *Drosophila* miRNA and siRNA (Zhou et al., 2008), DCR-1 Co-IP (Duchaine et al., 2006), ERI-1 Co-IP (Thivierge et al., 2012), AIN-2 Co-IP (Zhang et al., 2007), suppression of transgene silencing in *eri-1* and dsGFP RNAi (Kim et al., 2005), germline co-

suppression defect (Robert et al., 2005), SynMuv suppression (Cui et al., 2006). The generation and analysis of the 11 screens was previously described in Tabach et al. (2013). The hyper-geometric *p*-values were calculated from a population of 17,000 genes.

4.5.8 Gene Ontology (GO) term analysis.

GO term overrepresentation test (release 20150430) for GO cellular component annotations was determined using the PANTHER Classification System (http://www.pantherdb.org) (Mi et al., 2013; Thomas et al., 2003). Identified proteins listed in Table A3-1 (AIN-1 interactors) and Table A3-2 (NTL-1 interactors) served as the analyzed list, and the *C. elegans* genes in the PANTHER database served as the reference list.

4.5.9 Nuclease sensitivity assay.

At the end of a three-hour deadenylation reaction, 0.005 U/µl of micrococcal nuclease (MNase, Roche) and 1 mM $CaCl_2$ was added to the reaction mixture (a 1x 12.5-µl reaction consisted of 9.136 µl supplemented *C. elegans* embryonic extract, 2.364 µl water, and 1 µl radiolabeled RNA). A 1x 12.5-µl aliquot of the MNase-treated reaction mixture was withdrawn at each time point over a 15-minute treatment and the MNase treatment was stopped by the addition of 20 mM EGTA. RNA was extracted and analyzed by autoradiography as described in Wu et al. (2010).

To quantify the RNA integrity following MNase treatment, the intensity of the RNAs from the autoradiographs was quantified using ImageJ from triplicate experiments conducted using the same extract preparation. A logarithmic regression using a linear model was used to analyze the rate of RNA reporter decay. Autoradiograph from one replicate is presented. Experiment was reproduced at least twice in independent extract preparations. Error bars indicate standard deviation. Statistical significance was calculated using one-tailed Student's t-Test.

4.5.10 Biotinylated isoxazole (b-isox)-mediated precipitation.

C. elegans embryonic pellets were resuspended in a lysis buffer (50 mM HEPES pH 7.5, 150 mM NaCl, 0.1% NP-40, 1 mM EDTA, 2.5 mM EGTA, 10% glycerol, 1 μM DTT) supplemented with proteases, phosphatases, and RNase inhibitors. The extracts were homogenized with a pre-chilled Kontes dounce homogenizer and then centrifuged three times at 14,000 rpm for 10 min at 4°C. The samples were exposed to 100 μM of the b-isox chemical (Sigma Aldrich) and rotated at 4°C for 90 min. The incubated reaction was then centrifuged at 10,000 x g for 10 min to pellet the precipitates. The pellet was washed twice in the lysis buffer and resuspended in 1× SDS loading buffer for protein analysis. Proteins in the supernatant fractions were precipitated by addition of four volumes of cold acetone, incubated for 1 hour at -20°C, and centrifuged at 15,000 x g for 10 min to pellet the precipitates.

4.5.11 Western blotting

Protein samples from DRIP were separated on a 6% SDS-PAGE and analyzed by western blot. Protein samples for CCR-4 and CCF-1 western blot analysis were separated on a 10% SDS-PAGE. Samples from b-isox-mediated precipitation were resolved on NuPAGE 4-12% Tris-Glycine gradient gels (Invitrogen). Antibodies used were: mouse monoclonals against GFP (Roche), alpha tubulin (Abcam), FLAG (Sigma-Aldrich); rabbit polyclonals against PAB-1/2 (4569, Flamand et al., 2016), DCR-1, ALG-1/2, RDE-4 (Duchaine et al., 2006), CGH-1 (Boag et al., 2005), GLH-1 (Gruidl et al., 1996), PAN-1 (Gao et al., 2012), IFE-1, IFE-2 (Jankowska-Anyszka et al., 1998), and AIN-1 (gift from Dr. Martin Simard); rat polyclonal against DCAP-2 (Lall et al., 2005). HRP-conjugated goat anti-rabbit, anti-mouse, and anti-rat (Sigma-Aldrich) and mouse TrueBlot® (eBioscience) were used as secondary antibodies. Rabbit polyclonal antisera for CCF-1 and CCR-4 were raised against the following peptides at Capralogics Inc.

(Hardwick, Massachussetts): KGGLQEVADQLDVKRQGVR (CCF-1, 3755) and VHRVLTEDEIASGRSTRWTELE (CCR-4, 3756). For NTL-1, the region corresponding to amino acid position 650-950 was amplified from cDNA using forward primer: 5'-ATAATAGGATCCAGGTAATGAAAGAGAACTCGG-3' (Tdo1707); and reverse primer: 5'-TATTATGGATCCCAAATTTTCCACTGACATCGC-3' (Tdo1708), and cloned into pCAL-KC via BamHI/BamHI. This construct was used as a template for generating the antigen for mouse polyclonal against NTL-1. Sera for CCF-1, CCR-4, and NTL-1 were used at 1:1000 dilution in 5% non-fat dry milk in 0.1% Tween-PBS overnight at 4°C.

4.6 Acknowledgments

We thank Dr. Martin J. Simard for providing the *alg-2::gfp* strain and AIN-1 antibody, Dr. Christian Eckmann and the *C. elegans* TransgeneOme platform for the *ain-1::lap* and *ntl-1::lap* strains, and Dr. Valerie Reinke and the Caenorhabditis Genetics Center (CGC) for the *meg-1* and *meg-2* strains used in this study. We also thank Dr. Geraldine Seydoux and Dr. Deepika Calidas for the *meg-1::1xflag* strain and comments on the manuscript. This work was supported by the Canadian Institutes of Health Research (CIHR) MOP 123352 (T.F.D.), and the Fonds de la Rercherche en Santé du Québec (FRQS), Chercheur-Boursier Salary Award J2 to (T.F.D.). E.W. was supported by the CIHR Frederick Banting and Charles Best Doctoral Research Award.

Chapter 5: General Discussion

5.1 Main findings and impact

Since its introduction as a model organism by Sydney Brenner in the 1960s, *C. elegans* has brought about major contributions to biology. Its celebrated contributions include being the first whole-organism mapping of cell lineages, sequencing of the first multi-cellular organism genome, discovery of the genetic program underlying programmed cell death, and several seminal contributions to asymmetric cell divisions, germ line and early embryonic development. Most relevant to this thesis, however, were the discoveries of the genes involved in RNAi and miRNAs, amongst which *lin-4* and *let-7* are the founding members. These seminal discoveries clearly highlight the power of *C. elegans* genetics in building the framework for regulatory pathways that govern animal development. However powerful, genetics also has limitations that were recognized early on by Brenner himself; "only when genetics was coupled with methods of analyzing other properties of the mutants, by assays of enzymes or *in vitro* assembly, did the full power of this approach develop" (Brenner, 1974).

This last statement precisely captures the essence of my thesis. I have applied biochemistry, proteomics, cell-free assays, transgenics, and other molecular approaches to extend genetics for a fuller understanding of miRNAs and their impingement on gene expression. My first goal was to develop a system that faithfully recapitulated miRNA-mediated silencing. In Chapter 2, I detailed the properties of such an extract, derived from *C. elegans* embryo, and its optimization for miRNA-mediated translation repression assays. In Chapter 3, I further exploited this system in miRNA-directed deadenylation assays. I demonstrated that the miRISC directs rapid deadenylation of reporter mRNAs with a variety of natural 3'UTRs, with each target displaying a distinct pattern of deadenylation. Two particular 3'UTRs were examined in greater detail: the *tollish* family member *toh-1* and the BH3-encoding *egl-1* mRNAs. Both mRNAs are

also targeted by the *miR-58* family members (ortholog of *D. melanogaster bantam* miRNA), and require functional cooperativity between the two miRNA-binding sites on target 3'UTRs for deadenylation to occur. This contribution highlights i) the prevalence of miRNA-mediated deadenylation in *C. elegans* embryos, and ii) functional cooperation between miRNA-binding sites within the same 3'UTR to promote deadenylation.

In the years leading up to my thesis work, miRISC components had been shown to co-localize with mRNA decay components into the P body mRNPs (Behm-Ansmant et al., 2006; Ding et al., 2005; Jakymiw et al., 2005; Liu et al., 2005b; Meister et al., 2005; Pillai et al., 2005; Sen and Blau, 2005). This hinted to mRNA decay as an outcome of miRNA-mediated silencing. However, the nature of this association was correlative, and the functional role of mRNPs in miRNA-mediated silencing was poorly defined. In Chapter 4, I described the sequential assembly of miRISC on mRNA targets with its effector CCR4-NOT deadenylase and mRNA decay machineries into miRNP particles. I also revealed the extensive network of interactions between core miRISC AIN-1, CCR4-NOT deadenylase, and mRNP components of P bodies and germ granules. Several novel P bodies and germ granules interactions were identified, among which the intrinsically-disordered MEG-2 potentiated silencing effected by the embryonic *lsy-6* miRNA *in vivo*. In the course of this work, I developed yet more innovative assays to i) profile target association with miRISC and CCR4-NOT deadenylase complex (DRIP), and ii) to monitor miRNP assembly on target reporters (MNase sensitivity assay). While developing such assays was laborious, they expanded the reach of my *C. elegans* cell-free system beyond simple outcome of silencing and deadenylation. Overall, my findings point to a continuum of mRNP granule types and functionalities in miRNA-mediated silencing. Indeed, my data and others support a view of a dynamic specialization of mRNP, which can atone the mechanistic outcome

of silencing to cell lineage and developmental context, rather than mere localization into static, distinct entities.

5.2 Elucidating the mechanisms of miRNA-mediated silencing

My thesis work represents a significant contribution in direct logical line from the genetic discovery of the first miRNAs in 1993, and adds to the complex but comprehensive model that currently explains their gene silencing activities. Eight years after the discovery of *lin-4* and *let-7*, the first genome-wide investigations revealed that the two *C. elegans* heterochronic miRNAs were just the tip of the iceberg. Abundant small RNAs, miRNAs and others, were being discovered across metazoans (Lagos-Quintana et al., 2001; Lau et al., 2001; Lee and Ambros, 2001). Conservation of the miRNA sequences themselves, but also conservation of their biogenesis machineries and their co-factors, suggested that they might function in a similar manner in species as diverse as nematodes and humans. A fruitful convergence of experiments carried out across species and cell types rapidly followed, which would largely reveal the mechanisms underlying miRNA-mediated gene silencing. The earliest mechanistic studies, performed in *C. elegans*, were interpreted as evidence for inhibition at the translation level without an effect on mRNA stability (Olsen and Ambros, 1999). Shortly after, a handful of studies performed in *C. elegans* (Bagga et al., 2005), *D. melanogaster* (Behm-Ansmant et al., 2006), and zebrafish (Giraldez et al., 2006), instead provided evidence that silencing was correlated with mRNA deadenylation and/or decay. Particularly compelling was the role of *miR-430*, in the process of maternal-to-zygotic transition in zebrafish. On its own, this single miRNA can direct the deadenylation and destabilization of a wide variety of maternal mRNA targets (Giraldez et al., 2006), to enable the expression of zygotic cellular fates. The apparent contradictions of the early mechanistic studies raised some degree of controversy within the

community, and prompted yet more targeted investigations on the mechanism of miRNA-mediated silencing. It soon became clear, however, that *in vivo,* and genetic studies could not provide the sensitivity necessary to fully and unambiguously dissect the mechanism. The miRNA community soon turned to develop cell-free systems that recapitulated miRNA activities, starting with rabbit reticulocyte lysates (Wang et al., 2006), Krebs ascites mouse extract (Mathonnet et al., 2007), human cell culture (Beilharz et al., 2009; Wakiyama et al., 2007), and *D. melanogaster* embryos and cultured cells (Iwasaki et al., 2009; Thermann and Hentze, 2007). These systems proved invaluable in revealing some of the events of miRNA-mediated translation repression, mRNA deadenylation and decay.

My work represents a series of contributions along those investigations. However, our miRNA-mediated silencing system is unique, and remains irreplaceable in several aspects. First, our system is based on abundant, phenocritical, and endogenous miRNAs. Few miRNA families are essential for development and viability in *C. elegans* (Alvarez-Saavedra and Horvitz, 2010; Miska et al., 2007). Mutation of members of the *miR-35-42*, *miR-51-56*, and *Ce*Bantam (*miR-58/80-82*/*1834/2209a*), which are the focus of my molecular investigations, result in striking abnormalities ranging from locomotion and organogenesis to lethality (Alvarez-Saavedra and Horvitz, 2010; Ibanez-Ventoso et al., 2008; Lau et al., 2001; Stoeckius et al., 2009). These miRNA families are also abundantly expressed in the embryo, with *miR-51-56* family broadly expressed from mid-embryogenesis onward (Lau et al., 2001; Lim et al., 2003; Shaw et al., 2010; Stoeckius et al., 2009). As such, while certain *in vitro* miRNA silencing systems require ectopic programming of the extract by adding exogenously synthesized miRNAs (Iwasaki et al., 2009; Wakiyama et al., 2007), this step is not needed in our *C. elegans* cell-free system. In turn this

allowed us to study their endogenous properties and molecular behaviors in deadenylation and silencing.

Second, our cell-free system remains the only one to date to recapitulate miRNA-mediated deadenylation and silencing on natural 3'UTR sequences. Indeed, most cell-free studies examined the effects of individual miRNAs on artificial reporter mRNAs, and other systems that have been investigated in the lab, such as Krebs or HeLa extracts fail to deadenylate mammalian natural 3'UTRs. It is still unclear why it is so. It may be due to the particular abundance of the investigated miRNA families, a particularly primed miRISC machinery in *C. elegans* embryo, the pervasive nature of the deadenylation cues dictated by *C. elegans* 3'UTRs, or their exquisitely short and A/U-rich nature in comparison to other model systems (Jan et al., 2011). Notwithstanding the reasons, this enabled a unique glimpse at the 3'UTR-specific modulation of miRNA-mediated silencing activities (Chapter 3).

Third, the genetics and transgenic flexibilities available in *C. elegans* provided our system a unique versatility, and a conjuncture of molecular sensitivity and biological relevance. Such properties were instrumental in the successful generation of a miRNA-depleted extract with the *alg-2; alg-1(RNAi)* (Chapter 3), extracts wherein the *ccr-4* and *ccf-1* catalytic subunits of the CCR4-NOT deadenylase complex were partially depleted (Chapter 4), or extracts wherein ALG-2, AIN-1, and NTL-1 were tagged (Chapter 4).

Finally, my work like few other studies provides an understanding of the molecular mechanics for miRNA action within the embryonic context. Indeed, most cell-free systems are derived from somatic cells of a single lineage, sometimes transformed, and often grown outside of their physiological niche. This distinctive property was key in revealing the contribution of the

germ granule mRNP component and intrinsically disordered MEG-2 in embryonic miRNA-mediated silencing (Chapter 4).

5.3 On the cooperative nature of embryonic miRNA-mediated silencing

Each of the unique aforementioned properties of our cell-free system was key for one of the most significant findings of my thesis work: the profoundly cooperative nature of embryonic miRNA-mediated deadenylation. Using the natural 3'UTRs of *egl-1* and *toh-1* mRNAs, I showed in Chapter 3 that deadenylation absolutely requires cooperation of two distinct miRNA-binding sites. Previous studies based on mammalian cell culture had hinted that several miRNA-binding sites on artificial reporters are required for silencing (Pillai et al., 2005), and genomic studies had indicated that on average, a minimal distance separating binding sites enhanced silencing by miRNAs (Grimson et al., 2007; Saetrom et al., 2007). Our findings go beyond those previous observations in the sense that a single miRNA-binding site, however structured, cannot trigger deadenylation or silencing in the embryo. As such, miRNA-binding sites have to be considered as combinations, or functional constellations in this context. Synergism or strong cooperativity bears important biological implications during embryonic development. A fundamental consequence of this property is that mRNA targets of embryonic miRNAs are subjected to the combined stoichiometry, and thus an exquisitely precise control by several miRNAs with distinct expression patterns. This feature may be crucial in the case of threshold-sensitive proteins, such as with the BH3 homolog *egl-1*. Its precisely tuned protein level in cell types is literally a matter of life and death, as minor changes trigger apoptosis in a large number of cell lineages in *C. elegans* (Nehme and Conradt, 2008).

Cooperativity between *cis*-elements likely extends far beyond miRNA-binding sites. As pointed out in chapter 3, 3'UTRs are not only platforms for miRNAs, but also for diverse RNA-

binding proteins and other factors mediating post-transcriptional regulation mechanisms that are dictated by RNA elements often found in close proximity. These factors and their corresponding *cis*-elements likely interact and cooperate in fine-tuning gene expression by enabling diverse regulatory effects during development. An illustrative example of this is the case of *nos* mRNA regulation in *D. melanogaster*. In the fly embryo, *nos* mRNA is translationally repressed by the RNA-binding protein, Smaug, in the bulk of the embryo, but is translationally active at the posterior end (Dahanukar and Wharton, 1996; Gavis and Lehmann, 1994; Gavis et al., 1996; Smibert et al., 1996). Smaug recruits the CCR4-NOT deadenylase complex, resulting in rapid deadenylation and decay of *nos* mRNA (Zaessinger et al., 2006). Interestingly, the piRNA pathway was also reported to mediate post-transcriptional gene silencing of *nos* mRNA, and the piRNA-specific AGOs, Ago3 and Aubergine, form a complex with Smaug and CCR4 (Rouget et al., 2010). Although it remains unclear how the mechanisms of piRNA-mediated silencing and deadenylation by the CCR4-NOT complex co-regulate *nos* mRNA, these findings highlight cooperativity between distinct regions within *nos* mRNA 3'UTR in the fly embryo.

In line with this, I consider the interactions between RNA-binding proteins and the RNAi pathways on 3'UTRs an important area of research uniquely enabled by the system and biochemical assays I developed in this thesis. I discuss strategies to develop this important theme further, using the NHL-2/miRISC paradigm, in the *Future Directions* section below.

5.4 Untangling the events of translation repression, deadenylation, decapping and decay

My data revealed that deadenylation is a pervasive regulation mechanism employed by *C. elegans* embryonic miRNAs (Chapter 3). The poly(A) tail plays a central role in protecting mRNAs from decay (Bernstein et al., 1989), and in synergizing with the 5' cap in translation

initiation (Gallie, 1991; Wells et al., 1998). In several metazoan cell types, deadenylation is rapidly followed by mRNA decapping and mRNA decay by exonucleases (Wilusz et al., 2001). As such, the components of translation repression, mRNA deadenylation, decapping and decay are often intimately entangled in miRNA-mediated silencing. Current challenges in the field lie in discerning their relative contributions, and their individual biological significances.

Translation repression without impact on mRNA stability was noticed early on in *C. elegans* using ribosome sucrose gradient fractionation (Olsen and Ambros, 1999). More precise resolution was later provided *in vitro* in Krebs mouse ascites extracts as translation repression was shown to precede target deadenylation in this system (Fabian et al., 2009). More recently, detailed kinetic analyses conducted in mammalian (Bethune et al., 2012) and *D. melanogaster* cells (Djuranovic et al., 2012), and ribosome profiling in zebrafish embryos (Bazzini et al., 2012) reached similar conclusions. The latter study by the Giraldez group particularly highlighted the importance of context, as developmental progression marked a switch in mechanisms from translation repression to mRNA destabilization. These studies are in striking contrast to those from genome-wide studies, where comparison of transcriptomes and proteomes led to claims that mRNA destabilization was predominantly responsible for miRNA-mediated gene repression. This conclusion was reached in mammalian cells (Eichhorn et al., 2014; Guo et al., 2010; Subtelny et al., 2014) and in *C. elegans* larval stages (Subasic et al., 2015).

My work in Chapter 3 revealed the 3'UTR-specific behavior of miRNA-mediated deadenylation. On this basis, one should interpret cautiously the significance of the aforementioned transcriptome studies, which seek to conclude with genome-wide rules on such diverse and finely tuned determinants as those encoded in 3'UTRs. On a related matter, it is important to note that the L4 animals utilized in the Subasic et al. study are heterogeneous in

cellular diversity and tissue composition, and therefore context-dependent mechanistic aspects of miRNA-mediated silencing may be masked.

Given the tight consonance of events leading from translation repression, to deadenylation, to decay, a detailed time course of mRNA processing and translation should be conducted to monitor the effects on the mRNA target and on the protein levels. This was indeed a key feature in the zebrafish early embryo (Bazzini et al., 2012), and in a later study by the Bartel group (Subtelny et al., 2014). A major increment of this later study was the integration of a next-generation sequencing-based poly(A) tail profiling on RNAs isolated from various species, tissues, and cell lines, which provided better resolution of the tail length of global mRNAs (Subtelny et al., 2014).

Just like translation repression is difficult to disentangle from deadenylation, so is mRNA deadenylation from decapping and decay. In some systems such as *Drosophila* S2 cells, decapping and decay are extremely well coupled. In fact, one cannot capture or even detect a miRNA reporter without knocking down the decapping enzymes Dcp1 and Dcp2, which are only then revealed in their deadenylated form (Behm-Ansmant et al., 2006). This observation illustrates the challenge of clearly pinpointing and separating the events involved, and their contributions to overall silencing. However, it also hints to genetic depletion (knock down), and mRNA target integrity analyses as a powerful strategy to link novel miRISC or NTL-1 interactions specifically to steps of deadenylation, decapping and decay (see *Future Directions* section).

With this in perspective, it is also important to point out that while the CCR4-NOT complex is most notably characterized for its deadenylation function, recent reports have shown the ability of CCR4-NOT to act in translation repression independent of its deadenylase activity.

In *X. laevis*, HEK293T, and *Drosophila* S2 cells, a tethering-based assay showed a repressive effect by the CCR4-NOT even when it is recruited to reporter mRNAs lacking a poly(A) tail (Chekulaeva et al., 2011; Cooke et al., 2010). When the residues in the catalytic domain of CAF1 are mutated, CAF1 is still capable of impinging on translation of the reporters without any effects on the mRNA levels, indicating CAF1 can act as a translational repressor independent of its enzymatic deadenylase activity (Chekulaeva et al., 2011).

A challenge in the future will be to dissect the multi-faceted functions of CCR4-NOT in translation repression, deadenylation, decapping and decay. This complex involvement may be particularly important in the context of early embryonic development, in which cell fate determination and polarity is heavily dependent on spatiotemporal mRNA regulation. A particularly interesting paradigm for such a problem is the *C. elegans nos-2* maternal mRNA. *nos-2* is translationally repressed in the oocyte and early embryo (Gallo et al., 2008). But starting at the 4-cell stage, *nos-2* mRNA is degraded in somatic blastomeres yet maintained in germ cells, where it is activated in 28 cell-stage embryos. Interestingly, translation repression of *nos-2* in the oocyte and its degradation in somatic compartments are dependent on *ntl-1* (Gallo et al., 2008). It would be of great interest to dissect the dual functionality of the CCR4-NOT complex in the post-transcriptional gene regulation of *nos-2* and other maternal mRNAs during embryogenesis.

5.5 The diversity of mRNP particles in miRNA-mediated gene silencing

My work supports a model wherein mRNPs assembly with miRISC on mRNA targets is an integral and functional part in the events underlying miRNA-mediated silencing. A key observation of my thesis work is the extent and the diversity of interactions between the miRISC, CCR4-NOT and mRNP components of P bodies and germ granules. Because P bodies and germ granule mRNPs serve quite distinct biological purposes in silencing, processing, and storing

mRNAs, and because their compositions change with context, we propose that mRNP specialization could modulate the mechanisms and the outcome of miRNA-mediated silencing.

Previous studies conducted in mammalian cells and *D. melanogaster* S2 cells had identified physical interactions between CCR4-NOT, and the decapping and decay machineries (Chen et al., 2014; Mathys et al., 2014; Rouya et al., 2014). As specific determinants of GW182 directly interact with CCR4-NOT components *in vitro*, models favored a static view wherein mRNA decay would necessarily, and rapidly follow miRISC-triggered deadenylation. However, the biochemistry that occurs within mRNPs has remained largely evasive. With mRNPs being membrane-less and highly dynamic in nature, they have proven notoriously difficult to purify or fractionate without disrupting important interactions and dynamics that help define them. As a consequence, their functions were largely inferred based on the co-localization of proteins, recombinant protein interactions *in vitro*, and the enzymatic functions attributed to their resident proteins. For example, decapping enzymes are often used as P body markers. Because a significant fraction of AGO and GW182 co-localize with Dcp1 and Dcp2, P bodies were considered likely to be a site of miRNA target decay (Eystathioy et al., 2002; Eystathioy et al., 2003; Liu et al., 2005b; Meister et al., 2005; Pillai et al., 2005). However, the processes of decapping and decay require several co-factors in addition to the enzymatic proteins, most of which were not systematically considered in individual studies. This left open the possibility that mRNP particles, P body and others, may in fact be heterogeneous in composition and functions, and possibly much more diverse than reflected in the literature. Indeed, substantial evidence already exists on the spatiotemporal and functional specialization of mRNP particles. For example, the decapping enzymes, DCAP-1/2, and decapping activators, PATR-1 and LSM-1/3 are expressed at distinct moments during *C. elegans* embryogenesis. DCAP-1 and DCAP-2 co-

localize with PGL proteins in the early *C. elegans* embryo, but are gradually inherited in somatic cells (Lall et al., 2005). Expression of PATR-1, LSM-1, and LSM-3 was only detected in the 3/4-cell stage, and selectively in somatic blastomeres (Gallo et al., 2008). These findings suggest that even though early embryo germ granule mRNPs contain DCAP-1 and DCAP-2, they have not yet acquired essential decapping activators, and are presumed unfit to be primed sites for decapping and decay.

As such, the decision to decap and decay the mRNA target, or simply to deadenylate and store, may be rendered through the unique biochemical niche that prevails within individual mRNPs. Because mRNP composition is distinct with cell fate, developmental stage, mRNA target, and even the sub-cellular location, we suggest that mRNPs may serve to modulate the mechanistic outcome of miRNA-mediated silencing.

Recently, studies have turned to the insightful use of super-resolution fluorescence microscopy, or single-molecule imaging to better resolve RNP dynamics both spatially and temporally. Using high-resolution live imaging studies to track P granule components, Anthony Hyman's group showed that P granules exhibit liquid-like behaviors that allow them to rapidly undergo phase transitions of dissolution and condensation in *C. elegans* embryos (Brangwynne et al., 2009). Along those lines, Michael Rosen and his group showed that the concentration needed to form liquid droplets is related to the valency of interacting proteins. The parallel was made with the assembly of multivalent proteins-RNA complexes into large cellular bodies in the cytoplasm, such as P bodies and germ granules (Li et al., 2012). The group of Steven McKnight identified low complexity (LC) regions (or intrinsically disordered regions, IDRs) as key determinants for the assembly and disassembly of mRNP structures (Han et al., 2012; Kato et al., 2012). Incidentally, many RNA-binding proteins (RBPs) are enriched in LC sequences. When

maintained at low temperatures, recombinant LC sequences derived from some of these RBPs, such as FUS and hnRNPA2, promoted phase transition to a hydrogel-like state in a concentration-dependent manner (Kato et al., 2012). Recent studies have also experimentally assessed the importance of IDRs, by dissecting their abilities to form liquid droplets or gel-like states *in vitro* on their own, or through heterotypic interactions with other IDR recombinant proteins (Elbaum-Garfinkle et al., 2015; Kato et al., 2012; Lin et al., 2015; Nott et al., 2015). As such, LC-containing proteins seem to promote the formation of a "supramolecular structure" more organized than the proteins on their own (Turoverov et al., 2010), and consistent with the structural behavior of P bodies or germ granules.

Key to my research project were the findings from the Seydoux group, as they revealed the intrinsically disordered nature of MEG-1 and MEG-2 proteins, and their function as scaffolds for RNA granules in the *C. elegans* embryo (Wang et al., 2014). My discovery of their interaction with NTL-1, and of their function in gene silencing by the *lsy-6* miRNA *in vivo* is particularly striking as MEG-1 and MEG-2 appear to be only constituted of intrinsically disordered sequences. As such, this contributes to the powerful evidence that the structural scaffold of mRNPs itself, or the microenvironment that prevails within them is functionally important for miRNA function.

Given the rather restricted expression of MEG-1 and MEG-2 (Leacock and Reinke, 2008), with MEG-2 more broadly expressed and extends to somatic blastomeres, it is likely that other LC-containing or intrinsically disordered proteins may contribute a similar role in later cell types in *C. elegans* or in other organisms. In particular, aside from a recognizable ubiquitin-associated domain and an RNA recognition motif, mammalian GW182 homologs encode extensive regions that are predicted to be intrinsically disordered (Huang et al., 2013). Given the

scaffolding function of GW182 in bridging the CCR4-NOT complex to the Argonautes, the LC regions of GW182 may directly contribute, alone or in combination with other proteins, in the nucleation or the stabilization of mRNPs. Interestingly, GW182 encodes several potential serine/threonine phosphorylation sites (Eystathioy et al., 2002) within the LC region (Huang et al., 2013). Functional assays on phosphomimetic or phosphonull mutations of residues within the LC sequences compromised the silencing function of GW182 (Huang et al., 2013). This raises the enticing possibility that post-translational modification of GW182 in mammalian cells can impinge on its silencing activities by modulating mRNP structures.

mRNP specialization is likely to be a widespread feature in the many aspects of mRNA regulation. In Chapter 4, I highlighted parallels between embryonic miRISC mRNPs in *C. elegans* and RNA localization mRNPs in *Drosophila* oogenesis. A similar phenomenon may be at work in the piRNA pathway, required for the maintenance of germline genome integrity. In flies, oocyte germ granules are also referred to as nuage, due to the electron-dense structure that surrounds nuclei (Eddy, 1975; Mahowald, 1971). Nuage depends on the protein composition of assembled complexes to carry out distinct steps of piRNA biogenesis and target silencing events, at both transcriptional and post-transcriptional levels (Klattenhoff and Theurkauf, 2008; Pal-Bhadra et al., 2002; Pal-Bhadra et al., 2004; Rangan et al., 2011). Many of the piRNA pathway-related proteins are enriched in nuage, including Ago3 and Aubergine (Brennecke et al., 2007; Harris and Macdonald, 2001), the nucleases Zucchini and Squash (Pane et al., 2007), the Tudor-domain proteins Krimper, Qin, and SpindleE (Lim and Kai, 2007; Zhang et al., 2011), and DEAD box helicase UAP56 and Vasa (Zhang et al., 2012). It is also striking that several of the proteins required for nuage assembly and functions in piRNAs serve other crucial roles in the regulated translation of germline and posterior pole determinants (Voronina et al., 2011).

5.6 Future directions

The past decade of miRNA research has witnessed extensive progress in understanding their mechanism of action. The work presented in this thesis provides a clearer view of the molecular interactions involved, the order of events during miRNA-mediated silencing, the functional organization of miRNP particle assembly, and the importance of 3'UTR and developmental contexts in regulating miRNA activities. Yet, several significant questions remain to be addressed.

- *What determines target decay in embryonic miRNA-mediated silencing?*

The mechanistic outcome and the mRNA fate remain to be formally and more systematically investigated *in vivo* for endogenous miRNA targets in the embryo. miRNA targets can be silenced as a result of direct translational repression, deadenylation, decapping and decay. In metazoans, deadenylation and decapping occur rapidly one after the other, or they are coupled, which misleads several authors to equate deadenylation with decay. Reporter mRNAs with artificial or natural 3'UTRs remain stable in our *C. elegans* embryonic cell-free extract. Furthermore, my work and multiple lines of published evidence support the idea that silenced and even deadenylated mRNAs can remain stable *in vivo*, leaving open the possibility of re-adenylation, storage, or delayed decay. This thesis work strongly suggests that whether to silence, deadenylate, decay or not will be 3'UTR- and context-dependent. In light of the discovered order of events, one distinct possibility is that this decision is taken while the mRNA target is in mRNPs.

The use of the CRISPR/Cas9 technology to engineer, or mutate binding sites for miRNAs or RNA-binding proteins from 3'UTRs of genes of interest offers a more precise and specific series of strategies for a gene-to-gene approach. Genetic interaction of embryonic miRNAs with

decapping enzymes (*dcap-1* and *dcap-2*), co-activators (*edc-3, edc-4, patr-1*), or intrinsically disordered proteins should be assayed using sensitized embryonic miRNA backgrounds as it was done with *meg-1* and *meg-2* with *lsy-6* (Chapter 4). Finally, the impact of depletion of these factors on the embryonic transcriptome could also be visited using RNA-seq or 3'UTR capture libraries in wild-type or in mutant backgrounds.

- *Is miRNA-mediated deadenylation reversible?*

Closely related to the first question, it is tempting to speculate that temporarily silenced target mRNAs may be stored to undergo delayed re-adenylation and translation. Translational activation by cytoplasmic polyadenylation of maternal mRNAs is essential for early development in mouse (Gebauer and Richter, 1995), *D. melanogaster* (Salles et al., 1994), *X. laevis* (Sheets et al., 1995), and *C. elegans* (Kim et al., 2010; Suh et al., 2006). The phenomenon of re-adenylation is most characterized in *X. laevis*, in which during oocyte maturation, a subset of translationally dormant maternal mRNAs is polyadenylated (Huarte et al., 1987; Sheets et al., 1994; Stebbins-Boaz and Richter, 1994; Vassalli et al., 1989). This event is mediated by the cytoplasmic polyadenylation element (CPE)-binding protein (CPEB) (Hake and Richter, 1994; Huarte et al., 1992; Paris et al., 1991) and the cytoplasmic poly(A) polymerase, GLD2 (Barnard et al., 2004). CPEB controls the polyadenylation of cyclin, Cdk2, and c-mos maternal mRNAs, which is essential for meiotic cell cycle progression during oocyte maturation (Stebbins-Boaz et al., 1996). Interestingly, the poly(A)-specific ribonuclease PARN, also interacts with CPEB and GLD2 (Kim and Richter, 2006). This latter finding indicates opposing enzymatic activities of PARN and GLD2 in modulating poly(A) tail length during oocyte maturation, reflecting yet again the dynamics of mRNP remodeling on target mRNAs. A seminal study by the Filipowicz group suggests potential implications for reversible deadenylation in mammalian somatic cells.

Under the conditions of amino acid deprivation and arsenite treatment, the cationic amino acid transporter 1 (CAT-1) mRNA and reporters bearing its 3'UTR were relieved from *miR-122* translation repression (Bhattacharyya et al., 2006). Such relief is accompanied by the relocation of CAT-1 mRNA from P bodies to polysomes (Bhattacharyya et al., 2006). While the poly(A) tail status was not assessed in this study, these findings lend support to the reversibility of miRNA-mediated silencing under the context of cellular stress, and subsequent changes to the CAT-1:mRNP granule specialized to respond to stress, altering the silencing effects by miRNAs on CAT-1 target.

- *Specialized miRISCs: What is the function of AIN-2?*

Another interesting aspect to investigate with regards to the contributions of translation repression and deadenylation towards miRNA-mediated silencing will be to dissect the roles of the two *C. elegans* GW182 orthologs, AIN-1 and AIN-2. AIN-1 and AIN-2 are partially redundant for miRNA-mediated silencing in *C. elegans* (Ding and Grosshans, 2009; Zhang et al., 2007). However, the possibility that they function through distinct mechanisms was raised with the AIN-1 proteomics presented in Chapter 4. AIN-1 and NTL-1 interactions largely overlapped on the decapping and decay machineries. In contrast, a previous study by Min Han's group identified AIN-2 interactions with components of the translation initiation machinery, but none of the deadenylase, decapping, or decay components were detected (Zhang et al., 2007). Based on these findings, it is possible that AIN-1 and AIN-2 drive distinct mechanistic routes through the miRISC, and thus may play distinct biological roles. *In vitro* assays using the *C. elegans* cell-free system derived from *ain-1* and *ain-2*-depleted mutants will be useful in dissecting their contributions to translation repression and/or deadenylation. It is important to mention, however, that the AIN-2 proteomics by Min Han's group was conducted in mixed stage animals, which

may obscure developmental and cellular context-dependent interactions. Thus, the AIN-2 interactions should be revisited in the embryo to verify whether the interactions between the miRISC and deadenylase and decay machineries are indeed absent.

- *What are the functions of novel AIN-1 and NTL-1 interactions?*

NHL-2. All the *in vitro* assays I developed using the *C. elegans* embryonic system can be extended to characterize other AIN-1 and NTL-1 associated proteins. An intriguing candidate to revisit would be NHL-2, a member of the TRIM-NHL family of proteins and a putative RNA-binding protein. NHL-2 was characterized as a miRISC cofactor in the silencing of a subset of endogenous miRNA targets (Hammell et al., 2009). NHL-2 interacts with CGH-1 and with the miRISC, but this interaction was weakened by RNase treatment, suggesting the complex between CGH-1:NHL-2 to miRISC may occur or be stabilized on the target mRNA (Hammell et al., 2009). This later observation somewhat contrasts with our observations, as NHL-2 co-purified with AIN-1 and NTL-1 even after RNase treatment (Chapter 4). Interestingly, NHL-2 is also detected in distinct foci in germ cells (Hyenne et al., 2008). Whether NHL-2 directly binds RNA remains to be addressed, but in *D. melanogaster* its TRIM-NHL homolog BRAT was recently reported to directly bind to mRNA targets in the embryo (Loedige et al., 2015; Loedige et al., 2014). An enticing possibility is that NHL-2 may directly cooperate with miRISC in triggering target deadenylation. Alternatively, NHL-2 may be important in fine-tuning the expression of specific miRNA targets during embryogenesis.

LIN-66. Another interesting protein that should be revisited is LIN-66. *lin-66* plays a role in developmental timing, with loss of *lin-66* function leading to defects in vulva precursors and seam cell differentiation (Morita and Han, 2006). LIN-66 also negatively regulates the heterochronic gene, *lin-28,* which is also a phenocritical miRNA target. As such, *lin-66* belongs

in the same genetic cascade as *lin-4* and other miRNAs. Previous work has shown that LIN-66 does not co-immunoprecipitate with miRNAs from larval preparations, and that *lin-4* and *let-7* miRNA levels are not affected in *lin-66* mutants (Morita and Han, 2006). Our data instead indicates that LIN-66 stably interacts with AIN-1 in the embryo, and thus it may play a different role in early development by directly participating in miRNA-mediated silencing. Biochemical studies using the framework I developed with cell-free assays (translation repression, deadenylation, and DRIP, and MNase sensitivity) and genetic assays could be advantageously exploited in resolving its mechanistic role(s).

5.7 Conclusion

The work presented in this thesis revealed the pervasiveness of deadenylation and identified the fundamental contribution of miRISC cooperativity in miRNA-mediated gene silencing in *C. elegans* embryos. Additionally, we resolved and delineated the temporal order of events from target recognition by miRISC, to the recruitment of effector CCR4-NOT complex assembly, to mRNP nucleation. I further defined the physical and functional interactions between miRNA-mediated silencing and intrinsically disordered proteins. Finally, my findings substantiate a model wherein different mRNP granules and their context-dependent specialization modulate the mechanisms of gene silencing by miRNAs. In light of such progress, it is once more made obvious that the integrated use of genetics and biochemistry provides a fuller and more insightful comprehension of even the most complex biological mechanisms, such as miRNA-mediated silencing.

References

Abrahante, J.E., Daul, A.L., Li, M., Volk, M.L., Tennessen, J.M., Miller, E.A., and Rougvie, A.E. (2003). The Caenorhabditis elegans hunchback-like gene lin-57/hbl-1 controls developmental time and is regulated by microRNAs. Developmental cell *4*, 625-637.

Alvarez-Saavedra, E., and Horvitz, H.R. (2010). Many families of C. elegans microRNAs are not essential for development or viability. Curr Biol *20*, 367-373.

Amaral, P.P., Dinger, M.E., Mercer, T.R., and Mattick, J.S. (2008). The eukaryotic genome as an RNA machine. Science (New York, NY *319*, 1787-1789.

Ambros, V., and Horvitz, H.R. (1984). Heterochronic mutants of the nematode Caenorhabditis elegans. Science (New York, NY *226*, 409-416.

Ambros, V., Lee, R.C., Lavanway, A., Williams, P.T., and Jewell, D. (2003). MicroRNAs and other tiny endogenous RNAs in C. elegans. Curr Biol *13*, 807-818.

Amiri, A., Keiper, B.D., Kawasaki, I., Fan, Y., Kohara, Y., Rhoads, R.E., and Strome, S. (2001). An isoform of eIF4E is a component of germ granules and is required for spermatogenesis in C. elegans. Development (Cambridge, England) *128*, 3899-3912.

Anderson, J.S., and Parker, R.P. (1998). The 3' to 5' degradation of yeast mRNAs is a general mechanism for mRNA turnover that requires the SKI2 DEVH box protein and 3' to 5' exonucleases of the exosome complex. The EMBO journal *17*, 1497-1506.

Anderson, P., and Kedersha, N. (2006). RNA granules. The Journal of cell biology *172*, 803-808.

Andrei, M.A., Ingelfinger, D., Heintzmann, R., Achsel, T., Rivera-Pomar, R., and Luhrmann, R. (2005). A role for eIF4E and eIF4E-transporter in targeting mRNPs to mammalian processing bodies. RNA (New York, NY *11*, 717-727.

Aravin, A.A., Naumova, N.M., Tulin, A.V., Vagin, V.V., Rozovsky, Y.M., and Gvozdev, V.A. (2001). Double-stranded RNA-mediated silencing of genomic tandem repeats and transposable elements in the D. melanogaster germline. Curr Biol *11*, 1017-1027.

Ashe, A., Sapetschnig, A., Weick, E.M., Mitchell, J., Bagijn, M.P., Cording, A.C., Doebley, A.L., Goldstein, L.D., Lehrbach, N.J., Le Pen, J.*, et al.* (2012). piRNAs can trigger a multigenerational epigenetic memory in the germline of C. elegans. Cell *150*, 88-99.

Azuma-Mukai, A., Oguri, H., Mituyama, T., Qian, Z.R., Asai, K., Siomi, H., and Siomi, M.C. (2008). Characterization of endogenous human Argonautes and their miRNA partners in RNA silencing. Proceedings of the National Academy of Sciences of the United States of America *105*, 7964-7969.

Baek, D., Villen, J., Shin, C., Camargo, F.D., Gygi, S.P., and Bartel, D.P. (2008). The impact of microRNAs on protein output. Nature *455*, 64-71.

Bagga, S., Bracht, J., Hunter, S., Massirer, K., Holtz, J., Eachus, R., and Pasquinelli, A.E. (2005). Regulation by let-7 and lin-4 miRNAs results in target mRNA degradation. Cell *122*, 553-563.

Barbee, S.A., Lublin, A.L., and Evans, T.C. (2002). A novel function for the Sm proteins in germ granule localization during C. elegans embryogenesis. Curr Biol *12*, 1502-1506.

Barnard, D.C., Ryan, K., Manley, J.L., and Richter, J.D. (2004). Symplekin and xGLD-2 are required for CPEB-mediated cytoplasmic polyadenylation. Cell *119*, 641-651.

Baron-Benhamou, J., Gehring, N.H., Kulozik, A.E., and Hentze, M.W. (2004). Using the lambdaN peptide to tether proteins to RNAs. Methods in molecular biology *257*, 135-154.

Bartel, D.P. (2004). MicroRNAs: genomics, biogenesis, mechanism, and function. Cell *116*, 281-297.

Bartel, D.P. (2009). MicroRNAs: target recognition and regulatory functions. Cell *136*, 215-233.

Baumberger, N., and Baulcombe, D.C. (2005). Arabidopsis ARGONAUTE1 is an RNA Slicer that selectively recruits microRNAs and short interfering RNAs. Proceedings of the National Academy of Sciences of the United States of America *102*, 11928-11933.

Bazzini, A.A., Lee, M.T., and Giraldez, A.J. (2012). Ribosome profiling shows that miR-430 reduces translation before causing mRNA decay in zebrafish. Science (New York, NY *336*, 233-237.

Behm-Ansmant, I., Rehwinkel, J., Doerks, T., Stark, A., Bork, P., and Izaurralde, E. (2006). mRNA degradation by miRNAs and GW182 requires both CCR4:NOT deadenylase and DCP1:DCP2 decapping complexes. Genes & development *20*, 1885-1898.

Beilharz, T.H., Humphreys, D.T., Clancy, J.L., Thermann, R., Martin, D.I., Hentze, M.W., and Preiss, T. (2009). microRNA-mediated messenger RNA deadenylation contributes to translational repression in mammalian cells. PloS one *4*, e6783.

Bernstein, E., Caudy, A.A., Hammond, S.M., and Hannon, G.J. (2001). Role for a bidentate ribonuclease in the initiation step of RNA interference. Nature *409*, 363-366.

Bernstein, P., Peltz, S.W., and Ross, J. (1989). The poly(A)-poly(A)-binding protein complex is a major determinant of mRNA stability in vitro. Molecular and cellular biology *9*, 659-670.

Berthet, C., Morera, A.M., Asensio, M.J., Chauvin, M.A., Morel, A.P., Dijoud, F., Magaud, J.P., Durand, P., and Rouault, J.P. (2004). CCR4-associated factor CAF1 is an essential factor for spermatogenesis. Molecular and cellular biology *24*, 5808-5820.

Bethune, J., Artus-Revel, C.G., and Filipowicz, W. (2012). Kinetic analysis reveals successive steps leading to miRNA-mediated silencing in mammalian cells. EMBO reports *13*, 716-723.

Bhattacharyya, S.N., Habermacher, R., Martine, U., Closs, E.I., and Filipowicz, W. (2006). Relief of microRNA-mediated translational repression in human cells subjected to stress. Cell *125*, 1111-1124.

Blaszczyk, J., Tropea, J.E., Bubunenko, M., Routzahn, K.M., Waugh, D.S., Court, D.L., and Ji, X. (2001). Crystallographic and modeling studies of RNase III suggest a mechanism for double-stranded RNA cleavage. Structure *9*, 1225-1236.

Boag, P.R., Atalay, A., Robida, S., Reinke, V., and Blackwell, T.K. (2008). Protection of specific maternal messenger RNAs by the P body protein CGH-1 (Dhh1/RCK) during Caenorhabditis elegans oogenesis. The Journal of cell biology *182*, 543-557.

Boag, P.R., Nakamura, A., and Blackwell, T.K. (2005). A conserved RNA-protein complex component involved in physiological germline apoptosis regulation in C. elegans. Development (Cambridge, England) *132*, 4975-4986.

Boeck, R., Tarun, S., Jr., Rieger, M., Deardorff, J.A., Muller-Auer, S., and Sachs, A.B. (1996). The yeast Pan2 protein is required for poly(A)-binding protein-stimulated poly(A)-nuclease activity. The Journal of biological chemistry *271*, 432-438.

Bohmert, K., Camus, I., Bellini, C., Bouchez, D., Caboche, M., and Benning, C. (1998). AGO1 defines a novel locus of Arabidopsis controlling leaf development. The EMBO journal *17*, 170-180.

Boland, A., Chen, Y., Raisch, T., Jonas, S., Kuzuoglu-Ozturk, D., Wohlbold, L., Weichenrieder, O., and Izaurralde, E. (2013). Structure and assembly of the NOT module of the human CCR4-NOT complex. Nature structural & molecular biology *20*, 1289-1297.

Bonisch, C., Temme, C., Moritz, B., and Wahle, E. (2007). Degradation of hsp70 and other mRNAs in Drosophila via the 5' 3' pathway and its regulation by heat shock. The Journal of biological chemistry *282*, 21818-21828.

Bos, J.L. (1989). ras oncogenes in human cancer: a review. Cancer research *49*, 4682-4689.

Bouasker, S., and Simard, M.J. (2012). The slicing activity of miRNA-specific Argonautes is essential for the miRNA pathway in C. elegans. Nucleic acids research *40*, 10452-10462.

Brangwynne, C.P., Eckmann, C.R., Courson, D.S., Rybarska, A., Hoege, C., Gharakhani, J., Julicher, F., and Hyman, A.A. (2009). Germline P granules are liquid droplets that localize by controlled dissolution/condensation. Science (New York, NY *324*, 1729-1732.

Branscheid, A., Marchais, A., Schott, G., Lange, H., Gagliardi, D., Andersen, S.U., Voinnet, O., and Brodersen, P. (2015). SKI2 mediates degradation of RISC 5'-cleavage fragments and prevents secondary siRNA production from miRNA targets in Arabidopsis. Nucleic acids research.

Braun, J.E., Huntzinger, E., Fauser, M., and Izaurralde, E. (2011). GW182 proteins directly recruit cytoplasmic deadenylase complexes to miRNA targets. Molecular cell *44*, 120-133.

Brengues, M., Teixeira, D., and Parker, R. (2005). Movement of eukaryotic mRNAs between polysomes and cytoplasmic processing bodies. Science (New York, NY *310*, 486-489.

Brennecke, J., Aravin, A.A., Stark, A., Dus, M., Kellis, M., Sachidanandam, R., and Hannon, G.J. (2007). Discrete small RNA-generating loci as master regulators of transposon activity in Drosophila. Cell *128*, 1089-1103.

Brennecke, J., Hipfner, D.R., Stark, A., Russell, R.B., and Cohen, S.M. (2003). bantam encodes a developmentally regulated microRNA that controls cell proliferation and regulates the proapoptotic gene hid in Drosophila. Cell *113*, 25-36.

Brennecke, J., Stark, A., Russell, R.B., and Cohen, S.M. (2005). Principles of microRNA-target recognition. PLoS biology *3*, e85.

Brenner, J.L., Jasiewicz, K.L., Fahley, A.F., Kemp, B.J., and Abbott, A.L. (2010). Loss of individual microRNAs causes mutant phenotypes in sensitized genetic backgrounds in C. elegans. Curr Biol *20*, 1321-1325.

Brenner, S. (1974). The genetics of Caenorhabditis elegans. Genetics *77*, 71-94.

Brown, C.E., Tarun, S.Z., Jr., Boeck, R., and Sachs, A.B. (1996). PAN3 encodes a subunit of the Pab1p-dependent poly(A) nuclease in Saccharomyces cerevisiae. Molecular and cellular biology *16*, 5744-5753.

Buchan, J.R. (2014). mRNP granules. Assembly, function, and connections with disease. RNA biology *11*, 1019-1030.

Buckley, B.A., Burkhart, K.B., Gu, S.G., Spracklin, G., Kershner, A., Fritz, H., Kimble, J., Fire, A., and Kennedy, S. (2012). A nuclear Argonaute promotes multigenerational epigenetic inheritance and germline immortality. Nature *489*, 447-451.

Burkhart, K.B., Guang, S., Buckley, B.A., Wong, L., Bochner, A.F., and Kennedy, S. (2011). A pre-mRNA-associating factor links endogenous siRNAs to chromatin regulation. PLoS genetics *7*, e1002249.

Burton, N.O., Burkhart, K.B., and Kennedy, S. (2011). Nuclear RNAi maintains heritable gene silencing in Caenorhabditis elegans. Proceedings of the National Academy of Sciences of the United States of America *108*, 19683-19688.

Bushati, N., Stark, A., Brennecke, J., and Cohen, S.M. (2008). Temporal reciprocity of miRNAs and their targets during the maternal-to-zygotic transition in Drosophila. Curr Biol *18*, 501-506.

Bussing, I., Slack, F.J., and Grosshans, H. (2008). let-7 microRNAs in development, stem cells and cancer. Trends Mol Med *14*, 400-409.

Calin, G.A., Cimmino, A., Fabbri, M., Ferracin, M., Wojcik, S.E., Shimizu, M., Taccioli, C., Zanesi, N., Garzon, R., Aqeilan, R.I.*, et al.* (2008). MiR-15a and miR-16-1 cluster functions in human leukemia. Proc Natl Acad Sci U S A *105*, 5166-5171.

Calin, G.A., Dumitru, C.D., Shimizu, M., Bichi, R., Zupo, S., Noch, E., Aldler, H., Rattan, S., Keating, M., Rai, K.*, et al.* (2002). Frequent deletions and down-regulation of micro- RNA genes miR15 and miR16 at 13q14 in chronic lymphocytic leukemia. Proceedings of the National Academy of Sciences of the United States of America *99*, 15524-15529.

Calin, G.A., Sevignani, C., Dumitru, C.D., Hyslop, T., Noch, E., Yendamuri, S., Shimizu, M., Rattan, S., Bullrich, F., Negrini, M.*, et al.* (2004). Human microRNA genes are frequently located at fragile sites and genomic regions involved in cancers. Proceedings of the National Academy of Sciences of the United States of America *101*, 2999-3004.

Catalanotto, C., Azzalin, G., Macino, G., and Cogoni, C. (2000). Gene silencing in worms and fungi. Nature *404*, 245.

Chalfie, M., Horvitz, H.R., and Sulston, J.E. (1981). Mutations that lead to reiterations in the cell lineages of C. elegans. Cell *24*, 59-69.

Chan, J.A., Krichevsky, A.M., and Kosik, K.S. (2005). MicroRNA-21 is an antiapoptotic factor in human glioblastoma cells. Cancer research *65*, 6029-6033.

Chang, H.M., Triboulet, R., Thornton, J.E., and Gregory, R.I. (2013). A role for the Perlman syndrome exonuclease Dis3l2 in the Lin28-let-7 pathway. Nature *497*, 244-248.

Chekulaeva, M., Mathys, H., Zipprich, J.T., Attig, J., Colic, M., Parker, R., and Filipowicz, W. (2011). miRNA repression involves GW182-mediated recruitment of CCR4-NOT through conserved W-containing motifs. Nature structural & molecular biology *18*, 1218-1226.

Cheloufi, S., Dos Santos, C.O., Chong, M.M., and Hannon, G.J. (2010). A dicer-independent miRNA biogenesis pathway that requires Ago catalysis. Nature *465*, 584-589.

Chen, J., Rappsilber, J., Chiang, Y.C., Russell, P., Mann, M., and Denis, C.L. (2001). Purification and characterization of the 1.0 MDa CCR4-NOT complex identifies two novel components of the complex. Journal of molecular biology *314*, 683-694.

Chen, J.X., Cipriani, P.G., Mecenas, D., Polanowska, J., Piano, F., Gunsalus, K.C., and Selbach, M. (2016). In vivo interaction proteomics in C. elegans embryos provides new insights into P granule dynamics. Mol Cell Proteomics.

Chen, Y., Boland, A., Kuzuoglu-Ozturk, D., Bawankar, P., Loh, B., Chang, C.T., Weichenrieder, O., and Izaurralde, E. (2014). A DDX6-CNOT1 complex and W-binding pockets in CNOT9 reveal direct links between miRNA target recognition and silencing. Molecular cell *54*, 737-750.

Chendrimada, T.P., Finn, K.J., Ji, X., Baillat, D., Gregory, R.I., Liebhaber, S.A., Pasquinelli, A.E., and Shiekhattar, R. (2007). MicroRNA silencing through RISC recruitment of eIF6. Nature *447*, 823-828.

Chu, C.Y., and Rana, T.M. (2006). Translation repression in human cells by microRNA-induced gene silencing requires RCK/p54. PLoS biology *4*, e210.

Cifuentes, D., Xue, H., Taylor, D.W., Patnode, H., Mishima, Y., Cheloufi, S., Ma, E., Mane, S., Hannon, G.J., Lawson, N.D*., et al.* (2010). A novel miRNA processing pathway independent of Dicer requires Argonaute2 catalytic activity. Science (New York, NY *328*, 1694-1698.

Cimmino, A., Calin, G.A., Fabbri, M., Iorio, M.V., Ferracin, M., Shimizu, M., Wojcik, S.E., Aqeilan, R.I., Zupo, S., Dono, M*., et al.* (2005). miR-15 and miR-16 induce apoptosis by targeting BCL2. Proceedings of the National Academy of Sciences of the United States of America *102*, 13944-13949.

Claycomb, J.M., Batista, P.J., Pang, K.M., Gu, W., Vasale, J.J., van Wolfswinkel, J.C., Chaves, D.A., Shirayama, M., Mitani, S., Ketting, R.F*., et al.* (2009). The Argonaute CSR-1 and its 22G-RNA cofactors are required for holocentric chromosome segregation. Cell *139*, 123-134.

Cohen, L.S., Mikhli, C., Jiao, X., Kiledjian, M., Kunkel, G., and Davis, R.E. (2005). Dcp2 Decaps m2,2,7GpppN-capped RNAs, and its activity is sequence and context dependent. Molecular and cellular biology *25*, 8779-8791.

Collart, M.A., and Struhl, K. (1993). CDC39, an essential nuclear protein that negatively regulates transcription and differentially affects the constitutive and inducible HIS3 promoters. The EMBO journal *12*, 177-186.

Collart, M.A., and Struhl, K. (1994). NOT1(CDC39), NOT2(CDC36), NOT3, and NOT4 encode a global-negative regulator of transcription that differentially affects TATA-element utilization. Genes & development *8*, 525-537.

Coller, J.M., Tucker, M., Sheth, U., Valencia-Sanchez, M.A., and Parker, R. (2001). The DEAD box helicase, Dhh1p, functions in mRNA decapping and interacts with both the decapping and deadenylase complexes. RNA (New York, NY *7*, 1717-1727.

Consortium, E.P., Birney, E., Stamatoyannopoulos, J.A., Dutta, A., Guigo, R., Gingeras, T.R., Margulies, E.H., Weng, Z., Snyder, M., Dermitzakis, E.T*., et al.* (2007). Identification and analysis of functional elements in 1% of the human genome by the ENCODE pilot project. Nature *447*, 799-816.

Cooke, A., Prigge, A., and Wickens, M. (2010). Translational repression by deadenylases. The Journal of biological chemistry *285*, 28506-28513.

Cougot, N., Babajko, S., and Seraphin, B. (2004). Cytoplasmic foci are sites of mRNA decay in human cells. The Journal of cell biology *165*, 31-40.

Couttet, P., Fromont-Racine, M., Steel, D., Pictet, R., and Grange, T. (1997). Messenger RNA deadenylylation precedes decapping in mammalian cells. Proceedings of the National Academy of Sciences of the United States of America *94*, 5628-5633.

Cox, D.N., Chao, A., Baker, J., Chang, L., Qiao, D., and Lin, H. (1998). A novel class of evolutionarily conserved genes defined by piwi are essential for stem cell self-renewal. Genes & development *12*, 3715-3727.

Cox, D.N., Chao, A., and Lin, H. (2000). piwi encodes a nucleoplasmic factor whose activity modulates the number and division rate of germline stem cells. Development (Cambridge, England) *127*, 503-514.

Crick, F.H. (1958). On protein synthesis. Symp Soc Exp Biol *12*, 138-163.

Cui, M., Kim, E.B., and Han, M. (2006). Diverse chromatin remodeling genes antagonize the Rb-involved SynMuv pathways in C. elegans. PLoS genetics *2*, e74.

Dahanukar, A., and Wharton, R.P. (1996). The Nanos gradient in Drosophila embryos is generated by translational regulation. Genes & development *10*, 2610-2620.

Daugeron, M.C., Mauxion, F., and Seraphin, B. (2001). The yeast POP2 gene encodes a nuclease involved in mRNA deadenylation. Nucleic acids research *29*, 2448-2455.

Davis, E., Caiment, F., Tordoir, X., Cavaille, J., Ferguson-Smith, A., Cockett, N., Georges, M., and Charlier, C. (2005). RNAi-mediated allelic trans-interaction at the imprinted Rtl1/Peg11 locus. Curr Biol *15*, 743-749.

Decker, C.J., and Parker, R. (1993). A turnover pathway for both stable and unstable mRNAs in yeast: evidence for a requirement for deadenylation. Genes & development *7*, 1632-1643.

Decker, C.J., and Parker, R. (2012). P-bodies and stress granules: possible roles in the control of translation and mRNA degradation. Cold Spring Harb Perspect Biol *4*, a012286.

Decker, C.J., Teixeira, D., and Parker, R. (2007). Edc3p and a glutamine/asparagine-rich domain of Lsm4p function in processing body assembly in Saccharomyces cerevisiae. J Cell Biol *179*, 437-449.

Denis, C.L. (1984). Identification of new genes involved in the regulation of yeast alcohol dehydrogenase II. Genetics *108*, 833-844.

Denis, C.L., and Chen, J. (2003). The CCR4-NOT complex plays diverse roles in mRNA metabolism. Prog Nucleic Acid Res Mol Biol *73*, 221-250.

Denis, C.L., and Malvar, T. (1990). The CCR4 gene from Saccharomyces cerevisiae is required for both nonfermentative and spt-mediated gene expression. Genetics *124*, 283-291.

Deppe, U., Schierenberg, E., Cole, T., Krieg, C., Schmitt, D., Yoder, B., and von Ehrenstein, G. (1978). Cell lineages of the embryo of the nematode Caenorhabditis elegans. Proceedings of the National Academy of Sciences of the United States of America *75*, 376-380.

Ding, L., and Han, M. (2007). GW182 family proteins are crucial for microRNA-mediated gene silencing. Trends in cell biology *17*, 411-416.

Ding, L., Spencer, A., Morita, K., and Han, M. (2005). The developmental timing regulator AIN-1 interacts with miRISCs and may target the argonaute protein ALG-1 to cytoplasmic P bodies in C. elegans. Molecular cell *19*, 437-447.

Ding, X.C., and Grosshans, H. (2009). Repression of C. elegans microRNA targets at the initiation level of translation requires GW182 proteins. The EMBO journal *28*, 213-222.

Ding, X.C., Slack, F.J., and Grosshans, H. (2008). The let-7 microRNA interfaces extensively with the translation machinery to regulate cell differentiation. Cell cycle (Georgetown, Tex *7*, 3083-3090.

Djuranovic, S., Nahvi, A., and Green, R. (2012). miRNA-mediated gene silencing by translational repression followed by mRNA deadenylation and decay. Science (New York, NY *336*, 237-240.

Doench, J.G., Petersen, C.P., and Sharp, P.A. (2003). siRNAs can function as miRNAs. Genes & development *17*, 438-442.

Doench, J.G., and Sharp, P.A. (2004). Specificity of microRNA target selection in translational repression. Genes & development *18*, 504-511.

Douris, N., Kojima, S., Pan, X., Lerch-Gaggl, A.F., Duong, S.Q., Hussain, M.M., and Green, C.B. (2011). Nocturnin regulates circadian trafficking of dietary lipid in intestinal enterocytes. Curr Biol *21*, 1347-1355.

Drinnenberg, I.A., Weinberg, D.E., Xie, K.T., Mower, J.P., Wolfe, K.H., Fink, G.R., and Bartel, D.P. (2009). RNAi in budding yeast. Science (New York, NY *326*, 544-550.

Duchaine, T.F., Wohlschlegel, J.A., Kennedy, S., Bei, Y., Conte, D., Jr., Pang, K., Brownell, D.R., Harding, S., Mitani, S., Ruvkun, G.*, et al.* (2006). Functional proteomics reveals the biochemical niche of C. elegans DCR-1 in multiple small-RNA-mediated pathways. Cell *124*, 343-354.

Easow, G., Teleman, A.A., and Cohen, S.M. (2007). Isolation of microRNA targets by miRNP immunopurification. RNA (New York, NY *13*, 1198-1204.

Eddy, E.M. (1975). Germ plasm and the differentiation of the germ cell line. Int Rev Cytol *43*, 229-280.

Eichhorn, S.W., Guo, H., McGeary, S.E., Rodriguez-Mias, R.A., Shin, C., Baek, D., Hsu, S.H., Ghoshal, K., Villen, J., and Bartel, D.P. (2014). mRNA destabilization is the dominant effect of mammalian microRNAs by the time substantial repression ensues. Molecular cell *56*, 104-115.

Elbaum-Garfinkle, S., Kim, Y., Szczepaniak, K., Chen, C.C., Eckmann, C.R., Myong, S., and Brangwynne, C.P. (2015). The disordered P granule protein LAF-1 drives phase separation into droplets with tunable viscosity and dynamics. Proceedings of the National Academy of Sciences of the United States of America *112*, 7189-7194.

Elkayam, E., Kuhn, C.D., Tocilj, A., Haase, A.D., Greene, E.M., Hannon, G.J., and Joshua-Tor, L. (2012). The structure of human argonaute-2 in complex with miR-20a. Cell *150*, 100-110.

Ephrussi, A., and Lehmann, R. (1992). Induction of germ cell formation by oskar. Nature *358*, 387-392.

Esquela-Kerscher, A., Trang, P., Wiggins, J.F., Patrawala, L., Cheng, A., Ford, L., Weidhaas, J.B., Brown, D., Bader, A.G., and Slack, F.J. (2008). The let-7 microRNA reduces tumor growth in mouse models of lung cancer. Cell cycle (Georgetown, Tex *7*, 759-764.

Eulalio, A., Behm-Ansmant, I., and Izaurralde, E. (2007a). P bodies: at the crossroads of post-transcriptional pathways. Nature reviews *8*, 9-22.

Eulalio, A., Behm-Ansmant, I., Schweizer, D., and Izaurralde, E. (2007b). P-body formation is a consequence, not the cause, of RNA-mediated gene silencing. Molecular and cellular biology *27*, 3970-3981.

Eulalio, A., Helms, S., Fritzsch, C., Fauser, M., and Izaurralde, E. (2009a). A C-terminal silencing domain in GW182 is essential for miRNA function. RNA (New York, NY *15*, 1067-1077.

Eulalio, A., Huntzinger, E., and Izaurralde, E. (2008). GW182 interaction with Argonaute is essential for miRNA-mediated translational repression and mRNA decay. Nature structural & molecular biology *15*, 346-353.

Eulalio, A., Huntzinger, E., Nishihara, T., Rehwinkel, J., Fauser, M., and Izaurralde, E. (2009b). Deadenylation is a widespread effect of miRNA regulation. RNA (New York, NY *15*, 21-32.

Eulalio, A., Rehwinkel, J., Stricker, M., Huntzinger, E., Yang, S.F., Doerks, T., Dorner, S., Bork, P., Boutros, M., and Izaurralde, E. (2007c). Target-specific requirements for enhancers of decapping in miRNA-mediated gene silencing. Genes & development *21*, 2558-2570.

Eulalio, A., Tritschler, F., Buttner, R., Weichenrieder, O., Izaurralde, E., and Truffault, V. (2009c). The RRM domain in GW182 proteins contributes to miRNA-mediated gene silencing. Nucleic acids research *37*, 2974-2983.

Eulalio, A., Tritschler, F., and Izaurralde, E. (2009d). The GW182 protein family in animal cells: new insights into domains required for miRNA-mediated gene silencing. RNA (New York, NY *15*, 1433-1442.

Eystathioy, T., Chan, E.K., Tenenbaum, S.A., Keene, J.D., Griffith, K., and Fritzler, M.J. (2002). A phosphorylated cytoplasmic autoantigen, GW182, associates with a unique population of human mRNAs within novel cytoplasmic speckles. Molecular biology of the cell *13*, 1338-1351.

Eystathioy, T., Jakymiw, A., Chan, E.K., Seraphin, B., Cougot, N., and Fritzler, M.J. (2003). The GW182 protein colocalizes with mRNA degradation associated proteins hDcp1 and hLSm4 in cytoplasmic GW bodies. RNA (New York, NY *9*, 1171-1173.

Fabian, M.R., Cieplak, M.K., Frank, F., Morita, M., Green, J., Srikumar, T., Nagar, B., Yamamoto, T., Raught, B., Duchaine, T.F.*, et al.* (2011). miRNA-mediated deadenylation is

orchestrated by GW182 through two conserved motifs that interact with CCR4-NOT. Nature structural & molecular biology *18*, 1211-1217.

Fabian, M.R., Mathonnet, G., Sundermeier, T., Mathys, H., Zipprich, J.T., Svitkin, Y.V., Rivas, F., Jinek, M., Wohlschlegel, J., Doudna, J.A*., et al.* (2009). Mammalian miRNA RISC recruits CAF1 and PABP to affect PABP-dependent deadenylation. Molecular cell *35*, 868-880.

Fagard, M., Boutet, S., Morel, J.B., Bellini, C., and Vaucheret, H. (2000). AGO1, QDE-2, and RDE-1 are related proteins required for post-transcriptional gene silencing in plants, quelling in fungi, and RNA interference in animals. Proceedings of the National Academy of Sciences of the United States of America *97*, 11650-11654.

Fenger-Gron, M., Fillman, C., Norrild, B., and Lykke-Andersen, J. (2005). Multiple processing body factors and the ARE binding protein TTP activate mRNA decapping. Molecular cell *20*, 905-915.

Ferraiuolo, M.A., Basak, S., Dostie, J., Murray, E.L., Schoenberg, D.R., and Sonenberg, N. (2005). A role for the eIF4E-binding protein 4E-T in P-body formation and mRNA decay. The Journal of cell biology *170*, 913-924.

Filipowicz, W., Bhattacharyya, S.N., and Sonenberg, N. (2008). Mechanisms of post-transcriptional regulation by microRNAs: are the answers in sight? Nature reviews *9*, 102-114.

Fire, A., Xu, S., Montgomery, M.K., Kostas, S.A., Driver, S.E., and Mello, C.C. (1998). Potent and specific genetic interference by double-stranded RNA in Caenorhabditis elegans. Nature *391*, 806-811.

Flamand, M.N., Wu, E., Vashisht, A., Jannot, G., Keiper, B.D., Simard, M.J., Wohlschlegel, J., and Duchaine, T.F. (2016). Poly(A)-binding proteins are required for microRNA-mediated silencing and to promote target deadenylation in C. elegans. Nucleic acids research *44*, 5924-5935.

Fouts, D.E., True, H.L., and Celander, D.W. (1997). Functional recognition of fragmented operator sites by R17/MS2 coat protein, a translational repressor. Nucleic acids research *25*, 4464-4473.

Friedman, R.C., Farh, K.K., Burge, C.B., and Bartel, D.P. (2009). Most mammalian mRNAs are conserved targets of microRNAs. Genome research *19*, 92-105.

Fukaya, T., Iwakawa, H.O., and Tomari, Y. (2014). MicroRNAs block assembly of eIF4F translation initiation complex in Drosophila. Molecular cell *56*, 67-78.

Fukaya, T., and Tomari, Y. (2011). PABP is not essential for microRNA-mediated translational repression and deadenylation in vitro. The EMBO journal *30*, 4998-5009.

Fukaya, T., and Tomari, Y. (2012). MicroRNAs mediate gene silencing via multiple different pathways in drosophila. Molecular cell *48*, 825-836.

Gallie, D.R. (1991). The cap and poly(A) tail function synergistically to regulate mRNA translational efficiency. Genes & development *5*, 2108-2116.

Gallo, C.M., Munro, E., Rasoloson, D., Merritt, C., and Seydoux, G. (2008). Processing bodies and germ granules are distinct RNA granules that interact in C. elegans embryos. Developmental biology *323*, 76-87.

Gao, G., Deeb, F., Mercurio, J.M., Parfenova, A., Smith, P.A., and Bennett, K.L. (2012). PAN-1, a P-granule component important for C. elegans fertility, has dual roles in the germline and soma. Developmental biology *364*, 202-213.

Garneau, N.L., Wilusz, J., and Wilusz, C.J. (2007). The highways and byways of mRNA decay. Nature reviews *8*, 113-126.

Gavis, E.R., and Lehmann, R. (1994). Translational regulation of nanos by RNA localization. Nature *369*, 315-318.

Gavis, E.R., Lunsford, L., Bergsten, S.E., and Lehmann, R. (1996). A conserved 90 nucleotide element mediates translational repression of nanos RNA. Development (Cambridge, England) *122*, 2791-2800.

Gebauer, F., and Hentze, M.W. (2007). Studying translational control in Drosophila cell-free systems. Methods in enzymology *429*, 23-33.

Gebauer, F., and Richter, J.D. (1995). Cloning and characterization of a Xenopus poly(A) polymerase. Molecular and cellular biology *15*, 1422-1430.

Ghildiyal, M., and Zamore, P.D. (2009). Small silencing RNAs: an expanding universe. Nature reviews *10*, 94-108.

Gibbings, D.J., Ciaudo, C., Erhardt, M., and Voinnet, O. (2009). Multivesicular bodies associate with components of miRNA effector complexes and modulate miRNA activity. Nature cell biology *11*, 1143-1149.

Giraldez, A.J., Cinalli, R.M., Glasner, M.E., Enright, A.J., Thomson, J.M., Baskerville, S., Hammond, S.M., Bartel, D.P., and Schier, A.F. (2005). MicroRNAs regulate brain morphogenesis in zebrafish. Science (New York, NY *308*, 833-838.

Giraldez, A.J., Mishima, Y., Rihel, J., Grocock, R.J., Van Dongen, S., Inoue, K., Enright, A.J., and Schier, A.F. (2006). Zebrafish MiR-430 promotes deadenylation and clearance of maternal mRNAs. Science (New York, NY *312*, 75-79.

Godwin, A.R., Kojima, S., Green, C.B., and Wilusz, J. (2013). Kiss your tail goodbye: the role of PARN, Nocturnin, and Angel deadenylases in mRNA biology. Biochim Biophys Acta *1829*, 571-579.

Goldstrohm, A.C., and Wickens, M. (2008). Multifunctional deadenylase complexes diversify mRNA control. Nature reviews *9*, 337-344.

Gorgoni, B., and Gray, N.K. (2004). The roles of cytoplasmic poly(A)-binding proteins in regulating gene expression: a developmental perspective. Briefings in functional genomics & proteomics *3*, 125-141.

Green, C.B., and Besharse, J.C. (1996). Identification of a novel vertebrate circadian clock-regulated gene encoding the protein nocturnin. Proceedings of the National Academy of Sciences of the United States of America *93*, 14884-14888.

Gregory, R.I., Yan, K.P., Amuthan, G., Chendrimada, T., Doratotaj, B., Cooch, N., and Shiekhattar, R. (2004). The Microprocessor complex mediates the genesis of microRNAs. Nature *432*, 235-240.

Grimson, A., Farh, K.K., Johnston, W.K., Garrett-Engele, P., Lim, L.P., and Bartel, D.P. (2007). MicroRNA targeting specificity in mammals: determinants beyond seed pairing. Molecular cell *27*, 91-105.

Grishok, A., Pasquinelli, A.E., Conte, D., Li, N., Parrish, S., Ha, I., Baillie, D.L., Fire, A., Ruvkun, G., and Mello, C.C. (2001). Genes and mechanisms related to RNA interference regulate expression of the small temporal RNAs that control C. elegans developmental timing. Cell *106*, 23-34.

Grosshans, H., Johnson, T., Reinert, K.L., Gerstein, M., and Slack, F.J. (2005). The temporal patterning microRNA let-7 regulates several transcription factors at the larval to adult transition in C. elegans. Developmental cell *8*, 321-330.

Grudzien-Nogalska, E., Stepinski, J., Jemielity, J., Zuberek, J., Stolarski, R., Rhoads, R.E., and Darzynkiewicz, E. (2007). Synthesis of anti-reverse cap analogs (ARCAs) and their applications in mRNA translation and stability. Methods in enzymology *431*, 203-227.

Gruidl, M.E., Smith, P.A., Kuznicki, K.A., McCrone, J.S., Kirchner, J., Roussell, D.L., Strome, S., and Bennett, K.L. (1996). Multiple potential germ-line helicases are components of the germ-line-specific P granules of Caenorhabditis elegans. Proceedings of the National Academy of Sciences of the United States of America *93*, 13837-13842.

Gu, S.G., Pak, J., Guang, S., Maniar, J.M., Kennedy, S., and Fire, A. (2012). Amplification of siRNA in Caenorhabditis elegans generates a transgenerational sequence-targeted histone H3 lysine 9 methylation footprint. Nature genetics *44*, 157-164.

Gu, W., Shirayama, M., Conte, D., Jr., Vasale, J., Batista, P.J., Claycomb, J.M., Moresco, J.J., Youngman, E.M., Keys, J., Stoltz, M.J*., et al.* (2009). Distinct argonaute-mediated 22G-RNA pathways direct genome surveillance in the C. elegans germline. Molecular cell *36*, 231-244.

Guang, S., Bochner, A.F., Burkhart, K.B., Burton, N., Pavelec, D.M., and Kennedy, S. (2010). Small regulatory RNAs inhibit RNA polymerase II during the elongation phase of transcription. Nature *465*, 1097-1101.

Guang, S., Bochner, A.F., Pavelec, D.M., Burkhart, K.B., Harding, S., Lachowiec, J., and Kennedy, S. (2008). An Argonaute transports siRNAs from the cytoplasm to the nucleus. Science (New York, NY *321*, 537-541.

Guo, H., Ingolia, N.T., Weissman, J.S., and Bartel, D.P. (2010). Mammalian microRNAs predominantly act to decrease target mRNA levels. Nature *466*, 835-840.

Hafner, M., Landthaler, M., Burger, L., Khorshid, M., Hausser, J., Berninger, P., Rothballer, A., Ascano, M., Jr., Jungkamp, A.C., Munschauer, M., *et al.* (2010). Transcriptome-wide identification of RNA-binding protein and microRNA target sites by PAR-CLIP. Cell *141*, 129-141.

Hagan, J.P., Piskounova, E., and Gregory, R.I. (2009). Lin28 recruits the TUTase Zcchc11 to inhibit let-7 maturation in mouse embryonic stem cells. Nature structural & molecular biology *16*, 1021-1025.

Hake, L.E., and Richter, J.D. (1994). CPEB is a specificity factor that mediates cytoplasmic polyadenylation during Xenopus oocyte maturation. Cell *79*, 617-627.

Hammell, C.M., Lubin, I., Boag, P.R., Blackwell, T.K., and Ambros, V. (2009). nhl-2 Modulates microRNA activity in Caenorhabditis elegans. Cell *136*, 926-938.

Hammell, M., Long, D., Zhang, L., Lee, A., Carmack, C.S., Han, M., Ding, Y., and Ambros, V. (2008). mirWIP: microRNA target prediction based on microRNA-containing ribonucleoprotein-enriched transcripts. Nature methods *5*, 813-819.

Han, B.W., Hung, J.H., Weng, Z., Zamore, P.D., and Ameres, S.L. (2011). The 3'-to-5' exoribonuclease Nibbler shapes the 3' ends of microRNAs bound to Drosophila Argonaute1. Curr Biol *21*, 1878-1887.

Han, J., Lee, Y., Yeom, K.H., Nam, J.W., Heo, I., Rhee, J.K., Sohn, S.Y., Cho, Y., Zhang, B.T., and Kim, V.N. (2006). Molecular basis for the recognition of primary microRNAs by the Drosha-DGCR8 complex. Cell *125*, 887-901.

Han, T.W., Kato, M., Xie, S., Wu, L.C., Mirzaei, H., Pei, J., Chen, M., Xie, Y., Allen, J., Xiao, G., *et al.* (2012). Cell-free formation of RNA granules: bound RNAs identify features and components of cellular assemblies. Cell *149*, 768-779.

Harris, A.N., and Macdonald, P.M. (2001). Aubergine encodes a Drosophila polar granule component required for pole cell formation and related to eIF2C. Development (Cambridge, England) *128*, 2823-2832.

He, W., and Parker, R. (2001). The yeast cytoplasmic LsmI/Pat1p complex protects mRNA 3' termini from partial degradation. Genetics *158*, 1445-1455.

Heo, I., Ha, M., Lim, J., Yoon, M.J., Park, J.E., Kwon, S.C., Chang, H., and Kim, V.N. (2012). Mono-uridylation of pre-microRNA as a key step in the biogenesis of group II let-7 microRNAs. Cell *151*, 521-532.

Heo, I., Joo, C., Kim, Y.K., Ha, M., Yoon, M.J., Cho, J., Yeom, K.H., Han, J., and Kim, V.N. (2009). TUT4 in concert with Lin28 suppresses microRNA biogenesis through pre-microRNA uridylation. Cell *138*, 696-708.

Hock, J., Weinmann, L., Ender, C., Rudel, S., Kremmer, E., Raabe, M., Urlaub, H., and Meister, G. (2007). Proteomic and functional analysis of Argonaute-containing mRNA-protein complexes in human cells. EMBO reports *8*, 1052-1060.

Hope, I.A. (1999). C. elegans : a practical approach (Oxford: Oxford University Press).

Horvitz, H.R., and Sulston, J.E. (1980). Isolation and genetic characterization of cell-lineage mutants of the nematode Caenorhabditis elegans. Genetics *96*, 435-454.

Hsu, C.L., and Stevens, A. (1993). Yeast cells lacking 5'-->3' exoribonuclease 1 contain mRNA species that are poly(A) deficient and partially lack the 5' cap structure. Molecular and cellular biology *13*, 4826-4835.

Huang, K.L., Chadee, A.B., Chen, C.Y., Zhang, Y., and Shyu, A.B. (2013). Phosphorylation at intrinsically disordered regions of PAM2 motif-containing proteins modulates their interactions with PABPC1 and influences mRNA fate. RNA (New York, NY *19*, 295-305.

Huarte, J., Belin, D., Vassalli, A., Strickland, S., and Vassalli, J.D. (1987). Meiotic maturation of mouse oocytes triggers the translation and polyadenylation of dormant tissue-type plasminogen activator mRNA. Genes & development *1*, 1201-1211.

Huarte, J., Stutz, A., O'Connell, M.L., Gubler, P., Belin, D., Darrow, A.L., Strickland, S., and Vassalli, J.D. (1992). Transient translational silencing by reversible mRNA deadenylation. Cell *69*, 1021-1030.

Hubstenberger, A., Cameron, C., Noble, S.L., Keenan, S., and Evans, T.C. (2015). Modifiers of solid RNP granules control normal RNP dynamics and mRNA activity in early development. The Journal of cell biology *211*, 703-716.

Humphreys, D.T., Westman, B.J., Martin, D.I., and Preiss, T. (2005). MicroRNAs control translation initiation by inhibiting eukaryotic initiation factor 4E/cap and poly(A) tail function. Proceedings of the National Academy of Sciences of the United States of America *102*, 16961-16966.

Huntzinger, E., Braun, J.E., Heimstadt, S., Zekri, L., and Izaurralde, E. (2010). Two PABPC1-binding sites in GW182 proteins promote miRNA-mediated gene silencing. The EMBO journal *29*, 4146-4160.

Hutvagner, G., McLachlan, J., Pasquinelli, A.E., Balint, E., Tuschl, T., and Zamore, P.D. (2001). A cellular function for the RNA-interference enzyme Dicer in the maturation of the let-7 small temporal RNA. Science (New York, NY *293*, 834-838.

Hutvagner, G., and Simard, M.J. (2008). Argonaute proteins: key players in RNA silencing. Nature reviews *9*, 22-32.

Hutvagner, G., Simard, M.J., Mello, C.C., and Zamore, P.D. (2004). Sequence-specific inhibition of small RNA function. PLoS biology *2*, E98.

Hyenne, V., Desrosiers, M., and Labbe, J.C. (2008). C. elegans Brat homologs regulate PAR protein-dependent polarity and asymmetric cell division. Developmental biology *321*, 368-378.

Ibanez-Ventoso, C., Vora, M., and Driscoll, M. (2008). Sequence relationships among C. elegans, D. melanogaster and human microRNAs highlight the extensive conservation of microRNAs in biology. PloS one *3*, e2818.

Ibrahim, F., Rohr, J., Jeong, W.J., Hesson, J., and Cerutti, H. (2006). Untemplated oligoadenylation promotes degradation of RISC-cleaved transcripts. Science (New York, NY *314*, 1893.

Ingelfinger, D., Arndt-Jovin, D.J., Luhrmann, R., and Achsel, T. (2002). The human LSm1-7 proteins colocalize with the mRNA-degrading enzymes Dcp1/2 and Xrnl in distinct cytoplasmic foci. RNA (New York, NY *8*, 1489-1501.

Inomata, M., Tagawa, H., Guo, Y.M., Kameoka, Y., Takahashi, N., and Sawada, K. (2009). MicroRNA-17-92 down-regulates expression of distinct targets in different B-cell lymphoma subtypes. Blood *113*, 396-402.

Iwasaki, S., Kawamata, T., and Tomari, Y. (2009). Drosophila argonaute1 and argonaute2 employ distinct mechanisms for translational repression. Molecular cell *34*, 58-67.

Jacobson, A., and Favreau, M. (1983). Possible involvement of poly(A) in protein synthesis. Nucleic acids research *11*, 6353-6368.

Jakymiw, A., Lian, S., Eystathioy, T., Li, S., Satoh, M., Hamel, J.C., Fritzler, M.J., and Chan, E.K. (2005). Disruption of GW bodies impairs mammalian RNA interference. Nature cell biology *7*, 1267-1274.

Jan, C.H., Friedman, R.C., Ruby, J.G., and Bartel, D.P. (2011). Formation, regulation and evolution of Caenorhabditis elegans 3'UTRs. Nature *469*, 97-101.

Jankowska-Anyszka, M., Lamphear, B.J., Aamodt, E.J., Harrington, T., Darzynkiewicz, E., Stolarski, R., and Rhoads, R.E. (1998). Multiple isoforms of eukaryotic protein synthesis initiation factor 4E in Caenorhabditis elegans can distinguish between mono- and trimethylated mRNA cap structures. The Journal of biological chemistry *273*, 10538-10542.

Ji, Q., Hao, X., Zhang, M., Tang, W., Yang, M., Li, L., Xiang, D., Desano, J.T., Bommer, G.T., Fan, D.*, et al.* (2009). MicroRNA miR-34 inhibits human pancreatic cancer tumor-initiating cells. PLoS One *4*, e6816.

Jinek, M., Fabian, M.R., Coyle, S.M., Sonenberg, N., and Doudna, J.A. (2010). Structural insights into the human GW182-PABC interaction in microRNA-mediated deadenylation. Nature structural & molecular biology *17*, 238-240.

Jing, Q., Huang, S., Guth, S., Zarubin, T., Motoyama, A., Chen, J., Di Padova, F., Lin, S.C., Gram, H., and Han, J. (2005). Involvement of microRNA in AU-rich element-mediated mRNA instability. Cell *120*, 623-634.

Johnson, C.D., Esquela-Kerscher, A., Stefani, G., Byrom, M., Kelnar, K., Ovcharenko, D., Wilson, M., Wang, X., Shelton, J., Shingara, J.*, et al.* (2007). The let-7 microRNA represses cell proliferation pathways in human cells. Cancer research *67*, 7713-7722.

Johnson, S.M., Grosshans, H., Shingara, J., Byrom, M., Jarvis, R., Cheng, A., Labourier, E., Reinert, K.L., Brown, D., and Slack, F.J. (2005). RAS is regulated by the let-7 microRNA family. Cell *120*, 635-647.

Johnston, R.J., and Hobert, O. (2003). A microRNA controlling left/right neuronal asymmetry in Caenorhabditis elegans. Nature *426*, 845-849.

Jonas, S., and Izaurralde, E. (2013). The role of disordered protein regions in the assembly of decapping complexes and RNP granules. Genes & development *27*, 2628-2641.

Jonas, S., and Izaurralde, E. (2015). Towards a molecular understanding of microRNA-mediated gene silencing. Nature reviews *16*, 421-433.

Kamath, R.S., and Ahringer, J. (2003). Genome-wide RNAi screening in Caenorhabditis elegans. Methods *30*, 313-321.

Karginov, F.V., Cheloufi, S., Chong, M.M., Stark, A., Smith, A.D., and Hannon, G.J. (2010). Diverse endonucleolytic cleavage sites in the mammalian transcriptome depend upon microRNAs, Drosha, and additional nucleases. Molecular cell *38*, 781-788.

Kato, M., Han, T.W., Xie, S., Shi, K., Du, X., Wu, L.C., Mirzaei, H., Goldsmith, E.J., Longgood, J., Pei, J.*, et al.* (2012). Cell-free formation of RNA granules: low complexity sequence domains form dynamic fibers within hydrogels. Cell *149*, 753-767.

Kawasaki, I., Amiri, A., Fan, Y., Meyer, N., Dunkelbarger, S., Motohashi, T., Karashima, T., Bossinger, O., and Strome, S. (2004). The PGL family proteins associate with germ granules and function redundantly in Caenorhabditis elegans germline development. Genetics *167*, 645-661.

Kawasaki, I., Shim, Y.H., Kirchner, J., Kaminker, J., Wood, W.B., and Strome, S. (1998). PGL-1, a predicted RNA-binding component of germ granules, is essential for fertility in C. elegans. Cell *94*, 635-645.

Ketting, R.F., Fischer, S.E., Bernstein, E., Sijen, T., Hannon, G.J., and Plasterk, R.H. (2001). Dicer functions in RNA interference and in synthesis of small RNA involved in developmental timing in C. elegans. Genes & development *15*, 2654-2659.

Khorshid, M., Hausser, J., Zavolan, M., and van Nimwegen, E. (2013). A biophysical miRNA-mRNA interaction model infers canonical and noncanonical targets. Nature methods *10*, 253-255.

Kim, J.H., and Richter, J.D. (2006). Opposing polymerase-deadenylase activities regulate cytoplasmic polyadenylation. Molecular cell *24*, 173-183.

Kim, J.K., Gabel, H.W., Kamath, R.S., Tewari, M., Pasquinelli, A., Rual, J.F., Kennedy, S., Dybbs, M., Bertin, N., Kaplan, J.M.*, et al.* (2005). Functional genomic analysis of RNA interference in C. elegans. Science (New York, NY *308*, 1164-1167.

Kim, K.W., Wilson, T.L., and Kimble, J. (2010). GLD-2/RNP-8 cytoplasmic poly(A) polymerase is a broad-spectrum regulator of the oogenesis program. Proceedings of the National Academy of Sciences of the United States of America *107*, 17445-17450.

Kimble, J., and Hirsh, D. (1979). The postembryonic cell lineages of the hermaphrodite and male gonads in Caenorhabditis elegans. Developmental biology *70*, 396-417.

Kiriakidou, M., Tan, G.S., Lamprinaki, S., De Planell-Saguer, M., Nelson, P.T., and Mourelatos, Z. (2007). An mRNA m7G cap binding-like motif within human Ago2 represses translation. Cell *129*, 1141-1151.

Klattenhoff, C., and Theurkauf, W. (2008). Biogenesis and germline functions of piRNAs. Development (Cambridge, England) *135*, 3-9.

Kloosterman, W.P., Wienholds, E., Ketting, R.F., and Plasterk, R.H. (2004). Substrate requirements for let-7 function in the developing zebrafish embryo. Nucleic acids research *32*, 6284-6291.

Knaut, H., Pelegri, F., Bohmann, K., Schwarz, H., and Nusslein-Volhard, C. (2000). Zebrafish vasa RNA but not its protein is a component of the germ plasm and segregates asymmetrically before germline specification. The Journal of cell biology *149*, 875-888.

Knight, S.W., and Bass, B.L. (2001). A role for the RNase III enzyme DCR-1 in RNA interference and germ line development in Caenorhabditis elegans. Science (New York, NY *293*, 2269-2271.

Kozlov, G., Safaee, N., Rosenauer, A., and Gehring, K. (2010). Structural basis of binding of P-body-associated proteins GW182 and ataxin-2 by the Mlle domain of poly(A)-binding protein. The Journal of biological chemistry *285*, 13599-13606.

Krutzfeldt, J., Rajewsky, N., Braich, R., Rajeev, K.G., Tuschl, T., Manoharan, M., and Stoffel, M. (2005). Silencing of microRNAs in vivo with 'antagomirs'. Nature *438*, 685-689.

Kshirsagar, M., and Parker, R. (2004). Identification of Edc3p as an enhancer of mRNA decapping in Saccharomyces cerevisiae. Genetics *166*, 729-739.

Kuznicki, K.A., Smith, P.A., Leung-Chiu, W.M., Estevez, A.O., Scott, H.C., and Bennett, K.L. (2000). Combinatorial RNA interference indicates GLH-4 can compensate for GLH-1; these two P granule components are critical for fertility in C. elegans. Development (Cambridge, England) *127*, 2907-2916.

Kuzuoglu-Ozturk, D., Huntzinger, E., Schmidt, S., and Izaurralde, E. (2012). The Caenorhabditis elegans GW182 protein AIN-1 interacts with PAB-1 and subunits of the PAN2-PAN3 and CCR4-NOT deadenylase complexes. Nucleic acids research *40*, 5651-5665.

Lagos-Quintana, M., Rauhut, R., Lendeckel, W., and Tuschl, T. (2001). Identification of novel genes coding for small expressed RNAs. Science (New York, NY *294*, 853-858.

Lall, S., Piano, F., and Davis, R.E. (2005). Caenorhabditis elegans decapping proteins: localization and functional analysis of Dcp1, Dcp2, and DcpS during embryogenesis. Molecular biology of the cell *16*, 5880-5890.

Landthaler, M., Gaidatzis, D., Rothballer, A., Chen, P.Y., Soll, S.J., Dinic, L., Ojo, T., Hafner, M., Zavolan, M., and Tuschl, T. (2008). Molecular characterization of human Argonaute-containing ribonucleoprotein complexes and their bound target mRNAs. RNA (New York, NY *14*, 2580-2596.

Lau, N.C., Lim, L.P., Weinstein, E.G., and Bartel, D.P. (2001). An abundant class of tiny RNAs with probable regulatory roles in Caenorhabditis elegans. Science (New York, NY *294*, 858-862.

Lazzaretti, D., Tournier, I., and Izaurralde, E. (2009). The C-terminal domains of human TNRC6A, TNRC6B, and TNRC6C silence bound transcripts independently of Argonaute proteins. RNA (New York, NY *15*, 1059-1066.

Leacock, S.W., and Reinke, V. (2008). MEG-1 and MEG-2 are embryo-specific P-granule components required for germline development in Caenorhabditis elegans. Genetics *178*, 295-306.

Leaman, D., Chen, P.Y., Fak, J., Yalcin, A., Pearce, M., Unnerstall, U., Marks, D.S., Sander, C., Tuschl, T., and Gaul, U. (2005). Antisense-mediated depletion reveals essential and specific functions of microRNAs in Drosophila development. Cell *121*, 1097-1108.

Lee, J.E., Lee, J.Y., Trembly, J., Wilusz, J., Tian, B., and Wilusz, C.J. (2012). The PARN deadenylase targets a discrete set of mRNAs for decay and regulates cell motility in mouse myoblasts. PLoS genetics *8*, e1002901.

Lee, M., Choi, Y., Kim, K., Jin, H., Lim, J., Nguyen, T.A., Yang, J., Jeong, M., Giraldez, A.J., Yang, H.*, et al.* (2014). Adenylation of maternally inherited microRNAs by Wispy. Molecular cell *56*, 696-707.

Lee, M.T., Bonneau, A.R., Takacs, C.M., Bazzini, A.A., DiVito, K.R., Fleming, E.S., and Giraldez, A.J. (2013). Nanog, Pou5f1 and SoxB1 activate zygotic gene expression during the maternal-to-zygotic transition. Nature *503*, 360-364.

Lee, R.C., and Ambros, V. (2001). An extensive class of small RNAs in Caenorhabditis elegans. Science (New York, NY *294*, 862-864.

Lee, R.C., Feinbaum, R.L., and Ambros, V. (1993). The C. elegans heterochronic gene lin-4 encodes small RNAs with antisense complementarity to lin-14. Cell *75*, 843-854.

Lee, Y., Ahn, C., Han, J., Choi, H., Kim, J., Yim, J., Lee, J., Provost, P., Radmark, O., Kim, S., *et al.* (2003). The nuclear RNase III Drosha initiates microRNA processing. Nature *425*, 415-419.

Lee, Y., Jeon, K., Lee, J.T., Kim, S., and Kim, V.N. (2002). MicroRNA maturation: stepwise processing and subcellular localization. The EMBO journal *21*, 4663-4670.

Lee, Y., Kim, M., Han, J., Yeom, K.H., Lee, S., Baek, S.H., and Kim, V.N. (2004). MicroRNA genes are transcribed by RNA polymerase II. The EMBO journal *23*, 4051-4060.

Lee, Y.S., Pressman, S., Andress, A.P., Kim, K., White, J.L., Cassidy, J.J., Li, X., Lubell, K., Lim do, H., Cho, I.S., *et al.* (2009). Silencing by small RNAs is linked to endosomal trafficking. Nature cell biology *11*, 1150-1156.

Lehmann, R., and Nusslein-Volhard, C. (1986). Abdominal segmentation, pole cell formation, and embryonic polarity require the localized activity of oskar, a maternal gene in Drosophila. Cell *47*, 141-152.

Lejeune, F., Li, X., and Maquat, L.E. (2003). Nonsense-mediated mRNA decay in mammalian cells involves decapping, deadenylating, and exonucleolytic activities. Molecular cell *12*, 675-687.

Lewis, B.P., Burge, C.B., and Bartel, D.P. (2005). Conserved seed pairing, often flanked by adenosines, indicates that thousands of human genes are microRNA targets. Cell *120*, 15-20.

Li, P., Banjade, S., Cheng, H.C., Kim, S., Chen, B., Guo, L., Llaguno, M., Hollingsworth, J.V., King, D.S., Banani, S.F., *et al.* (2012). Phase transitions in the assembly of multivalent signalling proteins. Nature *483*, 336-340.

Lian, S.L., Li, S., Abadal, G.X., Pauley, B.A., Fritzler, M.J., and Chan, E.K. (2009). The C-terminal half of human Ago2 binds to multiple GW-rich regions of GW182 and requires GW182 to mediate silencing. RNA (New York, NY *15*, 804-813.

Lim, A.K., and Kai, T. (2007). Unique germ-line organelle, nuage, functions to repress selfish genetic elements in Drosophila melanogaster. Proceedings of the National Academy of Sciences of the United States of America *104*, 6714-6719.

Lim, L.P., Lau, N.C., Garrett-Engele, P., Grimson, A., Schelter, J.M., Castle, J., Bartel, D.P., Linsley, P.S., and Johnson, J.M. (2005). Microarray analysis shows that some microRNAs downregulate large numbers of target mRNAs. Nature *433*, 769-773.

Lim, L.P., Lau, N.C., Weinstein, E.G., Abdelhakim, A., Yekta, S., Rhoades, M.W., Burge, C.B., and Bartel, D.P. (2003). The microRNAs of Caenorhabditis elegans. Genes & development *17*, 991-1008.

Lin, H., and Spradling, A.C. (1997). A novel group of pumilio mutations affects the asymmetric division of germline stem cells in the Drosophila ovary. Development (Cambridge, England) *124*, 2463-2476.

Lin, S.Y., Johnson, S.M., Abraham, M., Vella, M.C., Pasquinelli, A., Gamberi, C., Gottlieb, E., and Slack, F.J. (2003). The C elegans hunchback homolog, hbl-1, controls temporal patterning and is a probable microRNA target. Developmental cell *4*, 639-650.

Lin, Y., Protter, D.S., Rosen, M.K., and Parker, R. (2015). Formation and Maturation of Phase-Separated Liquid Droplets by RNA-Binding Proteins. Molecular cell *60*, 208-219.

Lingel, A., Simon, B., Izaurralde, E., and Sattler, M. (2004). Nucleic acid 3'-end recognition by the Argonaute2 PAZ domain. Nature structural & molecular biology *11*, 576-577.

Little, S.C., Sinsimer, K.S., Lee, J.J., Wieschaus, E.F., and Gavis, E.R. (2015). Independent and coordinate trafficking of single Drosophila germ plasm mRNAs. Nature cell biology *17*, 558-568.

Liu, H., Rodgers, N.D., Jiao, X., and Kiledjian, M. (2002). The scavenger mRNA decapping enzyme DcpS is a member of the HIT family of pyrophosphatases. The EMBO journal *21*, 4699-4708.

Liu, H.Y., Badarinarayana, V., Audino, D.C., Rappsilber, J., Mann, M., and Denis, C.L. (1998). The NOT proteins are part of the CCR4 transcriptional complex and affect gene expression both positively and negatively. The EMBO journal *17*, 1096-1106.

Liu, J., Carmell, M.A., Rivas, F.V., Marsden, C.G., Thomson, J.M., Song, J.J., Hammond, S.M., Joshua-Tor, L., and Hannon, G.J. (2004). Argonaute2 is the catalytic engine of mammalian RNAi. Science (New York, NY *305*, 1437-1441.

Liu, J., Rivas, F.V., Wohlschlegel, J., Yates, J.R., 3rd, Parker, R., and Hannon, G.J. (2005a). A role for the P-body component GW182 in microRNA function. Nature cell biology *7*, 1261-1266.

Liu, J., Valencia-Sanchez, M.A., Hannon, G.J., and Parker, R. (2005b). MicroRNA-dependent localization of targeted mRNAs to mammalian P-bodies. Nature cell biology *7*, 719-723.

Liu, N., Abe, M., Sabin, L.R., Hendriks, G.J., Naqvi, A.S., Yu, Z., Cherry, S., and Bonini, N.M. (2011). The exoribonuclease Nibbler controls 3' end processing of microRNAs in Drosophila. Curr Biol *21*, 1888-1893.

Llave, C., Xie, Z., Kasschau, K.D., and Carrington, J.C. (2002). Cleavage of Scarecrow-like mRNA targets directed by a class of Arabidopsis miRNA. Science (New York, NY *297*, 2053-2056.

Loeb, G.B., Khan, A.A., Canner, D., Hiatt, J.B., Shendure, J., Darnell, R.B., Leslie, C.S., and Rudensky, A.Y. (2012). Transcriptome-wide miR-155 binding map reveals widespread noncanonical microRNA targeting. Molecular cell *48*, 760-770.

Loedige, I., Jakob, L., Treiber, T., Ray, D., Stotz, M., Treiber, N., Hennig, J., Cook, K.B., Morris, Q., Hughes, T.R.*, et al.* (2015). The Crystal Structure of the NHL Domain in Complex

with RNA Reveals the Molecular Basis of Drosophila Brain-Tumor-Mediated Gene Regulation. Cell Rep *13*, 1206-1220.

Loedige, I., Stotz, M., Qamar, S., Kramer, K., Hennig, J., Schubert, T., Loffler, P., Langst, G., Merkl, R., Urlaub, H.*, et al.* (2014). The NHL domain of BRAT is an RNA-binding domain that directly contacts the hunchback mRNA for regulation. Genes & development *28*, 749-764.

Lund, E., Liu, M., Hartley, R.S., Sheets, M.D., and Dahlberg, J.E. (2009). Deadenylation of maternal mRNAs mediated by miR-427 in Xenopus laevis embryos. RNA (New York, NY *15*, 2351-2363.

Luteijn, M.J., van Bergeijk, P., Kaaij, L.J., Almeida, M.V., Roovers, E.F., Berezikov, E., and Ketting, R.F. (2012). Extremely stable Piwi-induced gene silencing in Caenorhabditis elegans. The EMBO journal *31*, 3422-3430.

Lykke-Andersen, J. (2002). Identification of a human decapping complex associated with hUpf proteins in nonsense-mediated decay. Molecular and cellular biology *22*, 8114-8121.

Lytle, J.R., Yario, T.A., and Steitz, J.A. (2007). Target mRNAs are repressed as efficiently by microRNA-binding sites in the 5' UTR as in the 3' UTR. Proceedings of the National Academy of Sciences of the United States of America *104*, 9667-9672.

Ma, J.B., Ye, K., and Patel, D.J. (2004). Structural basis for overhang-specific small interfering RNA recognition by the PAZ domain. Nature *429*, 318-322.

MacCoss, M.J., McDonald, W.H., Saraf, A., Sadygov, R., Clark, J.M., Tasto, J.J., Gould, K.L., Wolters, D., Washburn, M., Weiss, A.*, et al.* (2002). Shotgun identification of protein modifications from protein complexes and lens tissue. Proceedings of the National Academy of Sciences of the United States of America *99*, 7900-7905.

Mahowald, A.P. (1971). Polar granules of drosophila. IV. Cytochemical studies showing loss of RNA from polar granules during early stages of embryogenesis. J Exp Zool *176*, 345-352.

Mallory, A., and Vaucheret, H. (2010). Form, function, and regulation of ARGONAUTE proteins. The Plant cell *22*, 3879-3889.

Maroney, P.A., Yu, Y., Fisher, J., and Nilsen, T.W. (2006). Evidence that microRNAs are associated with translating messenger RNAs in human cells. Nature structural & molecular biology *13*, 1102-1107.

Mathonnet, G., Fabian, M.R., Svitkin, Y.V., Parsyan, A., Huck, L., Murata, T., Biffo, S., Merrick, W.C., Darzynkiewicz, E., Pillai, R.S.*, et al.* (2007). MicroRNA inhibition of translation initiation in vitro by targeting the cap-binding complex eIF4F. Science (New York, NY *317*, 1764-1767.

Mathys, H., Basquin, J., Ozgur, S., Czarnocki-Cieciura, M., Bonneau, F., Aartse, A., Dziembowski, A., Nowotny, M., Conti, E., and Filipowicz, W. (2014). Structural and

biochemical insights to the role of the CCR4-NOT complex and DDX6 ATPase in microRNA repression. Molecular cell *54*, 751-765.

Mattick, J.S. (2003). Challenging the dogma: the hidden layer of non-protein-coding RNAs in complex organisms. Bioessays *25*, 930-939.

Mayr, C., Hemann, M.T., and Bartel, D.P. (2007). Disrupting the pairing between let-7 and Hmga2 enhances oncogenic transformation. Science (New York, NY *315*, 1576-1579.

Meister, G., Landthaler, M., Peters, L., Chen, P.Y., Urlaub, H., Luhrmann, R., and Tuschl, T. (2005). Identification of novel argonaute-associated proteins. Curr Biol *15*, 2149-2155.

Mello, C.C., Schubert, C., Draper, B., Zhang, W., Lobel, R., and Priess, J.R. (1996). The PIE-1 protein and germline specification in C. elegans embryos. Nature *382*, 710-712.

Mi, H., Muruganujan, A., and Thomas, P.D. (2013). PANTHER in 2013: modeling the evolution of gene function, and other gene attributes, in the context of phylogenetic trees. Nucleic acids research *41*, D377-386.

Miller, L.M., Gallegos, M.E., Morisseau, B.A., and Kim, S.K. (1993). lin-31, a Caenorhabditis elegans HNF-3/fork head transcription factor homolog, specifies three alternative cell fates in vulval development. Genes & development *7*, 933-947.

Miska, E.A., Alvarez-Saavedra, E., Abbott, A.L., Lau, N.C., Hellman, A.B., McGonagle, S.M., Bartel, D.P., Ambros, V.R., and Horvitz, H.R. (2007). Most Caenorhabditis elegans microRNAs are individually not essential for development or viability. PLoS genetics *3*, e215.

Mitchell, P., Petfalski, E., Shevchenko, A., Mann, M., and Tollervey, D. (1997). The exosome: a conserved eukaryotic RNA processing complex containing multiple 3'-->5' exoribonucleases. Cell *91*, 457-466.

Mittal, S., Aslam, A., Doidge, R., Medica, R., and Winkler, G.S. (2011). The Ccr4a (CNOT6) and Ccr4b (CNOT6L) deadenylase subunits of the human Ccr4-Not complex contribute to the prevention of cell death and senescence. Molecular biology of the cell *22*, 748-758.

Miyoshi, K., Okada, T.N., Siomi, H., and Siomi, M.C. (2009). Characterization of the miRNA-RISC loading complex and miRNA-RISC formed in the Drosophila miRNA pathway. RNA (New York, NY *15*, 1282-1291.

Molin, L., and Puisieux, A. (2005). C. elegans homologue of the Caf1 gene, which encodes a subunit of the CCR4-NOT complex, is essential for embryonic and larval development and for meiotic progression. Gene *358*, 73-81.

Molliex, A., Temirov, J., Lee, J., Coughlin, M., Kanagaraj, A.P., Kim, H.J., Mittag, T., and Taylor, J.P. (2015). Phase separation by low complexity domains promotes stress granule assembly and drives pathological fibrillization. Cell *163*, 123-133.

Moretti, F., Kaiser, C., Zdanowicz-Specht, A., and Hentze, M.W. (2012). PABP and the poly(A) tail augment microRNA repression by facilitated miRISC binding. Nature structural & molecular biology *19*, 603-608.

Morita, K., and Han, M. (2006). Multiple mechanisms are involved in regulating the expression of the developmental timing regulator lin-28 in Caenorhabditis elegans. The EMBO journal *25*, 5794-5804.

Morris, J.Z., Hong, A., Lilly, M.A., and Lehmann, R. (2005). twin, a CCR4 homolog, regulates cyclin poly(A) tail length to permit Drosophila oogenesis. Development (Cambridge, England) *132*, 1165-1174.

Moss, E.G., Lee, R.C., and Ambros, V. (1997). The cold shock domain protein LIN-28 controls developmental timing in C. elegans and is regulated by the lin-4 RNA. Cell *88*, 637-646.

Mukherjee, D., Gao, M., O'Connor, J.P., Raijmakers, R., Pruijn, G., Lutz, C.S., and Wilusz, J. (2002). The mammalian exosome mediates the efficient degradation of mRNAs that contain AU-rich elements. The EMBO journal *21*, 165-174.

Nakamura, M., Ando, R., Nakazawa, T., Yudazono, T., Tsutsumi, N., Hatanaka, N., Ohgake, T., Hanaoka, F., and Eki, T. (2007). Dicer-related drh-3 gene functions in germ-line development by maintenance of chromosomal integrity in Caenorhabditis elegans. Genes Cells *12*, 997-1010.

Nakamura, T., Yao, R., Ogawa, T., Suzuki, T., Ito, C., Tsunekawa, N., Inoue, K., Ajima, R., Miyasaka, T., Yoshida, Y.*, et al.* (2004). Oligo-astheno-teratozoospermia in mice lacking Cnot7, a regulator of retinoid X receptor beta. Nature genetics *36*, 528-533.

Nakanishi, K., Weinberg, D.E., Bartel, D.P., and Patel, D.J. (2012). Structure of yeast Argonaute with guide RNA. Nature *486*, 368-374.

Navarro, R.E., Shim, E.Y., Kohara, Y., Singson, A., and Blackwell, T.K. (2001). cgh-1, a conserved predicted RNA helicase required for gametogenesis and protection from physiological germline apoptosis in C. elegans. Development (Cambridge, England) *128*, 3221-3232.

Nehme, R., and Conradt, B. (2008). egl-1: a key activator of apoptotic cell death in C. elegans. Oncogene *27 Suppl 1*, S30-40.

Nguyen Chi, M., Chalmel, F., Agius, E., Vanzo, N., Khabar, K.S., Jegou, B., and Morello, D. (2009). Temporally regulated traffic of HuR and its associated ARE-containing mRNAs from the chromatoid body to polysomes during mouse spermatogenesis. PloS one *4*, e4900.

Nishimura, T., Padamsi, Z., Fakim, H., Milette, S., Dunham, W.H., Gingras, A.C., and Fabian, M.R. (2015). The eIF4E-Binding Protein 4E-T Is a Component of the mRNA Decay Machinery that Bridges the 5' and 3' Termini of Target mRNAs. Cell Rep *11*, 1425-1436.

Noble, S.L., Allen, B.L., Goh, L.K., Nordick, K., and Evans, T.C. (2008). Maternal mRNAs are regulated by diverse P body-related mRNP granules during early Caenorhabditis elegans development. The Journal of cell biology *182*, 559-572.

Nott, T.J., Petsalaki, E., Farber, P., Jervis, D., Fussner, E., Plochowietz, A., Craggs, T.D., Bazett-Jones, D.P., Pawson, T., Forman-Kay, J.D., *et al.* (2015). Phase transition of a disordered nuage protein generates environmentally responsive membraneless organelles. Molecular cell *57*, 936-947.

Nottrott, S., Simard, M.J., and Richter, J.D. (2006). Human let-7a miRNA blocks protein production on actively translating polyribosomes. Nature structural & molecular biology *13*, 1108-1114.

Nousch, M., Techritz, N., Hampel, D., Millonigg, S., and Eckmann, C.R. (2013). The Ccr4-Not deadenylase complex constitutes the main poly(A) removal activity in C. elegans. Journal of cell science *126*, 4274-4285.

Okamura, K., Hagen, J.W., Duan, H., Tyler, D.M., and Lai, E.C. (2007). The mirtron pathway generates microRNA-class regulatory RNAs in Drosophila. Cell *130*, 89-100.

Olsen, P.H., and Ambros, V. (1999). The lin-4 regulatory RNA controls developmental timing in Caenorhabditis elegans by blocking LIN-14 protein synthesis after the initiation of translation. Developmental biology *216*, 671-680.

Orom, U.A., Kauppinen, S., and Lund, A.H. (2006). LNA-modified oligonucleotides mediate specific inhibition of microRNA function. Gene *372*, 137-141.

Ozgur, S., Chekulaeva, M., and Stoecklin, G. (2010). Human Pat1b connects deadenylation with mRNA decapping and controls the assembly of processing bodies. Molecular and cellular biology *30*, 4308-4323.

Pal-Bhadra, M., Bhadra, U., and Birchler, J.A. (2002). RNAi related mechanisms affect both transcriptional and posttranscriptional transgene silencing in Drosophila. Molecular cell *9*, 315-327.

Pal-Bhadra, M., Leibovitch, B.A., Gandhi, S.G., Chikka, M.R., Bhadra, U., Birchler, J.A., and Elgin, S.C. (2004). Heterochromatic silencing and HP1 localization in Drosophila are dependent on the RNAi machinery. Science (New York, NY *303*, 669-672.

Palatnik, C.M., Wilkins, C., and Jacobson, A. (1984). Translational control during early Dictyostelium development: possible involvement of poly(A) sequences. Cell *36*, 1017-1025.

Pane, A., Wehr, K., and Schupbach, T. (2007). zucchini and squash encode two putative nucleases required for rasiRNA production in the Drosophila germline. Developmental cell *12*, 851-862.

Paris, J., Swenson, K., Piwnica-Worms, H., and Richter, J.D. (1991). Maturation-specific polyadenylation: in vitro activation by p34cdc2 and phosphorylation of a 58-kD CPE-binding protein. Genes & development *5*, 1697-1708.

Parker, R., and Sheth, U. (2007). P bodies and the control of mRNA translation and degradation. Molecular cell *25*, 635-646.

Parry, D.H., Xu, J., and Ruvkun, G. (2007). A whole-genome RNAi Screen for C. elegans miRNA pathway genes. Curr Biol *17*, 2013-2022.

Pase, L., Layton, J.E., Kloosterman, W.P., Carradice, D., Waterhouse, P.M., and Lieschke, G.J. (2009). miR-451 regulates zebrafish erythroid maturation in vivo via its target gata2. Blood *113*, 1794-1804.

Pasquinelli, A.E., Reinhart, B.J., Slack, F., Martindale, M.Q., Kuroda, M.I., Maller, B., Hayward, D.C., Ball, E.E., Degnan, B., Muller, P.*, et al.* (2000). Conservation of the sequence and temporal expression of let-7 heterochronic regulatory RNA. Nature *408*, 86-89.

Peters, L., and Meister, G. (2007). Argonaute proteins: mediators of RNA silencing. Molecular cell *26*, 611-623.

Petersen, C.P., Bordeleau, M.E., Pelletier, J., and Sharp, P.A. (2006). Short RNAs repress translation after initiation in mammalian cells. Molecular cell *21*, 533-542.

Pham, J.W., Pellino, J.L., Lee, Y.S., Carthew, R.W., and Sontheimer, E.J. (2004). A Dicer-2-dependent 80s complex cleaves targeted mRNAs during RNAi in Drosophila. Cell *117*, 83-94.

Pillai, R.S., Bhattacharyya, S.N., Artus, C.G., Zoller, T., Cougot, N., Basyuk, E., Bertrand, E., and Filipowicz, W. (2005). Inhibition of translational initiation by Let-7 MicroRNA in human cells. Science (New York, NY *309*, 1573-1576.

Rangan, P., Malone, C.D., Navarro, C., Newbold, S.P., Hayes, P.S., Sachidanandam, R., Hannon, G.J., and Lehmann, R. (2011). piRNA production requires heterochromatin formation in Drosophila. Curr Biol *21*, 1373-1379.

Raymond, C.K., Roberts, B.S., Garrett-Engele, P., Lim, L.P., and Johnson, J.M. (2005). Simple, quantitative primer-extension PCR assay for direct monitoring of microRNAs and short-interfering RNAs. RNA (New York, NY *11*, 1737-1744.

Rehwinkel, J., Behm-Ansmant, I., Gatfield, D., and Izaurralde, E. (2005). A crucial role for GW182 and the DCP1:DCP2 decapping complex in miRNA-mediated gene silencing. RNA (New York, NY *11*, 1640-1647.

Reijns, M.A., Alexander, R.D., Spiller, M.P., and Beggs, J.D. (2008). A role for Q/N-rich aggregation-prone regions in P-body localization. Journal of cell science *121*, 2463-2472.

Reinhart, B.J., Slack, F.J., Basson, M., Pasquinelli, A.E., Bettinger, J.C., Rougvie, A.E., Horvitz, H.R., and Ruvkun, G. (2000). The 21-nucleotide let-7 RNA regulates developmental timing in Caenorhabditis elegans. Nature *403*, 901-906.

Ren, Z., Veksler-Lublinsky, I., Morrissey, D., and Ambros, V. (2016). Staufen Negatively Modulates microRNA Activity in Caenorhabditis elegans. G3 (Bethesda).

Rinn, J.L., Kertesz, M., Wang, J.K., Squazzo, S.L., Xu, X., Brugmann, S.A., Goodnough, L.H., Helms, J.A., Farnham, P.J., Segal, E.*, et al.* (2007). Functional demarcation of active and silent chromatin domains in human HOX loci by noncoding RNAs. Cell *129*, 1311-1323.

Rivas, F.V., Tolia, N.H., Song, J.J., Aragon, J.P., Liu, J., Hannon, G.J., and Joshua-Tor, L. (2005). Purified Argonaute2 and an siRNA form recombinant human RISC. Nature structural & molecular biology *12*, 340-349.

Robert, V.J., Sijen, T., van Wolfswinkel, J., and Plasterk, R.H. (2005). Chromatin and RNAi factors protect the C. elegans germline against repetitive sequences. Genes & development *19*, 782-787.

Rouget, C., Papin, C., Boureux, A., Meunier, A.C., Franco, B., Robine, N., Lai, E.C., Pelisson, A., and Simonelig, M. (2010). Maternal mRNA deadenylation and decay by the piRNA pathway in the early Drosophila embryo. Nature *467*, 1128-1132.

Rouya, C., Siddiqui, N., Morita, M., Duchaine, T.F., Fabian, M.R., and Sonenberg, N. (2014). Human DDX6 effects miRNA-mediated gene silencing via direct binding to CNOT1. RNA (New York, NY *20*, 1398-1409.

Ruby, J.G., Jan, C.H., and Bartel, D.P. (2007). Intronic microRNA precursors that bypass Drosha processing. Nature *448*, 83-86.

Ruvkun, G., and Giusto, J. (1989). The Caenorhabditis elegans heterochronic gene lin-14 encodes a nuclear protein that forms a temporal developmental switch. Nature *338*, 313-319.

Saetrom, P., Heale, B.S., Snove, O., Jr., Aagaard, L., Alluin, J., and Rossi, J.J. (2007). Distance constraints between microRNA target sites dictate efficacy and cooperativity. Nucleic acids research *35*, 2333-2342.

Salles, F.J., Lieberfarb, M.E., Wreden, C., Gergen, J.P., and Strickland, S. (1994). Coordinate initiation of Drosophila development by regulated polyadenylation of maternal messenger RNAs. Science (New York, NY *266*, 1996-1999.

Sarin, S., O'Meara, M.M., Flowers, E.B., Antonio, C., Poole, R.J., Didiano, D., Johnston, R.J., Jr., Chang, S., Narula, S., and Hobert, O. (2007). Genetic screens for Caenorhabditis elegans mutants defective in left/right asymmetric neuronal fate specification. Genetics *176*, 2109-2130.

Sasaki, T., Shiohama, A., Minoshima, S., and Shimizu, N. (2003). Identification of eight members of the Argonaute family in the human genome. Genomics *82*, 323-330.

Schisa, J.A. (2012). New insights into the regulation of RNP granule assembly in oocytes. Int Rev Cell Mol Biol *295*, 233-289.

Schneider, M.D., Najand, N., Chaker, S., Pare, J.M., Haskins, J., Hughes, S.C., Hobman, T.C., Locke, J., and Simmonds, A.J. (2006). Gawky is a component of cytoplasmic mRNA processing bodies required for early Drosophila development. The Journal of cell biology *174*, 349-358.

Schubert, C.M., Lin, R., de Vries, C.J., Plasterk, R.H., and Priess, J.R. (2000). MEX-5 and MEX-6 function to establish soma/germline asymmetry in early C. elegans embryos. Molecular cell *5*, 671-682.

Scott, M.P., Storti, R.V., Pardue, M.L., and Rich, A. (1979). Cell-free protein synthesis in lysates of Drosophila melanogaster cells. Biochemistry *18*, 1588-1594.

Seggerson, K., Tang, L., and Moss, E.G. (2002). Two genetic circuits repress the Caenorhabditis elegans heterochronic gene lin-28 after translation initiation. Developmental biology *243*, 215-225.

Seitz, H., Ghildiyal, M., and Zamore, P.D. (2008). Argonaute loading improves the 5' precision of both MicroRNAs and their miRNA* strands in flies. Curr Biol *18*, 147-151.

Selbach, M., Schwanhausser, B., Thierfelder, N., Fang, Z., Khanin, R., and Rajewsky, N. (2008). Widespread changes in protein synthesis induced by microRNAs. Nature *455*, 58-63.

Sen, G.L., and Blau, H.M. (2005). Argonaute 2/RISC resides in sites of mammalian mRNA decay known as cytoplasmic bodies. Nature cell biology *7*, 633-636.

Sengupta, M.S., Low, W.Y., Patterson, J.R., Kim, H.M., Traven, A., Beilharz, T.H., Colaiacovo, M.P., Schisa, J.A., and Boag, P.R. (2013). ifet-1 is a broad-scale translational repressor required for normal P granule formation in C. elegans. Journal of cell science *126*, 850-859.

Seydoux, G., and Fire, A. (1994). Soma-germline asymmetry in the distributions of embryonic RNAs in Caenorhabditis elegans. Development (Cambridge, England) *120*, 2823-2834.

Shaw, W.R., Armisen, J., Lehrbach, N.J., and Miska, E.A. (2010). The conserved miR-51 microRNA family is redundantly required for embryonic development and pharynx attachment in Caenorhabditis elegans. Genetics *185*, 897-905.

Sheets, M.D., Fox, C.A., Hunt, T., Vande Woude, G., and Wickens, M. (1994). The 3'-untranslated regions of c-mos and cyclin mRNAs stimulate translation by regulating cytoplasmic polyadenylation. Genes & development *8*, 926-938.

Sheets, M.D., Wu, M., and Wickens, M. (1995). Polyadenylation of c-mos mRNA as a control point in Xenopus meiotic maturation. Nature *374*, 511-516.

Shen, B., and Goodman, H.M. (2004). Uridine addition after microRNA-directed cleavage. Science (New York, NY *306*, 997.

Sheth, U., and Parker, R. (2003). Decapping and decay of messenger RNA occur in cytoplasmic processing bodies. Science (New York, NY *300*, 805-808.

Shirayama, M., Seth, M., Lee, H.C., Gu, W., Ishidate, T., Conte, D., Jr., and Mello, C.C. (2012). piRNAs initiate an epigenetic memory of nonself RNA in the C. elegans germline. Cell *150*, 65-77.

Smibert, C.A., Wilson, J.E., Kerr, K., and Macdonald, P.M. (1996). smaug protein represses translation of unlocalized nanos mRNA in the Drosophila embryo. Genes & development *10*, 2600-2609.

Soderstrom, K.O., and Parvinen, M. (1976). Incorporation of (3H)uridine by the chromatoid body during rat spermatogenesis. The Journal of cell biology *70*, 239-246.

Souret, F.F., Kastenmayer, J.P., and Green, P.J. (2004). AtXRN4 degrades mRNA in Arabidopsis and its substrates include selected miRNA targets. Molecular cell *15*, 173-183.

Spike, C., Meyer, N., Racen, E., Orsborn, A., Kirchner, J., Kuznicki, K., Yee, C., Bennett, K., and Strome, S. (2008). Genetic analysis of the Caenorhabditis elegans GLH family of P-granule proteins. Genetics *178*, 1973-1987.

Squirrell, J.M., Eggers, Z.T., Luedke, N., Saari, B., Grimson, A., Lyons, G.E., Anderson, P., and White, J.G. (2006). CAR-1, a protein that localizes with the mRNA decapping component DCAP-1, is required for cytokinesis and ER organization in Caenorhabditis elegans embryos. Molecular biology of the cell *17*, 336-344.

Stebbins-Boaz, B., Hake, L.E., and Richter, J.D. (1996). CPEB controls the cytoplasmic polyadenylation of cyclin, Cdk2 and c-mos mRNAs and is necessary for oocyte maturation in Xenopus. The EMBO journal *15*, 2582-2592.

Stebbins-Boaz, B., and Richter, J.D. (1994). Multiple sequence elements and a maternal mRNA product control cdk2 RNA polyadenylation and translation during early Xenopus development. Molecular and cellular biology *14*, 5870-5880.

Stoeckius, M., Maaskola, J., Colombo, T., Rahn, H.P., Friedlander, M.R., Li, N., Chen, W., Piano, F., and Rajewsky, N. (2009). Large-scale sorting of C. elegans embryos reveals the dynamics of small RNA expression. Nature methods *6*, 745-751.

Strome, S., and Wood, W.B. (1982). Immunofluorescence visualization of germ-line-specific cytoplasmic granules in embryos, larvae, and adults of Caenorhabditis elegans. Proceedings of the National Academy of Sciences of the United States of America *79*, 1558-1562.

Subasic, D., Brummer, A., Wu, Y., Pinto, S.M., Imig, J., Keller, M., Jovanovic, M., Lightfoot, H.L., Nasso, S., Goetze, S.*, et al.* (2015). Cooperative target mRNA destabilization and translation inhibition by miR-58 microRNA family in C. elegans. Genome research *25*, 1680-1691.

Subtelny, A.O., Eichhorn, S.W., Chen, G.R., Sive, H., and Bartel, D.P. (2014). Poly(A)-tail profiling reveals an embryonic switch in translational control. Nature *508*, 66-71.

Suh, N., Jedamzik, B., Eckmann, C.R., Wickens, M., and Kimble, J. (2006). The GLD-2 poly(A) polymerase activates gld-1 mRNA in the Caenorhabditis elegans germ line. Proceedings of the National Academy of Sciences of the United States of America *103*, 15108-15112.

Sulston, J.E., and Horvitz, H.R. (1977). Post-embryonic cell lineages of the nematode, Caenorhabditis elegans. Developmental biology *56*, 110-156.

Sulston, J.E., and Horvitz, H.R. (1981). Abnormal cell lineages in mutants of the nematode Caenorhabditis elegans. Developmental biology *82*, 41-55.

Tabach, Y., Billi, A.C., Hayes, G.D., Newman, M.A., Zuk, O., Gabel, H., Kamath, R., Yacoby, K., Chapman, B., Garcia, S.M.*, et al.* (2013). Identification of small RNA pathway genes using patterns of phylogenetic conservation and divergence. Nature *493*, 694-698.

Tabara, H., Sarkissian, M., Kelly, W.G., Fleenor, J., Grishok, A., Timmons, L., Fire, A., and Mello, C.C. (1999). The rde-1 gene, RNA interference, and transposon silencing in C. elegans. Cell *99*, 123-132.

Tabara, H., Yigit, E., Siomi, H., and Mello, C.C. (2002). The dsRNA binding protein RDE-4 interacts with RDE-1, DCR-1, and a DExH-box helicase to direct RNAi in C. elegans. Cell *109*, 861-871.

Takamizawa, J., Konishi, H., Yanagisawa, K., Tomida, S., Osada, H., Endoh, H., Harano, T., Yatabe, Y., Nagino, M., Nimura, Y.*, et al.* (2004). Reduced expression of the let-7 microRNAs in human lung cancers in association with shortened postoperative survival. Cancer research *64*, 3753-3756.

Takimoto, K., Wakiyama, M., and Yokoyama, S. (2009). Mammalian GW182 contains multiple Argonaute-binding sites and functions in microRNA-mediated translational repression. RNA (New York, NY *15*, 1078-1089.

Tang, G., Reinhart, B.J., Bartel, D.P., and Zamore, P.D. (2003). A biochemical framework for RNA silencing in plants. Genes & development *17*, 49-63.

Teixeira, D., Sheth, U., Valencia-Sanchez, M.A., Brengues, M., and Parker, R. (2005). Processing bodies require RNA for assembly and contain nontranslating mRNAs. RNA (New York, NY *11*, 371-382.

Temme, C., Zaessinger, S., Meyer, S., Simonelig, M., and Wahle, E. (2004). A complex containing the CCR4 and CAF1 proteins is involved in mRNA deadenylation in Drosophila. The EMBO journal *23*, 2862-2871.

Temme, C., Zhang, L., Kremmer, E., Ihling, C., Chartier, A., Sinz, A., Simonelig, M., and Wahle, E. (2010). Subunits of the Drosophila CCR4-NOT complex and their roles in mRNA deadenylation. RNA (New York, NY *16*, 1356-1370.

Tharun, S., He, W., Mayes, A.E., Lennertz, P., Beggs, J.D., and Parker, R. (2000). Yeast Sm-like proteins function in mRNA decapping and decay. Nature *404*, 515-518.

Tharun, S., and Parker, R. (2001). Targeting an mRNA for decapping: displacement of translation factors and association of the Lsm1p-7p complex on deadenylated yeast mRNAs. Molecular cell *8*, 1075-1083.

Thermann, R., and Hentze, M.W. (2007). Drosophila miR2 induces pseudo-polysomes and inhibits translation initiation. Nature *447*, 875-878.

Thivierge, C., Makil, N., Flamand, M., Vasale, J.J., Mello, C.C., Wohlschlegel, J., Conte, D., Jr., and Duchaine, T.F. (2012). Tudor domain ERI-5 tethers an RNA-dependent RNA polymerase to DCR-1 to potentiate endo-RNAi. Nature structural & molecular biology *19*, 90-97.

Thomas, P.D., Kejariwal, A., Campbell, M.J., Mi, H., Diemer, K., Guo, N., Ladunga, I., Ulitsky-Lazareva, B., Muruganujan, A., Rabkin, S.*, et al.* (2003). PANTHER: a browsable database of gene products organized by biological function, using curated protein family and subfamily classification. Nucleic acids research *31*, 334-341.

Till, S., Lejeune, E., Thermann, R., Bortfeld, M., Hothorn, M., Enderle, D., Heinrich, C., Hentze, M.W., and Ladurner, A.G. (2007). A conserved motif in Argonaute-interacting proteins mediates functional interactions through the Argonaute PIWI domain. Nature structural & molecular biology *14*, 897-903.

Timmons, L., Court, D.L., and Fire, A. (2001). Ingestion of bacterially expressed dsRNAs can produce specific and potent genetic interference in Caenorhabditis elegans. Gene *263*, 103-112.

Tolia, N.H., and Joshua-Tor, L. (2007). Slicer and the argonautes. Nature chemical biology *3*, 36-43.

Tomari, Y., Du, T., and Zamore, P.D. (2007). Sorting of Drosophila small silencing RNAs. Cell *130*, 299-308.

Tops, B.B., Plasterk, R.H., and Ketting, R.F. (2006). The Caenorhabditis elegans Argonautes ALG-1 and ALG-2: almost identical yet different. Cold Spring Harbor symposia on quantitative biology *71*, 189-194.

Tritschler, F., Huntzinger, E., and Izaurralde, E. (2010). Role of GW182 proteins and PABPC1 in the miRNA pathway: a sense of deja vu. Nature reviews *11*, 379-384.

Tucker, M., Valencia-Sanchez, M.A., Staples, R.R., Chen, J., Denis, C.L., and Parker, R. (2001). The transcription factor associated Ccr4 and Caf1 proteins are components of the major cytoplasmic mRNA deadenylase in Saccharomyces cerevisiae. Cell *104*, 377-386.

Turoverov, K.K., Kuznetsova, I.M., and Uversky, V.N. (2010). The protein kingdom extended: ordered and intrinsically disordered proteins, their folding, supramolecular complex formation, and aggregation. Progress in biophysics and molecular biology *102*, 73-84.

Uchida, N., Hoshino, S., and Katada, T. (2004). Identification of a human cytoplasmic poly(A) nuclease complex stimulated by poly(A)-binding protein. The Journal of biological chemistry *279*, 1383-1391.

Valegard, K., Murray, J.B., Stonehouse, N.J., van den Worm, S., Stockley, P.G., and Liljas, L. (1997). The three-dimensional structures of two complexes between recombinant MS2 capsids

and RNA operator fragments reveal sequence-specific protein-RNA interactions. Journal of molecular biology *270*, 724-738.

van Dijk, E., Cougot, N., Meyer, S., Babajko, S., Wahle, E., and Seraphin, B. (2002). Human Dcp2: a catalytically active mRNA decapping enzyme located in specific cytoplasmic structures. The EMBO journal *21*, 6915-6924.

van Hoof, A., Staples, R.R., Baker, R.E., and Parker, R. (2000). Function of the ski4p (Csl4p) and Ski7p proteins in 3'-to-5' degradation of mRNA. Molecular and cellular biology *20*, 8230-8243.

Vasquez-Rifo, A., Bosse, G.D., Rondeau, E.L., Jannot, G., Dallaire, A., and Simard, M.J. (2013). A new role for the GARP complex in microRNA-mediated gene regulation. PLoS genetics *9*, e1003961.

Vasquez-Rifo, A., Jannot, G., Armisen, J., Labouesse, M., Bukhari, S.I., Rondeau, E.L., Miska, E.A., and Simard, M.J. (2012). Developmental characterization of the microRNA-specific C. elegans Argonautes alg-1 and alg-2. PloS one *7*, e33750.

Vassalli, J.D., Huarte, J., Belin, D., Gubler, P., Vassalli, A., O'Connell, M.L., Parton, L.A., Rickles, R.J., and Strickland, S. (1989). Regulated polyadenylation controls mRNA translation during meiotic maturation of mouse oocytes. Genes & development *3*, 2163-2171.

Ventura, A., Young, A.G., Winslow, M.M., Lintault, L., Meissner, A., Erkeland, S.J., Newman, J., Bronson, R.T., Crowley, D., Stone, J.R.*, et al.* (2008). Targeted deletion reveals essential and overlapping functions of the miR-17 through 92 family of miRNA clusters. Cell *132*, 875-886.

Verdel, A., Jia, S., Gerber, S., Sugiyama, T., Gygi, S., Grewal, S.I., and Moazed, D. (2004). RNAi-mediated targeting of heterochromatin by the RITS complex. Science (New York, NY *303*, 672-676.

Voronina, E., Seydoux, G., Sassone-Corsi, P., and Nagamori, I. (2011). RNA granules in germ cells. Cold Spring Harb Perspect Biol *3*.

Waghray, S., Williams, C., Coon, J.J., and Wickens, M. (2015). Xenopus CAF1 requires NOT1-mediated interaction with 4E-T to repress translation in vivo. RNA (New York, NY *21*, 1335-1345.

Wakiyama, M., Takimoto, K., Ohara, O., and Yokoyama, S. (2007). Let-7 microRNA-mediated mRNA deadenylation and translational repression in a mammalian cell-free system. Genes & development *21*, 1857-1862.

Wang, B., Love, T.M., Call, M.E., Doench, J.G., and Novina, C.D. (2006). Recapitulation of short RNA-directed translational gene silencing in vitro. Molecular cell *22*, 553-560.

Wang, J.T., Smith, J., Chen, B.C., Schmidt, H., Rasoloson, D., Paix, A., Lambrus, B.G., Calidas, D., Betzig, E., and Seydoux, G. (2014). Regulation of RNA granule dynamics by phosphorylation of serine-rich, intrinsically disordered proteins in C. elegans. eLife *3*, e04591.

Wang, Z., Jiao, X., Carr-Schmid, A., and Kiledjian, M. (2002). The hDcp2 protein is a mammalian mRNA decapping enzyme. Proceedings of the National Academy of Sciences of the United States of America *99*, 12663-12668.

Wang, Z., and Kiledjian, M. (2001). Functional link between the mammalian exosome and mRNA decapping. Cell *107*, 751-762.

Washburn, M.P., Wolters, D., and Yates, J.R., 3rd (2001). Large-scale analysis of the yeast proteome by multidimensional protein identification technology. Nature biotechnology *19*, 242-247.

Wells, S.E., Hillner, P.E., Vale, R.D., and Sachs, A.B. (1998). Circularization of mRNA by eukaryotic translation initiation factors. Molecular cell *2*, 135-140.

Wightman, B., Ha, I., and Ruvkun, G. (1993). Posttranscriptional regulation of the heterochronic gene lin-14 by lin-4 mediates temporal pattern formation in C. elegans. Cell *75*, 855-862.

Williams, R.W., and Rubin, G.M. (2002). ARGONAUTE1 is required for efficient RNA interference in Drosophila embryos. Proceedings of the National Academy of Sciences of the United States of America *99*, 6889-6894.

Wilusz, C.J., Wormington, M., and Peltz, S.W. (2001). The cap-to-tail guide to mRNA turnover. Nature reviews *2*, 237-246.

Wolters, D.A., Washburn, M.P., and Yates, J.R., 3rd (2001). An automated multidimensional protein identification technology for shotgun proteomics. Analytical chemistry *73*, 5683-5690.

Wu, C.C., and MacCoss, M.J. (2002). Shotgun proteomics: tools for the analysis of complex biological systems. Curr Opin Mol Ther *4*, 242-250.

Wu, E., and Duchaine, T.F. (2011). Cell-free microRNA-mediated translation repression in Caenorhabditis elegans. Methods in molecular biology *725*, 219-232.

Wu, E., Thivierge, C., Flamand, M., Mathonnet, G., Vashisht, A.A., Wohlschlegel, J., Fabian, M.R., Sonenberg, N., and Duchaine, T.F. (2010). Pervasive and cooperative deadenylation of 3'UTRs by embryonic microRNA families. Molecular cell *40*, 558-570.

Wu, L., and Belasco, J.G. (2005). Micro-RNA regulation of the mammalian lin-28 gene during neuronal differentiation of embryonal carcinoma cells. Molecular and cellular biology *25*, 9198-9208.

Wu, L., Fan, J., and Belasco, J.G. (2006). MicroRNAs direct rapid deadenylation of mRNA. Proceedings of the National Academy of Sciences of the United States of America *103*, 4034-4039.

Wu, P.H., Isaji, M., and Carthew, R.W. (2013). Functionally diverse microRNA effector complexes are regulated by extracellular signaling. Molecular cell *52*, 113-123.

Xu, P., Vernooy, S.Y., Guo, M., and Hay, B.A. (2003). The Drosophila microRNA Mir-14 suppresses cell death and is required for normal fat metabolism. Curr Biol *13*, 790-795.

Yamashita, A., Chang, T.C., Yamashita, Y., Zhu, W., Zhong, Z., Chen, C.Y., and Shyu, A.B. (2005). Concerted action of poly(A) nucleases and decapping enzyme in mammalian mRNA turnover. Nature structural & molecular biology *12*, 1054-1063.

Yekta, S., Shih, I.H., and Bartel, D.P. (2004). MicroRNA-directed cleavage of HOXB8 mRNA. Science (New York, NY *304*, 594-596.

Yi, R., Qin, Y., Macara, I.G., and Cullen, B.R. (2003). Exportin-5 mediates the nuclear export of pre-microRNAs and short hairpin RNAs. Genes & development *17*, 3011-3016.

Yi, X., Hong, M., Gui, B., Chen, Z., Li, L., Xie, G., Liang, J., Wang, X., and Shang, Y. (2012). RNA processing and modification protein, carbon catabolite repression 4 (Ccr4), arrests the cell cycle through p21-dependent and p53-independent pathway. The Journal of biological chemistry *287*, 21045-21057.

Yigit, E., Batista, P.J., Bei, Y., Pang, K.M., Chen, C.C., Tolia, N.H., Joshua-Tor, L., Mitani, S., Simard, M.J., and Mello, C.C. (2006). Analysis of the C. elegans Argonaute family reveals that distinct Argonautes act sequentially during RNAi. Cell *127*, 747-757.

Yu, F., Yao, H., Zhu, P., Zhang, X., Pan, Q., Gong, C., Huang, Y., Hu, X., Su, F., Lieberman, J.*, et al.* (2007). let-7 regulates self renewal and tumorigenicity of breast cancer cells. Cell *131*, 1109-1123.

Yu, J.H., Yang, W.H., Gulick, T., Bloch, K.D., and Bloch, D.B. (2005). Ge-1 is a central component of the mammalian cytoplasmic mRNA processing body. RNA (New York, NY *11*, 1795-1802.

Zaessinger, S., Busseau, I., and Simonelig, M. (2006). Oskar allows nanos mRNA translation in Drosophila embryos by preventing its deadenylation by Smaug/CCR4. Development (Cambridge, England) *133*, 4573-4583.

Zekri, L., Huntzinger, E., Heimstadt, S., and Izaurralde, E. (2009). The silencing domain of GW182 interacts with PABPC1 to promote translational repression and degradation of microRNA targets and is required for target release. Molecular and cellular biology *29*, 6220-6231.

Zeng, Y., Yi, R., and Cullen, B.R. (2005). Recognition and cleavage of primary microRNA precursors by the nuclear processing enzyme Drosha. The EMBO journal *24*, 138-148.

Zhang, F., Wang, J., Xu, J., Zhang, Z., Koppetsch, B.S., Schultz, N., Vreven, T., Meignin, C., Davis, I., Zamore, P.D.*, et al.* (2012). UAP56 couples piRNA clusters to the perinuclear transposon silencing machinery. Cell *151*, 871-884.

Zhang, L., Ding, L., Cheung, T.H., Dong, M.Q., Chen, J., Sewell, A.K., Liu, X., Yates, J.R., 3rd, and Han, M. (2007). Systematic identification of C. elegans miRISC proteins, miRNAs, and

mRNA targets by their interactions with GW182 proteins AIN-1 and AIN-2. Molecular cell *28*, 598-613.

Zhang, P., and Zhang, H. (2013). Autophagy modulates miRNA-mediated gene silencing and selectively degrades AIN-1/GW182 in C. elegans. EMBO reports *14*, 568-576.

Zhang, Z., Xu, J., Koppetsch, B.S., Wang, J., Tipping, C., Ma, S., Weng, Z., Theurkauf, W.E., and Zamore, P.D. (2011). Heterotypic piRNA Ping-Pong requires qin, a protein with both E3 ligase and Tudor domains. Molecular cell *44*, 572-584.

Zheng, D., Ezzeddine, N., Chen, C.Y., Zhu, W., He, X., and Shyu, A.B. (2008). Deadenylation is prerequisite for P-body formation and mRNA decay in mammalian cells. The Journal of cell biology *182*, 89-101.

Zhou, R., Hotta, I., Denli, A.M., Hong, P., Perrimon, N., and Hannon, G.J. (2008). Comparative analysis of argonaute-dependent small RNA pathways in Drosophila. Molecular cell *32*, 592-599.

Zinovyeva, A.Y., Bouasker, S., Simard, M.J., Hammell, C.M., and Ambros, V. (2014). Mutations in conserved residues of the C. elegans microRNA Argonaute ALG-1 identify separable functions in ALG-1 miRISC loading and target repression. PLoS genetics *10*, e1004286.

Zipprich, J.T., Bhattacharyya, S., Mathys, H., and Filipowicz, W. (2009). Importance of the C-terminal domain of the human GW182 protein TNRC6C for translational repression. RNA (New York, NY *15*, 781-793.

Zuo, Y., and Deutscher, M.P. (2001). Exoribonuclease superfamilies: structural analysis and phylogenetic distribution. Nucleic acids research *29*, 1017-1026.

Appendix 1: Supplemental information to Chapter 2

List of modifications for *C. elegans* cell-free extract preparation

Since the release of the manuscript (Chapter 2) for publication, several changes to the extract preparation have been made. I would like to acknowledge Mathieu Flamand, another user of the cell-free system in Thomas Duchaine's laboratory, in finding optimal conditions for preparing the extract and for his assistance in compiling the following list of changes and conditions:

Materials:

- The calf-liver tRNA product from Novagen has since been discontinued. We have noticed that translation activity can still be recapitulated without supplementing tRNA from any source. Thus, we have omitted tRNA from our list of supplements (Table 2-1A). As a result, the amount of water needs to be readjusted to 2.364 µl for a 1x reaction, instead of 2.114 µl (Table 2-1B).
- Stock concentrations of 8 µg/µl creatine phosphokinase can also be used.
- Luciferase activity can also be measured using Synergy™ H1 Hybrid Reader (Biotek), however, it is important to note that the luciferase counts obtained using this machine are ten-fold lower than those obtained with the GloMax 20/20 Luminometer.
- TCEP (Tris(2-carboxyethyl)phosphine hydrochloride) can substitute for DTT at a 2 mM concentration with no deleterious effect detected.

Methods:

- During harvesting, embryos can be transferred to 5 ml tubes (Eppendorf or Diamed) and flash-frozen in these tubes. This saves considerable space in the freezer.
- Optimally, the bed of Sephadex G-25 Superfine beads should sit into the narrowest region of the 10-ml Polyprep columns (below the 2-ml mark), thus limiting the scale of extract preparation. To scale up extract preparation, Glass Econo-Columns® Columns (BIO-RAD)

can also be used in order to obtain a larger bed of beads and thus migration front. Only 10x1.5 cm Glass Econo-Columns® columns have been tested.

For two particular genotypes, we were unable to obtain extracts capable of recapitulating translation (or potent translation) from each extract preparation ($n \geq 3$).

- In the transgenic strain, *qeIs6(pab-2::gfp)*, whose phenotype resembles wild-type animals, we experienced difficulties in recapitulating translation activity from several preparations of these embryonic extracts. None of the extract preparations produced any luciferase counts when assayed for translation. It is unclear why it is so. This event is rare, as we can only record one genotype from our library with this behavior. Thus, we ask users to keep in mind that cell-free extracts may not be obtained for certain genotypes. Such conclusion should only be made after several trials of extract preparation for the genotype of interest.
- For *pab-2 null (ok1851)*, extracts prepared from this strain failed to produce potent translation counts when assayed for luciferase activity. However, this extract was competent for deadenylation, suggesting that translation activity in this genetic background, or at least this extract, is not required for other silencing steps.

Appendix 2: Supplemental information to Chapter 3

Edlyn Wu, Caroline Thivierge, Mathieu Flamand, Geraldine Mathonnet, Ajay A. Vashisht, James Wohlschlegel, Marc R. Fabian, Nahum Sonenberg & Thomas F. Duchaine (**2010**). *Molecular Cell* (40): 558-570.

Name	Sequence
Starfire probes	
α-miR-35	5'-ACTGCTAGTTTCCACCCGGTGA/3StarFire/-3'
α-miR-52	5'-AGCACGGAAACATATGTACGGGTG/3StarFire/-3'
α-miR-58	5'-ATTGCCGTACTGAACGATCTCA/3StarFire/-3'
α-miR-60	5' ACTAGAAAATGTGCATAATA/3StarFire/-3'
α-miR-86	5'-GACTGTGGCAAAGCATTCACTTA/3StarFire/-3'
α-miR-87	5'ACACCTGAAACTTTGCTCAC/3StarFire/-3'
α-miR-230	5' TCTCCTGGTCGCACAACTAATAC/3StarFire/-3'
α-miR-232	5' TCACCGCAGTTAAGATGCATTTA/3StarFire/-3'
qRT-PCR	
Universal primer	5'-CATGATCAGCTGGGCCAAGA-3'
miR-35 specific primer	5'-CATGATCAGCTGGGCCAAGAACTGCTA GTT-3'
miR-35 LNA	5'-T+CACCGGGTGGAAAC-3'
2'-*O*-Me oligos	
α-miR-1	5'-UCUUCCUCCAUACUUCUUUACAUUCCAACCUU-3'
α-miR-35	5'-UUAAUACUGCUAGUUUCCACCCGGUGAUUAAU-3'
α-miR-52	5'-UUAAUAGCACGGAAACAUAUGUACGGGUGUUAAU-3'
α-miR-58	5'-UUAAUUGCCGUACUGAACGAUCUCAUUAAU-3'
α-miR-81	5'-UUAAUACUGGCUUUCACGAUGAUCUCAUUAAU-3'
hsa-miR-16	5'-UUAAUCGCCAAUAUUUACGUGCUGCUAUUAAU-3'
α-miR-86	5'-UUAAUGACUGUGGCAAAGCAUUCACUUAUUAAU-3'
α-miR-87	5'-UUAAUACACCUGAAACUUUGCUCACUUAAU-3'
miR-35 targets 3'UTR cloning	
c34h3.1 fwd	5'-ATAAACTAGTGCAATGCTTGATTCTACCACA-3'
c34h3.1 rev	5'-TATTGCGGCCGCTAATGGAATCTGTGAGCAACG-3'
hlh-11 fwd	5'-ACTAGTGCCTGACTTTTGACAAATGTAG-3'
hlh-11 rev	5'-GCGGCCGCATTGGTACTCTTGTCTCAGTGG-3'
nhl-2 fwd	5'-ATAAACTAGTGGAGGTTACCCCAATTCCTAT-3'
nhl-2 rev	5'-TATTGCGGCCGCGGGCGAGCTGAAATTCAAATT-3'
r05h11.2 fwd	5'-ATAAACTAGTATTGAATACTTATAGACCTCAAG-3'
r05h11.2 rev	5'-TATTGCGGCCGCTCTAACCGTCTGAATATTATCTG-3'
spn-4 fwd	5'-ATAAACTAGTTCAGTTCAACTGATACGCCC-3'
spn-4 rev	5'-TATTGCGGCCGCTATGGCGAAGCACTTCATTTG-3'
toh-1 fwd	5'-ACTAGTATTCATTTTCTAGTTCTTCTACTC-3'
toh-1 rev	5'-GCGGCCGCAAGACTCAAATGTTTCATTGGG-3'
y71f9b.8 fwd	5'-ATAAACTAGTATTTTCAGGCTTTCAAGCCCA-3'

y71f9b.8 rev	5’-TATTGCGGCCGCTTTATAGTTAATAAATTTATTTGATTTA-3’
Cloning	
miR-52 1X fwd	5’-CTAGAGATTTTTCCCAGCAGCGAAAATGTACGGGTGAATTCGC-3’
miR-52 1X rev	5’-GGCCGCGAATTCACCCGTACATTTTCCGTGCTGGGAAAAATCT-3’
miR-52 2X fwd	5’ CTAGA A GCA CGG AAA ATG TAC GGG TG CTCGAG A GCA CGG AAA ATG TAC GGG TG GC-3’
miR-52 2X rev	5’-GGCCGC C ACC CGT ACA TTT TCC GTG CT CTCGAG C ACC CGT ACA TTT TCC GTG CT T-3’
miR-52 3X fwd	5’-CTAGA A GCA CGG AAA ATG TAC GGG TG CTCGAG A GCA CGG AAA ATG TAC GGG TG CTCGAG A GCA CGG AAA ATG TAC GGG TG GC-3’
miR-52 3X rev	5’-GGCCGC C ACC CGT ACA TTT TCC GTG CT CTCGAG C ACC CGT ACA TTT TCC GTG CT CTCGAG C ACC CGT ACA TTT TCC GTG CT T-3’
miR-52 4X fwd	5’-AATTC A GCA CGG AAA ATG TAC GGG TG CTCGAG A GCA CGG AAA ATG TAC GGG TG CTCGAG A GCA CGG AAA ATG TAC GGG TG G-3’
miR-52 4X rev	5’-AATTC C ACC CGT ACA TTT TCC GTG CT CTCGAG C ACC CGT ACA TTT TCC GTG CT CTCGAG C ACC CGT ACA TTT TCC GTG CT G-3’
miR-35 short linker fwd	5’-ATAAGCTGCAATAAACAAGTTG-3’
miR-35 short linker rev	5’-CTA AAG GGA AGC GGC CGC-3’
miR-35 long linker fwd	5’-GCGGCCGCTTCCCTTTAG-3’
miR-35 long linker rev	5’-GCGGCCGCAATAAAGCATTTTTTTCACTGCA-3’
miR-35 1X fwd	5’-CTAGTACTGCTAGTTTCCACCCGGTGAGC-3’
miR-35 1X rev	5’-GCCCGCTCACCGGGTGGAAACTAGCAGTA-3’
miR-35 2X fwd	5’-CTAGAACTGCTAGCCACCCGGTGAG AATTCACTGCTAGCCACCCGGTGAGC-3’
miR-35 2X rev	5’-GGCCGCTCACCGGGTGGCTAGCAG TGAATTCTCACCGGGTGGCTAGCAGTT-3’
miR-35 3X fwd	5’-CTAGAACTGCTAGCCACCCGGTGATTAATACTGCTAGCCACCC GGTGATTAATACTGCTAGCCACCCGGTGAGC-3’
miR-35 3X rev	5’-GGCCGCTCACCGGGTGGCTAGCAGTATTAATCACCGGGT GGCTAGCAGTATTAATCACCGGGTGGCTAGCAGTT-3’
miR-35 4X fwd	5’-AATTGACTGCTAGCCACCCGGTGATTAATACTGCTAGCCA CCCGGTGATTAATACTGCTAGCCACCCGGTGATTAATG-3’
miR-35 4X rev	5’-AATTCATTAATCACCGGGTGGCTAGCAGTATTAATCACC GGGTGGCTAGCAGTATTAATCACCGGGTGGCTAGCAGTC-3’

Table A2-1: Primer sequences for northern analyses, qRT-PCR, translation and stability assays, and cloning

(Relates to section 3.5 Materials and Methods).

A

qRT-PCR

Fractions	Ct mean	Dilution Factor	miR-35 conc. [nM]
NF	16.33 ± 0.23	1062	**8.38 ± 1.16**
1	16.78 ± 0.23	487.5	**2.91 ± 0.40**
2	16.22 ± 0.10	808.3	**6.81 ± 0.43**
3	16.26 ± 0.23	1006	**8.31 ± 1.18**
4	16.60 ± 0.09	819.2	**5.41 ± 0.30**
5	16.42 ± 0.33	429.0	**3.23 ± 0.78**

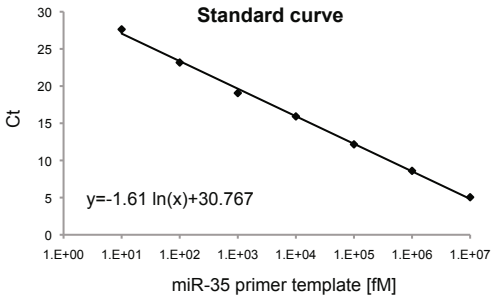

B

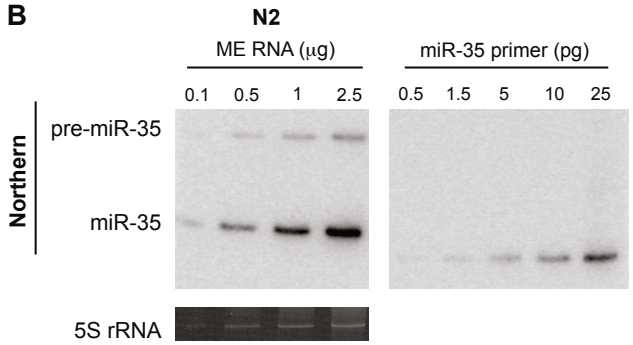

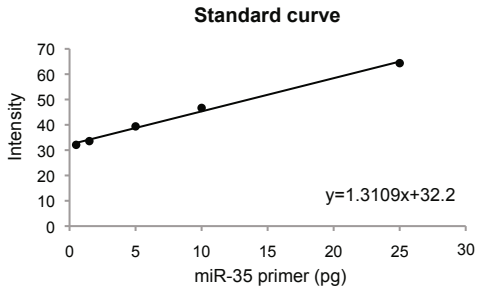

C

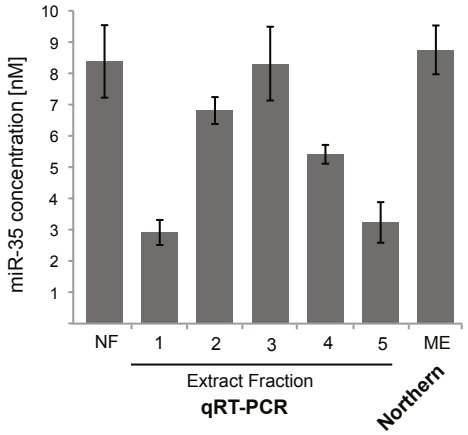

D

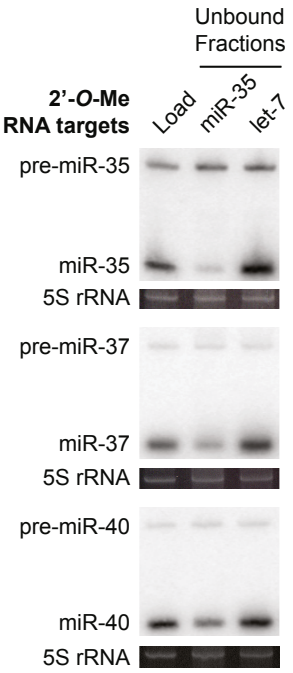

Figure A2-1: miR-35 quantification in *C. elegans* embryonic extracts and fractions

(A) miR-35 real-time (qRT)-PCR analysis. Total RNA was isolated from fractions of wild-type (N2) *C. elegans* embryonic extract not filtered (NF) or filtered fractions (1-5). A standard curve was made with different concentrations of miR-35 template primer (fM). miR-35 concentration per reaction was multiplied by the dilution factor to obtain miR-35 concentration per fraction (nM). Dilution factor: RNA concentration from the stock divided by 0.0025 (final concentration in qRT-PCR reaction). (B) miR-35 northern blot analysis. A standard curve was made with different amounts of miR-35 DNA primer (pg) to determine the concentration of miR-35 in the middle embryo (me) lysate from wild-type (N2). 5S rRNA was used as a loading control for RNA. (C) miR-35 concentration (nM) per fraction from the data obtained in (A) and (B). (D) Northern blot analysis of miR-35-42 family members on 2'-*O*-Me depletions. Extracts prepared from wild-type (N2) *C. elegans* embryos were incubated with either α-miR-35 or α-let-7 2'-*O*-Me to pull down miRISC, and unbound fractions were probed for miR-35, miR-37 and miR-41. 5S rRNA was used as a loading control. (Relates to Figure 3-1).

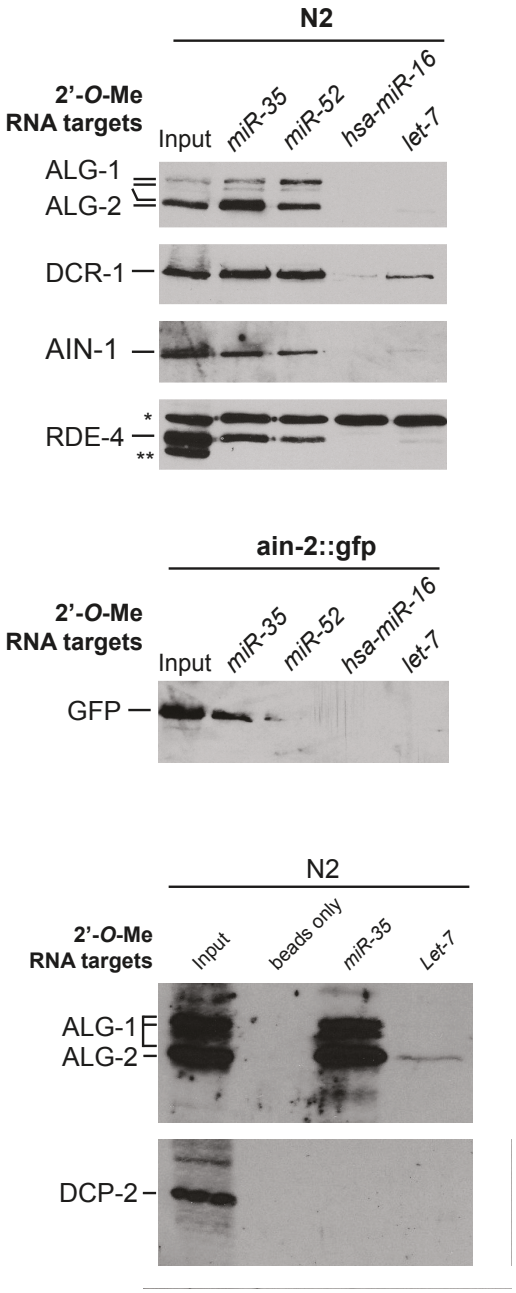
N2
2'-O-Me RNA targets
Input
miR-35
miR-52
hsa-miR-16
let-7
ALG-1
ALG-2
DCR-1
AIN-1
RDE-4
*
**
ain-2::gfp
2'-O-Me RNA targets
Input
miR-35
miR-52
hsa-miR-16
let-7
GFP
N2
2'-O-Me RNA targets
Input
beads only
miR-35
Let-7
ALG-1
ALG-2
DCP-2

Figure A2-2: Characterization of miR-35-RISC pulldown from *C. elegans* embryos

Western blot analysis on affinity-purified miRISC to confirm results obtained by MudPIT analysis. N2 embryonic extracts were incubated with 2'-*O*-Me, as indicated. Proteins were probed with polyclonal antibodies against ALG-1/2, DCR-1, AIN-1, RDE-4, and GFP. * and ** indicate non-specific bands. Bottom panel: western blot analysis of DCP-2 on affinity-purified miRISC. Wild-type embryonic extracts were incubated with either no 2'-*O*-Me (beads only), α-miR-35, or α-let-7 2'-*O*-Me. Proteins were probed with polyclonal antibodies against ALG-1/ALG-2 and DCP-2. (Relates to Table 3-1).

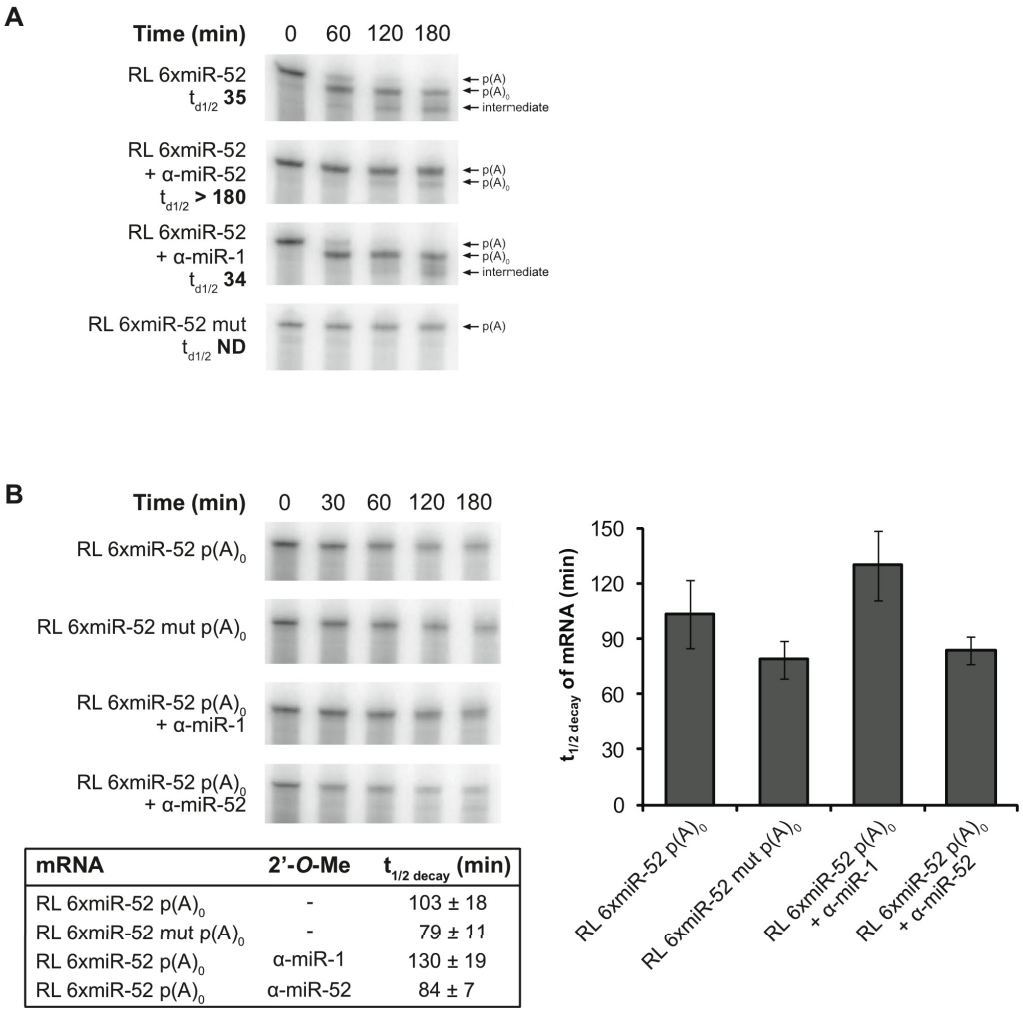

Figure A2-3: Deadenylation and decay time course of miR-52 reporters

(A) Time course of RL 6xmiR-52 deadenylation in wild-type embryos. Full-length reporters contain a poly(A) tail of 87 nucleotides. Images are representative of three independent experiments. (B) Time course of mRNA stability of RL 6xmiR-52 reporters lacking a poly(A) tail in the absence or presence of specific (α-miR-52) or non-specific (α-miR-1) 2'-*O*-Me. Images are representative of a triplicate experiment conducted in the same wild-type embryonic extract. Values represent the average from the triplicate experiment, and error bars indicate standard deviation. Quantification of the mRNA half-deadenylation time ($t_{d1/2}$) and half-life ($t_{1/2\ decay}$) was obtained using ImageJ. (Relates to Figure 3-3).

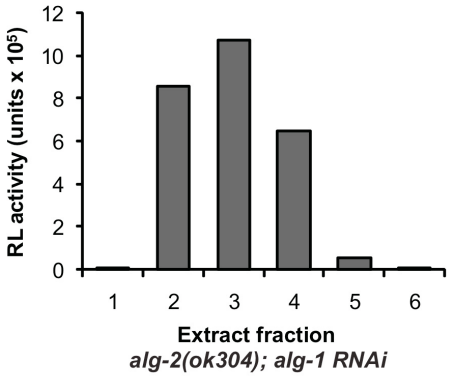

Figure A2-4: Translation of RL in *C. elegans* embryos prepared from *alg-2(ok304); alg-1 RNAi*

Luciferase activity from each fraction was measured following 3-hours translation incubation. (Relates to Figure 3-4).

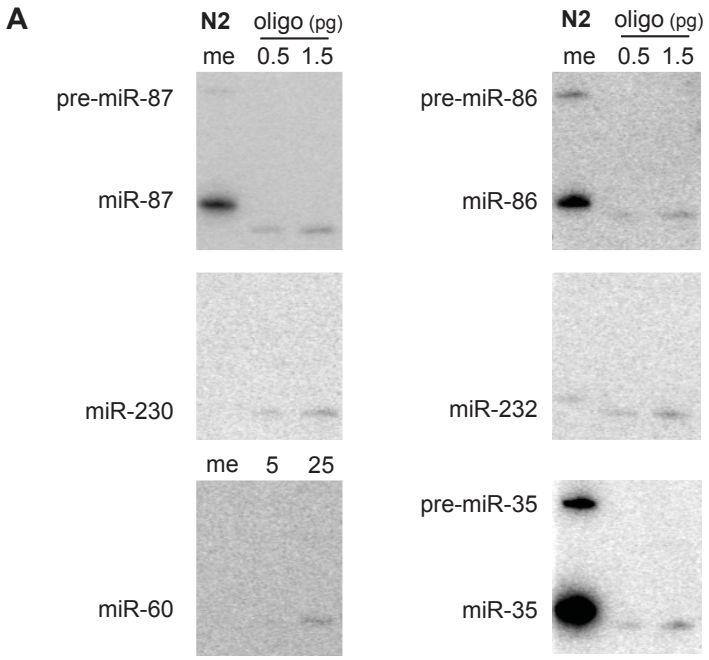
A
N2
oligo (pg)
me
0.5
1.5
pre-miR-87
miR-87
pre-miR-86
miR-86
miR-230
miR-232
me
5
25
miR-60
pre-miR-35
miR-35

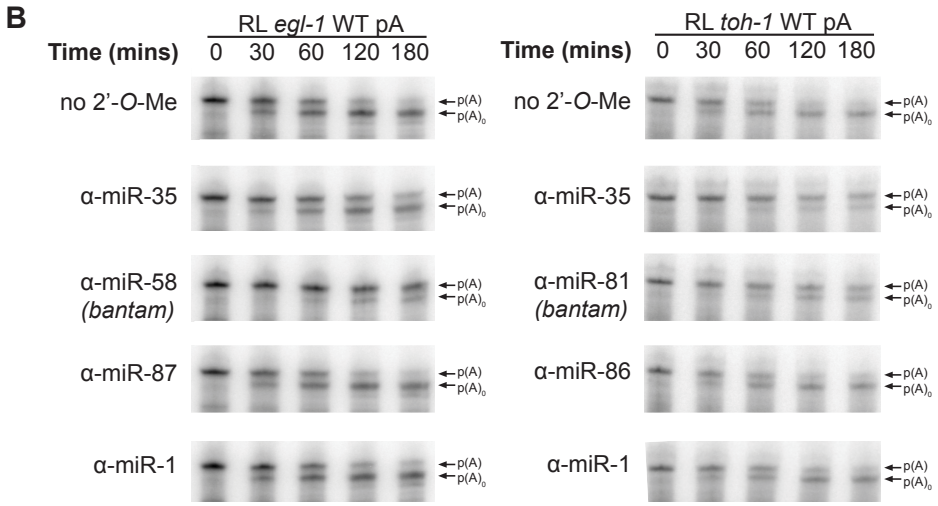
B
RL egl-1 WT pA
RL toh-1 WT pA
Time (mins)
0
30
60
120
180
no 2'-O-Me
α-miR-35
α-miR-58
(bantam)
α-miR-81
(bantam)
α-miR-87
α-miR-86
α-miR-1
p(A)
p(A)0

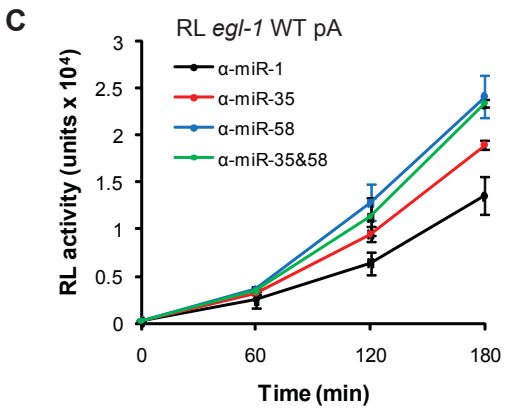
C
RL egl-1 WT pA
α-miR-1
α-miR-35
α-miR-58
α-miR-35&58
RL activity (units x 10⁴)
3
2.5
2
1.5
1
0.5
0
0
60
120
180
Time (min)

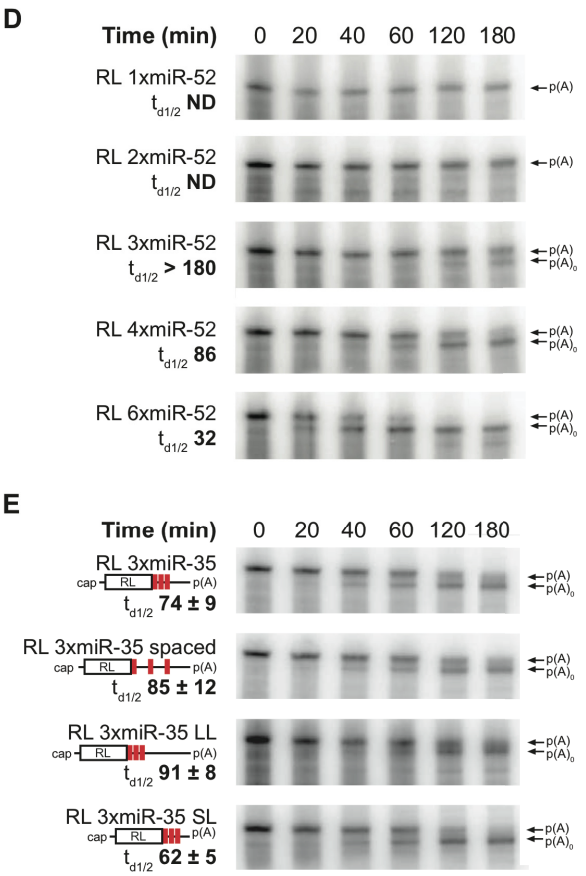

Figure A2-5: miRISC cooperation is required to potentiate miRNA target deadenylation

(A) Northern blot analysis of candidate miRNAs affecting the 3'UTR of *egl-1* and *toh-1* mRNAs. RNA was prepared from wild-type (N2) mid-development embryo (me). Primers complementary to the probe (0.5 and 1.5 pg or 5 and 25 pg in the case of miR-60) were used as positive controls. (B) Time course of RL *egl-1* 3'UTR and RL *toh-1* 3'UTR deadenylation in N2 embryo extract. Reporter mRNAs were incubated in the presence or absence of 50 nM of α-miR-35, α-miR-58, α-miR-81, α-miR-86 and α-miR-87 or the negative control α-miR-1. (C) Time course of RL *egl-1* 3'UTR translation in N2 embryo extract. The reporter mRNA was incubated with 50 nM of 2'-*O*-Me, as indicated. α-miR-1 served as a negative control. Values represent averages from a triplicate experiment conducted in the same extract, and error bars indicate standard deviation. (D) Time course of RL reporter mRNAs deadenylation fused to various copies of miR-52 binding

sites (1x-6x). (E) Time course of RL 3xmiR-35 reporter mRNAs deadenylation. For all the 3xmiR-35 reporters, miR-35 binding sites were separated by five nucleotides, with the exception of RL 3xmiR-35 spaced, in which the miR-35 binding sites are separated by 50 nucleotides. The size of the linker (sequence between the miR-35 sites and the poly(A) tail) are as follows: 161 nts (RL 3xmiR-35 and RL 3xmiR-35 spaced), 261 nts (RL 3xmiR-35 LL), and 32 nts (RL 3xmiR-35 SL). Images in D and E are representative of three independent experiments. Values for time of half-deadenylation ($t_{d1/2}$) were obtained by measuring the intensity of the bands using ImageJ. (Relates to Figure 3-5).

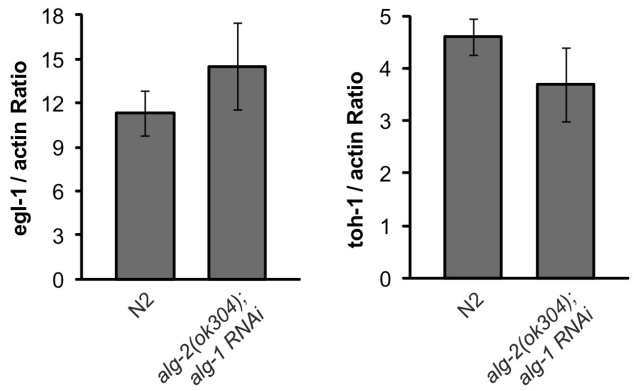

Figure A2-6: qRT-PCR analysis of the expression levels of *egl-1* and *toh-1* mRNA.

Total RNA from embryonic preparations was isolated from wild-type (N2) and *alg-2(ok304); alg-1 RNAi*. *egl-1* and *toh-1* mRNA levels were normalized against actin mRNA. qRT-PCR results are presented as the mean from triplicate independent preparations and error bars represent standard deviation. (Relates to a point in section 3.4 Discussion).

Supplemental Materials and Methods

Construction of reporters

To generate RL reporters containing miR-35 sites, annealed primers were inserted into XbaI-NotI sites of pCI neo RL p(A). miR-35 targets 3'UTR: 3'UTR sequences were amplified by PCR from genomic DNA or cDNA isolated from *C. elegans* embryos using primers listed in Table A2-1 and cloned into XbaI/NotI in pCI neo truncated RL, in which the RL cds region between NheI and BsaBI (position 1-764) was removed. For c34h3.1 3'UTR reporter, RL cDNA contained only region 491-936. The sequences of 6xmiR-35 mutant, 6xmiR-52, 6xmiR-52 mutant, egl-1 3'UTR (wild-type, miR-35 mutant, bantam mutant, miR-35 + bantam mutant), and toh-1 3'UTR (miR-35 mutant, bantam mutant, miR-35 and bantam mutant) were purchased from IDT, as pIDTSMART-KAN clones and were subcloned into pCI neo RL in XbaI-NotI sites.

Embryonic extract preparation

C. elegans embryonic pellets were homogenized in hypotonic buffer [10 mM HEPES-KOH pH 7.4, 15 mM KCl, 1.8 mM $Mg(OAc)_2$, 2 mM DTT] with a pre- chilled Kontes dounce homogenizer. The extract was then centrifuged twice at 13,200 rpm for 10 minutes at 4°C. The supernatant was loaded onto a Column-Prep (BioRad) stacked with Sephadex G-25 Superfine beads (volume of beads was four-times the volume of the supernatant, Amersham Bioscience) and pushed into the matrix with 1 supernatant volume of isotonic buffer (30 mM HEPES-KOH pH 7.4, 100 mM KOAc, 1.8 mM $Mg(OAc)_2$, 2 mM DTT). Multiple elutions (5-7) were gathered and protein concentrations were determined by Bradford. The average concentration of active fractions ranged from 10-30 mg/mL.

In vitro translation assays

Reactions were typically set up as follows: each 12.5 µl reaction contained 5 µl embryonic extract, 0.1 mM spermidine, 60 uM amino acids, 36 mM HEPES-KOH (pH 7.4), 2 mM $Mg(OAc)_2$, 65 mM KOAc, 0.1 µg/µl calf liver tRNA, 0.096 U/µl RiboLock RNase Inhibitor (Fermentas), 16.8 mM creatine phosphate, 81.6 ng/µl creatine phosphokinase, 0.8 mM ATP, and 0.2 mM GTP). Reactions were incubated with mRNA (1 nM final) at 17°C for 0 to 3 hours, as indicated. Luciferase activities were analyzed with the Dual-Luciferase® Reporter Assay System (Promega). To assay for miRNA activity, reactions were pre-incubated with 50 nM (except where indicated) 2'-*O*-Me oligonucleotides (Dharmacon) prior to mRNA addition for 30 minutes at 17°C. The 2'-*O*-Me miRNA inhibitors were designed as antisense oligonucleotides to the mature miRNAs according to Wormbase registry (www.wormbase.org).

Appendix 3: Supplemental information to Chapter 4

Edlyn Wu, Ajay A. Vashisht, Clément Chapat, Mathieu Flamand, Emiliano Cohen, Mihail Sarov, Yuval Tabach, Nahum Sonenberg, James Wohlschlegel & Thomas F. Duchaine.

Manuscript in preparation

Sequence ID	Protein	# datasets detected	Coverage (peptide counts)	Homology/Domain	Description
T07D3.7	ALG-2 (*)	6/6	68% (72)	AGO1	miRISC
F48F7.1	ALG-1 (*)	6/6	63% (76)	AGO1	miRISC
C06G1.4	AIN-1 (*)	6/6	53% (37)	TNRC6, GW182	miRISC
W02D3.11	HRPF-1	6/6	31% (12)	hnRNP F/H	splicing
Y116A8C.35	UAF-2	6/6	23% (5)	U2AF35, RRM	splicing
R10E4.2	SUP-26	6/6	22% (7)	RRM	sex determination
ZC518.3	CCR-4	6/6	19% (6)	Ccr4/CNOT6 and CNOT6L	CCR4-NOT subunit
K07C11.2	AIR-1	6/6	18% (4)	Aurora-A S/T kinase family	spindle assembly
B0513.1	LIN-66	6/6	17% (6)	unknown	translational regulation
Y22F5A.4	LYS-1	6/6	17% (4)	glycoside hydrolase	carbohydrate metabolism
Y95B8A.8	Y95B8A.8	6/6	16% (8)	ZFR, ZFR2	nucleic acid binding
K08F4.2	GTBP-1	6/6	16% (6)	G3BP2, GTPase	DNA repair
Y23H5A.3	Y23H5A.3	6/6	16% (4)	none detected	cell division
Y48C3A.14	Y48C3A.14	6/6	15% (7)	TOP3B	DNA topoisomerase
B0041.2	AIN-2	6/6	15% (6)	TNRC6, GW182	miRISC
T28D6.6	T28D6.6	6/6	15% (4)	DRG1	GTP binding
Y48B6A.3	XRN-2	6/6	13% (7)	XRN2	5'-3' exoribonuclease
Y44E3A.6	Y44E3A.6	6/6	13% (7)	EDC4	decapping activator
Y50D4C.3	Y50D4C.3	6/6	13% (5)	Tdrd3	RNA binding
F52B5.3	F52B5.3	6/6	13% (12)	DEAH helicase, SpindleE	RNA processing
D2005.5	DRH-3	6/6	12% (8)	DEAH/D-box helicase	germline RNAi
C05E4.9	ICL-1	6/6	12% (8)	malate synthase	TCA
C07G1.5	HGRS-1	6/6	12% (6)	Vps27p, FYVE Zn finger	endocytosis
C17G10.9	EIF3.L	6/6	11% (4)	EIF3L	translation initiation
T07D4.3	RHA-1	6/6	10% (8)	DEAD box helicase	RNAi
F10C2.4	F10C2.4	6/6	10% (7)	DNA polymerase subunit A	DNA replication
F26F4.7	NHL-2	6/6	10% (6)	TRIM-NHL	miRISC component
T09E8.2	HIM-17	6/6	10% (5)	coiled coil domain	DNA recombination
F43G6.9	PATR-1	6/6	10% (5)	PAT1	mRNA decay
F29C4.7	GRLD-1	6/6	10% (4)	RBM15, Nito	uncharacterized
F57B9.2	NTL-1	6/6	10% (16)	CNOT1	CCR4-NOT subunit
F52G3.1	F52G3.1	6/6	9% (6)	proline-rich, coiled coil	uncharacterized
F31E3.4	PANL-2	6/6	9% (6)	PAN2	PAN2 exonuclease
Y53C12B.3	NOS-3	6/6	8% (4)	Nanos	germline development
Y113G7A.3	SEC-23	6/6	8% (4)	Sec23p	COPII component
K12H4.8	DCR-1	6/6	7% (7)	DCR1	RNAi, endoribonuclease
T20F5.6	T20F5.6	6/6	7% (4)	RNF208, RNF183	Zn ion binding
Y38C9A.2	CGP-1	6/6	7% (3)	GTPBP1	GTPase activity
Y113G7B.18	MDT-17	6/6	7% (3)	MED17	RNA pol II cofactor
F48F7.4	PQN-39	6/6	7% (3)	Q/N-rich domain	rRNA synthesis
C12D8.1	C12D8.1	6/6	7% (2)	KH domain, RNA-binding	uncharacterized
C05C10.2	C05C10.2	6/6	6% (6)	IGHMBP2	helicase
F54D8.6	F54D8.6	6/6	6% (3)	unknown	uncharacterized
Y54E2A.4	Y54E2A.4	6/6	5% (7)	ASCC3	protein translocation
D2030.2	D2030.2	6/6	5% (3)	CLPX	ATP binding activity
C14B9.4	PLK-1	6/6	5% (3)	Polo, CDC5	meiosis
ZC518.2	SEC-24.2	6/6	5% (3)	SEC24A/B	zinc-ion binding activity
R10E11.1	CBP-1	6/6	4% (5)	CBP, p300	chromatin remodeling
C01G8.9	LET-526	6/6	4% (4)	SWI/SNF	SWI/SNF component
C47D12.1	TRR-1	6/6	2% (5)	TRAAP family	let-60/Ras signaling
Y77E11A.13	NPP-20	5/6	20% (3)	SEC13	NPC component
Y73B6BL.33	HRPF-2	5/6	19% (7)	HNRNPH	nucleic acid binding activity
ZK418.9	ZK418.9	5/6	19% (7)	KH domain, RNA-binding	uncharacterized

EEED8.1	MEL-47	5/6	19% (4)	SLIRP	embryonic development
Y56A3A.20	CCF-1	5/6	18% (4)	Caf1/CNOT7	CCR4-NOT subunit
C34G6.7	STAM-1	5/6	16% (4)	Q/N-rich domain, SH3	protein transport
W01B11.3	NOL-5	5/6	15% (5)	NOP58	nucleolar RNP
W02B12.3	RSP-1	5/6	15% (4)	SRp75	splicing
C18D11.4	RSP-8	5/6	15% (4)	Tra2beta splicing activator	splicing
DNJ-13	DNJ-13	5/6	13% (3)	DnaJ domain	stress response
F31E3.3	RFC-4	5/6	13% (3)	RFC4	DNA replication
B0511.10	EIF3.E	5/6	12% (4)	EIF3E	translation initiation
Y6D1A.1	Y6D1A.1	5/6	12% (4)	none detected	uncharacterized
F53A2.6	IFE-1	5/6	12% (3)	eIF4E	cap-binding protein
E01A2.2	E01A2.2	5/6	11% (5)	SRRT	cap binding complex
Y46G5A.13	TIAR-2	5/6	11% (3)	TIAL-1, TIA-1	stress granule
Y34D9A.10	VPS-4	5/6	11% (3)	VPS4B, VPS4A	vacuolar protein sorting
T25G12.5	ACDH-7	5/6	10% (3)	ACADM	acyl-CoA dehydrogenase
F22G12.4	F22G12.4	5/6	9% (6)	AHKFY1	metal-ion binding activity
C18E9.3	SZY-20	5/6	8% (3)	coiled coil domain	chromosome segregation
F31D4.3	FKB-6	5/6	8% (2)	TPR repeat	protein folding
K07H8.10	K07H8.10	5/6	7% (5)	coiled coil domain	uncharacterized
T20B5.1	APA-2	5/6	7% (4)	AP2	endocytosis
C23G10.8	C23G10.8	5/6	7% (4)	none detected	apoptosis
F16D3.2	RSD-6	5/6	7% (4)	Tdrd5/10/TDRKH	uncharacterized
R05D3.7	UNC-116	5/6	7% (4)	kinesin-1 heavy chain	intracellular transport
C36E6.1	C36E6.1	5/6	7% (3)	coiled coil, KH domains	splicing
F56F3.1	IFET-1	5/6	7% (3)	eIF4E Transporter	translation repressor
T01B7.6	TRCS-2	5/6	7% (3)	unknown	uncharacterized
Y77E11A.7	Y77E11A.7	5/6	7% (3)	none detected	development and reproduction
F44B9.8	F44B9.8	5/6	7% (2)	RFC5	DNA replication factor
D2045.1	ATX-2	5/6	6% (4)	ataxin-2	early embryo patterning
Y39A1A.15	CNT-2	5/6	6% (3)	Arf GAP	asymmetric cell division
R74.8	R74.8	5/6	6% (2)	none detected	uncharacterized
M106.1	MIX-1	5/6	5% (4)	SMC2	chromosome segregation
H04J21.3	GIP-1	5/6	5% (3)	Spc98p	mitotic spindle organization
C01B10.8	C01B10.8	5/6	5% (2)	METTL13	methyltransferase
ZK381.4	PGL-1	5/6	5% (2)	RGG box motif	P granule component
T14G8.1	CHD-3	5/6	4% (4)	SNF2,chromodomain	chromatin remodeling
K10D2.3	CID-1	5/6	4% (3)	ZCCHC6/1	poly(U) polymerase
R04A9.2	NRDE-3	5/6	4% (3)	Argonaute	nuclear RNAi
C18H9.3	C18H9.3	5/6	4% (2)	GIGYF1/2	GYF domain-containing protein
Y67D8C.5	EEL-1	5/6	2% (4)	Mule	early embryo development
C49G7.11	DJR-1.2	4/6	37% (5)	DJ-1	glyoxals detoxification
C56C10.3	VPS-32.1	4/6	26% (3)	CHMP4	endosome trafficking
Y74C10AR.1	EIF-3.i	4/6	20% (5)	EIF3I	translation initiation
Y37E11AL.7	MAP-1	4/6	19% (3)	METAP1	metalloexopeptidase
W08E3.2	W08E3.2	4/6	18% (6)	CASC3	RNA binding
F02E9.2	LIN-28	4/6	17% (3)	CCHC-Zn finger	developmental timing
T26E3.3	PAR-6	4/6	17% (3)	PDZ domain	embryo polarity
R04A9.4	IFE-2	4/6	16% (3)	eIF-4E	translation initiation
C35E7.5	C35E7.5	4/6	16% (11)	none detected	uncharacterized
R11D1.8	RPL-28	4/6	15% (2)	RPL28	translation
C44B7.2	C44B7.2	4/6	14% (4)	HNRNPL	RNA binding
T04D3.2	SDZ-30	4/6	13% (7)	coiled coil domain	development and reproduction
M01E5.6	SEPA-1	4/6	13% (7)	KIX domain	autophagy
K10C3.6	NHR-49	4/6	13% (5)	HNF4 family of NHR	fat metabolism, lifespan
W02D9.1	PRI-2	4/6	13% (3)	DNA polymerase subunit C	DNA replication
AH6.5	MEX-6	4/6	12% (4)	CCCH Zn finger	embryo polarity

Y55F3AM.12	DCAP-1	4/6	12% (3)	Dcp1	mRNA decapping
H28G03.1	H28G03.1	4/6	12% (3)	RNA-binding	uncharacterized
R11H6.5	R11H6.5	4/6	12% (3)	ILF2	lipid storage
C46A5.9	HCF-1	4/6	11% (6)	HCF-1	transcription regulation
Y55F3AM.6	Y55F3AM.6	4/6	11% (3)	MKRN1/2/3	Zn ion binding
T06A10.1	MEL-46	4/6	10% (7)	DDX20	endocytosis
C35E7.3	C35E7.3	4/6	10% (4)	none detected	uncharacterized
T23G7.1	DPL-1	4/6	10% (4)	DP	transcription regulation
Y48G8AL.5	Y48G8AL.5	4/6	10% (4)	NSUN2	tRNA methyltransferase
W05G11.6	PCK-1	4/6	9% (4)	PEPCK	gluconeogenesis
K08E3.5	K08E3.5	4/6	9% (3)	UGP2	glucose metabolism
Y47D3A.16	RSKS-1	4/6	9% (3)	RPS6KB1/2	protein synthesis
F41E6.6	TAG-196	4/6	9% (3)	CTSF	endopeptidase
C01G10.8	C01G10.8	4/6	9% (2)	AHSA1	ATPase
W08D2.7	MTR-4	4/6	8% (6)	Mtr4p	TRAMP complex
Y56A3A.1	NTL-3	4/6	8% (4)	CNOT3	CCR4-NOT component
Y65B4BL.2	DEPS-1	4/6	8% (3)	none detected	P granule component
C17H12.1	DYCI-1	4/6	8% (3)	coiled coil, WD repeat	embryo development
F44E7.4	F44E7.4	4/6	7% (4)	IDE	metal ion binding
B0336.3	B0336.3	4/6	7% (3)	RBM26/27	metal ion binding
D1081.8	CDC-5L	4/6	7% (3)	CDC5L	DNA repair
T12F5.5	LARP-5	4/6	7% (3)	La-related protein	RNA-binding
W02D3.9	UNC-37	4/6	7% (3)	Groucho, WD-repeat	neuronal fate specification
T22H6.2	ALH-13	4/6	6% (3)	ALDH18A1	glutamate dehydrogenase
T19B4.2	NPP-7	4/6	6% (3)	NUP153	nuclear pore complex
Y40B1B.6	SPR-5	4/6	6% (3)	LSD1	chromatin remodeling
F27D4.4	F27D4.4	4/6	6% (2)	ZC3H15	metal ion binding
Y47D3A.29	Y47D3A.29	4/6	5% (5)	DNA polymerase alpha	DNA replication
Y71H2B.10	APB-1	4/6	5% (4)	AP1	protein transport
F16B12.6	F16B12.6	4/6	5% (4)	uncharacterized	reproduction
R05D3.4	RFP-1	4/6	5% (4)	RNF20, RNF40	ubiquitin-protein ligase
T12E12.4	DRP-1	4/6	5% (3)	DRP1	dynamin-related protein
D1007.7	NRD-1	4/6	5% (3)	SCAF8, SCAF4	vulval development
R02D3.4	R02D3.4	4/6	5% (3)	ASUN	uncharacterized
Y56A3A.27	TOP-3	4/6	5% (3)	DNA topoisomerase	DNA recombination
Y51A2D.7	Y51A2D.7	4/6	5% (3)	INTS5	embryo development
Y57A10A.13	Y57A10A.13	4/6	5% (3)	3’-5' exonuclease	uncharacterized
C18G1.4	PGL-3	4/6	5% (2)	coiled coil domain	P granule component
Y39G8C.1	XRN-1	4/6	4% (4)	Xrn1	5'-3’ exonuclease
C34B2.6	C34B2.6	4/6	4% (3)	Lon domain	protease
D2045.6	CUL-1	4/6	4% (3)	CUL1	G1-S transition
D1081.7	D1081.7	4/6	4% (2)	none detected	reproduction
F37A4.8	ISW-1	4/6	3% (3)	ISWI	chromatin remodeling
F44B9.6	LIN-36	4/6	3% (2)	THAP-type Zn finger	larval development
H39E23.1	PAR-1	4/6	3% (2)	kinase domain	embryo polarity
Y71F9AL.18	PARP-1	4/6	3% (2)	PARP1	DNA repair
C23F12.1	FLN-2	4/6	2% (3)	unknown	locomotion
Y71F9B.4	SNR-7	3/6	53% (3)	snRNP-G	splicing
R07E5.14	RNP-4	3/6	50% (4)	Tsunagi	exon-exon junction complex
F43E2.2	RPB-4	3/6	36% (4)	POLR2D	DNA polymerase
ZK593.7	LSM-7	3/6	28% (2)	LSM7	RNA processing
F32A5.7	LSM-4	3/6	23% (2)	LSM4	RNA processing
T16G1.11	EIF-3.K	3/6	22% (4)	EIF3K	translation initiation
K07C11.1	PAX-1	3/6	21% (4)	PAX1/9	transcription regulation
C07A9.2	C07A9.2	3/6	20% (2)	BUD31	DNA repair
C41D11.2	EIF-3.H	3/6	18% (4)	EIF3H	translation initiation

Y75B8A.30	PPH-4.1	3/6	18% (4)	PPP4C	mitotic spindle organization
C18A3.5	TIAR-1	3/6	18% (4)	TIA1	stress granule component
F25B5.7	NONO-1	3/6	17% (5)	NONO	transcription regulation
F23H11.1	BRA-2	3/6	17% (3)	BRAM1	TGF-beta signaling
R09B3.5	MAG-1	3/6	17% (3)	MAGOH	Poly(A) RNA binding
H20J04.8	MOG-2	3/6	17% (3)	U2 snRNP	splicing
F43G9.5	CFIM-1	3/6	17% (2)	NUDIX hydrolase	mRNA polyadenylation
Y39A1A.3	Y39A1A.3	3/6	17% (2)	SSSCA1	uncharacterized
Y39A3CR.1	SMI-1	3/6	16% (3)	Gemin2	snRNP assembly
F13D12.2	LDH-1	3/6	15% (4)	LDHB	lactate dehydrogenase
D2013.7	EIF-3.F	3/6	15% (2)	EIF3F	translation initiation
F08G12.2	F08G12.2	3/6	13% (3)	SNRNP40	splicing
Y54G9A.6	BUB-3	3/6	12% (3)	BUB3	mitotic checkpoint
K10B3.8	GPD-2	3/6	11% (3)	GAPDH	glycolysis
K10B3.7	GPD-3	3/6	11% (3)	GAPDH	glycolysis
Y48G1A.3	DAF-25	3/6	11% (2)	Ankmy2, MYND domain	osmotic stress
T12G3.2	T12G3.2	3/6	10% (6)	coiled coil domain	uncharacterized
F18E2.2	ABCF-1	3/6	10% (3)	ABCF1	ATP binding
Y54G11A.6	CTL-1	3/6	10% (2)	catalase	oxidative stress
F35G12.2	IDHG-1	3/6	10% (2)	isocitrate dehydrogenase	tricarboxylic acid cycle
K04F10.7	K04F10.7	3/6	10% (2)	FAM76A/B family	splicing
C26E6.3	NTL-9	3/6	10% (2)	RQCD1	CCR4-NOT component
C33H5.7	SWD-2.2	3/6	10% (2)	WDR82	development and reproduction
T09B4.5a	T09B4.5	3/6	10% (2)	transmembrane helix	unknown
H28G03.2	H28G03.2	3/6	9% (4)	CPSF7	cleavage and polyadenylation
Y105E8A.17	EKL-4	3/6	9% (3)	DMAP1	endocytosis
F18A1.2	LIN-26	3/6	9% (2)	C2H2 Zn finger	cell differentiation
T01G1.3	SEC-31	3/6	8% (5)	SEC31	development and reproduction
T05F1.2	T05F1.2	3/6	8% (4)	none detected	uncharacterized
D1046.1	CFIM-2	3/6	8% (3)	CPSF6/7	cleavage and polyadenylation
Y73F8A.25a	NTL-11	3/6	8% (3)	CNOT11	CCR4-NOT component
F54D8.3	ALH-1	3/6	8% (2)	ALDH2	aldehyde dehydrogenase
B0261.7	B0261.7	3/6	8% (2)	none detected	uncharacterized
C14B9.8	C14B9.8	3/6	7% (4)	PHKA2	glycogen metabolism
R06C7.1	WAGO-1	3/6	7% (4)	AGO1	RNAi
C37C3.2	C37C3.2	3/6	7% (3)	eIF5	translation initiation
F19F10.12	F19F10.12	3/6	7% (3)	INTS9	snRNA processing
F26A1.13	F26A1.13	3/6	7% (3)	NEDD4-binding, coiled coil	uncharacterized
ZK863.4	USIP-1	3/6	7% (3)	TUT1	terminal uridylyl transferase
K02B12.7	K02B12.7	3/6	7% (2)	ARFGAP1	GTPase
W09C5.2	UNC-59	3/6	6% (2)	Septin	locomotion
T23B5.1a	PRMT-3	3/6	5% (3)	PRMT9	methyltransferase
Y59A8B.6	PRP-6	3/6	5% (3)	PRPF6	pre-mRNA processing
F58G1.1	WAGO-4	3/6	5% (3)	AGO1	RNAi
Y92H12A.4	Y92H12A.4	3/6	5% (3)	INTS3	reproduction
ZK520.4	CUL-2	3/6	5% (2)	E3 ubiquitin ligase	ubiquitination
F56D2.6	DDX-15	3/6	5% (2)	DEAD box helicase, DDX15	RNA processing
R06C7.7	LIN-61	3/6	5% (2)	MBT repeat	genome stability
F09E5.1	PKC-3	3/6	5% (2)	kinase domain	embryonic AP axis
Y50D7A.2	XPD-1	3/6	5% (2)	ERCC2	transcription factor
Y69A2AR.1	Y69A2AR.1	3/6	5% (2)	none detected	uncharacterized
Y23H5A.7	CARS-1	3/6	4% (3)	CysRS	tRNA synthetase
B0379.3	MUT-16	3/6	4% (3)	Q/N-rich domain	RNAi
F56A3.4	SPD-5	3/6	4% (3)	coiled coil domain	cell division
K02F2.3	TEG-4	3/6	4% (3)	SAP130	splicing

F12F6.6	SEC-24.1	3/6	4% (2)	Sec24	COPII complex component
C47D12.6	TARS-1	3/6	4% (2)	TARS	tRNA ligase
Y57G11C.9	Y57G11C.9	3/6	4% (2)	coiled coil domain	nucleic acid binding
Y111B2A.22	SSL-1	3/6	3% (5)	Q/N-rich domain	chromatin remodeling
T16G12.5	EKL-6	3/6	3% (3)	TANGO6	uncharacterized
R05D3.11	MET-2	3/6	3% (3)	SET family	histone methyltransferase
T12D8.1	SET-16	3/6	3% (3)	SET family	H3K methyltransferase
F08B4.1	DIC-1	3/6	3% (2)	DDX26	Integrator complex component
ZK1053.4	ZK1053.4	3/6	3% (2)	coiled-coil domain	SEPA-1 family, autophagy
F22B5.7	ZYG-9	3/6	3% (2)	HEAT repeat	microtubule organization
R11A8.7	R11A8.7	3/6	2% (3)	Q/N-rich domain	uncharacterized
R09E10.7	EBAX-1	3/6	2% (2)	BC-box	axon guidance
T13F2.3	PIS-1	3/6	2% (2)	Pax-interacting domain	uncharacterized
F44E2.8	F44E2.8	2/6	37% (5)	none detected	uncharacterized
M28.5	M28.5	2/6	31% (3)	NHP2L1	involved in reproduction
Y51F10.2	Y51F10.2	2/6	26% (6)	ring finger protein	Zn ion binding
C33H5.12	RSP-6	2/6	24% (2)	SFRS3/SRp20	splicing
Y82E9BR.15	ELC-1	2/6	23% (2)	elongin C	proteolysis of germ plasm components
C11D2.7	C11D2.7	2/6	18% (2)	MCTS1	RNA binding
K11H3.3	K11H3.3	2/6	17% (3)	SLC25A1	transport
C07D10.5	C07D10.5	2/6	16% (4)	coiled coil domain	uncharacterized
C25H3.9	C25H3.9	2/6	15% (2)	NDUFB5/SGDH	ubiquinone complex
F52B5.2	F52B5.2	2/6	14% (3)	kinase domain	locomotion
F08B4.5	POLE-2	2/6	14% (3)	POL2	DNA replication
Y110A2AL.13	PINN-1	2/6	14% (2)	PIN1	isomerase
ZC404.8	SPN-4	2/6	14% (2)	RNA-binding	translational regulator
T17E9.2	NMT-1	2/6	13% (4)	N-myristoyl transferase	development, locomotion, apoptosis
F46E10.10	MDH-1	2/6	13% (2)	malate dehydrogenase	carbohydrate metabolism
T21G5.3	GLH-1	2/6	12% (7)	Vasa	P granule component
C49H3.5	NTL-4	2/6	12% (5)	CNOT4, RING finger, RRM	CCR4-NOT component
C44B12.5	PERM-4	2/6	12% (3)	none detected	uncharacterized
T25F10.6	CLIK-1	2/6	12% (2)	CNN1/3, TAGLN	Calponon-like protein
Y66H1A.4	Y66H1A.4	2/6	12% (2)	GAR1	endocytosis
F49H12.1	LSY-2	2/6	11% (4)	C2H2-type Zn finger	transcription factor
C27A12.8	ARI-1	2/6	11% (3)	ARIH1, Zn finger	ubiquitination
C18C4.10	KLC-2	2/6	10% (3)	TPR, coiled coil domains	kinesin light chain
Y37D8A.9	MRG-1	2/6	10% (2)	MRG15, chromodomain	transcription regulation
B0286.4	NTL-2	2/6	10% (2)	CNOT2	CCR4-NOT component
Y49E10.14	PIE-1	2/6	10% (2)	CCCH Zn finger	germ cell fate determination
F12F6.1	F12F6.1	2/6	9% (5)	coiled coil domain	uncharacterized
F58A4.4	PRI-1	2/6	9% (3)	DNA polymerase subunit D	DNA polymerase
C39E9.13	RFC-3	2/6	9% (3)	RFC3	DNA replication
R10H10.1	DIV-1	2/6	9% (2)	DNA polymerase subunit B	DNA replication
W02A2.7	MEX-5	2/6	9% (2)	CCCH Zn finger	embryonic polarity
R05F9.6	R05F9.6	2/6	9% (2)	PGM1/5	phosphotransferase
Y40B1A.4	SPTF-3	2/6	9% (2)	C2H2 Zn finger	transcription factor
F08C6.4	STO-1	2/6	9% (2)	NPHS2	membrane protein
F53C11.8	SWAN-1	2/6	9% (2)	WD repeat	cell migration
W03F9.5	TTB-1	2/6	9% (2)	GTF2B	transcription regulation
W03F9.10	W03F9.10	2/6	9% (2)	SF3B2	development and reproduction
R144.7	LARP-1	2/6	8% (5)	La-related protein	Ras-MAPK signaling
T09A5.10	LIN-5	2/6	8% (4)	coiled coil domain	microtubule organization
T22D1.10	RUVB-2	2/6	8% (3)	RUVBL2	DNA helicase
Y55F3AM.15	CSN-4	2/6	8% (2)	COP9 subunit 4	signaling processes
R09E12.3	STI-1	2/6	8% (2)	Sti/Hop family	heat shock protein

T12G3.4	T12G3.4	2/6	8% (2)	APMAP	hydrolase
Y39G10AR.12	TPXL-1	2/6	8% (2)	TPX2	mitotic spindle orientation
Y53G8AR.8	Y53G8AR.8	2/6	8% (2)	ATP5SL	adult lifespan
Y56A3A.31	Y56A3A.31	2/6	8% (2)	C7orf26	uncharacterized
F23B12.8	BMK-1	2/6	7% (5)	BimC/kinesin-5	microtubule organization
C50F2.3	C50F2.3	2/6	7% (4)	XAB2	development and reproduction
C26C6.5	DCP-66	2/6	7% (3)	NuRD component	histone deacetylase
F22B7.5	DNJ-10	2/6	7% (3)	DnaJ	mitochondrial organization
F25B4.5	F25B4.5	2/6	7% (3)	PRPF39	mRNA processing
K01C8.9	NST-1	2/6	7% (3)	GNL3	ribosome biogenesis
F38A5.13	DNJ-11	2/6	7% (2)	ZRF1 family	mitotic spindle orientation
F59E12.4	NPL-4.1	2/6	7% (2)	NPLOC4	endocytosis
F59E12.5	NPL-4.2	2/6	7% (2)	NPLOC4	endocytosis
ZC302.1	MRE-11	2/6	6% (3)	MRE11	DNA recombination
ZK112.2	NCL-1	2/6	6% (3)	BRAT, B-box Zn finger	rRNA RNA transcription regulation
F49D11.1	PRP-17	2/6	6% (3)	PRP17	splicing
Y50D4C.1	UNC-34	2/6	6% (3)	EVH1 domain	cell migration
F22D6.6	EKL-1	2/6	6% (2)	Tudor domain	RNAi
M01E11.6	KLP-15	2/6	6% (2)	kinesin family	microtubule organization
C41G7.2	KLP-16	2/6	6% (2)	Ncd, Kar3	neuronal development
T26A8.4	T26A8.4	2/6	6% (2)	Caf120	CCR4-NOT component
C14B1.4	WDR-5.1	2/6	6% (2)	WD40 repeat	chromatin remodeling
Y66D12A.15	XPB-1	2/6	6% (2)	ERCC3	uncharacterized
Y39A1B.3	DPY-28	2/6	5% (4)	condensin subunit homolog	chromatin regulation
F45F2.10	F45F2.10	2/6	5% (4)	ankyrin repeat	development and reproduction
T19E10.1	ECT-2	2/6	5% (3)	RhoGEF	cytokinesis in early embryos
Y76A2B.1	POD-1	2/6	5% (3)	coronin-like protein	embryonic AP axis
Y39G10AR.10	EPG-2	2/6	5% (2)	Coiled coil domain	autophagy
F10B5.8	F10B5.8	2/6	5% (2)	CPSF3L	cleavage and polyadenylation
R12B2.5	MDT-15	2/6	5% (2)	MED15	fatty acid metabolism
R10E4.1	R10E4.1	2/6	5% (2)	BTB domain	uncharacterized
Y39G10AR.2	ZWL-1	2/6	5% (2)	SWILCH	embryo development
B0334.8	AGE-1	2/6	4% (3)	PI3K catalytic subunit p110	insulin signaling pathway
C02C6.1	DYN-1	2/6	4% (3)	dynamin GTPase	endocytosis, vesicular trafficking
Y43F4B.6	KLP-19	2/6	4% (3)	kinesin family	microtubule organization
Y41D4B.19	NPP-8	2/6	4% (3)	none detected	nucleocytoplasmic transport
T04H1.4	RAD-50	2/6	4% (3)	Rad50	DNA repair
T05H10.1	T05H10.1	2/6	4% (3)	USP47	ubiquitination
T13C2.6	T13C2.6	2/6	4% (3)	LDLR	calcium ion binding
C03D6.3	CEL-1	2/6	4% (2)	RNA triphosphatase	mRNA capping enzyme
C06G3.2	KLP-18	2/6	4% (2)	kinesin family	microtubule organization
Y48E1B.7	LIN-38	2/6	4% (2)	C2H2-type Zn finger	synmuv protein
F21H12.1	RBBP-5	2/6	4% (2)	WD40 repeat	chromatin remodeling
ZK1236.3	SOR-1	2/6	4% (2)	sop-2 related protein	hox gene regulation
F18C12.2	RME-8	2/6	3% (5)	DnaJ	endocytosis
W07E11.1	W07E11.1	2/6	3% (4)	NADP binding	glutamate biosynthesis
F11C1.5	F11C1.5	2/6	3% (3)	VWA8	ATPase
C16A3.3	LET-716	2/6	3% (3)	PDCD11	development and reproduction
K08B12.5	MRCK-1	2/6	3% (3)	MRCK	embryonic elongation
D2021.1	UTX-1	2/6	3% (3)	UTX	transcription regulation
T08A9.1	ATG-11	2/6	3% (2)	RB1CC1, coiled coil	autophagy
C07H4.2	CLH-5	2/6	3% (2)	CLC1	endocytosis
M18.5	DDB-1	2/6	3% (2)	DDB1	DNA repair
R05H10.3	R05H10.3	2/6	3% (2)	TIGD1 transposable element	uncharacterized
T23E7.2	T23E7.2	2/6	3% (2)	Coiled coil domain	uncharacterized

T25G3.4	T25G3.4	2/6	3% (2)	GPD2	glycerol degradation
Y57A10A.31	Y57A10A.31	2/6	3% (2)	RNF216	reproduction
K12D12.2	NPP-3	2/6	2% (3)	Nup205	nuclear transport of proteins
Y51H4A.12	SET-26	2/6	2% (3)	PHD Zn finger, SET domain	histone methyltransferase
F15E6.1	SET-9	2/6	2% (3)	PHD Zn finger, SET domain	Zn ion binding
ZK1067.2	ZK1067.2	2/6	2% (3)	ZNFX1	transcription factor
F33H2.5	POLE-1	2/6	2% (2)	POLE	DNA polymerase
F26A3.8	RRF-1	2/6	2% (2)	RdRP	RNAi
T08A11.2	T08A11.2	2/6	2% (2)	SAP155	splicing
F47A4.2	DPY-22	2/6	1% (3)	TRAP230	Wnt and Ras signaling

Table A3-1: AIN-1 interactors

Proteins (n=340) identified by MuDPIT in AIN-1::LAP purifications. Proteins are ordered based on number of detections out of six independent immunoprecipitations, followed by peptide coverage (%). Homology data and description for each protein were obtained from Wormbase WS250 and UniProt database. (*) ALG-1, ALG-2, and AIN-1 were the most abundant proteins detected in the AIN-1 IP. The proteins were also detected in the negative control (wild-type non-transgenic FLAG IP samples), but at a much lower peptide count and coverage (4 peptide counts and 7% peptide coverage for ALG-1/2, and 2 peptide counts and 6% coverage for AIN-1). The interactions between ALG-1/2 with AIN-1 were previously validated (Zhang et al., 2007). (Relates to Figure 4-1 and Table 4-1).

Sequence ID	Protein	# datasets detected	Coverage (peptide counts)	Homology/Domain	Description
ZC518.3	CCR-4	3/3	61% (40)	Ccr4/CNOT6 and CNOT6L	CCR4-NOT subunit
Y56A3A.1	NTL-3	3/3	58% (44)	CNOT3	CCR4-NOT component
C26E6.3	NTL-9	3/3	45% (18)	RQCD1	CCR4-NOT component
K04B12.2	K04B12.2	3/3	44% (12)	Cul9/NEDD4L	uncharacterized
F57B9.2	NTL-1	3/3	43% (121)	CNOT1	CCR4-NOT subunit
B0286.4	NTL-2	3/3	42% (14)	CNOT2	CCR4-NOT component
Y56A3A.20	CCF-1	3/3	39% (19)	Caf1/CNOT7	CCR4-NOT subunit
F44A2.1	TAG-153	3/3	33% (23)	CNOT2	uncharacterized
T12G3.1	SQST-1	3/3	22% (12)	Sqstm1/p62	autophagy
M02D8.4	ASNS-2	3/3	22% (10)	Asn synthetase	Asn biosynthesis
ZK652.4	RPL-35	3/3	20% (2)	60S rpl-35	ribosomal protein
R05D11.8	EDC-3	3/3	18% (8)	Edc3	decapping activator
Y113G7B.17	PRMT-1	3/3	17% (4)	Argine methyltransferase	Argine methyltransferase
K10B3.8	GPD-2	3/3	14% (3)	GAPDH	glycolysis
K10B3.7	GPD-3	3/3	14% (3)	GAPDH	glycolysis
H28G03.1	H28G03.1	3/3	13% (3)	RNA-binding	uncharacterized
Y44E3A.6	Y44E3A.6	3/3	12% (7)	EDC4	decapping activator
F31E3.3	RFC-4	3/3	12% (3)	RFC4	DNA replication
F13D12.2	LDH-1	3/3	12% (3)	LDHB	lactate dehydrogenase
F47B10.1	F47B10.1	3/3	10% (4)	ATP Grasp domain	TCA cycle
B0513.1	LIN-66	3/3	10% (4)	unknown	translational regulation
K02B9.2	MEG-2	3/3	9% (5)	none detected	P granule component
C37E2.1	IDHB-1	3/3	9% (3)	NAD isocitrate dehydrogenase	TCA cycle
F26F4.7	NHL-2	3/3	8% (6)	TRIM-NHL	miRISC component
C07G1.5	HGRS-1	3/3	6% (3)	Vps27p, FYVE Zn finger	endocytosis
R11A8.7	R11A8.7	3/3	5% (9)	Q/N-rich domain	uncharacterized
H19N07.2	USP-7	3/3	4% (3)	MATH/Usp domain	ubiquitin-specific protease
C55B7.1	GLH-2	3/3	4% (3)	DEAD box RNA helicase	P granule component
C18H9.3	C18H9.3	3/3	4% (3)	GIGYF1/2	GYF domain-containing protein
T01B7.6	TRCS-2	3/3	4% (3)	unknown	uncharacterized
F56A3.4	SPD-5	3/3	4% (3)	coiled coil domain	cell division
ZK381.4	PGL-1	3/3	4% (2)	none detected	RGG box motif, P granules
F46G10.7	SIR-2.2	2/3	32% (8)	Sir2p	NAD-dependent histone deacetylase
Y74C10AR.1	EIF-3.i	2/3	18% (5)	EIF3I	translation initiation
Y116A8C.42	SNR-1	2/3	15% (3)	snRNP family	splicing
Y57A10A.18	PQN-87	2/3	14% (14)	Q/N-rich domain	uncharacterized
T08B2.7	ECH-1.2	2/3	13% (6)	HADHA	CoA hydratase/dehydrogenase
C34G6.7	STAM-1	2/3	12% (4)	Q/N-rich domain, SH3	protein transport
F31D4.3	FKB-6	2/3	12% (4)	TPR repeat	protein folding
C38C3.5	UNC-60	2/3	12% (3)	ADF family	actin polymerization
R05D3.7	UNC-116	2/3	11% (7)	kinesin-1 heavy chain	intracellular transport
T12E12.4	DRP-1	2/3	11% (6)	DRP1	dynamin-related protein
Y54G9A.6	BUB-3	2/3	10% (2)	BUB3	mitotic checkpoint
Y116A8C.35	UAF-2	2/3	10% (2)	U2AF35, RRM	splicing
T05G5.3	CDK-1	2/3	10% (2)	Cdc28	cell cycle
C12D8.11	ROP-1	2/3	9% (4)	Ro autoantigen	Y RNA stabilization
T05E7.5	VET-1	2/3	9% (3)	coiled coil domain	reproduction
R11G1.4	SAX-1	2/3	9% (3)	kinase domain	cell polarity
F20B6.2	VHA-12	2/3	9% (3)	ATPase	ATP metabolism
F32E10.4	IMA-3	2/3	9% (2)	Importin subunit	protein transport
F26E4.1	SUR-6	2/3	8% (3)	PP2A subunit B	signal transduction
K07A3.1	FBP-1	2/3	8% (2)	FBP1	carbohydrate metabolism

C53D5.6	IMB-3	2/3	7% (6)	Importin beta 3	nuclear transport
F43G6.9	PATR-1	2/3	7% (4)	PAT1	mRNA decay
T08B2.9	FARS-1	2/3	7% (3)	aminoacyl tRNA synthase	aminoacyl tRNA synthase
Y34D9A.10	VPS-4	2/3	7% (3)	VPS4B, VPS4A	vacuolar protein sorting
K10C9.3	K10C9.3	2/3	7% (2)	ribonuclease T2	RNA binding
T25G12.5	ACDH-7	2/3	7% (2)	ACADM	acyl-CoA dehydrogenase
Y65B4A.6	Y65B4A.6	2/3	7% (2)	DEAD box RNA helicase	splicing
F33D11.10	F33D11.10	2/3	7% (2)	DEAD box RNA helicase	splicing
C06G1.4	AIN-1	2/3	6% (3)	GW182/TNRC6	miRISC
ZK632.7	PANL-3	2/3	6% (3)	PAN3	PAN2/3 subunit
W01B11.3	NOL-5	2/3	6% (3)	NOP58	nucleolar RNP
W08G11.4	PPTR-1	2/3	5% (3)	PP2A regulatory subunit	P granule component
Y73F8A.25a	NTL-11	2/3	5% (3)	CNOT11	CCR4-NOT component
T23G5.1	RNR-1	2/3	5% (3)	ATP cone domain	DNA replication
E04F6.5	ACDH-12	2/3	5% (3)	Acyl Coa dehydrogenase	lipid homeostasis
Y48B6A.3	XRN-2	2/3	4% (3)	XRN2	5'-3' exoribonuclease
ZK1053.4	ZK1053.4	2/3	4% (2)	coiled-coil domain	SEPA-1 family, autophagy
F52G2.1	DCAP-2	2/3	4% (2)	Dcp2	mRNA decapping
Y46G5A.4	Y46G5A.4	2/3	3% (4)	putative RNA helicase	splicing
F55H2.6	CLU-1	2/3	3% (3)	CLU family	mitochondrial protein transport
Y59A8B.6	PRP-6	2/3	3% (2)	PRPF6	pre-mRNA processing
T23B5.1	PRMT-3	2/3	3% (2)	PRMT9	methyltransferase
H34C03.2	H34C03.2	2/3	3% (2)	Usp4	Protein catabolism
F35G12.2	IDHG-1	2/3	8% (2)	isocitrate dehydrogenase	tricarboxylic acid cycle
C44E4.1	C44E4.1	2/3	2% (5)	UBR4	ubiquitination
T21E12.4	DHC-1	2/3	1% (4)	Dynein heavy chain family	motor transport

Table A3-2: NTL-1 interactors

Proteins (n=78) identified by MuDPIT in NTL-1::LAP purifications. Proteins are ordered based on number of detections out of six independent immunoprecipitations, followed by peptide coverage (%). Homology data and description for each protein were obtained from Wormbase WS250 and UniProt database. (Relates to Figure 4-1 and Table 4-1).

	let-7 sensitized	*let-7* phenotype	*Drosophila* miRNA	AIN-2 Co-IP	DCR-1 Co-IP	ERI-1 Co-IP	*Drosophila* siRNA	dsGFP RNAi	Germline suppression defect	SynMuv suppression	Suppression of transgene silencing in *eri-1*	NTL-1 co-IP	AIN-1 co-IP	NTL-1 & AIN-1 co-IP
let-7 sensitized	319	78	7	3	3	5	11	7	5	1	68	3	25	2
let-7 phenotype	2.7E-68	296	7	1	4	6	12	13	5	2	63	6	29	4
Drosophila miRNA	0.0004	0.0002	71	2	2	4	63	4	0	2	13	0	17	0
AIN-2 Co-IP	0.0340	0.4874	0.0110	38	6	3	0	0	0	0	1	0	6	0
DCR-1 Co-IP	0.2640	0.0842	0.0599	6.2E-08	95	22	3	3	1	1	10	5	11	1
ERI-1 Co-IP	0.0260	0.0046	0.0005	0.0010	6.1E-31	89	5	4	1	0	9	3	10	1
Drosophila siRNA	1.6E-05	1.2E-06	6E-135	1	0.0297	0.0004	120	6	0	3	23	2	21	1
dsGFP RNAi	0.0015	5.2E-09	0.0005	1	0.0140	0.0013	4.2E-05	90	3	6	66	2	13	1
Germline suppression defect	0.0107	0.0079	1	1	0.3288	0.3116	1	0.0063	71	1	11	4	10	2
SynMuv suppression	0.4444	0.1011	0.0074	1	0.1596	1	0.0013	1.2E-08	0.1218	31	17	0	6	0
Suppression of transgene silencing in *eri-1*	1.5E-25	1.0E-23	3.4E-05	0.8507	0.0173	0.0293	1.5E-08	3.1E-67	0.0006	5.9E-15	829	11	61	8
NTL-1 co-IP	0.1805	0.0024	1	1	7.5E-05	0.0080	0.1051	0.0643	0.0003	1	0.0014	78	38	38
AIN-1 co-IP	6.6E-09	1.7E-12	3.4E-14	9.8E-05	3.0E-06	1.1E-05	2.6E-14	2.7E-08	1.4E-06	3.0E-05	5.0E-19	4.4E-44	340	38
NTL-1 & AIN-1 co-IP	0.1593	0.0042	1	1	0.1920	0.1810	0.2362	0.1828	0.0110	1	0.0004	2.5E-94	3.3E-66	38

Table A3-3: Proteins that bind to NTL-1 and AIN-1 in Co-IP assays overlap with proteins identified in previous siRNA and miRNA screens

The table shows the number of proteins identified in the present Co-IP study (NTL-1 and AIN-1) that overlap with proteins identified in previous screens (upper triangle) (Tabach et al., 2013) and the hyper-geometric *p*-value of the overlap (lower triangle). The gray diagonal represents the total number of proteins identified in each screen. The integrated studies are as follows: *let-7* phenotype (WormBase (WS220), Tabach et al., 2013), *let-7* sensitized (Parry et al., 2007), *Drosophila* miRNA and siRNA (Zhou et al., 2008), DCR-1 Co-IP (Duchaine et al., 2006), ERI-1 Co-IP (Thivierge et al., 2012), AIN-2 Co-IP (Zhang et al., 2007), suppression of transgene silencing in *eri-1* and dsGFP RNAi (Kim et al., 2005), germline co-suppression defect (Robert et al., 2005), SynMuv suppression (Cui et al., 2006). (Relates to Figure 4-1 and Table 4-1).

	Symbol	Transcript Name	let-7 sensitized	let-7 phenotype	Drosophila miRNA	AIN-2 Co-IP	DCR-1 Co-IP	Phylogenetic Profile	Expression	PPI	interologs	Genetic	Phenotype	**LR+ Score**
AIN-1 Co-IP overlap p-value = 1.14E-37	alg-2	T07D3.7	0.000	0.000	2.015	2.074	2.828	2.990	1.874	0.000	2.674	0.000	0.000	**14.455**
	alg-1	F48F7.1	0.000	0.000	2.015	2.074	2.828	2.990	1.402	0.000	2.674	0.000	0.062	**14.046**
	dcr-1	K12H4.8	2.118	1.368	0.000	0.000	0.000	2.146	0.000	0.000	2.674	1.998	0.000	**10.304**
	hrpf-2	Y73B6BL.33	0.000	0.000	2.015	0.000	0.000	1.552	0.000	0.000	2.674	0.000	0.062	**6.302**
	isw-1	F37A4.8	1.420	1.368	2.015	0.000	0.000	0.642	0.815	0.000	0.000	0.000	0.000	**6.260**
	unc-59	W09C5.2	2.118	1.368	0.000	0.000	0.000	0.837	0.815	0.000	0.000	0.000	0.062	**5.200**
	drh-3	D2005.5	0.000	0.000	0.000	0.000	2.828	0.837	1.402	0.000	0.000	0.000	0.000	**5.067**
	lin-28	F02E9.2	2.118	0.000	0.000	0.000	0.000	2.807	0.000	0.000	0.000	0.000	0.000	**4.925**
	dpl-1	T23G7.1	0.000	0.000	2.015	0.000	0.000	1.555	0.815	0.000	0.000	0.000	0.062	**4.447**
	rsp-8	C18D11.4	0.000	1.368	0.000	0.000	0.000	2.146	0.815	0.000	0.000	0.000	0.062	**4.391**
	npp-3	K12D12.2	0.000	1.368	0.000	0.000	0.000	2.191	0.815	0.000	0.000	0.000	0.000	**4.374**
	dyci-1	C17H12.1	2.118	0.000	0.000	0.000	0.000	2.146	0.000	0.000	0.000	0.000	0.000	**4.264**
	swd-2.2	C33H5.7	1.595	0.000	2.015	0.000	0.000	0.642	0.000	0.000	0.000	0.000	0.000	**4.252**
	E01A2.2	E01A2.2	0.000	0.000	2.015	0.000	0.000	0.262	1.874	0.000	0.000	0.000	0.000	**4.151**
	psf-1	F25B5.7	0.000	1.368	0.000	0.000	0.000	0.596	1.874	0.000	0.000	0.000	0.062	**3.900**
	fln-2	C23F12.1	1.595	1.368	0.000	0.000	0.000	0.837	0.000	0.000	0.000	0.000	0.062	**3.863**
	trr-1	C47D12.1	1.595	1.368	0.000	0.000	0.000	0.837	0.000	0.000	0.000	0.000	0.062	**3.863**
	ntl-4	C49H3.5	1.420	0.000	0.000	0.000	0.000	0.543	1.874	0.000	0.000	0.000	0.000	**3.836**
	nrde-3	R04A9.2	0.000	0.000	0.000	0.000	0.000	2.414	1.402	0.000	0.000	0.000	0.000	**3.817**
	ain-2	B0041.2	1.595	0.000	0.000	2.074	0.000	0.000	0.000	0.000	0.000	0.000	0.000	**3.670**
	eif-3.E	B0511.10	1.595	0.000	0.000	0.000	0.000	1.987	0.000	0.000	0.000	0.000	0.062	**3.645**
	mrck-1	K08B12.5	1.595	0.000	0.000	0.000	0.000	0.642	1.402	0.000	0.000	0.000	0.000	**3.640**
	cul-1	D2045.6	1.595	0.000	0.000	0.000	0.000	0.596	1.402	0.000	0.000	0.000	0.000	**3.594**
	B0336.3	B0336.3	0.000	0.000	0.000	0.000	0.000	2.191	1.402	0.000	0.000	0.000	0.000	**3.593**
	mtr-4	W08D2.7	0.000	1.368	0.000	0.000	0.000	0.642	1.402	0.000	0.000	0.000	0.062	**3.475**
	C12D8.1	C12D8.1	0.000	0.000	2.015	0.000	0.000	1.459	0.000	0.000	0.000	0.000	0.000	**3.474**
	T08A11.2	T08A11.2	0.000	0.000	2.015	0.000	0.000	0.596	0.815	0.000	0.000	0.000	0.000	**3.426**
	cfim-2	D1046.1	0.000	0.000	2.015	0.000	0.000	1.356	0.000	0.000	0.000	0.000	0.000	**3.371**
	C18A3.5	C18A3.5	0.000	1.368	0.000	0.000	0.000	0.596	1.402	0.000	0.000	0.000	0.000	**3.367**
	dpy-22	F47A4.2	1.595	0.000	0.000	0.000	0.000	0.305	1.402	0.000	0.000	0.000	0.062	**3.364**
	unc-37	W02D3.9	0.000	1.368	0.000	0.000	0.000	0.543	1.402	0.000	0.000	0.000	0.000	**3.314**
	K08F4.2	K08F4.2	0.000	0.000	0.000	0.000	1.773	0.000	1.402	0.000	0.000	0.000	0.000	**3.176**
	par-1	H39E23.1	1.595	0.000	0.000	0.000	0.000	0.642	0.815	0.000	0.000	0.000	0.000	**3.052**
	ekl-6	T16G12.5	1.420	1.368	0.000	0.000	0.000	0.262	0.000	0.000	0.000	0.000	0.000	**3.051**
	xrn-1	Y39G8C.1	0.000	0.000	0.000	0.000	0.000	2.990	0.000	0.000	0.000	0.000	0.000	**2.990**
	hrpf-1	W02D3.11	0.000	0.000	0.000	0.000	0.000	1.552	1.402	0.000	0.000	0.000	0.000	**2.954**
	dcap-1	Y55F3AM.12	0.000	0.000	0.000	0.000	0.000	0.262	0.000	0.000	2.674	0.000	0.000	**2.937**
	alh-1	F54D8.3	0.000	0.000	0.000	2.074	0.000	0.837	0.000	0.000	0.000	0.000	0.000	**2.912**
	rme-8	F18C12.2	1.420	0.000	0.000	0.000	0.000	1.336	0.000	0.000	0.000	0.000	0.062	**2.818**
	larp-5	T12F5.5	0.000	0.000	0.000	0.000	0.000	0.837	1.953	0.000	0.000	0.000	0.000	**2.790**
	R10E4.2b.3	R10E4.2	0.000	0.000	0.000	0.000	2.175	0.596	0.000	0.000	0.000	0.000	0.000	**2.771**
	lsy-2	F49H12.1	0.000	0.000	0.000	0.000	0.000	0.837	1.874	0.000	0.000	0.000	0.000	**2.711**
	swd-3.1	C14B1.4	0.000	0.000	2.015	0.000	0.000	0.642	0.000	0.000	0.000	0.000	0.000	**2.657**
	mrg-1	Y37D8A.9	0.000	0.000	0.000	0.000	0.000	1.834	0.815	0.000	0.000	0.000	0.000	**2.649**
	nst-1	K01C8.9	0.000	0.000	0.000	0.000	1.943	0.642	0.000	0.000	0.000	0.000	0.062	**2.647**
	W03F9.10	W03F9.10	0.000	0.000	2.015	0.000	0.000	0.543	0.000	0.000	0.000	0.000	0.000	**2.558**
	rfp-1	R05D3.4	0.000	1.368	0.000	0.000	0.000	0.305	0.815	0.000	0.000	0.000	0.062	**2.550**
	Y46G5A.13	Y46G5A.13	0.000	0.000	0.000	0.000	1.925	0.596	0.000	0.000	0.000	0.000	0.000	**2.521**
	dcp-66	C26C6.5	0.000	1.368	0.000	0.000	0.000	0.262	0.815	0.000	0.000	0.000	0.062	**2.508**

	klc-2	C18C4.10	0.000	0.000	0.000	0.000	0.000	1.657	0.815	0.000	0.000	0.000	0.000	**2.472**
	Y48C3A.14	Y48C3A.14	0.000	0.000	0.000	0.000	1.773	0.642	0.000	0.000	0.000	0.000	0.000	**2.416**
	F58G1.1	F58G1.1	0.000	0.000	0.000	0.000	0.000	2.414	0.000	0.000	0.000	0.000	0.000	**2.414**
	R06C7.1	R06C7.1	0.000	0.000	0.000	0.000	0.000	2.414	0.000	0.000	0.000	0.000	0.000	**2.414**
	F29C4.7	F29C4.7	0.000	0.000	2.015	0.000	0.000	0.383	0.000	0.000	0.000	0.000	0.000	**2.398**
	R02D3.4	R02D3.4	0.000	0.000	2.015	0.000	0.000	0.383	0.000	0.000	0.000	0.000	0.000	**2.398**
	gei-7	C05E4.9	0.000	0.000	0.000	2.074	0.000	0.305	0.000	0.000	0.000	0.000	0.000	**2.379**
	lys-1	Y22F5A.4	0.000	0.000	0.000	2.074	0.000	0.305	0.000	0.000	0.000	0.000	0.000	**2.379**
	T26A8.4	T26A8.4	0.000	0.000	2.015	0.000	0.000	0.262	0.000	0.000	0.000	0.000	0.062	**2.339**
	C07A9.2	C07A9.2	0.000	0.000	2.015	0.000	0.000	0.305	0.000	0.000	0.000	0.000	0.000	**2.320**
	H20J04.8.2	H20J04.8	0.000	0.000	2.015	0.000	0.000	0.305	0.000	0.000	0.000	0.000	0.000	**2.320**
NTL-1 Co-IP overlap p-value = 6.33E-12	ZK632.7	ZK632.7	0.000	0.000	0.000	0.000	1.907	0.837	1.402	0.000	0.000	0.000	0.000	**4.147**
	Y46G5A.4	Y46G5A.4	0.000	0.000	0.000	0.000	1.714	0.642	1.402	0.000	0.000	0.000	0.000	**3.759**
	sur-6	F26E4.1	0.000	1.368	0.000	0.000	0.000	0.837	1.402	0.000	0.000	0.000	0.062	**3.670**
	prmt-1	Y113G7B.17	1.595	1.368	0.000	0.000	0.000	0.596	0.000	0.000	0.000	0.000	0.000	**3.560**
	ima-3	F32E10.4	0.000	0.000	0.000	0.000	0.000	0.642	0.000	0.000	2.470	0.000	0.000	**3.112**
	T08B2.7	T08B2.7	0.000	0.000	0.000	0.000	1.814	0.837	0.000	0.000	0.000	0.000	0.000	**2.651**
	dcap-2	F52G2.1	0.000	0.000	0.000	0.000	0.000	0.305	0.000	0.000	2.143	0.000	0.000	**2.447**
NTL-1& AIN-1 Co-IP overlap p-value = 1.95E-09	ntl-2	B0286.4	0.000	1.368	0.000	0.000	0.000	0.837	1.874	0.000	0.000	0.000	0.062	**4.141**
	gpd-3	K10B3.7	0.000	0.000	0.000	0.000	1.821	2.129	0.000	0.000	0.000	0.000	0.000	**3.949**
	nhl-2	F26F4.7	0.000	0.000	0.000	0.000	0.000	2.990	0.815	0.000	0.000	0.000	0.000	**3.805**
	fkb-6	F31D4.3	1.420	1.368	0.000	0.000	0.000	0.642	0.000	0.000	0.000	0.000	0.000	**3.430**
	drp-1	T12E12.4	0.000	1.368	0.000	0.000	0.000	0.642	1.402	0.000	0.000	0.000	0.000	**3.413**
	unc-116	R05D3.7	1.595	0.000	0.000	0.000	0.000	0.642	0.815	0.000	0.000	0.000	0.062	**3.114**
	xrn-2	Y48B6A.3	0.000	0.000	0.000	0.000	0.000	2.990	0.000	0.000	0.000	0.000	0.062	**3.052**
	uaf-2	Y116A8C.35	0.000	0.000	0.000	0.000	0.000	2.146	0.815	0.000	0.000	0.000	0.000	**2.961**
	let-711	F57B9.2	0.000	1.368	0.000	0.000	0.000	0.543	0.815	0.000	0.000	0.000	0.062	**2.788**
	R11A8.7	R11A8.7	0.000	0.000	0.000	0.000	0.000	0.642	1.953	0.000	0.000	0.000	0.000	**2.595**
	ntl-3	Y56A3A.1	0.000	0.000	0.000	0.000	0.000	2.310	0.000	0.000	0.000	0.000	0.000	**2.310**

Table A3-4: Overlap of genes implicated in RNAi between different siRNA and miRNA screens

71 and 18 interactors of AIN-1 and NTL-1, respectively, overlap with previously identified proteins that have a high likelihood of being part of the siRNA and/or miRNA pathway. The last column is the combined likelihood from the individual datasets (columns 3-13) into one predictive score (Tabach et al., 2013). Moreover, 11 of the genes identified in our screen are interactors of both AIN-1 and NTL-1. The hyper-geometric *p*-values for the overlap are 1.14E-37 for AIN-1, 6.33E-12 for NTL-1 and 1.95E-09 for the shared proteins. (Relates to Figure 4-1 and Table 4-1).

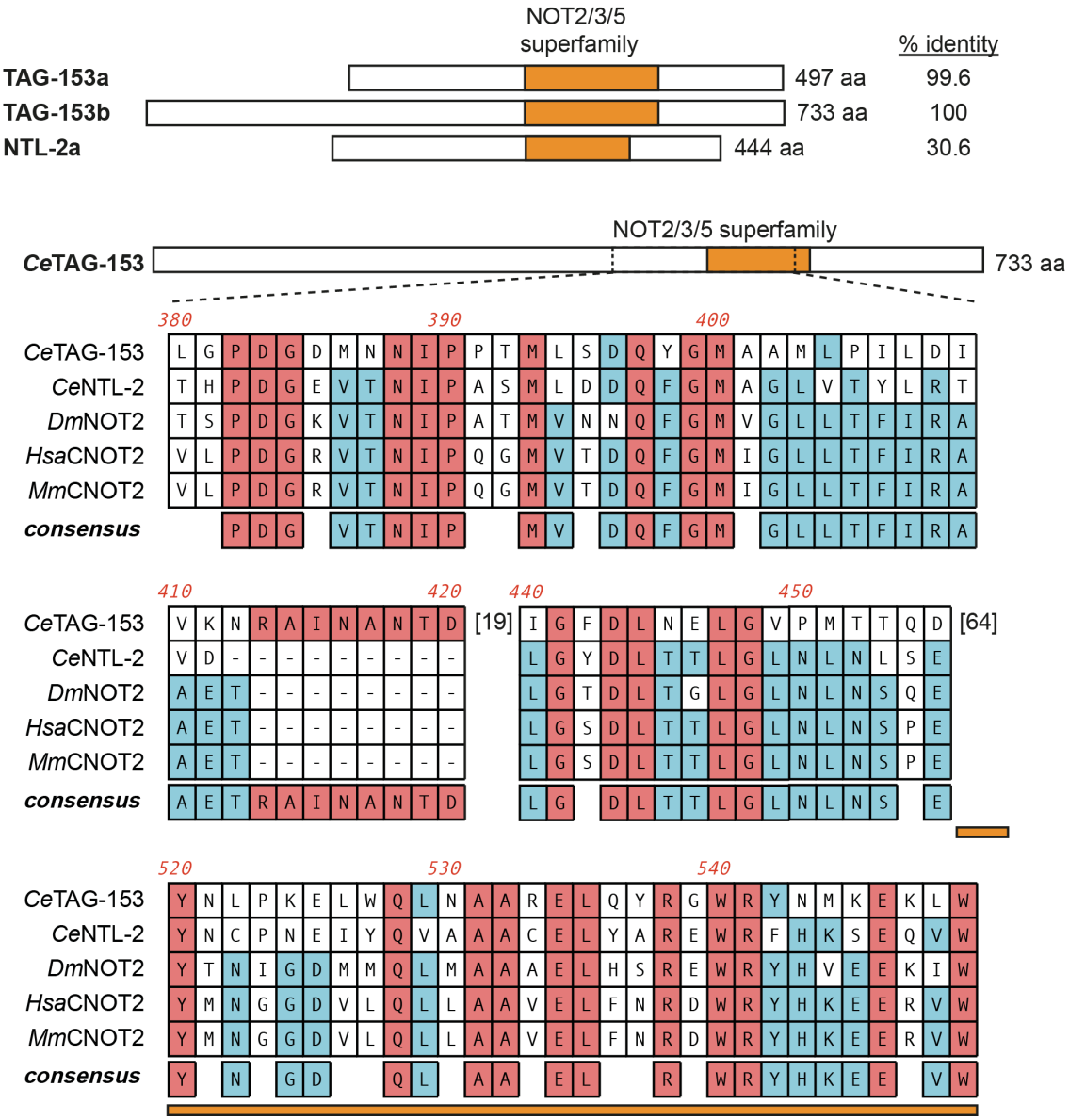

Figure A3-1: TAG-153, a homolog of NTL-2/CNOT2 subunit

Using NCBI Protein BLAST, *tag-153* (*f44a2.1*) was found to encode a protein that shares homologous sequences (amino acids 353-525: 30.6% identity, 51.4% similarity) with the NTL-2/CNOT2 subunit of the CCR4-NOT complex. Protein alignments of the homologous region near and at the NOT2/3/5 domain (orange) are provided. Species are as follows: *Homo sapiens* (*Hsa*), *Mus musculus* (*Mm*), *D. melanogaster* (*Dm*), *and C. elegans* (*Ce*). Residues that are conserved in all aligned proteins are highlighted in red, and residues that are less conserved are highlighted in blue. (Relates to Figure 4-1 and Table 4-1).

Sequence ID	Protein	# datasets detected	Coverage (peptide counts)	Homology/Domain	Description	AIN-1 IP?	NTL-1 IP?
2'-O-Me miR-35 pulldown							
C35D10.13	C35D10.13	3/3	27% (5)	coiled coil domain	apoptosis, embryo development	-	-
B0041.2	AIN-2	3/3	23% (17)	GW182/TNRC6	miRISC	3/6 (*)	-
C06G1.4	AIN-1	3/3	21% (12)	GW182/TNRC6	miRISC	6/6	2/3
T07D3.7	ALG-2	3/3	18% (15)	AGO1	miRISC	6/6 (*)	-
F48F7.1	ALG-1	3/3	13% (11)	AGO1	miRISC	6/6 (*)	-
K12H4.8	DCR-1	3/3	12% (18)	DCR1	RNAi, endoribonuclease	6/6	-
Y23H5A.3	Y23H5A.3	3/3	11% (3)	none detected	cell division, embryo development	6/6	-
R09B3.3	R09B3.3	2/3	33% (2)	CSTF2, RRM	embryo development		-
R10E4.2	SUP-26	2/3	21% (4)	RRM domain	translation regulation	3/6	-
T27E9.1	ANT-1.1	2/3	18% (2)	ADP/ATP exchange factor	mitochondrial adenine nucleotide transporter	-	-
T20G5.11	RDE-4	2/3	11% (3)	dsRBD	RNAi	-	-
EEED8.1	MEL-47	2/3	7% (2)	SLIRP	maternal early embryonic cell division	5/6	-
2'-O-Me miR-52 pulldown							
T07D3.7	ALG-2	6/6	16% (11)	AGO1	miRISC	6/6 (*)	-
F48F7.1	ALG-1	6/6	13% (10)	AGO1	miRISC	6/6 (*)	-
C06G1.4	AIN-1	6/6	14% (7)	GW182/TNRC6	miRISC	6/6 (*)	2/3
B0041.2	AIN-2	6/6	13% (8)	GW182/TNRC6	miRISC	3/6	-
K12H4.8	DCR-1	5/6	6% (8)	DCR1	RNAi, endoribonuclease	6/6	-
C56C10.8	ICD-1	4/6	27% (3)	BTF3	apoptosis, transcription regulation	-	-
F17C11.9	EEF-1G	3/6	9% (3)	EEF1G	translation elongation	-	-
Y25C1A.8	Y25C1A.8	3/6	9% (2)	ZRANB2	RNA binding	-	-
C06A1.1	CDC-48.1	3/6	8% (4)	Cdc-48.1	ubiquitin chaperone	-	-
Y47G6A.20	RNP-6	3/6	6% (3)	PUF60	splicing	-	-
F10G7.2	TSN-1	3/6	5% (3)	Tudor SN	miRISC	-	-
K08C7.3	EPI-1	3/6	2% (4)	laminin-like	development	-	-
C25A1.8	CLEC-87	2/6	18% (4)	C-type leptin domain	carbohydrate binding	-	-
F48E8.2	F48E8.2	2/6	11% (3)	E2F-associated phosphoprotein	transcription regulation	-	-
Y48B6A.14	HMG-1.1	2/6	11% (2)	HMG box	chromatin remodeling	-	-
Y53H1A.1	RSY-1	2/6	10% (3)	PNISR	synapse assembly	-	-
Y37E3.9	PHB-1	2/6	10% (2)	prohibitin family	embryo and germline development	-	-
F01G4.6	F01G4.6	2/6	9% (4)	SLC25A3	development	-	-
F20G4.3	NMY-2	2/6	8% (11)	coiled coil domain	embryo polarity	-	-
C54D1.5	LAM-2	2/6	4% (4)	laminin-like	embryo development	-	-

Table A3-5: Comparative proteomics of 2'-O-Me captured miRISC and NTL-1- and AIN-1-interacting proteins

Proteins detected in FLAG immunoprecipitations (IP) of AIN-1 and NTL-1 were cross-referenced with proteins that were previously detected with miR-35-42 (maternal and zygotic) and miR-51-56 (zygotic) miRISC by 2'-*O*-Me pulldown (Wu et al., 2010). Only proteins that were detected in at least two NTL-1 or AIN-1 purifications and not in the negative control (non-transgenic wild-type *N2* background) were retained (with the exception of ALG-1/2 and AIN-1, denoted by (*), as described in Table A3-1). Homology data and description for each protein were obtained from Wormbase WS250 and UniProt database. (Relates to Figure 4-3).

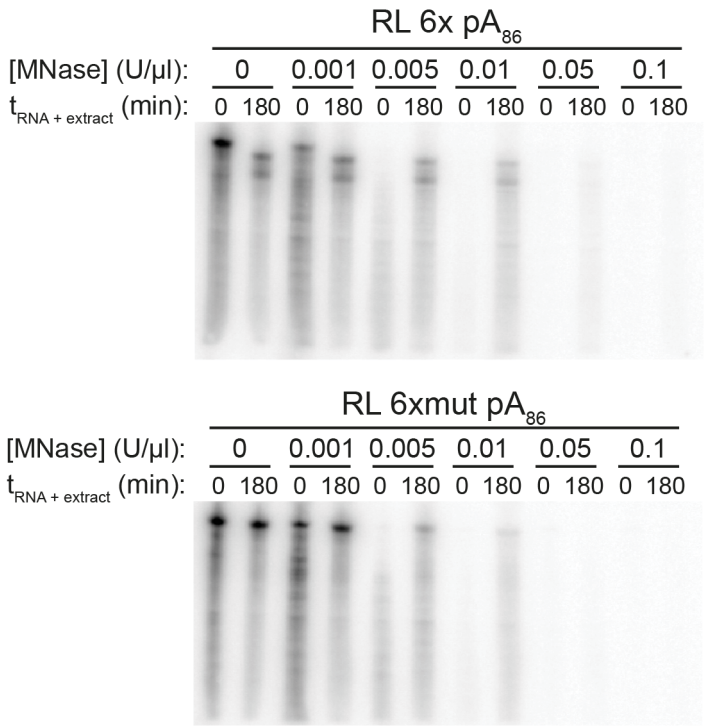

Figure A3-2: miRNP assembly secludes target mRNAs in nuclease-refractory mRNP

(A) Dose-response for sensitivity of 32P-radiolabeled reporter mRNAs (RL 6x pA86 and RL 6xmut pA86) to micrococcal nuclease (MNase). RNA was incubated in the cell-free extract for 0 or 180 minutes (min), followed by a 10-min MNase treatment at the indicated MNase concentrations. The integrity of the mRNA was examined by UREA-PAGE and autoradiography. (Relates to Figure 4-4).

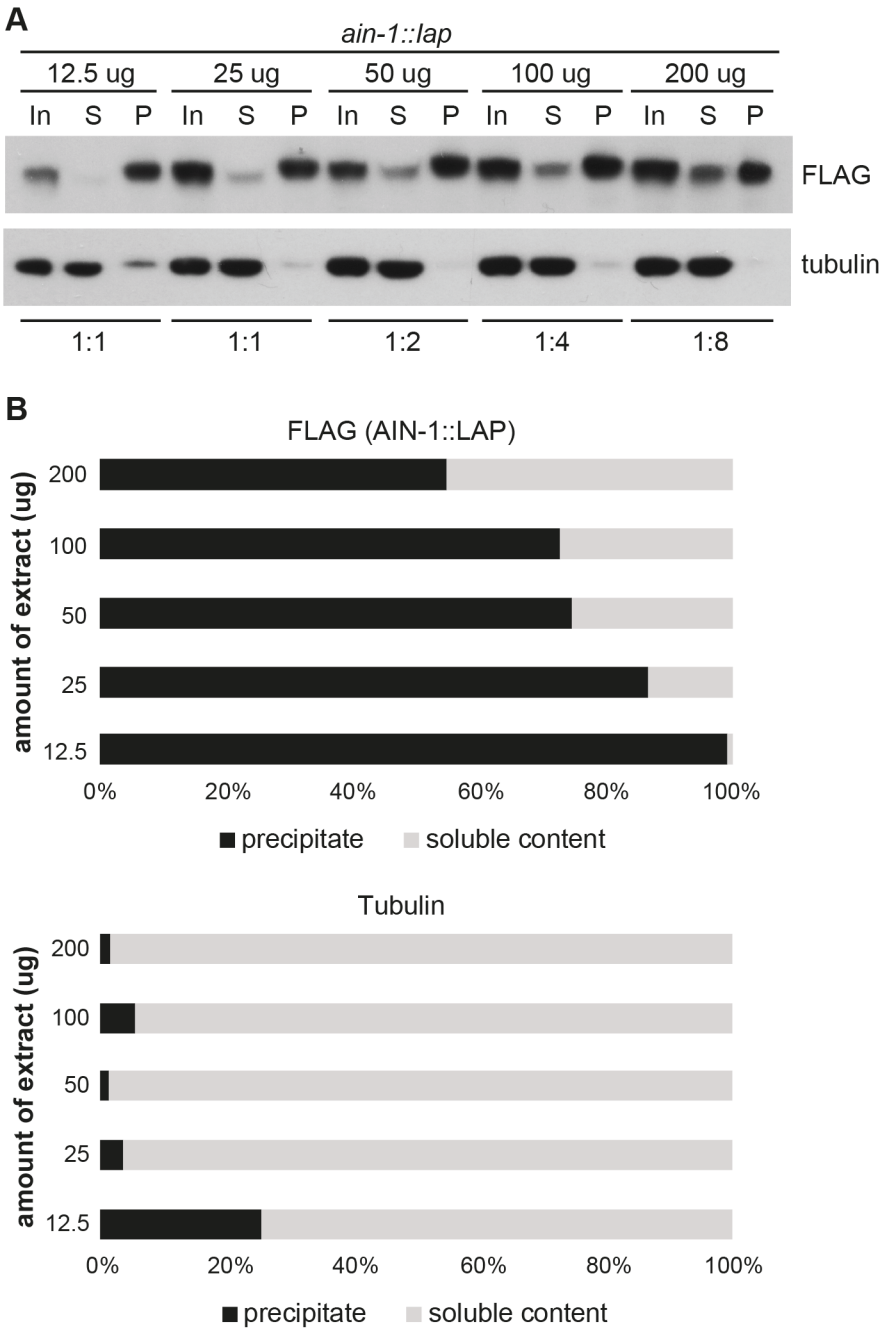
A
ain-1::lap
12.5 ug
25 ug
50 ug
100 ug
200 ug
In S P In S P In S P In S P In S P
FLAG
tubulin
1:1
1:1
1:2
1:4
1:8
B
FLAG (AIN-1::LAP)
amount of extract (ug)
200
100
50
25
12.5
0%
20%
40%
60%
80%
100%
precipitate
soluble content
Tubulin
amount of extract (ug)
200
100
50
25
12.5
0%
20%
40%
60%
80%
100%
precipitate
soluble content

Figure A3-3: Sensitivity of AIN-1 precipitation in response to b-isox

(A) Western blot analysis of *C. elegans* lysates treated with b-isox probed with anti-FLAG and anti-tubulin antibodies. B-isox treatment (100 μM final) was conducted on varying amounts of *C. elegans* lysates as indicated. Ratio denotes the proportion of protein used for b-isox treatment relative to input. In indicates input, S indicates soluble content, and P indicates precipitate. (B) Percentage of FLAG (AIN-1::LAP protein, top panel) and tubulin (bottom panel) detected in the precipitate (denoted by black bars) and in the soluble content (denoted by gray bars) following exposure to b-isox. Quantification of FLAG (AIN-1::LAP) and tubulin signals were obtained using ImageJ. (Relates to Figure 4-5).